Stony Brook University

Application of Transition Metal-Catalyzed Reactions in the Synthesis of *N*-Heterocyclic Natural Products

A Dissertation Presented

by

Stephen J. Chaterpaul

to

The Graduate School

in partial fulfillment of the

requirements

for the Degree of

Doctor of Philosophy

in

Chemistry

Stony Brook University

August 2010

Stony Brook University

The Graduate School

Stephen J. Chaterpaul

We, the dissertation committee for the above candidate for the

Doctor of Philosophy degree, hereby recommend

acceptance of this thesis

Professor Iwao Ojima
Dissertation Advisor
Department of Chemistry

Professor Francis Johnson
Chairman
Department of Chemistry

Professor Robert Kerber
Third Member
Department of Chemistry

Professor William Hersh
Outside Member
Professor Department of Chemistry
Queens College City University of New York

This dissertation is accepted by the Graduate School

Lawrence Martin
Dean of the Graduate School

Abstract of the Dissertation

Application of Transition Metal-Catalyzed Reactions in the Synthesis of *N*-Heterocyclic Natural Products

Stephen J. Chaterpaul

Doctor of Philosophy

Chemistry

Stony Brook University

2010

Metal-catalyzed carbon-carbon bond forming reactions have become one of the most powerful synthetic reactions of the modern organic chemistry reaction arsenal. These reactions have allowed for easier access to more complex structures, and brought about the development of various catalytic asymmetric and asymmetric transformations. At the core of metal-catalyzed asymmetric synthesis are chiral ligands, which are required for the asymmetric inductions afforded by these reactions.

From the very inception of asymmetric reactions, mono- and bidentate phosphorus-based ligands have played a critical role in achieving high enantioselectivity. Although, bidentate ligands have dominated the scene over the past thirty years, monodentate ligands have re-emerged from obscurity to become an essential asset in asymmetric catalysis.

The Ojima laboratory has developed a series of novel phosphorus ligands based on axially chiral 5,5`,6,6`-tetramethylbiphenyl-2,2`-diol. These novel ligands have the capacity to be fine-tuned, which is a particularly attractive feature as these ligands can be applied to a variety of reactions. Thus, a library of these axially chiral phosphorus ligands were designed and synthesized. Subsquently these ligands were successfully applied in a palladium-catalyzed bicycloannulation reaction, the key-step in the synthesis of the lycopodium alkaloid huperzine-A.

In addition to exploring asymmetric catalysis, we also explored cyclohydrocarbonylation as a means to access several classes of nitrogen-based heterocycles. The cyclohydrocarbonylative process can be described as a

hydroformylation reaction, followed by concomintant cyclization resulting from an intramolecular attack by an amide-nitrogen, forming an *N*-acyliminium ion. We studied the trapping of this species with various carbon nucleophiles, including electron rich aromatics, allyl silanes, and enols. This concomitant process permits facile access to several traditionally difficult to synthesize alkaloid classes. Successful application of cyclohydrocarbonylative trapping is demonstrated.

.

TABLE OF CONTENTS

List of Figures

Chapter 1

Chapter 2

Chapter 3

Chapter 4

List of Schemes

Chapter 1

Chapter 2

Chapter 3

Chapter 4

List of Tables

Chapter 1

Chapter 2

Chapter 3

Chapter 4

List of Abbreviations

acac	-	acetylacetonate
AChE	-	acetylcholine esterase
AD	-	Alzheimer's Disease
AH	-	asymmetric hydrogenation
atm	-	atmosphere
Ac	-	acetyl
BINAP	-	2,2'-bis(diphenylphosphino)-1-1'-binapthyl
BINOL	-	1,1'-bis-2-naphtol
BIPHEPHOS	-	6,6'-[(3,3'-Di-*t*-butyl-5,5'-dimethoxy-1,1'-biphenyl-2,2'-diyl)bis(oxy)]bis(dibenzo[d,f][1,3,2]dioxaphosphepin
BSA	-	(*N*,*O*-bis(trimethylsilyl)Acetamide)
CHC	-	cyclohydrocarbonylation
COD	-	cycloctadiene
d	-	doublet
DCM	-	dichloromethane
dd	-	doublet of doublets
DIOP	-	(diphenylphosphino(dimethyl))dioxolane
DMAP	-	4-dimethylaminopyridine
DME	-	dimethoxyethane
DMF	-	dimethylformamide
EDC	-	1-[3-(dimethylamino)propyl]-3-ethylcarbodiimide
ESI	-	electrospray ionization

ee	-	enantiomeric excess
EtOAc	-	ethyl acetate
FCC	-	flash column chromatography
FIA	-	flow-injection analysis
g	-	grams
GC- MS	-	gas chromatography mass spectrometry
HEX	-	hexanes
h	-	hour
HMPT	-	hexamethylphosphorotriamide
HPLC	-	high performance liquid chromatography
HRMS	-	high resolution mass spectrometry
Hz	-	hertz
IR	-	infrared spectroscopy
Kcal	-	kilocalorie
kD	-	kilodalton
L	-	liter
LC-MS	-	liquid chromatography mass spectrometry
LiHMDS	-	lithium hexamethyldisilizane
m	-	multiplet
mmol	-	millimole
M	-	molarity
mg	-	milligram
mL	-	milliliter

mp	-	melting point
MS	-	mass spectrometry
MW	-	microwave
NMDPP	-	neomenthyldiphenylphosphine
NMR	-	nuclear magnetic resonance
PCC	-	pyridinium chlorochromate
PPM	-	parts per million
PSI	-	pounds per square inch
RCM	-	ring-closing metathesis
Red-Al®		sodium bis(2-methoxyethoxy)aluminumhydride
rt	-	room temperature
s	-	singlet
t	-	triplet
TEA	-	triethylamine
TFA	-	trifluroacetic acid
THF	-	tetrahydrofuran
TESCl	-	triethylsilyl chloride
TLC	-	thin layer chromatography
TMG	-	tetramethylguanidine
TMS	-	trimethylsilyl
pTSA	-	*p*-toluenesulfonic acid

Acknowledgements

I would like to first thank, Professor Iwao Ojima for allowing me the opportunity to work in his research group. In addition I would like to thank him for his patience and guidance with both my experimental work and the writing process, he is a truly great mentor. I wish to say thanks to Mrs. Yoko Ojima for her wonderful hospitality on many different occasions. I would also like to thank each and every member of the Ojima Research Group for their help with everything from writing, to experimental work, to instrument training and teaching me various important techniques. Thank you to my mentors. Dr. Liang Sun and Dr. Ray Zhao. To all whom I had intellectual chemistry discussions, Dr. Olivier Marrec, Dr. Stan Jaracz, Dr. Bruno Chapsal, Dr. Ce Shi and all the current Ojima Group members Joseph Kaloko, Edison Zuniga, Alexandra Athan, Ilaria Zanrdi, Chi-Feng (Corey) Lin, Chi-Wei Chien, William Berger, Gary Teng, Lucy Li, and Kunal Kumar. I would like to especially thank Dr. Olivier Marec, Edison Zuniga, Joseph Kaloko, and Alexandra Athan for their help in proofreading my dissertation and their critical comments that helped to shape this work. I would also like to thank Mrs. Patricia Marinaccio for being a wonderful help, and encouragement to me. Without Pat, research would come to a halt in the Ojima group. A special thank you to Dr. James Maracek for his help with NMR techniques and his general advice on various synthetic problems. A special thank you to Dr. Alvin Silverstein and Mr. Michael Tetta for their help when the Chemistry building fought back. A thank you to my ACC committee, Prof. Robert Kerber, and Prof. Francis Johnson, for always pushing me to do my best and for their various advices. I would especially like to thank Prof. William Hersh for taking the time to be my Outside Member. In addition I would like to thank all the faculty members who I had throughout my course work (Professor Drueckhammer, Prof. Ojima, Prof. Parker, Prof Raleigh, and Prof. Wang); thank you for making organic chemistry an easier to understand subject. A special note of thanks to Prof. Robert Schneider, Prof Frank W. Fowler and Prof. Joseph W. Lauher, your commitment to education and particularly to students was truly inspiring. Thank you to the National Science Foundation (NSF) for the financial support for our research. A very special thank you to the entire main office staff for all your help throughout the years, Ms. Diane Godden, Ms. Katherine Hughes,

Mrs. Carol Brekke, Ms. Charmaine Yapchin and Ms. Lizandia Perez. Finally, I would like to especially thank my entire family Mom, Dad, my sister Nalini, Aunty Kamla, my cousins and grandma and my close friends for their love, support and encouragement. Thank you all for always believing in me. Thank you to everyone for all your help in making my career at Stony Brook a wonderful success. Most of all I must give God praise and thanks for giving me the opportunity, the understanding, the wisdom, and patience to pursue a career in the sciences. Thank you to everyone everywhere who made this effort possible.

Chapter 1

Chiral Ligands and Their Development

§1.1 Catalytic Asymmetric Synthesis

The origin of chirality was first observed in 1815 by Jean-Baptiste Biot and later determined to be of molecular origin by Louis Pasteur in 1848.[1] This single concept has become one of the most important ideas and principles in both organic chemistry and biochemistry. Undoubtedly, our understanding of the biological world would be vastly different without this notion. It has been well established since this time period that many biochemical processes can distinguish pairs of enantiomers. It was not, however, until the 20th century that the impact of chirality was really understood.

In the 1950s, Grünenthal Pharmaceuticals marketed the drug Thalidomide® (**Figure I-1**) as a sedative particularly for the treatment of nausea gravidarum.

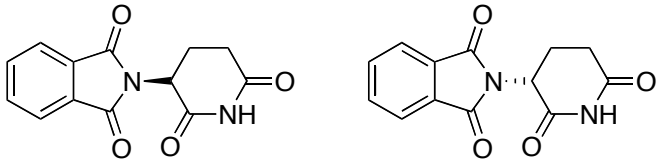

Figure I-1: (a) *(R)*-Thalidomide (b) (*S*)-Thalidomide

In 1961, a link between birth defects and thalidomide was established. After extensive studies, the teratogenic properties of thalidomide were attributed solely to the (*S*)-enantiomer, while clinical efficacy was due to the (*R*)-enantiomer.[2] It was evident that the stereochemical integrity of pharmaceutical agents is critical. Thus, synthesis of enantiopure drugs is vital. As organic synthesis has advanced since the thalidomide time period, the Food and Drug Administration in 1992 established the following policy:[3]

> ...Now that technological advances (large scale chiral separation procedures or asymmetric syntheses) permit production of many single enantiomers on a commercial scale, it is appropriate to consider what FDA's policy with respect to stereoisomeric mixtures should be…

As a result of this policy, enantiomeric drugs face stronger scrutiny than their achiral counterparts. TCI estimated that in 2000, 40% of all dosage-forms of drugs sold were

single-enantiomer forms.[4] This shift in policy has helped to foster the growth of asymmetric synthesis within organic chemistry. As a result, several chemical fields have emerged from this growth including catalytic asymmetric synthesis.

Catalytic asymmetric synthesis has become one of the most powerful synthetic methods for accessing chiral compounds in both, an efficient and an atom economical manner. This field afforded the 2001 Nobel Prize in Chemistry, shared by three field pioneers, Noyori, Knowles, "for their work on chirally catalysed hydrogenation reactions" and Sharpless "for his work on chirally catalysed oxidation reactions".[5]

The development of various types of chiral ligands has been the life-blood in sustaining and advancing asymmetric catalysis. Much of the early advancement of this field focused on the development of the chiral ligands for catalytic hydrogenation.[6] However, much of the last decade has seen a shift towards developing ligands for more complex catalytic reactions i.e. asymmetric allylic amination and asymmetric hydroformylation to name a few.[7]

§ 1.2 From Monodentate to Bidentate

The story of the chiral ligand development began to emerge in 1966 when Wilkinson and co-workers reported the use of $[RhCl(PPh_3)_3]$ (Wilkinson's Catalyst) for hydrogenation.[8] They demonstrated that triphenylphosphine could be used as a monodentate ligand in an active complex for rhodium catalyzed hydrogenation. This represented the first application of a phosphine ligand in a homogenous catalysis reaction. Additionally, Nozaki and co-workers identified that when a chiral-copper catalyst was employed for the cyclopropanation of styrene a modest amount of asymmetric induction could be obtained in 10 and 6% ee, respectively (**Scheme I-1**).[9] These findings further served as the "catalyst" for the development of new ligands for asymmetric hydrogenation.

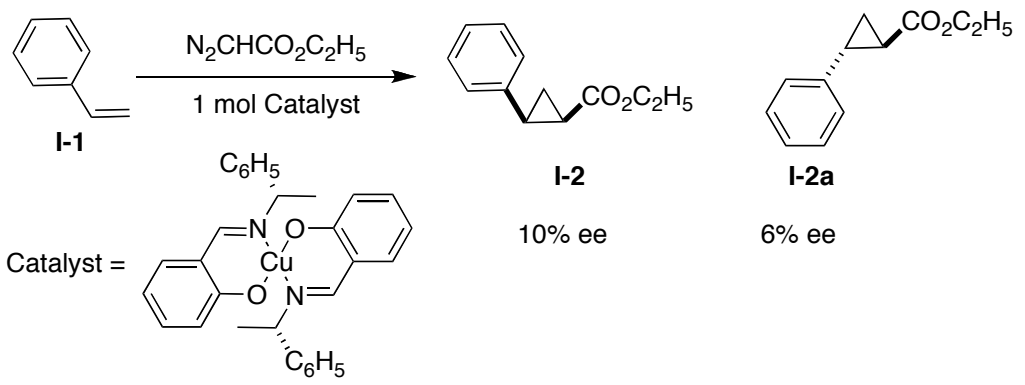

Scheme I-1: First reported asymmetric reaction by a metal-catalyst [9a]

In addition to these two developments, Mislow and Horner reported a method for the preparation of optically active phosphine.[10] With these reports the table was now set for the application of asymmetric homogenous catalysis with chiral phosphines. Horner and co-workers were the first to hypothesize that asymmetric induction could be afforded by chiral tertiary phosphines.[10]

In 1968, Knowles first reported the use of chiral monodentate phosphorus ligands in the Rh-catalyzed hydrogenation of α-phenylacrylic acid (**I-3**) with methylphenyl-*n*-propyl phosphine ligand **A (Scheme I-2)** which afforded (+)-hydratropic acid (**I-4**) in a modest 15% enantiomeric excess.[11]

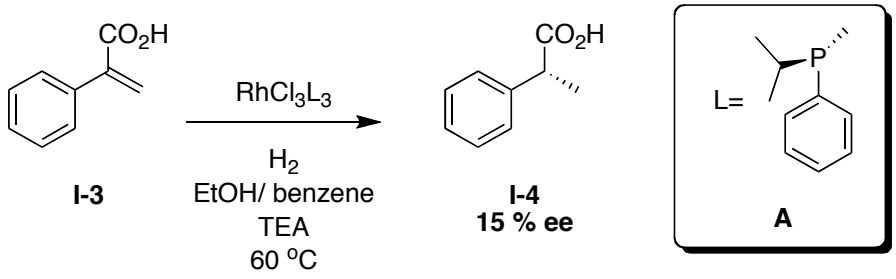

Scheme I-2: First example of Rh-catalyzed asymmetric hydrogenation with chiral monodentate phosphorus ligands [11]

Subsequent to this, Morrison *et al*. published the first example of asymmetric hydrogenation where the asymmetric center was derived from a carbon atom instead of the tertiary phosphorus atom (**Scheme I-3**) with the neomenthyldiphenylphosphine (**NMDPP)** ligand.[12] However, little was done to advance these ligand types, primarily due to the great success of the chiral phosphorus ligands later developed by Knowles.[6]

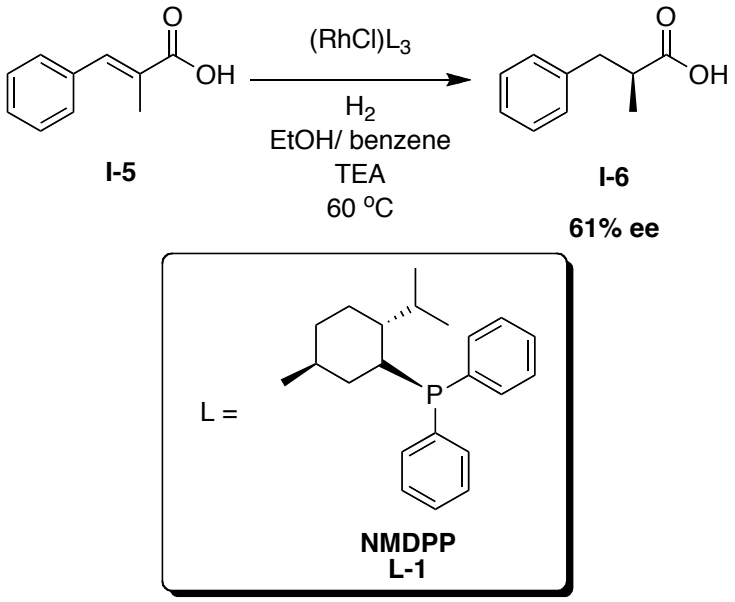

Scheme I-3: Hydrogenation with NMDPP (neomenthyldiphenylphosphine); the C-P Chiral Ligand [12]

Shortly after, Morrison, Knowles, and others unveiled several more efficacious ligands including **PAMP (*O*-anisylmethylphenylphosphine),** and **CAMP (*O*-anisylcyclohexylmethylphosphine)** affording an unprecedented 90% ee for the asymmetric hydrogenation (AH) of acylaminoacrylic acid **I-A** (**Scheme I-4**).[13]

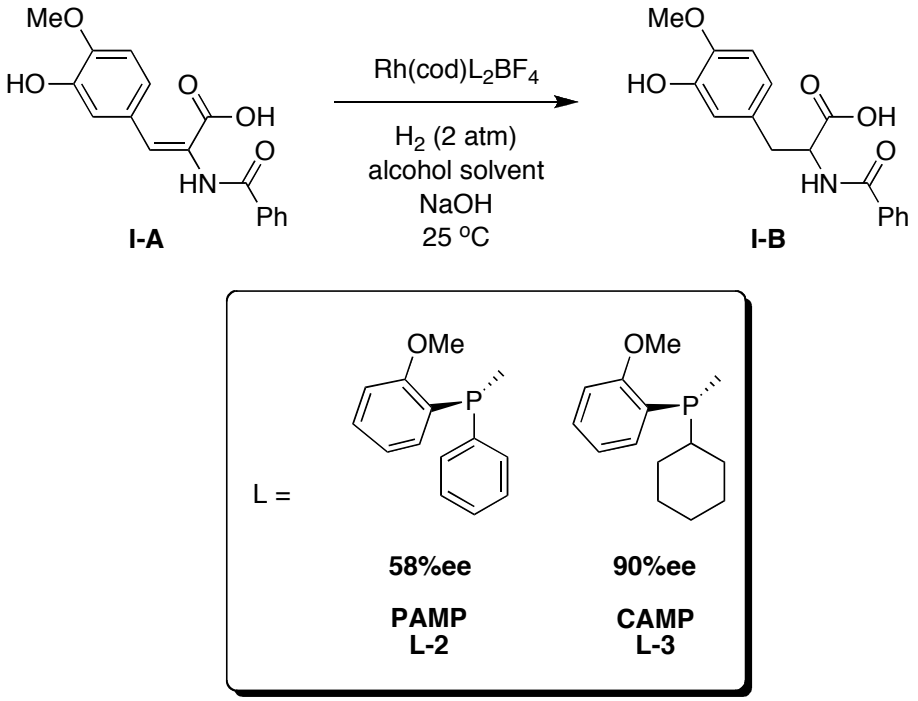

Scheme I- 4: PAMP, CAMP Ligands [13]

The **CAMP** ligand later became the first chiral ligand to be used in the commercial production of the anti-Parkinson's drug L-DOPA.[6]

In 1971, Kagan turned the commonly held idea that chirality at a single phosphorus atom is necessary for chiral induction on its head by introducing **DIOP** ((diphenylphosphino(dimethyl))dioxolane), (**Scheme I-5**) a bisphosphine joined by a chiral backbone, still affording 72% ee in the asymmetric hydrogenation of the α-acetoamidocinnamic (**I-C**) acid affording (*R*)-*N*-acetylphenylalanine (**I-D**) in 95% chemical yield.[14]

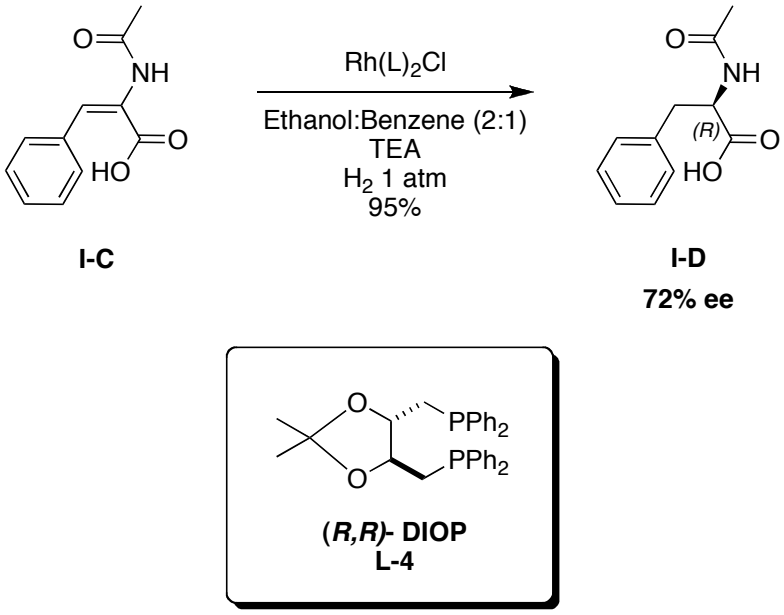

Scheme I- 5: Application of the DIOP ligand [14]

This ligand was particularly attractive because it could be easily synthesized from natural tartaric acid.[14a]

Following Kagan's development of the bidentate ligand **DIOP**, Knowles in 1977 unveiled his bidentate ligand **DiPAMP (**(*S*)-(2-methoxyphenyl)-[2-[(2-methoxyphenyl)-phenylphosphanyl]ethyl]-phenylphosphane) (**Figure I-2**), a dimer of the previous **PAMP** ligand, affording an unprecedented 95% ee for the hydrogenation of α-*N*-acylaminoacrylic acids.[15]

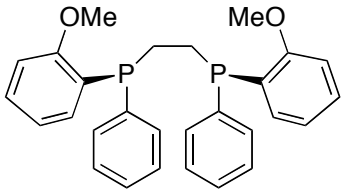

DiPAMP
L-32

Figure I-2: DiPAMP (*S*)-(2-methoxyphenyl)-[2-[(2-methoxyphenyl)-phenylphosphanyl]ethyl]-phenylphosphane Ligand

The discovery of these new bidentate type ligands allowed many novel related ligand types to be designed and synthesized. Thus the field proliferated with many novel bisphosphine ligands several of which are shown below in **Figure I-3**. Among these

early ligands, **Chiraphos** ((–)-(2*S*,3*S*)-Bis(diphenylphosphino)butane),[16] **BPPFA** ((*R*)-*N,N*-Dimethyl-1-[(*S*)-1′,2-bis(diphenylphosphino)ferrocenyl]ethylamine),[17] **BPPM** (2*S*,4*S*)-*N*-butoxycarbonyl-4-diphenlylphosphino-2-diphenylphosphinomethylpyrrolidine),[18] **CBD** (1,4-bis(diphenylphosphino)butane),[19] and **PNNP** ((*1S,2S*)-*N,N*′-Bis(diphenylphosphino)- 1,2-diphenylethylenediamine)[20] were among the most effective ligands for AH.

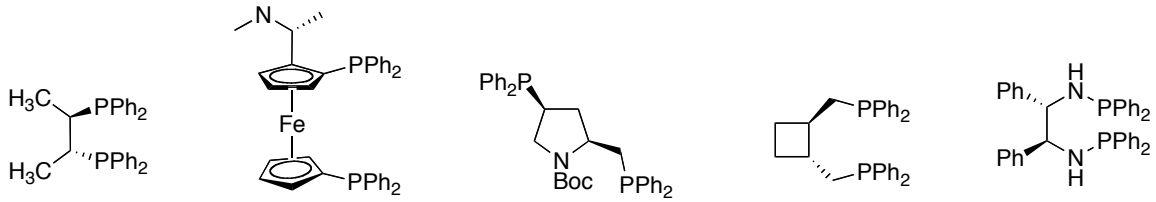

Chiraphos Bosnich L-5 | **BPPFA Kumada L-6** | **BPPM Achiwa L-7** | **CBD Rhone-Poulenc L-8** | **PNNP Giongo L-9**

Figure I-3: Early bidentate phosphorus ligands

Subsequent to the development of a chiral carbon-based phosphorus ligand Grubbs and DeVries extended the ligand types to include the atropisomeric system **NAPHOS (**2,2'-Bis((diphenylphosphino)methyl)-1,1'-binaphthyl)[21] (**Figure I-4**), with an asymmetric axis as opposed to a chiral center. The **NAPHOS** system, however, only afforded modest enantiomeric excesses.[21] Later in 1980, Noyori and co-workers published axially chiral **BINAP (**2,2'-bis(diphenylphosphino)-1,1'-binaphthyl)[22] (**Figure I-4**) that is arguably the most famous ligand to date. Although **NAPHOS** and **BINAP** differ only by a $-CH_2$ moiety, the efficacies of the two ligands are drastically different affording 56% and 100% ee, respectively for AH.[21-22]

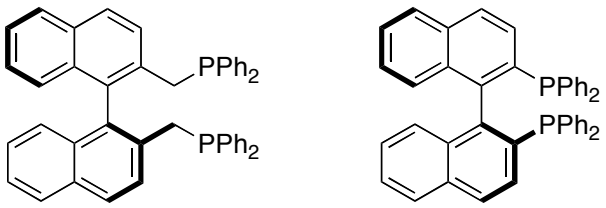

NAPHOS L-10 | **BINAP L-11**

Figure I-4: Atropisomeric bisphophine ligands

Derived from the great success of **BINAP** and other ligands, bidentate ligands continued to dominate the landscape. Although the bidentate diphosphine ligands have shown excellent efficacy in a variety of the asymmetric hydrogenation substrate applications, the diversity of the ligands were inherently limited by the connectivity with other systems, as functionalization of the napthyl system is quite arduous. Additionally, it was desirable to see asymmetric applications outside of hydrogenation. Logically, it was necessary to create a large number of ligand systems in order to expand to other reaction types. Thus, monodentate ligands systems were then extensively explored. [23]

§ 1.3 From Bidentate to Monodentate

During the past decade, chiral monodentate ligands began to re-emerge, as the dominant species. This is primarily due to the difficulty in synthesis of the diphosphine-based ligands, primarily in creating the phosphorus carbon bonds and limits afforded by structural diversity. Particular attention has been focused on the development of the monophosphite, monophosphonite and monophosphoramidite ligands (**Figure I-5**).[23b;c;24]

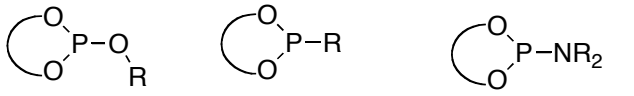

Phosphite **Phosphonite** **Phosphoramidite**

Figure I-5: Emerging monodenate phosphorus ligands

The re-birth of the monodentate ligands began in 1991 when Alexakis and co-workers published the first example of asymmetric conjugate addition of an organocuprate to 1,4-cyclohexenone using ligand **L-12** ((4*R*, 5*S*)-*N*,*N*-4-trimethyl-5-phenyl-1,3,2-dioxaphospholan-2-amine) derived from ephedrine and HMPT (hexamethylphosphorus triamide) (**Scheme I-6**), giving a modest 75% ee and 90% chemical yield under optimized conditions.[25] This finding demonstrated that monodentate ligands were indeed capable of inducing modest levels of asymmetric and were also

applicable to reactions other than asymmetric hydrogenation. Following Alexakis's successful application, a large number of chiral monodentate ligands have been synthesized and applied to various reaction types.[26]

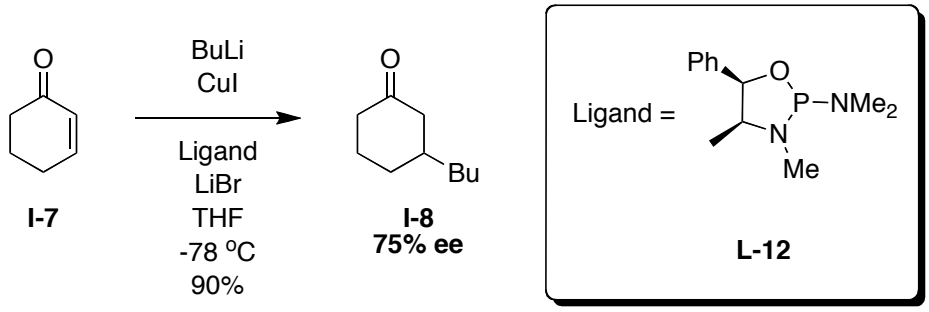

Scheme I-6: Early monodentate Ligand for 1,4-conjugate addition [25]

Alexakis later developed several novel ligand libraries of monodentate phosphonite-based ligands, which found excellent efficacy in asymmetric conjugate addition of diethyl zinc to cyclohexenone and other cyclic enone species. These ligands, **L-12,**[27] **TADDOL (L-13),** (*trans*-α, α'-(dimethyl-1,3-dioxolane-4,5-diyl)bis(diphenylmethanol)[28] **and BINOL (L-14)** (1,1'-binaphthalene-2,2'-diol),[29] afforded excellent enantiomeric excesses (**Figure I-6**) in various conjugate addition reactions. BINOL derivative **L-14A** demonstrated excellent enantiomeric excess in the conjugate addition of diethylzinc to linear nitroalkenes as shown in **Scheme I-7**.[30]

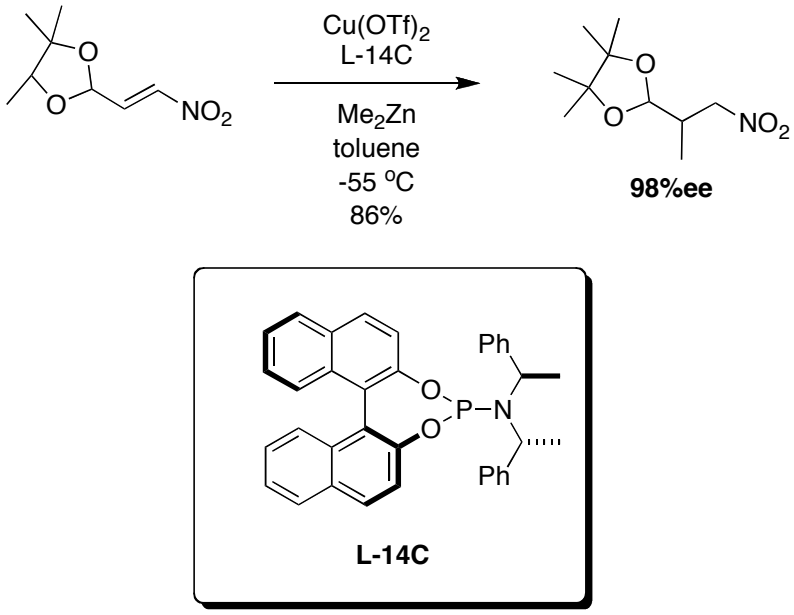

Scheme I-7: Addition of the dimethyl zinc to linear nitroalkenes [30]

In addition to the excellent enantiomeric excess achieved, these novel monodentate ligands were synthetically easy to access, being derived from either already chiral materials or racemic materials that can be easily resolved, thus making diversification promising.

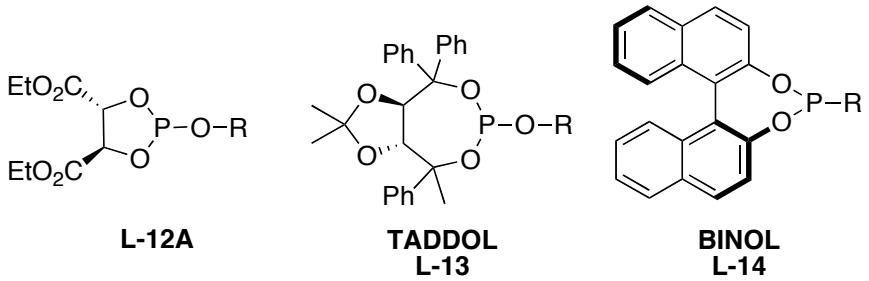

Figure I-6: Monodentate ligands developed by Alexakis

Likely stemming from the ease of access, Feringa and Alexakis further modified the monodentate phosphonite based ligands to develop a library of monodentate phosphoramidite ligands. In 1994, Feringa reported the application of **MonoPhos** ((*S*)-(−)-(3,5-Dioxa-4-phospha-cyclohepta[2,1-α:3,4-α′]di-naphthalen-4-yl)dimethylamine) (**Figure I-7**) to the copper triflate catalyzed 1,4-addition of diethyl zinc to chalcones and cyclohexenones achieving an impressive 90% ee.[31] Feringa also achieved moderate

enantioselectivities when using **TADDOL** based **L-15** for addition of diethyl zinc to cyclic eneones.[32]

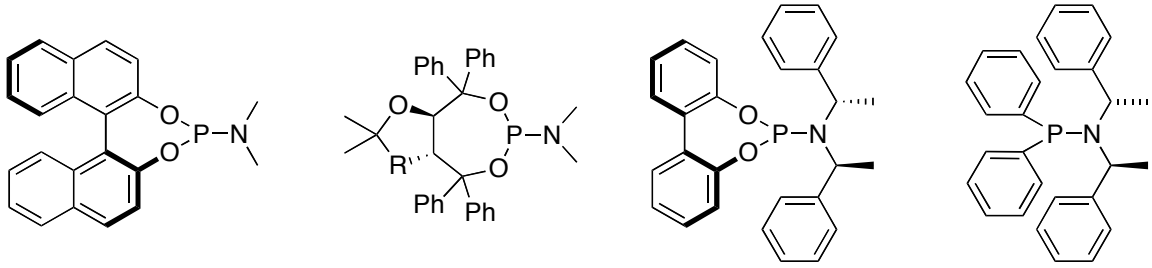

Figure I-7: Novel phosphoramidte ligands developed by Alexakis and Feringa

Alexakis *et al*. developed two atropisomeric ligands, **L-16** based stereoisomers obtained when achiral biphenol is reacted with a chiral amine and **SimplePhos (L-17)** **(**((diphenylphosphanyl)bis[(1*S*)-1-phenylethyl]amine), a phosphinamine type ligand.[33] Both systems afforded modest to excellent enantiomeric excess in conjugate addition type reactions (**Figure I-7**). [33]

The ever-increasing diversity and complexity of novel chiral phosphorus ligands demands new more sophisticated reactions to tackle. Asymmetric allylic alkylation is a powerful carbon-carbon or carbon-heteroatom bond-forming reaction that can afford new chiral carbon centers. The ligands for this reaction were developed along side of the early phosphorus-based ligands. **Table 1** depicts several novel ligands used in the asymmetric allylic alkylation and asymmetric conjugate addition reactions, demonstrating the structural diversity afforded by the monodentate ligand class.

Table I-1: Select phosphorus ligands

Allylic Alkylation Ligands:

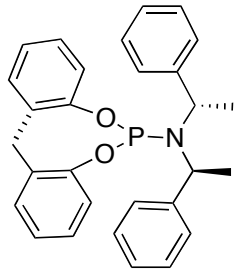

L-18

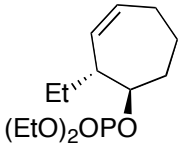

L-19

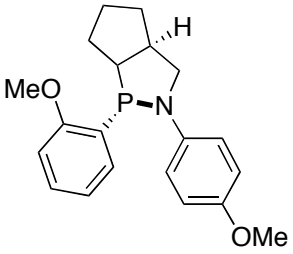

L-20

Asymmetric Conjugate Addition:

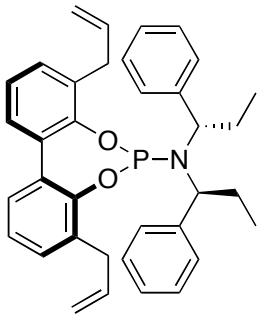

L-21

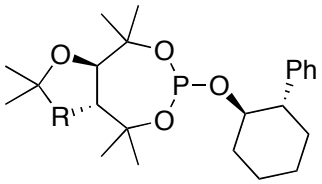

L-22

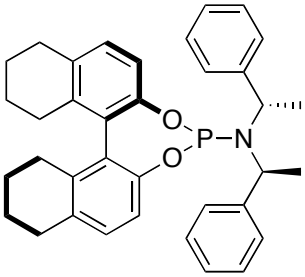

L-23

In addition to allylic alkylation, various monodentate ligands have been applied to asymmetric hydrogenation.[34] These various ligand types have also been applied to hydrovinylation,[35] hydroboration,[36] hydrosilylation,[37] hydroformylation,[38] allylic substitution,[39] and asymmetric intramolecular Heck reaction.[40]

Asymmetric allylic substitution is one of the most powerful asymmetric type reactions as it allows for both the regio- and stereoselective addition of a nucleophile to the π-allylic complex. This reaction has been applied in the synthesis of several important natural products.[41] Recently, Alexakis and co-workers published an iridium-catalyzed asymmetric allylic alkylation allowing access to chiral cyclopentanes from ω-ethylenic allylic substrates using the BINOL derivate **L-24** affording excellent selectivity toward the γ-isomer (**Scheme I-8**).[42]

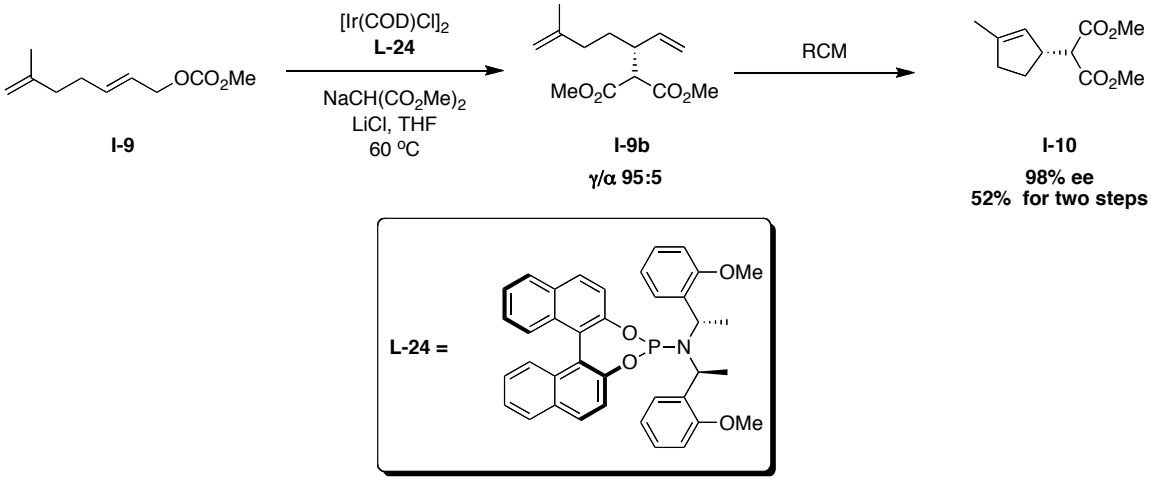

Scheme I-8: Iridium catalyzed asymmetric allylic alkylation [42]

In 2007, Pamies and Dieguez demonstrated that mixed phosphite-phosphoramidite D-xylose based ligand systems can be used in the Pd-catalyzed asymmetric allylic alkylation (**Scheme I-9**).[43]

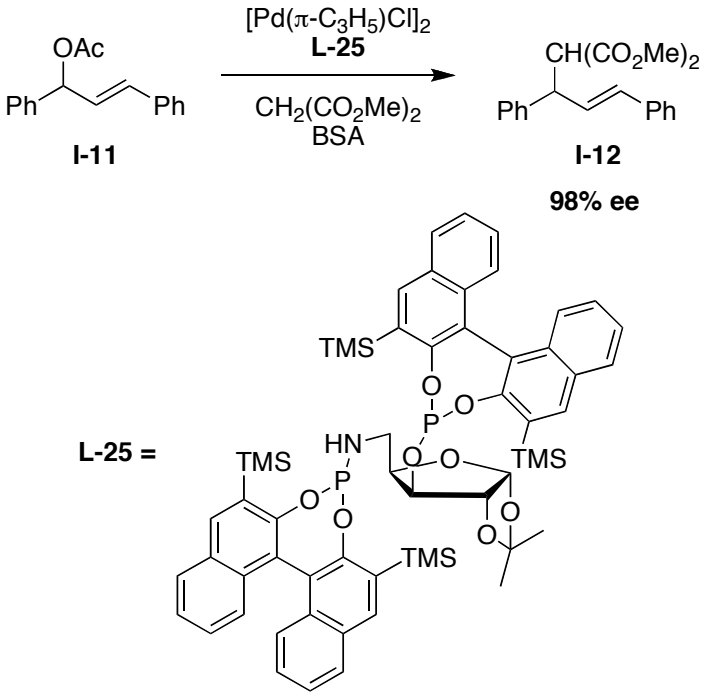

Scheme I-9: First mixed-ligand for asymmetric allylic alkylation [43]

§ 1.4 Novel Biphenol-Based Chiral Ligands and Applications

Recently, our laboratory proposed a new class of monodentate phosphorus ligands based on the atropisomeric biphenol backbone as shown in **Figure I-8**.[34a]

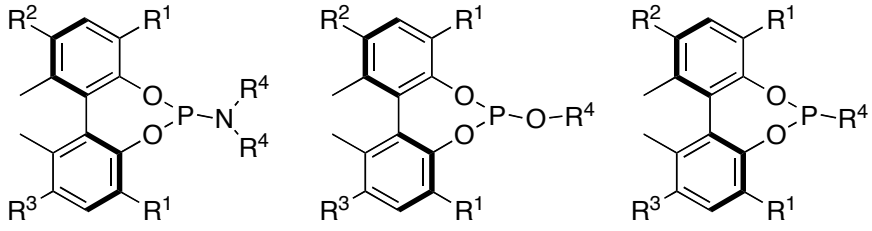

Figure I-8: Novel Biphenol-Based Chiral Ligand

The principal feature of these ligands lies in the four easily modifiable positions (R groups, **Figure I-8**), making them fine-tunable to each reaction type and substrate kind. The synthesis and development of fine-tunable ligand types is highly desirable, as no single so-called, "super-ligand" has been unveiled. Additionally, the development of a "super-ligand" is impractical because of the high substrate and reaction dependency previously observed.[38] Thus, easily tailored ligands are highly desirable in the world of asymmetric catalysis. Furthermore, as a result of the 6,6`-dimethyl groups these ligands are considerably more configurationally stable as compared to the corresponding chiral BINOLs.[34a]

We have successfully installed a wide-range of functional groups to the biphenol-core (at the R^1 position) structure including, bromo, methyl, chloromethyl, hydroxymethyl, aryl, and *t*-butyl.[34a;38;44] In addition to modifications at the biphenol core, modulations at the phosphorus center can afford phosphoramidite, phosphite, and phosphonite species, allowing a large library of biphenol-based ligands to be quickly synthesized and screened against a variety of reactions. This combinatorial approach to ligand screening allows for the application to a number of different reaction types.

In 2003,[34a] we applied our first series of biphenol-based phosphite ligands to the asymmetric hydrogenation of dimethyl itaconate (**I-13**) affording the (*R*)-dimethyl

methylsuccinate (**Scheme I-10**). Interestingly, in the absence of the *t*-butyl group of **L-26,** stereochemical control is completely lost, affording a nominal 2.7% ee. It is also noteworthy to mention that in absence of the secondary chiral center on the phosphorus atom (i.e. Whitesell's auxiliary) stereochemical control is also poor. The ligand system which showed the greatest efficacy in this reaction is **L-26** where the 3,3'-position is *t*-butyl and the phosphite center is derived from Whitesell's chiral auxiliary, affording the dimethyl methylsuccinate in 99.6% ee.[45]

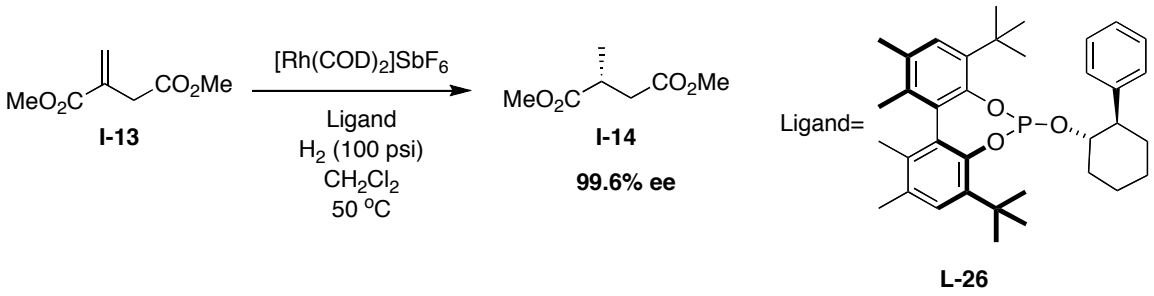

Scheme I-10: Hydrogenation of dimethyl itaconate [34a]

Several other phosphite-ligands bearing menthol derivatives at the phosphite position have also demonstrated excellent enantiomeric excesses.[34a]

Following the success of the asymmetric hydrogenation using the phosphite ligand system, the phosphoramidite types were then applied to asymmetric hydroformylation of allyl cyanide (**Scheme I-11**).[38] Once again the ligand with 3,3'-*t*-butyl groups was shown to be most effective affording 80% ee in 96:4 *branch:linear* (*b:l*) selectivity. Furthermore, no hydrogenated product was observed for these conditions.

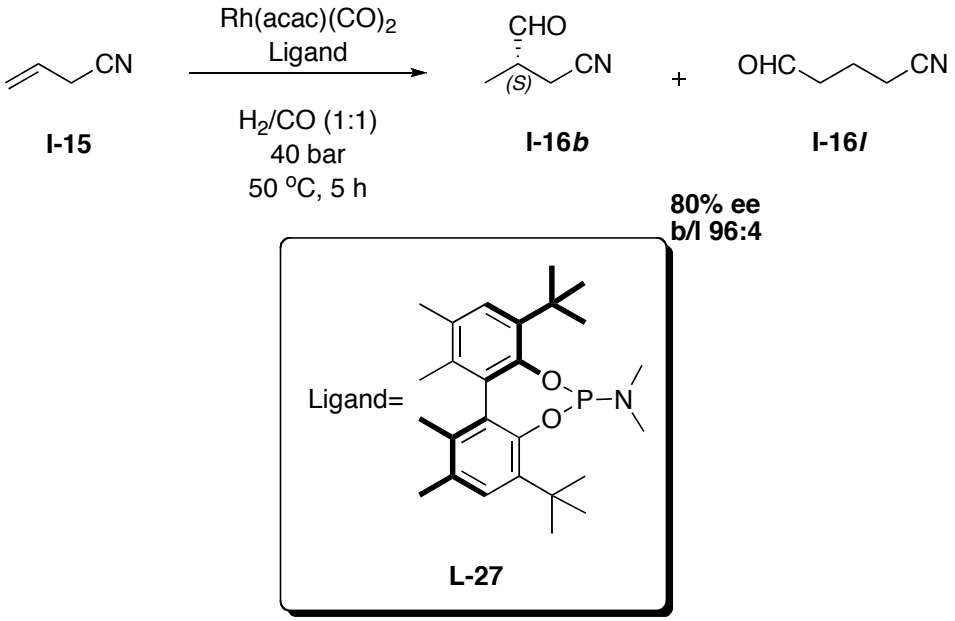

Scheme I-11: Asymmetric hydroformylation of allyl cyanide [38]

The asymmetric results observed for the biphenol-based ligands are dramatically superior to their BINOL-counterparts which afforded only 18% ee with a near 3:1 *b:l* ratio.[46]

The same series of phosphoramidite ligands were also tested for efficacy in the asymmetric conjugate addition of diethylzinc to cyclohexeneone, cycloheptеneone and cyclopentenone (**Scheme I-12**). The phosphoramidite ligands bearing the BIPEA (bisphenylethylamine) moiety showed the greatest efficacy in both six and seven-membered ring systems affording 98.4 and 97.5% ee, respectively.[38] However, only modest enantioselectivity was afforded in the case of the five-membered ring system. The same ligand **L-28** also demonstrated excellent efficacy, with a 94% ee in the conjugate addition of diethylzinc to α, β-unsaturated nitro-compounds.

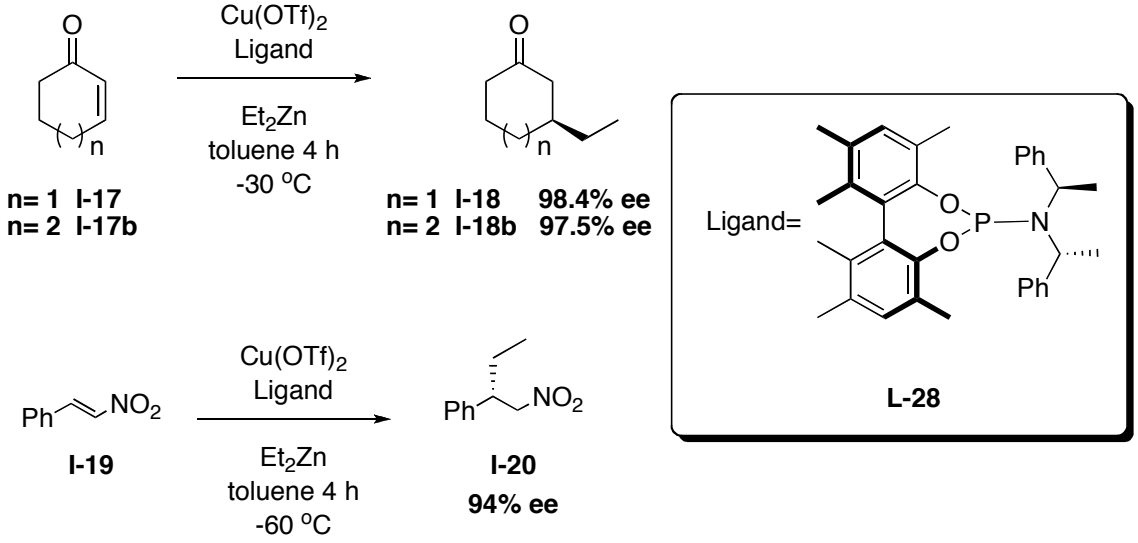

Scheme I-12: Asymmetric conjugate addition of diethyl zinc [38]

Following the many reports of BINOL-based (*vide supra*) ligands in asymmetric allylic alkylation, the Ojima laboratory successfully applied their novel phosphoramidite biphenol-based ligands to two asymmetric allylic substitution reactions. The first example reported involved the key step in the total synthesis of the alkaloid γ-lycorane, which following the key allylic alkylation step, was obtained in >99% enantiomeric excess (**Scheme I-13**).[44a;b]

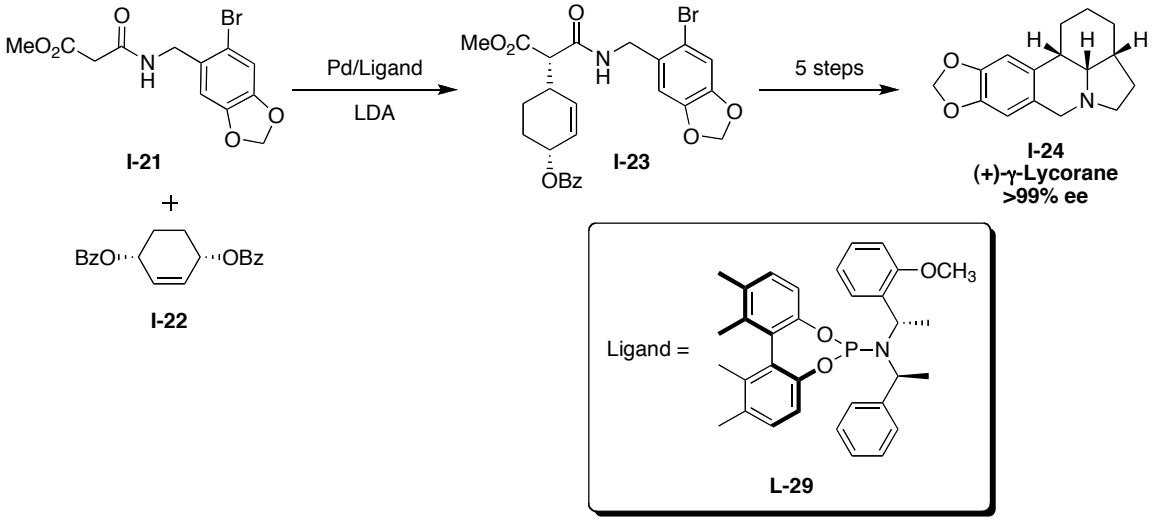

Scheme I-13: Asymmetric synthesis of γ-lycorane [44a;b]

Later in 2007, the phosphoramidite ligands were applied to the intramolecular allylic amination step toward the synthesis of the tetrahydroisoquinoline core (**Scheme I-14**).[44d] It was noted from this endeavor that both the nucleophile substituents and the allylic leaving groups played a critical role in the stereoselectivity of this reaction. In the case of allylic leaving groups, bulkier substituents afforded higher enantioselectivity when R_1 was tosyl (**I-25a)** (*t*-buty at R affording 77% ee). Higher enantioselectivity was achieved when the TFA amide (**I-25a)** was employed in place of the tosylamide. The highest enantiomeric excess, 95% ee, was obtained when R was the TFA amide and R^1 was the phenyl carbonate.

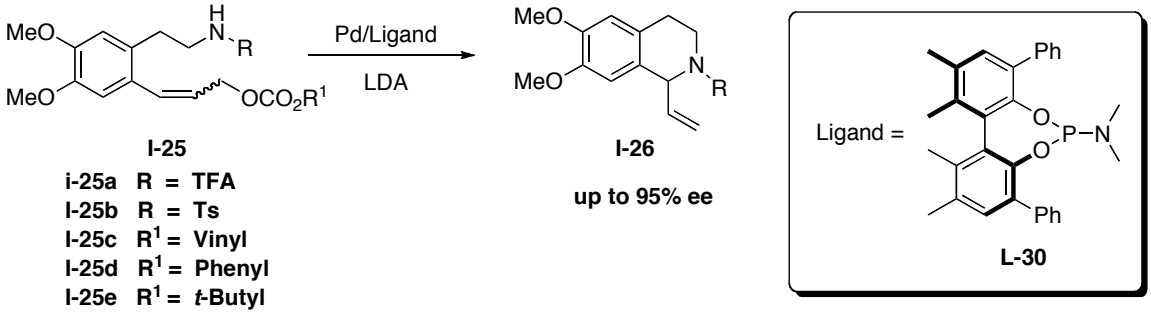

I-25

i-25a R = TFA
I-25b R = Ts
I-25c R^1 = Vinyl
I-25d R^1 = Phenyl
I-25e R^1 = *t*-Butyl

I-26

up to 95% ee

L-30

Scheme I-14: Asymmetric synthesis of the tetrahydroisoquinoline core.[44d]

Thus, our laboratory has demonstrated the efficacy of our biphenol-based ligands in the application to various metal-catalyzed reactions. We continue to expand on the applications of our ligand system to various different reaction types and substrates. In addition, we continue to design and screen our ligands for various different applications.

§ 1.5 Synthesis of Enantiopure Biphenols

In efforts to promote our asymmetric catalysis research program, we continue to synthesize enantiopure biphenol derivatives in order to develop novel ligands for various asymmetric metal-catalyzed reactions. Herein the synthesis of axially chiral biphenols (**Figure I-9**) is discussed.

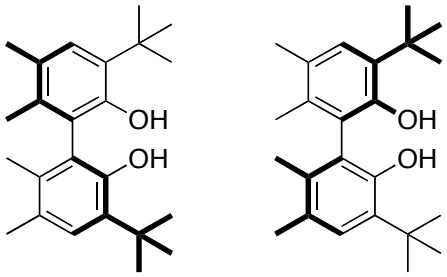

(*S*) I-27 (*R*) I-27

Figure I-9: Axially Chiral Enantiopure Biphenol

The enantiopure biphenol depicted in **Figure I-9** can readily be synthesized using a known literature procedure.[47] The core biphenol system was employed by Schrock and co-workers in efforts toward a molybdenum catalyst for enantioselective ring closing metathesis as shown in **Scheme I-15** starting with racemic compound **I-28**.

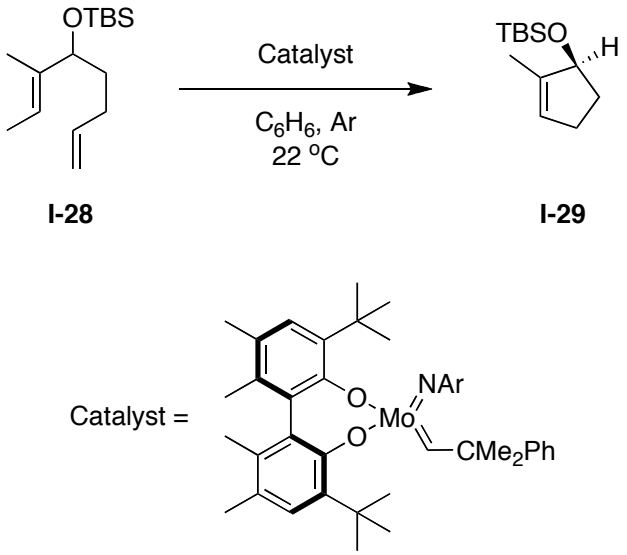

I-28 **I-29**

Scheme I-15: Biphenol-based molybdenum catalyst in asymmetric ring closing metathesis[47a]

The racemic form of compound **I-27** serves as the principal building block for all the biphenol ligands developed.

§ 1.5.1 Results and Discussion:

The synthesis of the enantiopure biphenol-based monodentate ligands began with the Friedel-Crafts alkylation of the 2,3-dimethylphenol with isobutene in the presence of a catalytic amount of sulfuric acid to afford compound **I-31**, which was directly subjected to oxidative coupling with Jones' Reagent to afford racemic biphenol **I-32** in 68% isolated yield over two steps (**Scheme I-16**).

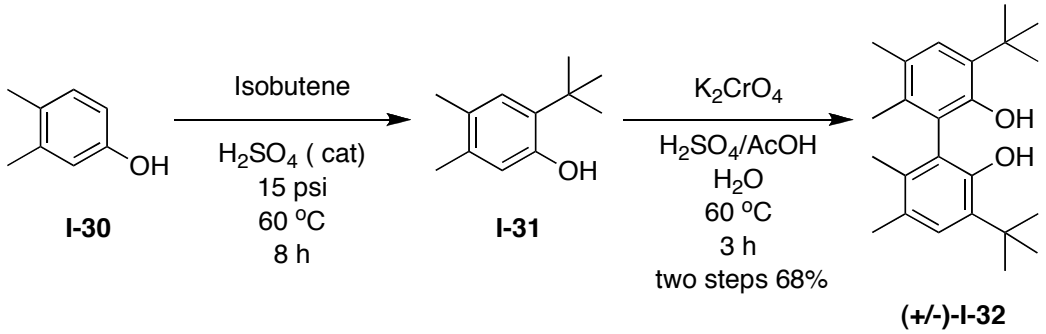

Scheme I-16: Synthesis of the racemic biphenol I-32

The chemo-resolution of the racemic biphenol ((**+/-)-I-32**) began with coupling optically pure (-)-menthol (**I-30**) to the racemic biphenol affording the intermediate phosphite that was immediately oxidized to the phosphate in the presence of hydrogen peroxide (**Scheme I-17**). The optically pure menthol was first converted to the phosphodichloride (**I-34**), directly reacted with racemic biphenol, and immediately subjected to oxidation with hydrogen peroxide affording diastereomeric-biphenol **I-35** as shown in **Scheme I-17**.

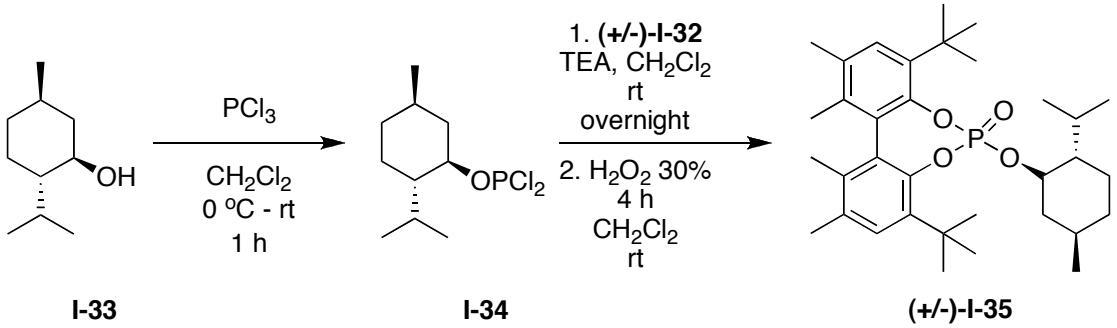

Scheme I-17: Synthesis of the Diastereoisomer

The diastereomeric mixture was resolved by consecutive crystallizations. The first crystallization, from acetic acid afforded diastereomerically enriched (***S***)-**I-35 (Scheme I-17**). The resultant mother liquor containing enriched (***R***) was then crystallized from methanol to afford the diastereomerically pure ***(R)*.** The enriched sets were then recrystallized from the same solvents, respectively to afford the diastereomerically pure compounds **I-35** (**Scheme I-18**), which were confirmed by ^{31}P NMR.

The resolved diastereoisomers were then reduced with commercial reducing agent, Red-Al® to afford the enantiopure axially chiral biphenol in good yield as shown in **Scheme I-18** to afford the optically pure 3,3`-di-*tert*-butyl-5,5`,6.6`-hexamethylbiphenyl-2,2`-diol.

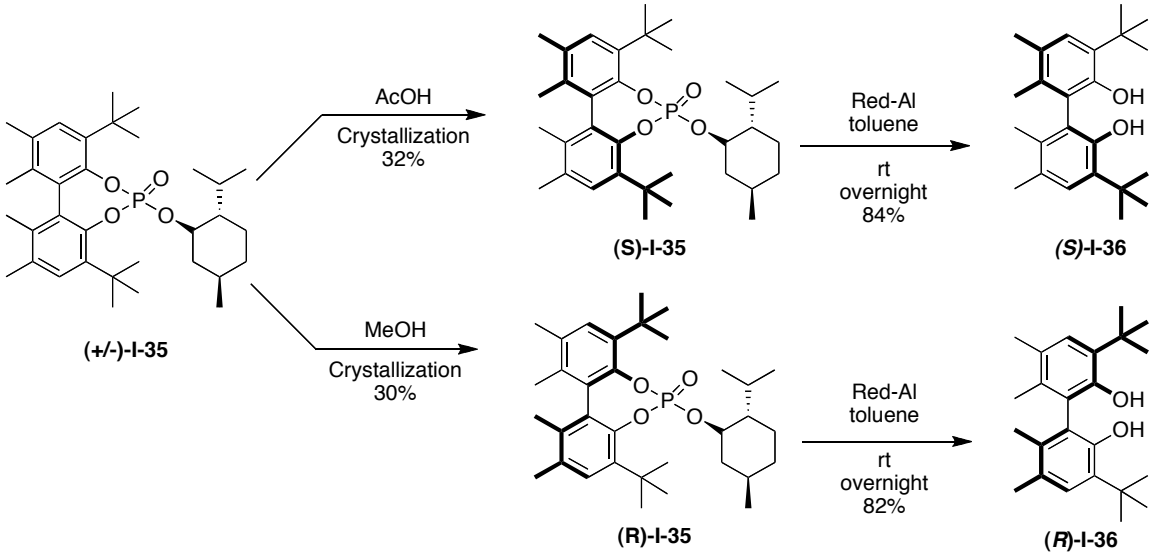

Scheme I-18: Resolution of diastereoisomers I-35 and phosphate reduction

One of the salient features of the ligand system is the modification that can be afforded at the 3,3'-position. This modification requires the removal of the *t*-butyl for the proper introduction of the various functional groups. The treatment of either biphenol stereoisomer with $AlCl_3$ in a toluene-nitromethane (1:1) mixture affords a Friedel-Crafts alkyl transfer from the biphenol to the toluene affording compounds **I-37** in 89% and 92% yield for the (*S*) and (*R*) enantiomers, respectively **(Scheme I- 19)**.

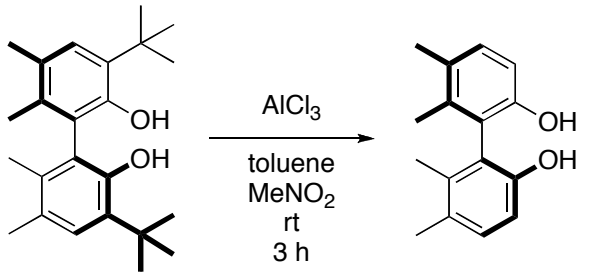

(*S*)- I-36 (*S*)- I-37 89%

(*R*)- I-36 (*R*)- I-37 92%

Scheme I-19: Friedel-Crafts Alkyl-transfer

From this key building-block a vast library of the novel biphenol-based ligands can be synthesized, limited only by availability of the desired modifying groups at either the 3,3`-position or the phosphorus atom.

A library of functionalized phosphoramidite ligands was then synthesized from building block **I-37**, and the final diverse ligands are as shown in **Figure I-10.**

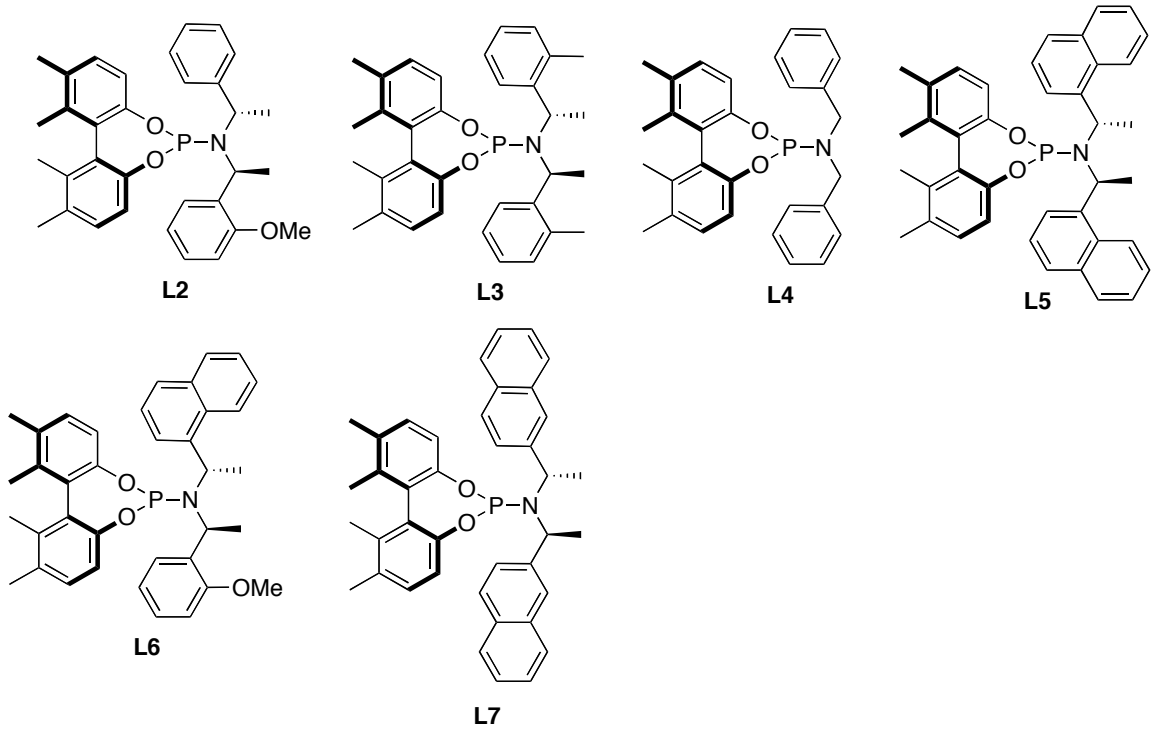

Figure I-10: Library of Phosphoramidite Ligands

The phosphoramidite ligands were synthesized *via* formation of the phosphorchloridite followed by treatment with a desired amine as seen the general form in **Scheme I-20**.

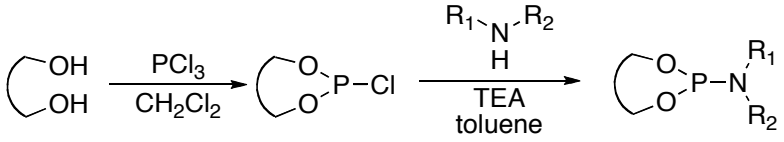

Scheme I-20: Generalized synthesis of the phosphoramidite ligands

The various amines were either purchased from commercial sources or synthesized *via* reductive amination, as per Alexakis, which affords a mixture of the diastereomers in a 9:1 ratio.[48] Amines used here were taken from our laboratory stockpile previously synthesized. The synthesis of biphenylethylamine ligand (**I-40**) began with formation of the phosphochloridite (**I-38**) intermediate, and after solvent removal the product is immediately reacted with the amine to afford the phosphoramidite ligand **I-40** in 62% isolated yield as shown in **Scheme I-21**.

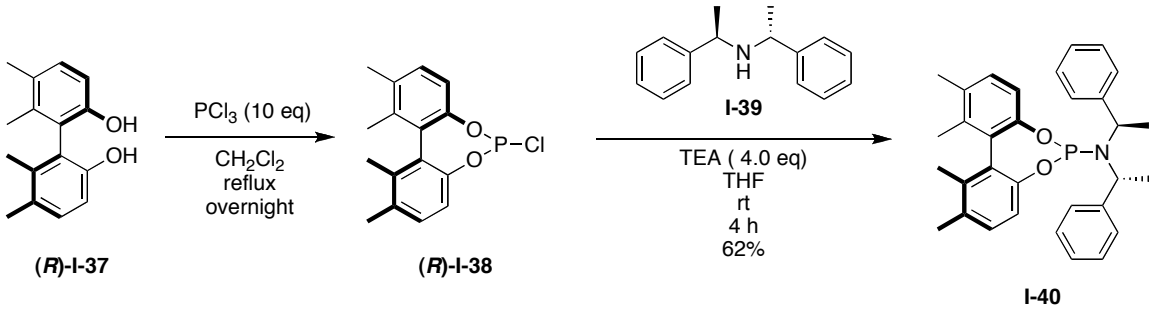

Scheme I-21: Synthesis of Phosphoramidite ligand I-40

The ligands shown in **Figure I-11** were also synthesized in a similar manner as shown in **Scheme I-21** with comparable yield.

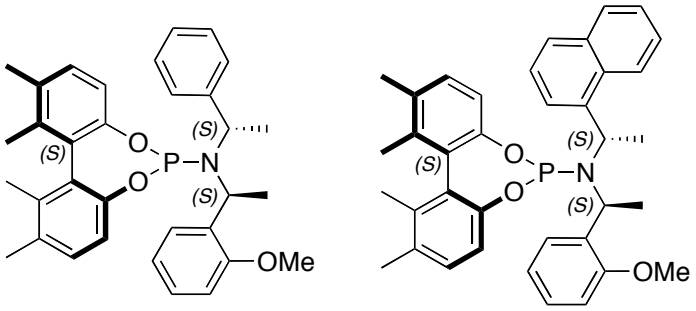

I-41
60%

I-42
45%

Figure I-11: Synthesized Phosphoramidite Ligands

The remaining ligands were screened from a house stockpile previously synthesized.

§ 1.6 Experimental Methods:

General Information:

All chemicals were obtained from either Sigma-Aldrich or Acros Organics and used as is unless otherwise noted. All reactions were performed under Schlenk conditions with oven-dried glassware unless otherwise noted. Anhydrous methylene chloride, toluene, tetrahydrofuran, and ethyl ether were degassed, kept under nitrogen and were dried using the PURESOLV system (Innovative Technologies, Newport, MA). Anhydrous dimethoxyethane (DME) was obtained from Acros Organics and used as is. Anhydrous methanol was obtained by distillation over calcium hydride. ^{1}H, ^{13}C and ^{31}P NMR data were obtained using either 300 MHz Varian Gemni 2300 (75 MHz ^{13}C, 121 MHz ^{31}P) spectrometer or the 400 MHz Varian INOVA 400 (100 MHz ^{13}C, 162 MHz ^{31}P) spectrometer in $CDCl_3$ as a solvent unless otherwise noted. Chemical shifts (δ) are reported in ppm and standardized with solvent as internal standard based on literature reported values.[49] Melting points were measured on Thomas Hoover Capillary melting point apparatus and are uncorrected. GC/MS was performed on Agilent 6890 GC/ 5973 Mass selective detector with electron ionization. LC/MS was complete using FIA (flow-injection analysis) using Agilent 1100 LS-MSD electrospray ionization (ESI) single quadrupole mass spectrometer. Ligands depicted in Figure I-10 we obtained from a stockpile library.

2-*tert*-Butyl-4,5-dimethylphenol (I-31):[47a]

3,4-Dimethylphenol (81.67 g, 66.8 mmol) was placed into 300-mL autoclave with a glass liner equipped with a stirring bar. Concentrated sulfuric acid (1 mL) was added dropwise to the solid. The autoclave was then pressurized with isobutene (20 psi) and heated to 80 ^{o}C with stirring for 8 h. The autoclaved was then cooled and carefully vented, after which the contents were analyzed by GC-MS and showed no remaining starting material. The resulting crude deep brown oil was used directly in the next step without any purification.

3,3`-Di-*tert*-butyl-5,5`,6,6`-tetramethyl-1-1`-biphenyl-2,2`-diol (+/- I-32): [47a]

Jones reagent was freshly prepared from potassium dichromate (60 g, 20.4 mmol) dissolved in concentrated sulfuric acid (120 mL) and water (44 mL). The hot solution was carefully added over a period of 15 min to a stirred solution of acetic acid (650 mL) and **I-31**. The solution of the acid was added slowly enough to maintain a reaction temperature below 60 ^{o}C. Upon addition of Jones' Reagent an off-white precipitate was quickly formed and the solution began to change from clear orange to cloudy green. After the complete addition of the Jones' reagent the mixture was stirred for one hour slowly cooling to room temperature. The resultant mixture was filtered on a Buchner funnel and washed with water, followed by cold methanol. After filtration, the solid is collected and dried under vacuum to afford the desired product **(+/-)-I-32** as a white solid (67.4 g, 58% yield): ^{1}H NMR (300 MHz, $CDCl_3$) δ 1.39 (s, 18H), 1.80 (s, 6H), 2.26 (s, 6H), 4.79 (s, 2H), 7.12 (s, 2H); ^{13}C (100 MHz, $CDCl_3$) δ 15.9, 20.0, 29.5, 34.7, 120.9, 108.0, 128.0, 128.7, 133.3, 134.1, 150.3. All data were accordance with literature reported values.[47a]

Preparation of Phosphate (I-35): [34a]

A solution of (-)-menthol (30.0 g, 19.2 mmol) in dichloromethane was slowly added to a stirred solution of phosphorous trichloride (32.13 g, 23.0 mmol) in 100 mL of dichloromethane at 0 ^{o}C. After the addition, the ice-bath was removed and solution was slowly warmed to ambient temperature over a one-hour period. The solvent and phosphorous trichloride was removed *in vacuo*. The remaining oily residue was re-dissolved in dichloromethane (208 mL) and a mixture of triethylamine (58.28 g, 57.6 mmol) and the biphenol **(-/+) I-32** in dichloromethane was added over 30 min. After stirring at room temperature for 3 h, the white solid was filtered off and filterate was cooled to 0 ^{o}C. A 35% w/w solution of hydrogen peroxide was carefully added with stirring. The reaction mixture was then further stirred for 4 h while slowly warming to room temperature. The biphasic mixture was separated and the organic layer was washed with water and brine. The organic phase was dried over $MgSO_4$, filtered and the solvent evaporated to afford crude mixture of diastereoisomers. The diastereomeric mixture was

recrystallized from hot acetic acid to afford (***S***)-**I-35** as a solid white needle crystals (32% yield, 32.80 g): mp 162-165; ^{31}P NMR (121.5 MHz) δ -4.46 (99% dr). All values are consistent with literature.[34a] The resultant mother liquor from the first crystallization was evaporated and recrystallized from hot methanol to afford **(*R*)-I-35** as white solid (31.20 g, 30% yield): mp 168-170 ^{o}C; ^{31}P NMR (121.5 MHz, $CDCl_3$) δ -4.93 (99% dr). All values are consistent with literature. [34a]

(*S*)-3,3'-Di-*tert*-butyl-5,5',6,6'-tetramethylbiphenyl-2,2'-diol ((*S*)-I-36): [34a]

The resolved ***(S)*-I-35** (32.78 g, 60.6 mmol) was dissolved in toluene (300 mL) in a two-necked flask equipped with a pressure equalizing dropping funnel and cooled to 0 ^{o}C. Red-Al® [sodium bis(2-methoxyethoxy)aluminum hydride)] was transferred into the addition funnel and then added drop-wise to the phosphate solution. The reaction mixture was stirred overnight and quenched with water (50 mL) followed by bleach (5% w/v) (50 mL). The two layers were allowed to separate and organic phase was collected and washed with bleach followed by brine. The organic phase was then dried over $MgSO_4$ filtered and evaporated to afford a white solid with a minty odor. The solid was then successively washed and filtered on Buchner funnel with ice cold methanol until the minty odor disappeared, affording compound **(*S*)-I-36** as a fluffy white solid (17.58 g, 82% yield): ^{1}H NMR (300 MHz, $CDCl_3$) δ 1.38 (s, 18H), 1.80 (s, 6H), 2.24 (s, 6H), 4.79 (s, 2H), 7.12 (s, 2H); ^{13}C (100 MHz, $CDCl_3$): δ 16.4, 20.5, 30.2, 35.2, 121.6, 127.7, 134.1, 134.6, 151.2. All values are consistent with literature.[34a]

(*R*)-3,3'-Di-*tert*-butyl-5,5',6,6'-tetramethylbiphenyl-2,2'-diol ((*R*)-I-36): [34a]

Same procedure as **(*S*)-II**. **(*R*)-I-36** was obtained as a fluffy white solid (16.90 g, 84% yield): ^{1}H NMR (300 MHz, $CDCl_3$) δ 1.38 (s, 18H), 1.80 (s, 6H), 2.24 (s, 6H), 4.79 (s, 2H), 7.12 (s, 2H); ^{13}C (100 MHz, $CDCl_3$): δ 16.4, 20.5, 30.2, 35.2, 121.6, 127.7, 134.1, 134.6, 151.2. All values are consistent with literature. [34a]

(*S*)-5,5',6,6'-Tetramethylbiphenyl-2,2'-diol ((*S*)-I-37): [34a]

A solution of $AlCl_3$ (4.202 g, 31.52 mmol), in a mixture of 25 mL of toluene and nitromethane (33 mL) was added *via* cannula to a solution of **(*S*)-I-36** (7.00 g, 19.7

mmol) in toluene (79 mL) at 0 ^{o}C over a 30 minute period. The reaction mixture was stirred at 0 ^{o}C for 30 min and then slowly warmed to room temperature over a 20 minute period. The mixture was quenched with water. The organic layer was separated and the aqueous layer was extracted with ether (100 mL x 3). The combined organic layers were washed with brine and dried over $MgSO_4$, filtered and solvent evaporated. The product was recrystallized from a mixture of hexanes and dichloromethane (5:1) to afford **(*S*)-I-37** as a white solid (4.24 g, 89% yield): ^{1}H NMR (300 MHz, $CDCl_3$) δ 1.90 (s, 6H), 2.26 (s, 6H), 4.52 (s, 2H), 6.82 (s, 2H); ^{13}C (100 MHz, $CDCl_3$) δ 16.5, 20.0, 30.2, 112.8, 120.4, 129.4, 131.5, 137.1, 152.0. All values are consistent with literature. [34a]

(*R*)-5,5',6,6'-Tetramethylbiphenyl-2,2'-diol ((*R*)-I-37): [34a]

The product was recrystallized from a mixture of hexanes and dichloromethane (5:1) to afford **(*R*)-I-37** as white solid (4.54 g, 92% yield): ^{1}H NMR (300 MHz, $CDCl_3$) δ 1.90 (s, 6H), 2.26 (s, 6H), 4.52 (s, 2H), 6.82 (s, 2H); ^{13}C (100 MHz, $CDCl_3$) δ 16.5, 20.0, 30.2, 112.8, 120.4, 129.4, 131.5, 137.1, 152.0. All values are consistent with literature. [34a]

General Procedure for Phosphoramidite Synthesis

Phosphorus trichloride (1.2 eq) was added dropwise to TEA (4.0 eq) at 0 ^{o}C under a nitrogen atmosphere. To this mixture was added a solution of the amine (10 mmol) in DCM (2 mL/mmol). The mixture was stirred at room temperature and monitored by phosphorus NMR until one phosphoramidite peak was observed. The solvent and excess phosphorus trichloride was removed *in vacuo.* The mixture was then cooled once again to 0 ^{o}C and a solution of the biphenol dissolved in THF was added dropwise. The resultant mixture was stirred overnight at room temperature. Following the overnight stirring, ether was added to mixture, which was then filtered over silica gel. The resultant solution was then concentrated *in vacuo.* The crude material was purified by column chromatography on silica gel with hexanes-ethyl acetate as eluent to afford the desired products given below.

***O,O'*-(*R*)-(5,5',6,6'-Tetramethylbiphenyl-2,2'-diyl) -*N,N*-bis[(*R,R*)-1-phenylethyl] phosphoramidite (I-40):**[34a]

white solid (465 mg, 71% yield): mp 58-61 ^{o}C (lit [44a] mp 62-63 ^{o}C) $[\alpha]^{D}_{22}$ -174.2 ($CHCl_3$,

c 0.52): ^{1}H-NMR (300 MHz, $CDCl_3$) δ 1.71 (d, *J*= 7.2 Hz, 6H), 2.03 (s, 3H), 2.08 (s, 3H), 2.35 (s, 3H), 4.40-4.46 (m, 2H), 6.84-7.28 (m, 14H),. All data are consistent with literature values. [44a]

_O,O'_-(_S_)-(5,5',6,6'-Tetramethylbiphenyl-2,2'-diyl)-_N,N_-[(_S_)-1-(napthalen-2-yl)ethyl]-[(_S_)-1-(2-methoxyphenyl)ethyl]phosphoramidite (L7):[44a]

white solid: mp 91-93 °C (lit [44a] mp 92-94 ^{o}C); $[\alpha]^{22}_{D}$ + 95.7 (*c* 1.21, $CHCl_3$); ^{1}H-NMR (400 MHz, CD_2Cl_2) δ 1.4 (d, J= 7.2 Hz, 3H), 1.60 (d, J= 7.2 Hz, 3H), 1.98 (s, 6H), 2.12 (s, 3H), 2.32 (s, 3H), 3.58 (s, 3H), 3.75 (m, 1H), 5.37 (m, 1H), 6.49-6.67 (m, 4H), 6.89 (td, J= 0.8, 7.2 Hz, 1H), 7.10 (d, J= 8 Hz, 1H), 7.22 (d, J= 8 Hz, 1H), 7.29 (t, J= 8 Hz, 1H), 7.37 (m, 2H), 7.58 (d, J= 8.4 Hz, 1H), 7.66 (d, J= 7.6 Hz, 1H), 7.71 (m, 1H), 7.81 (m, 1H); ^{13}C-NMR (100 MHz, CD_2Cl_2) δ 17.6, 17.8, 20.3, 20.6, 22.9, 23.0, 23.2, 23.3, 51.7, 50.7, 55.3, 109.9, 119.0, 119.4, 120.4, 124.1, 124.1, 124.7, 124.8, 125.4, 125.5, 125.8, 127.6, 127.7, 128.4, 128.4, 128.9, 129.8, 130.3, 131.7, 132.4, 133.1, 134.0, 134.20, 136.9, 137.9, 140.7, 140.8, 150.1, 150.3, 150.40, 156.4; ^{31}P-NMR (121.5 MHz, $CDCl_3$) δ 151.12. All values are consistent with literature. [44a]

1.7 References

(1). Trost, B., Asymmetric catalysis: An enabling science *Proc. Nat. Acad. Sci.* **2004**, *101*, 5348-5355.

(2). Somers, G. F., Thalidomide and congenital abnormalities. *Lancet* **1962**, *1*, 9123-9127.

(3). Administration, U. S. F. a. D. Development of new stereoisomeric drugs. http://www.fda.gov/Drugs/GuidanceComplianceRegulatoryInformation/Guidances/ucm122883.htm (accessed 4/23/2010).

(4). Stinson, S. C., Chiral Pharmaceuticals *Chem.l and Eng. News* **2001**, *79*, 79-97.

(5). The Nobel Prize in Chemistry 2001. http://nobelprize.org/nobel_prizes/chemistry/laureates/2001/index.html (accessed 4/24/10).

(6). Knowles, W. S., Asymmetric hydrogenation. *Acc. Chem. Res.* **1983** *16*, 106-112.

(7). (a) Trost, B. M.; Guangbin, D., New Class of Nucleophiles for Palladium-Catalyzed Asymmetric Allylic Alkylation. Total Synthesis of Agelastatin A. *J. Am. Chem. Soc.* **2006**, *128*, 6054-6055; (b) Toyota, M.; Hirota, M.; Niskikawa, Y.; Fukumoto, K.; Ihara, M., Palladium-catalyzed intramolecular allylic alkylation reaction in marine natural product Synthesis: enantioselective synthesis of (+)-methyl pederate, a key intermediate in syntheses of mycalamides. *J. Org. Chem.* **1998**, *63*, 5895-5902; (c) Trost, B. M.; Lee, C., Asymmetric allylic alkylation reactions. In *Catalytic Asymmetric Synthesis*, Ojima, I., Ed. Wiley-VCH: 2001.

(8). Osborn, J. A.; Jardine, F. J.; Young, J. F.; Wilkinson, G., The preparation and properties of tris(triphenylphosphine)halogenorhodium (I) and some reactions thereof including catalytic homogeneous hydrogenation of olefins and acetylenes and their derivatives. *J. Chem. Soc.* **1966**, *1711-1732*.

(9). (a) Nozaki, H.; Moriuti, S.; Takaya, H.; Noyori, R., Asymmetric induction in carbenoid reaction by means of a dissymmetric copper chelate *Tetrahedron Lett.* **1966**, *7*, 5239-5244; (b) Nozaki, H.; Takaya, H.; Moriuti, S.; Noyori, R., Homogenous catalysis in the decomposition of diazo compound by copper chelates: Asymmetric carbenoid reactions *Tetrahedron* **1968**, *24*, 3655-3669.

(10). Morrison, J. D.; Masler, W. F.; Neuberg, M. K., Asymmetric homogenous hydrogenation. In *Advances in catalysis and related subjects*, Eley, D. D.; Weisz, P. B., Eds. Academic Press: New York, 1976; Vol. 25.

(11). Knowles, W. S.; Sabacky, M. J., Catalytic asymmetric hydrogenation employing a soluble optically active, Rhodium Complexes. *Chem. Comm.* **1968**, 1445-1446.

(12). Morrison, J. D.; Burnett, R. E.; Adam M. Aguiar; Cary J. Morrow; Phillips, C., Asymmetric homogeneous hydrogenation with rhodium (I) complexes of chiral phosphines *J. Am. Chem. Soc.* **1971**, *93*, 1301-1302.

(13). Knowles, W. S.; Sabacky, M. J.; Vineyard, M. J., Catalytic asymmetric hydrogenation. *J. Chem. Soc., Chem. Commun* **1972**, 10-11.

(14). (a) Kagan, H. B.; Tuan-Phat, D., The asymmetric synthesis of hydratropic acid and amino-acids by homogeneous catalytic hydrogenation. *J. Chem. Soc. D* **1971**, 481-483; (b) Kagan, H. B.; Tuan-Phat, D., Asymmetric catalytic reduction with transition metal complexes. I. Catalytic system of rhodium(I) with (-)-2,3-0-isopropylidene-2,3-dihydroxy-1,4-bis(diphenylphosphino)butane, a new chiral diphosphine. *J. Am. Chem. Soc.* **1972**, *94*, 6429-6433.

(15). Vineyard, B. D.; Knowles, W. S.; Sabacky, M. J.; Bachman, G. L.; Weinkauff, D. J., Asymmetric hydrogenation. Rhodium chiral bisphosphine catalyst. *J. Am. Chem. Soc.* **1977**, *99*, 5946–5952.

(16). Fryzuk, M. D.; Bosnich, B., Asymmetric synthesis. Production of optically active amino acids by catalytic hydrogenation. *J. Am. Chem. Soc.* **1977**, *99*, 6262-6267.

(17). Hayashi, T.; Mise, T.; Fukushima, M.; Kagotani, M.; Nagashima, N.; Hamada, Y.; Matsumoto, A.; Kawakami, S.; Konishi, M.; Yamamoto, K.; Kumada, M., Asymmetric synthesis catalyzed by chiral ferrocenylphosphine–transition metal complexes. I. preparation of chiral ferrocenylphosphines. *Bull. Chem. Soc. Jpn.* **1980**, *53*, 1138-1151.

(18). Achiwa, K., Asymmetric hydrogenation with new chiral functionalized bisphosphine-rhodium complexes. *J. Am. Chem. Soc.* **1976**, *98*, 8265–8266.

(19). Shang, G.; Li, W.; Zhang, X., Transition metal-catalyzed homogenous asymmetric hydrgenation In *Catalytic Asymmetric Synthesis* 3rd ed.; Ojima, I., Ed. Hoboken 2010.

(20). Caplar, V.; Comisso, G.; Sunjic, V., Homogenous asymmetric hydrogenation *Synthesis* **1981**, 85-117.

(21). Grubbs, R. H.; DeVries, R. A., Asymmetric hydrogenation by an atropisomer diphosphinite rhodium complex *Tetrahedron Lett.* **1977**, *18*, 1879-1880.

(22). Miyashita, A.; Yasuda, A.; Takaya, H.; Toriumi, K.; Ito, T.; Souchi, T.; Noyori, R., Synthesis of 2,2'-bis(diphenylphosphino)-1,1'-binaphthyl (BINAP), an atropisomeric chiral bis(triaryl)phosphine, and its use in the rhodium(I)-catalyzed asymmetric hydrogenation of a (acylamino)acrylic acids. *J. Am. Chem. Soc.* **1980**, *102*, 7932–7934.

(23). (a) Guo, H.; Ding, K.; Dai, L., Recent advances in catalytic asymmetric hydrogenation: renaissance of the monodentate phosphorus ligands. *Chin. Sci. Bull.* **2004**, *49*, 2003-2016; (b) Minnaard, A. J.; Feringa, B. L.; Lefort, L.; de Vries, J. G., Asymmetric hydrogenation using monodentate phosphoramidite ligands. *Acc. Chem. Res.* **2007**, *40*, 1267–1277; (c) Reetz, M. T., Combinatorial transition-metal catalysis: Mixing monodentate ligands to control enantio-, diastereo-, and regioselectivity. *Angew. Chem. Int. Ed.* **2008**, *47*, 2556 - 2588.

(24). Kostas, I. D., Recent advances on *P,N*-containing ligands for transition-metal homogenous catalysis. *Curent. Org. Syn.* **2008**, *5*, 227-249.

(25). Alexakis, A.; Mutti, S.; Normant, J. F., A new chiral ligand for the asymmetric conjugate addition of organocopper reagents to enones. *J. Am. Chem. Soc.* **1991**, *113*, 6332–6334.

(26). Bruneau, C.; Renoud, J.-L., Monophosphinites, -aminophosphinites, -phosphonites, -phosphites, -phosphoramidites In *Phosphorus Ligands in Asymmetric Catalysis*, Borner, A., Ed. Wiley-VCH: 2008; Vol. 1.

(27). Alexakis, A.; Varta, J.; Burton, J.; Mangeney, P., Asymmetric conjugate addition of diethyl zinc to enones with tartrate chiral phosphite ligands. *Tetrahedron: Asymmetry* **1997**, *8*, 3193-3196.

(28). Alexakis, A.; Vastra, J.; Burton, J.; Benhaim, C.; Mangeney, P., Asymmetric conjugate addition of diethyl zinc to enones with chiral phosphorus ligands derived from TADDOL. *Tetrahedron Lett.* **1998**, *39*, 7869-7872.

(29). Alexakis, A.; Frutos, J. C.; Mangeney, P.; Meyers, A. I.; Moorlag, H., Determination of enantiomeric purity of hydroxy biaryls using 1H and 31P-NMR on their diazaphospholidine derivatives. *Tetrahedron Lett.* **1994**, *35*, 5125-5128.

(30). Duursma, A.; Minnaard, A. J.; Feringa, B. L., Highly enantioselective conjugate addition of dialkylzinc reagents to acyclic nitroalkenes: A catalytic route to β2-amino acids, aldehydes, and alcohols. *J. Am. Chem. Soc.* **2003**, *125*, 3700-3701.

(31). de Vries, A. H. M.; Meetsma, A.; Feringa, B. L., Enantioselective conjugate addition of dialkylzinc reagents to cyclic and acyclic enones catalyzed by chiral copper complexes of new phosphorus amidites. *Angew. Chem. Int. Ed.* **1996**, *35*, 2374-2376.

(32). Keller, E.; Maurer, J.; Naasz, R.; Schader, T.; Meetsma, A.; Feringa, B. L., Unexpected enhancement of enantioselectivity in copper (II) catalyzed conjugate addition of diethyzinc to cyclic enones with novel TADDOL phosphorus amidite ligands *Tetrahedron: Asymmetry* **1998**, *9*, 2409-2413.

(33). (a) Alexakis, A.; Polet, D.; Rosset, S.; Marc, S., Biphenol-based phosphoramidite ligands for the enantioselective copper-catalyzed conjugate addition of diethylzinc. *J. Org. Chem.* **2004** *69*, 5660-5567; (b) Palais, L.; Mikhel, I. S.; Bournaud, C.; Micouin, L.; Falciola, C. A.; Vuagnoux-d'Augustin, M.; Rosset, S.; Bernardinelli, G.; Alexakis, A., SimplePhos monodentate ligands: Synthesis and application in copper-catalyzed reactions *Angew. Chem. Int. Ed.* **2007**, *46*, 7462-7465.

(34). (a) Hua, Z.; Vassar, V. C.; Ojima, I., Syntheses of new chiral monodentate phosphite ligands and hteir use in catalytic asymmetric hydrogenations. *Org. Lett.* **2003**, *5*, 3831-3834; (b) Wu, S.; Zhang, W.; Zhang, Z.; Zhang, X., Synthesis of new monodentate spiro phosphoramidite ligand and its application in Rh-catalyzed asymmetric hydrogenation reactions. *Org. Lett.* **2004**, *6*, 3565-3567.

(35). Franciò, G.; Faraone, F.; Leitne, W., Highly enantioselective nickel-catalyzed hydrovinylation with chiral phosphoramidite ligands. *J. Am. Chem. Soc.* **2002**, *124*, 736-737.

(36). Korostylev, A.; Gridnev, I.; Brown, J. M., Mechanistic and synthetic aspects of hydroboration with a simple atropisomeric ligand prepared from 1-(1′-(isoquinolyl)-2-naphthol. *J. Organomet. Chem.* **2003**, *680*, 329-334.

(37). Guo, X.-X.; Xie, J.-H.; Hou, G.-H.; Shi, W.-J.; Wang, L.-X.; Zhou, Q.-L., Asymmetric palladium-catalyzed hydrosilylation of styrenes using efficient chiral spiro phosphoramidite ligands. *Tetrahedron: Asymmetry* **2004**, *15*, 2231-2234.

(38). Hua, Z.; Vassar, V. C.; Choi, H.; Ojima, I., New biphenol-based fine-tunable monodentate phosphoramidite ligands for catalytic asymmetric transformations. *Proc. Nat. Acad. Sci.* **2004** *101*, 5411-5416.

(39). (a) Bartels, B.; Helmchen, G., Ir-catalysed allylic substitution: mechanistic aspects and asymmetric synthesis with phosphorus amidites as ligands. *Chem. Commun.* **1999**, 741-742; (b) Malda, H.; van Zijl, A. W.; Arnold, L. A.; Feringa, B. L., Enantioselective copper-catalyzed allylic alkylation with dialkylzincs using

phosphoramidite ligands. *Org. Lett.* **2001**, *3*, 1169–1171; (c) Ohmura, T.; Hartwig, J. F., Regio- and enantioselective allylic amination of achiral allylic esters catalyzed by an Iridium−phosphoramidite complex. *J. Am. Chem. Soc.* **2002**, *124*, 15164–15165.

(40). Imbos, R.; Minnaard, A. J.; Feringa, B. L., A highly enantioselective intramolecular Heck reaction with a monodentate ligand
. *J. Am. Chem. Soc.* **2002**, *124*, 184-185.

(41). (a) Yoshizaki, H.; Satoh, H.; Sato, Y.; Nukui, S.; Shibasaki, M.; Mori, M., Palladium-mediated asymmetric synthesis of *cis*-3,6-disubstituted cyclohexenes. A short total synthesis of optically active (+)-γ -Lycorane. *J. Org. Chem.* **1995**, *60*, 2016-2021; (b) Nakanishi, M.; Mori, M., Total synthesis of (-)-strychnine. *Angew. Chem. Int. Ed* **2002**, *41*, 1934-1936; (c) Trost, B. M.; Dogra, K., Synthesis of (-)-Δ9-trans-tetrahydrocannabinol: Stereocontrol via Mo-catalyzed asymmetric allylic alkylation reaction. *Org. Lett.* **2007**, *9*, 861-863; (d) Trost, B. M.; Cook, G. R., An asymmetric synthesis of (−)-epibatidine. *Tetrahedron Lett.* **1996**, *37*, 7485-7488.

(42). Giacomina, F.; Riat, D.; Alexakis, A., ω-Ethylenic allylic substrates as alternatives to cyclic substrates in copper- and iridium-catalyzed asymmetric allylic alkylation. *Org. Lett.* **2010**, *12*, 1156-1159.

(43). Raluy, E.; Claver, C.; Pàmies, O.; Diéguez, M., First chiral phosphoroamidite-phosphite ligands for highly enantioselective and versatile Pd-catalyzed asymmetric allylic substitution reactions. *Org. Lett.* **2007**, *9*, 49-52.

(44). (a) Chapsal, B. D.; Ojima, I., Total synthesis of enantiopure (+)-γ-lycorane using highly efficient Pd-catalyzed asymmetric allylic alkylation. *Org. Lett.* **2005**, *8*, 1395-1398; (b) Chapsal, B. D.; Ojima, I., Catalytic asymmetric transformations with fine-tunable biphenol-based monodentate ligands. *Tetrahedron: Asymmetry* **2006**, *17*, 642-657; (c) Choi, H.; Hua, Z.; Ojima, I., Highly enantioselective copper-catalyzed conjugate addition of diethylzinc to nitroalkenes. *Org. Lett.* **2004** *6*,2689-2691; (d) Shi, C.; Ojima, I., Asymmetric synthesis of 1-vinyltetrahydroisoquinoline through Pd-catalyzed intramolecular allylic amination. *Tetrahedron* **2007**, *63*, 8563-8570.

(45). Reetz, M. T.; Mehle, G., Highly enantioselective Rh-catalyzed hydrogenation reactions based on chiral monophosphite ligands. *Angew. Chem.* **2000**, *39*, 3889-3890.

(46). Lambers-Verstappen, M. M. H.; De Vries, J. G., Rhodium-catalysed asymmetric hydroformylation of unsaturated nitriles. *Advan. Syn. Catal.* **2003**, *345*, 478-482.

(47). (a) Alexander, J. B.; La, D. S.; Cefalo, D. R.; Hoveyda, A. H.; Schrock, R. R., Catalytic enantioselective ring-closing metathesis by a chiral biphenol−Mo complex. *J. Am. Chem. Soc.* **1998**, *120*, 4041–4042; (b) Alexander, J. B.; Schrock, R. R.; Davis, W. M.; Hultzsch, K. C.; Hoveyda, A. H.; Houser, J. H., Synthesis of molybdenum imido alkylidene complexes that contain 3,3'-Dialkyl-5,5',6,6'-tetramethyl-1,1'-biphenyl-2,2'-doilates (Alkyl= *t*-Bu, Adamantyl), catalyst for enantioselective olefin metathesis reactions. *Organometallics* **2000**, *19*, 3700-3715.

(48). Polet, D.; Alexakis, A., Kinetic Study of various phosphoramidite ligands in the iridium-catalyzed allylic substitution. *Org. Lett.* **2005**, *7*, 1621-1624.

(49). Gottlieb, H. E.; Kotlyar, V.; Nudelman, A., NMR chemical shifts of common laboratory solvents as trace impurities. *J. Org. Chem.* **1997**, *62*, 7512-7515.

Chapter 2

Application of Biphenol Ligands to Asymmetric Allylic Alkylation

2.1 Introduction to Asymmetric Allylic Alkylation

Metal-catalyzed carbon-carbon bond forming reactions have become one of the most powerful synthetic reactions of the modern organic chemistry reaction arsenal.[1] These reactions have allowed for easier access to more complex structures, and brought about the development of various catalytic asymmetric and asymmetric transformations.

Among these transformations asymmetric allylic alkylation (AAA) is one of the most unique for several reasons. First, allylic alkylation can be catalyzed by several different transition metals including rhodium,[2] ruthenium,[3] iridium,[4] molybdenum,[5] tungsten,[6] and copper.[7] The nature of the transition metal has had a dramatic influence on the stereochemical outcome of allylic alkylation. Second, unlike many other metal-catalyzed reactions, AAA has several known possible enantiodiscrimination mechanisms *i.e* deracemization, enantiotopic faces and desymmetrization (**Scheme II-1**).[8]

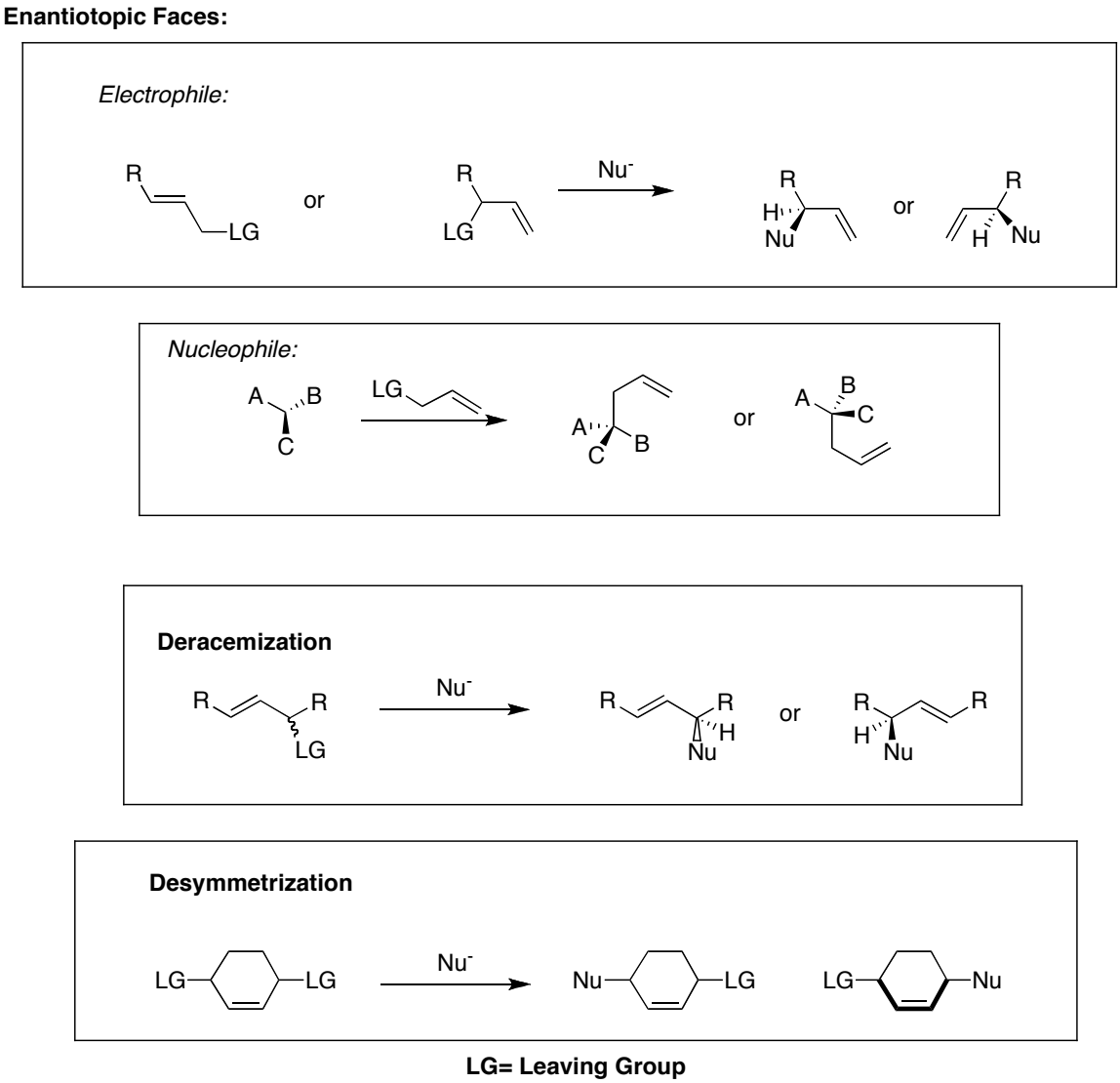

Scheme II-1: Enantioselective mechanisms for allylic allylation

Furthermore, both the electrophilic species and the nucleophilic species are capable of inducing asymmetry in asymmetric allylic alkylation. As a result, the most superior feature of AAA is vested in its ability to not only carbon-based nucleophiles but also hydrogen, nitrogen, oxygen and sulfur.[9] Thus, metal-catalyzed AAA is a robust reaction that allows simpler access to some very complex structures.

The transition metal-catalyzed allylic alkylation was first developed by Tsuji in 1965 using Pd, partly based on an earlier discovery by Smidt and Hafner of the Wacker process.[1b;9] This was the first example of a carbon-carbon bond-forming substitution through a π-allyl-palladium complex (**Scheme II-2**)

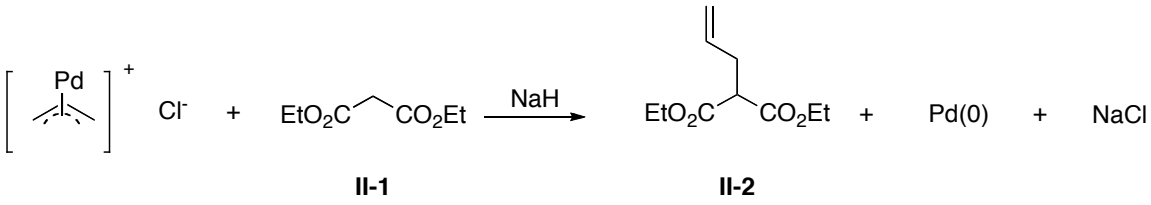

II-1 **II-2**

Scheme II-2: First example of allylic substitution [10]

This discovery opened the floodgates for new synthetic targets that have not been possible with previously known methods. During the time of this discovery several novel chiral ligands were being developed for asymmetric hydrogenation. In 1973, Trost reported the first asymmetric allylic alkylation using Kagan's **DIOP,** (diphenyl-phosphino(dimethyl))dioxolane, ligand that afforded enantioselectivities in the range of 2-22% ee for the substitution of *cis*-2-pentene with diethyl sodiomalonate.[11] Later in 1977, Trost published much higher enantioselectivity in conversion of other malonate derivates to cyclohexenes as shown in **Scheme II-3**.[10]

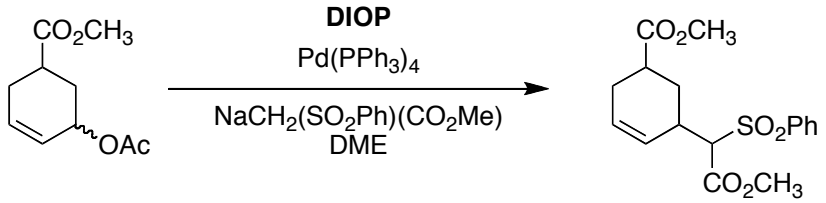

II-3 **II-4**

46% ee

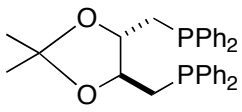

(*R,R*)- DIOP
L-4

Scheme II-3: First asymmetric allylic alkylation [10]

Since this time, great efforts have been put forth to understand both the mechanism and the origin of enantioselectivity of the reaction.[12] The generally accepted mechanism of allylic alkylation is summarized below in **Scheme II-4**.

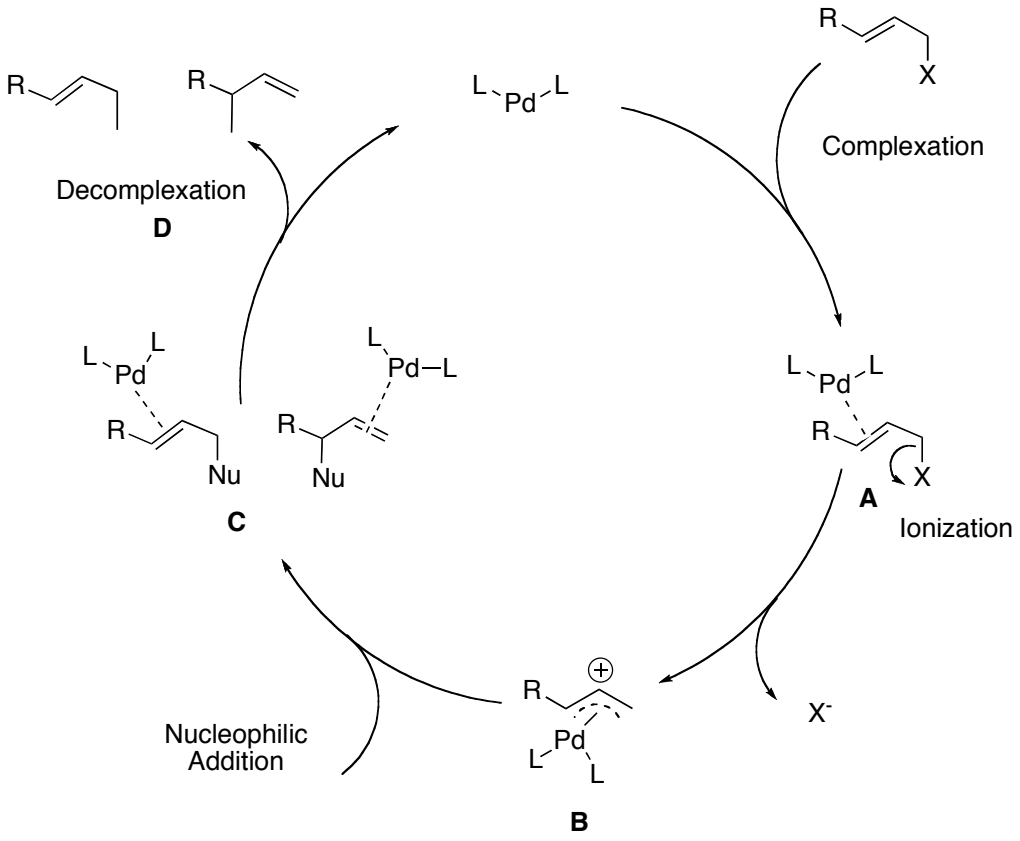

Scheme II-4: Generalized mechanism of allylic-substitution reaction[13]

The catalytic cycle begins with complexation of the allylic olefin to the palladium metal, Pd(0), **(A, Scheme II-4**) followed by oxidative addition of the palladium, where the X-group is cleaved from the allylic moiety forming the electrophilic π-allylic system (**Scheme II-4**). It has been observed that ionization of the X-group occurs *anti*- to the metal complex.[12b] The nucleophilic attack on the π-allyl-complex is dependent on the nucleophile type. In the case of soft nucleophiles (pKa <25), the attack occurs on the π -allyl complex *anti* to the palladium metal. Whereas, hard nucleophiles (pKa> 25) attack the metal center first, and are then transferred to the π-allylic system for an overall *syn*-addition of the nucleophile and overall trans-metallative mechanism.[9;13] The observed regioselectivity of the product in the case of the palladium is dependent primarily on (1) the sterics of the approaching nucleophile, (2) the stability of the π-allylic system, which is also influenced by the electronics of the metal center. The terminal step of the catalytic cycle is the decomplexation to release the newly formed compound and regenerate the active metal species.[13] As shown in the **Scheme II-4** mechanism, each step except the

terminal decomplexation, can be face selective, thus affording an overall asymmetric reaction.[12a]

Asymmetric allylic alkylation has become a very useful process in the total synthesis of various natural products. Several total-syntheses have been completed using the Pd-allylic substitution as the key-step.[13-14] Shown below in **Figure II-1** are several examples of natural products whose syntheses had employed asymmetric allylic alkylation as the key step in their total synthesis. The asymmetric synthesis of the lycorane was completed by Mori and co-workers affording the key intermediate in 54% ee and 66% isolated yield.[15] Later in 2005 Chapsal and Ojima reported the total synthesis of the γ-lycorane in >99% ee and 41% overall yield.[16]. α-Skytanthine was complete by Helmchem in 2002[17]; Pentobarital and Nitramine were synthesized in 81% ee and 86% ee respectively, by Trost;[18] the more structurally complex Amphidinolide A[19] and Galanthanmine[20] were also completed by Trost using Ru-catalyzed allylic alkylation and Pd-catalyzed allylic alkylation, respectively.

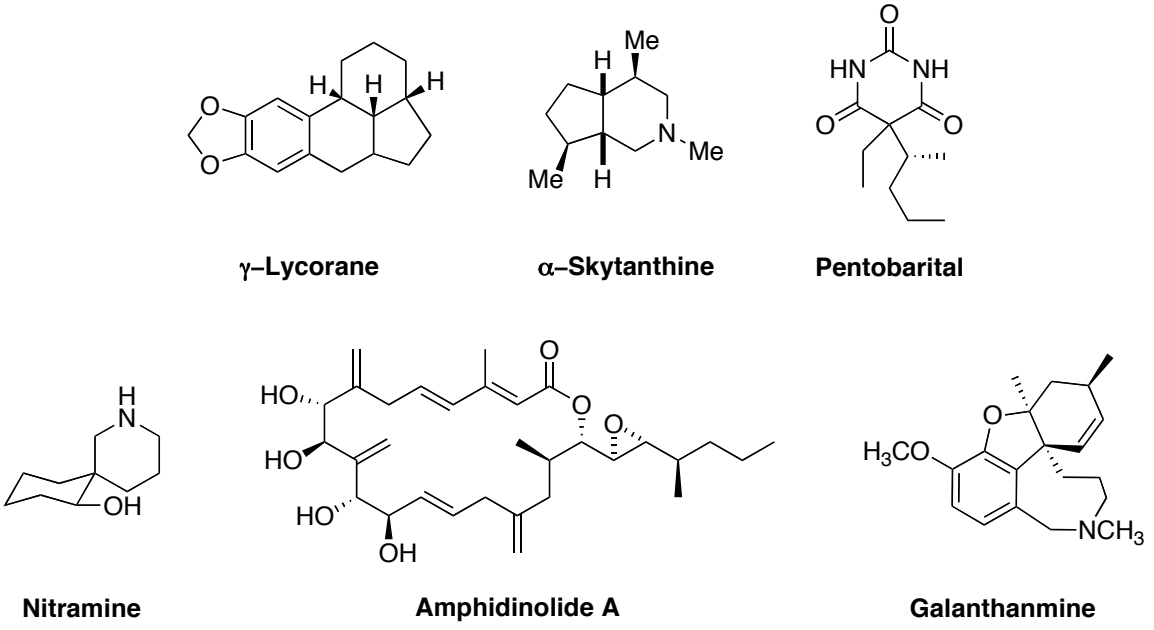

Figure II-1: Example of molecules with allylic alkylation used as key step in synthesis [14]

The examples shown in **Figure II-1** demonstrate the broad-spectrum application of asymmetric allylic alkylation in total synthesis.

Many of the compounds shown in **Figure II-1** were targeted primarily for their potential biological applications. Thus, AAA can be a very useful reaction in the development of more potent synthetic analogues of these natural products. The allylic alklyation was applied to develop analogues of the natural product Huperzine-A.[21]

In 1989, Kozikowski completed the first total synthesis of the alkaloid huperzine-A.[22] Later in 1993, Kozikowski revised the total synthesis to employ a racemic Pd-catalyzed allylic bicycloannulation as the key step to form the tricylic core of huperzine-A as shown in **Scheme II-5**.[23] He later developed several more potent derivatives employing allylic alkylation in the key step.

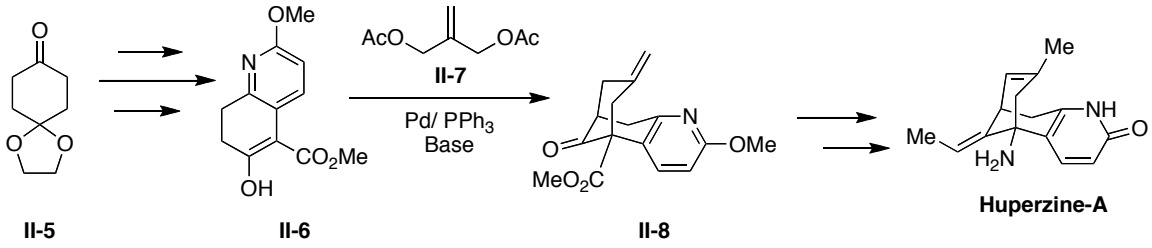

Scheme II-5: Key step in the total synthesis of Huperzine-A [23]

Following Kozikowski's description, Terashima and co-workers detailed the first catalytic asymmetric synthesis of huperzine-A, using a bidentate ferrocene-based ligand, affording a modest 64% ee.[24]

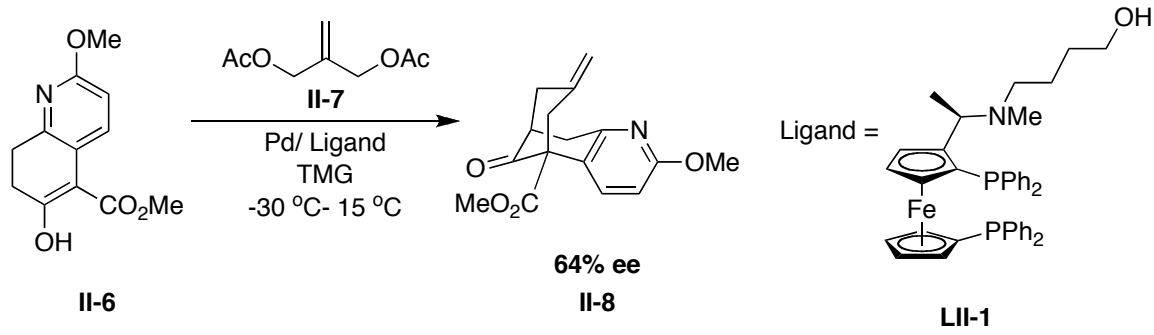

Scheme 6: Asymmetric allylic alkylation towards Huperzine-A [24]

Bai and co-workers synthesized a slightly modified version of Terashima's bidentate ferrocenyl-based ligand (**LII-2**, **Figure II-2**), which achieved a 90% ee under the same conditions as Terashima in the key step synthesis of huperzine-A.[25]

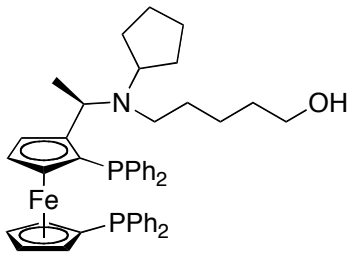

LII-2

Figure II-2: Bai's Ferrocenyl Ligand [25]

The results detailed by Bai still have room for improvement in the enantioselective synthesis of the huperzine-A. Furthermore, only bidentate ligands have been applied to the enantioselective synthesis of huperzine-A. Thus, this molecule represents an excellent target application of our novel monodentate biphenol ligands. While efforts to complete the synthesis of huperzine-A *via* a catalytic asymmetric synthesis were being accomplished, Langolis and co-workers reported an asymmetric version using diastereoselective catalysis with Whitesell's chiral auxiliary affording the desired product intermediate **B** in 92% d.r (**Scheme II-7**).[26]

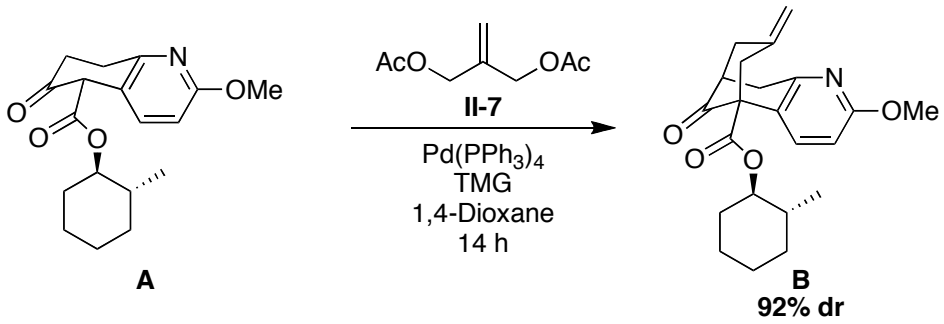

Scheme II-7: Diastereoselective synthesis of huperzine precursor.[26]

2.2 Huperzine-A

Huperzine-A (**Figure II-3**) is an alkaloid from the subclass lycopodine and a member of the larger class of lycopodium alkaloids.[27] It was isolated from the club moss *Huperzia serrata* in ~95 mg/g.[28] Huperzine-A, like many other alkaloids from Huperziace family have found many uses in traditional Chinese folk medicine.

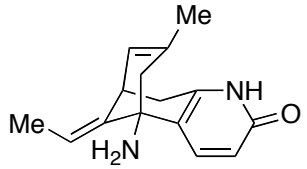

Huperzine-A

Figure II-3: Chemical structure of huperzine-A

Indeed, these compounds have been used to treat contusions, sprains, swelling, schizophrenia, myasthenia gravis, and organophosphate poisoning. Furthermore, pharmacological studies have confirmed that these alkaloids have a definite effect on cardiovascular and neuromuscular systems.[27-29]

Huperzine-A is a particularly promising alkaloid as it has been shown to be an inhibitor of acetylcholinesterase (AChE), and it has also been shown to attenuate b-amyloid induced apoptosis in cortical neurons along with several other neuroprotective effects.[28;30] Resulting from these various neuroprotective effects, huperzine-A holds excellent promise in the treatment of Alzheimer's disease (AD).[28] Huperzine is currently used as a first line drug in the treatment of AD in China and recently completed Phase II clinical trials in the United States.[28;31] By 2050, it is estimated that 1 in 85 people worldwide will be living with this disease.[32] Thus, continued research to expand the repertoire of the drug for the treatment of Alzheimer's is necessary.

2.2.1 Synthesis of Key-Step Substrate

The application of our biphenol-based ligands to the synthesis of huperzine-A begins with the preparation of materials needed for the catalytic step in order to screen our various ligands. The synthesis of the huperzine-A key intermediate was taken from a known procedure reported by Kozikowski.[33] The fused-bicyclic pyridine (**A**), can be obtained by alpha-functionalization of ketone **B** following deprotection of compound **C**, which can be obtained from commercial materials shown in **Figure II-4**.

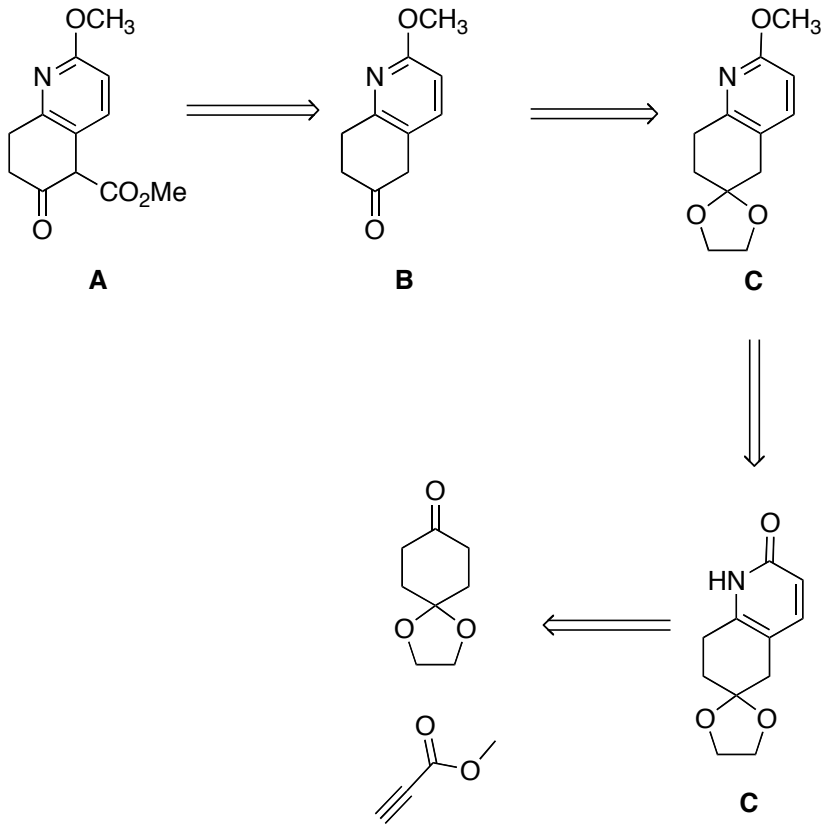

Figure II-4: Retrosynthesis for key-step intermediate

The preparation began with commercially available mono-protected 1,4-cyclohexanedione (**II-5**) that underwent a modified Stork-enamine synthesis with methyl-propriolate (**II-10**) to afford the alpha-pyridone (**II-11**) in a range of yields as shown in **Scheme II-8**. The wide range of yields for this reaction may have resulted from the

inconsistent concentrations of ammonia present in the solvent mixture, as it was a commercial preparation.

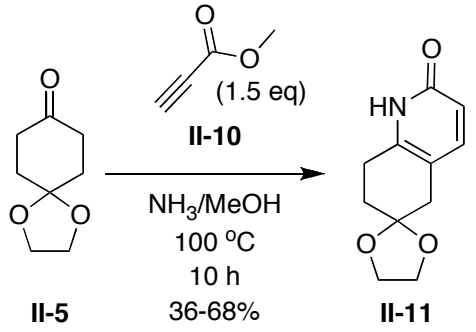

Scheme II-8: Synthesis of II-11

A reaction mechanism is shown in **Scheme II-9** for the formation of the **II-11**. Following the formation of the enamide **II-5a**, a Michael addition to **II-10** occurs and subsequent lactamization afforded **II-11**.

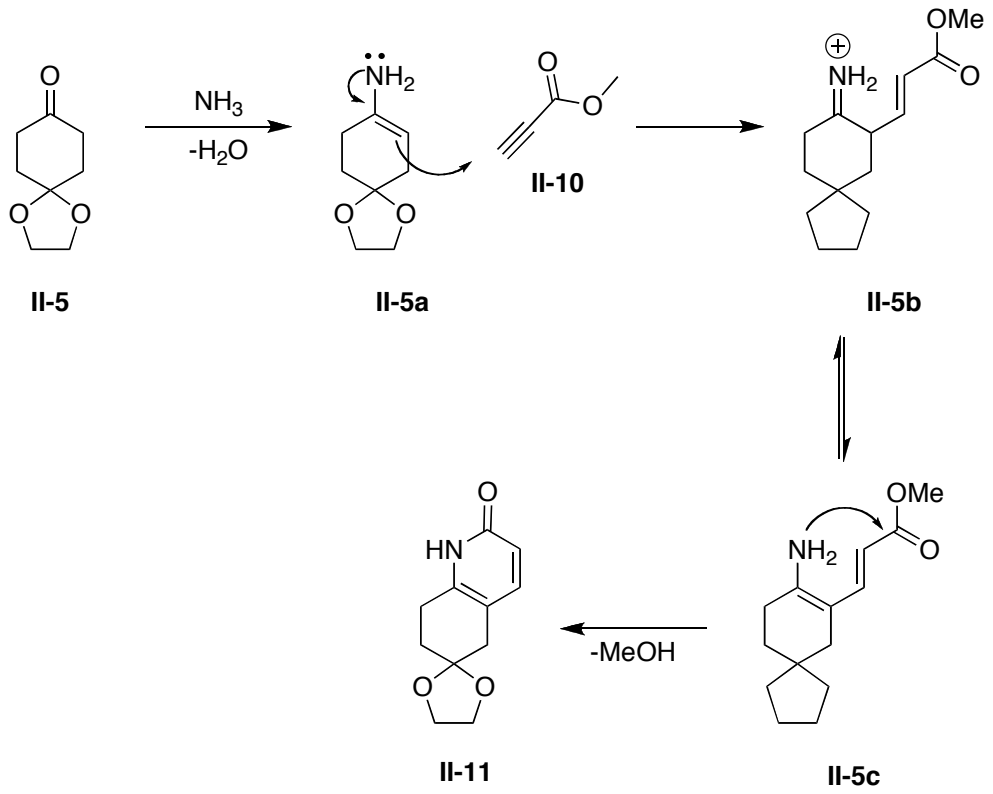

Scheme II-9: Mechanism for that formation of II-11

The subsequent silver carbonate-promoted methylation of the oxygen posed some difficulty (**Scheme II-10**). Although there were several literature reports of quantitative yield were reported [24;34] at no time were those reported yields reproduced under the given conditions. As such, various conditions for this reaction were explored and the data are summarized in **Table II-1**.

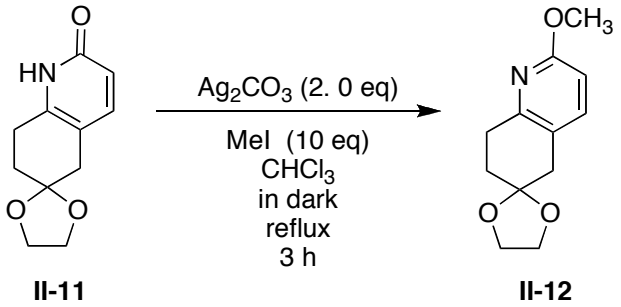

II-11 **II-12**

Scheme II-10: O-Methylation of II-11

Table II-1: Condition for Synthesis of II-12

Entry	Conditions	Yield
1	rt overnight (no sonication)	0%
2	overnight reflux (30 min. dry sonication)*	56%
3	overnight reflux (30 min solution sonication)	62%
4	2 h reflux (30 min. solution sonication)	71%

*No solvent was present in the reaction flask (Used mainly to break-up large chunks)

The best condition as seen in entry 4 requires 30 min of sonication prior to the start of the reaction. This likely improves the solubility of the silver carbonate. Furthermore, it appears that longer reflux times have an adverse affect on the yield (entries 3 and 4). Following *O*-methylation, the ketal was deprotected under acidic conditions to afford **II-13** which was then carboxymethoxylated at the most acidic position to give catalytic intermediate **II-14** in 72% isolated yield over two steps (**Scheme II-11**).

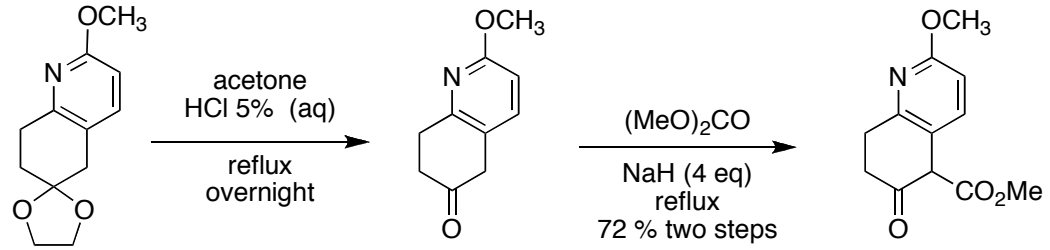

II-12 **II-13** **II-14**

Scheme II-11: Final steps to key intermediate II-14

Compound **II-14** can be drawn as both a ketone and its enol-tautomer.[23] The equilibrium in this case is shifted toward the enol-tautomer (**II-14b**) as there is a very stable intramolecular hydrogen-bond between the ester carbonyl and the enol-tautomer (**Scheme II-12**). This equilibrium will make the nucleophilic attack step in the allylic alkylation reaction more facile.

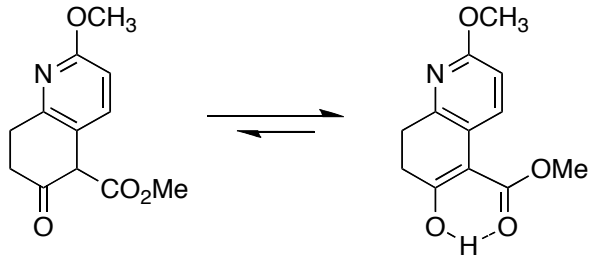

II-14 **II-14b**

Scheme II-12: Keto-Enol Tautomerization

With the desired substrate in hand the allylic group was synthesized from commercially available 2-methylene-1,3-propane-diol to afford the desired symmetric diacetate (**II-7)** in quantitative yield (**Scheme II-13**).

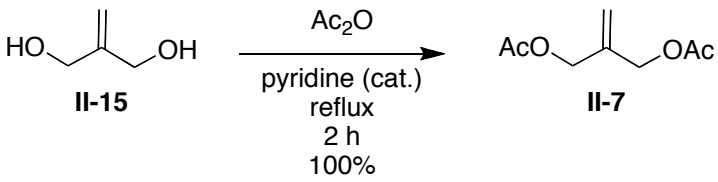

II-15 **II-7**

Scheme II-13: Synthesis of the allylic group bearing acetate moiety

2.3 Ligand Screening

Preliminary ligand screening was done by Dr. Hojae Choi.[35] The early screening results confirmed the experimental data of Terashima and co-workers.[24] Thus, palladium-allyl chloride dimer was chosen as the catalyst for this system and tetramethylguanidine (TMG) was chosen as the base for this reaction (**Figure II-5**). Furthermore, results demonstrated that the 3,3'-biphenol position need not contain a substituent, as this proves detrimental to the enantioselectivity.

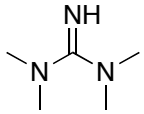

Tetramethylguanidine

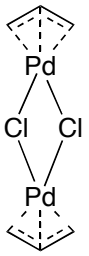

Allylpalladium(II) chloride dimer

Figure II-5: Base and Catalyst for Ligand Screening

Consequently, we continued ligand screening with chiral monodenatate phosphoramidite ligands that demonstrated efficacy in the lycorane reaction system as shown below in **Figure II-6**.

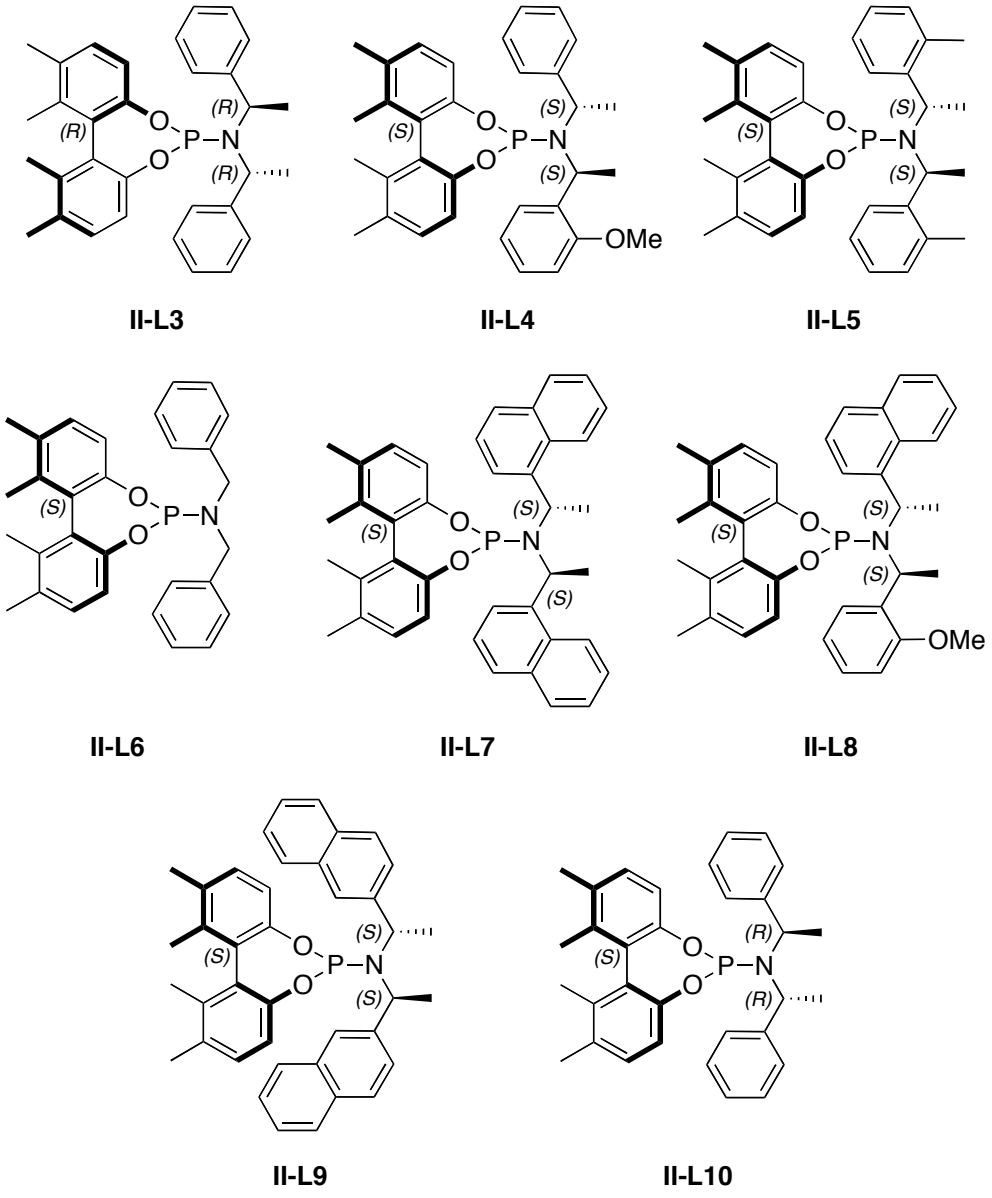

Figure II-6: Early Screening Ligand Library

The screening results are shown in **Table II-2**. One key finding to be noted here is the use of matched ligand pairing, where the biphenol stereochemistry is the same as the chiral amine moiety versus mismatched ligand pairing, where the biphenol stereochemistry is opposite to that of the biphenol backbone. As evidenced by entries 7 and 8, a matched ligand system affords better enantioselectivity.

Table II-2: Initial Ligand Screening

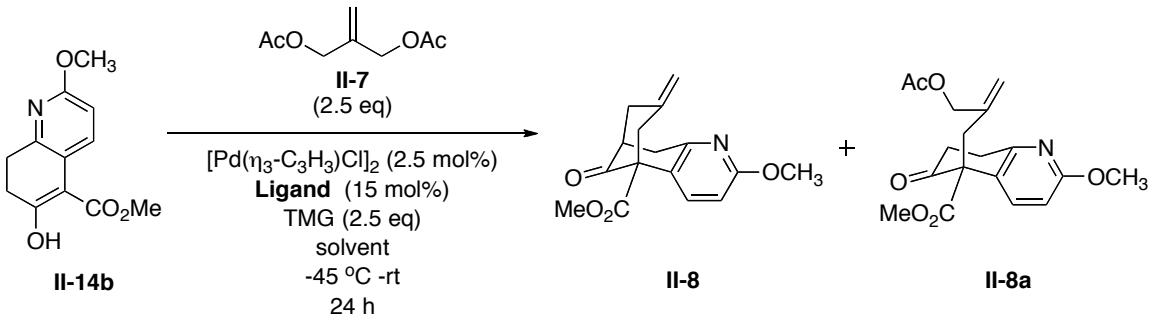

Entry	Ligand	Temp °C	Solvent	Product [a]	% ee [a]
1	**II-L3**	-45	toluene	**II-8**	69
2	**II-L4**	-45	toluene	**II-8**	47
3	**II-L5**	-45	toluene	**II-8**	10
4	**II-L6**	-45	toluene	**II-8**	-
5	**II-L7**	-45	toluene	**II-8**	41
6	**II-L9**	-45	toluene	**II-8**	46
7	**II-L8**	-45	toluene	**II-8**	44
8	**II-L8**	-45	DME	**II-8**	56
9	**II-L3**	-15	DME	**II-8**	39
10	**II-L10**	-15	DME	**II-8**	22
11	**II-L3**	-45	DME	**II-8**	69

[a] All reactions reported are based on 100% conversion
[b] Determined by chiral normal phase HPLC using chiral OD-H column

Furthermore, entry 4 demonstrates the necessity of the chiral centers derived from the alkylamine. A decrease in temperature as noted in entries 1 and 9 can afford modest improvements enantioselectivities. Furthermore, the enantioselectivity appears to be independent of solvent polarity as the enantioselectivities are the same for both toluene and DME (entries 1 and 11). Following these results, we began modification on the allylic substrate, stemming from a previous findings demonstrating that allylic groups can influence enantiomeric excesses.[36]

A series of four different carbonate-based allylic groups were synthesized as shown in **Scheme II-14**.

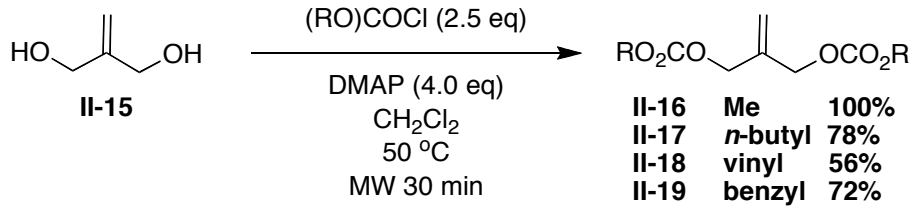

Scheme II-14: Synthesis of various carbonate-based allylic substrates

Following the synthesis, the carbonate-based allylic substrates were screened. The results for the first screening with methyl-carbonate are shown in **Scheme II-15**. The results demonstrate that >89% ee can be achieved using the bisnapthylethylamino base ligand **II-L9.** However, the reaction stalls at the monoalkylation, affording the desired bicycloannulated product as the minor product in this case.

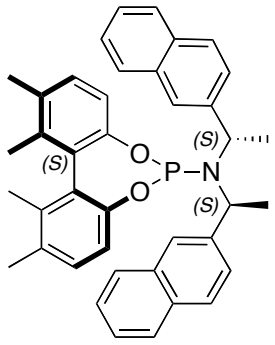

II-L9

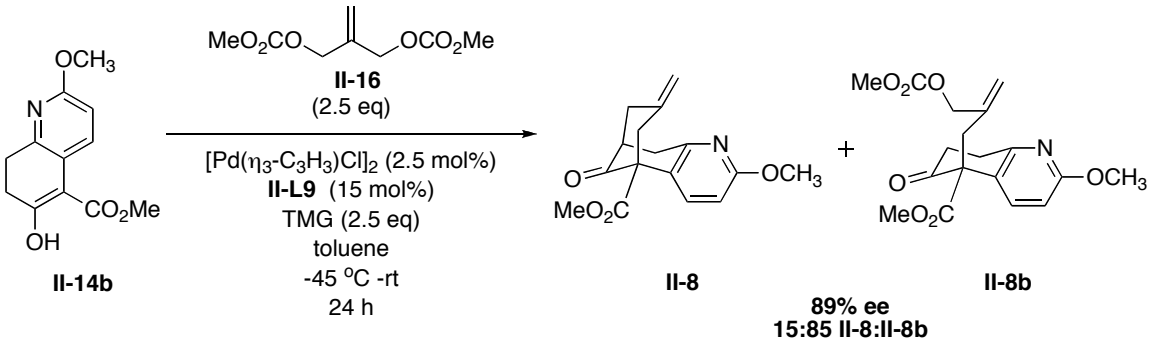

Scheme II-15: Optimization with methyl-carbonate allyl substrate

Attempts were made to drive the cyclization, including isolation of the monoalkylation adduct and continued heating in the presence of an achiral catalyst. However, this course did not show any improvement in the selectivity of the reaction. Thus, screening of ligands and conditions continued. Having seen promising results with the bisnapthyl-based ligand system, modification of the biphenyl ligand amine moiety was examined

more closely with a methyl-carbonate allylic leaving group. The results of this examination are shown in **Table II-3**.

Table II-3: Ligand Screening

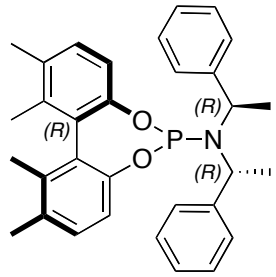

II-L3

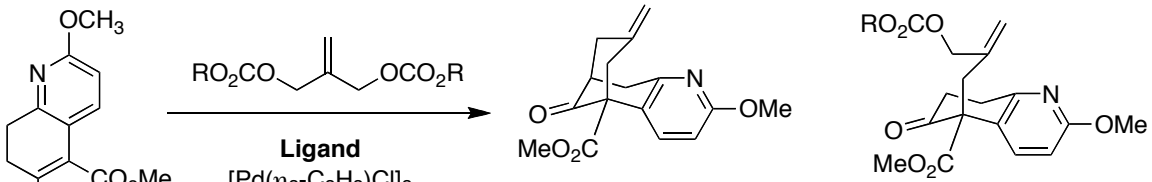

II-14b

Ligand
$[Pd(\eta_3\text{-}C_3H_3)Cl]_2$
DME, TMG
-45 °C- MW conditions

II-16	**Me**
II-17	***n*-butyl**
II-18	**vinyl**
II-19	**benzyl**

II-8

II-8c	**Me**
II-8d	***n*-butyl**
II-8e	**vinyl**
II-8f	**benzyl**

Entry	Ligand	R	MW Conditions	% ee [a]	Result [a] II8:II8c-f
1	**II-L3**	Me	60 °C, 90 min	>99 [b]	2:1
2	**II-L3**	Me	60 °C, 90 min	>99 [c]	1:1
3	**II-L3**	Me	80 °C, 60 min	>99 [d]	**II-8**
4	**II-L3**	n-Bu	80 °C, 60 min	>99	**II-8**
5	**II-L3**	vinyl	80 °C, 60 min	>99	**II-8**
6	**II-L3**	benzyl	80 °C, 60 min	48	**II-8**

[a] Determined by chiral HPLC/ [b] Based on 97% conversion/ [c] based on 95% conversion/ [d] based on 100% conversion

Having determined that conventional heating was unable to drive the second alkylation, we employed a microwave reactor.

Microwave reactors have been shown to improve results where conventional heating has either failed or provided only small amounts of the desired product.[37] This enhancement as a result of microwave heating has been attributed to even internal heating of the vessel, which eliminates localized super-heating of the vessel walls observed under thermal conditions. The increased wall temperature is known to cause catalyst

decomposition. The solvent was changed back to DME since no significant solvent effects were noted and it has a higher dielectric constant than toluene thus allowing full advantage of microwave heating.[38] Ligand **II-L3** afforded >99% ee in cases, but selectivity required high thermal conditions to bias the desired product as shown in **Table II-3**. When the system was heated to 60 ^{o}C for 90 min selectivity was inconsistent (entries 1 and 2), thus the temperature was increased and the microwave exposure time decreased. Finally >99% ee with exclusive selectivity to the desired product was obtained when the reaction mixture was heated to 80 ^{o}C for 60 min. Following the excellent success of the methyl-carbonate leaving groups, vinyl, *n*-butyl and benzyl carbonates (entries 4-6) were explored. Both the vinyl and *n*-butyl carbonates afforded the same selectivity as the methyl-carbonate. However, a dramatic decrease in selectivity is noted in the case of the benzyl-carbonate. This finding implies that carbonate leaving groups play a critical role in the enantioselectivity of this reaction. The leaving group is likely functioning to either block or hinder a particular approach of the incoming nucleophile as seen with high enantioselectivity afforded by the methyl, butyl, and vinyl carbonates.

Upon achieving excellent enantioselectivity using ligand **II-L3**, a larger scale reaction was completed and the desired product was obtained in 83% isolated yield with 97% ee (**Scheme II-16**). The decrease in enantiomeric excess can be attributed to localized heating of the reaction vessel during the addition of the base, which is an overall exothermic process.

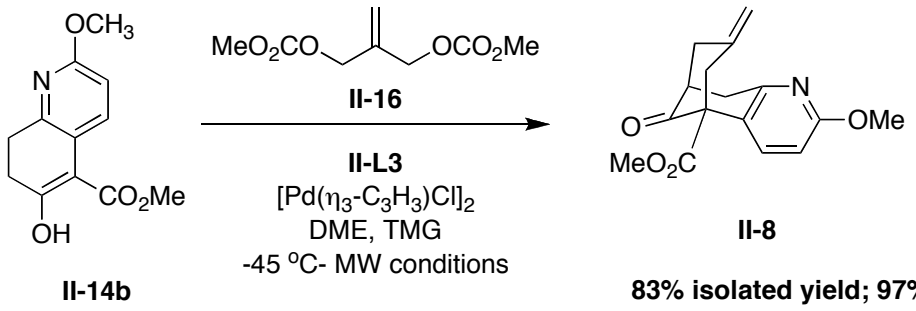

Scheme II-16: Larger scale for isolated yield determination

The mechanism of enantioselection is governed in this case, by the orientation of the nucleophilic species, relative to the steric freedom that π–allyl system posses. That is, the less hindered face of the nucleophile will approach the allylic system from the least

hindered face giving- rise to a single enantiomer. Thus enantioselectivity is dependent on the approach of nucleophile to the allylic system.

2.5 Experimental Methods

General Information:

All chemicals were obtained from either Sigma-Aldrich or Acros Organic and used as is unless otherwise noted. All reactions were performed under Schlenk conditions with oven-dried glassware unless otherwise noted. Anhydrous methylene chloride, toluene, tetrahydrofuran, and ethyl ether were degassed, kept under nitrogen and were dried using the PURESOLV system (Innovative Technologies, Newport, MA). Anhydrous dimethoxyethane (DME) was obtained from Acros Organics and used as is. Anhydrous methanol was obtained by distillation over calcium hydride. ^{1}H, ^{13}C and ^{31}P NMR data were obtained using either 300 MHz Varian Gemni 2300 (75 MHz ^{13}C, 121 MHz ^{31}P) spectrometer or the 400 MHz Varian INOVA 400 (100 MHz ^{13}C, 162 MHz ^{31}P) spectrometer in $CDCl_3$ as a solvent unless other wise noted. Chemical shifts (δ) are reported in ppm and standardized with solvent as internal standard based on literature reported values.[39] Melting points were measured on Thomas Hoover Capillary melting point apparatus and are uncorrected. GC/MS was performed on Agilent 6890 GC/ 5973 Mass selective detector with electron ionization. LC/MS was complete using FIA (flow-injection analysis) using Agilent 1100 LS-MSD electrospray ionization (ESI) single quadrupole mass spectrometer. Enantiomeric excess was determined by chiral HPLC using either Waters 486 HPLC system with UV-detector (254 nm) or Shimadazu LC-A210 with CHIRACEL OD-H column with 4% *i*-PrOH in hexanes as the mobile phase. Infrared spectra were taken on a Thermo-Nicolet IR using sodium chloride salt plates or AT-R attachment with ZnSe crystal. Microwave reactions were performed in 38-mL reaction vials using a CEM Discover Microwave system equipped with 48-position Explorer robotic arm. Temperatures were monitored by an internal infrared probe.

2',5',7',8'-Tetrahydro-1'H-spiro[1,3-dioxolane-2,6'-quinoline]-2'-one (II-11): [33]
1,4-Cyclohexanedione monoethylene ketal (3.00 g, 19.20 mmol), methyl propiolate (3.229 g, 38.41 mmol) were placed into a round-bottomed flask. A 7 N solution of ammonia in methanol (60 mL) was added to the reaction flask and the flask was sealed with a septa. Two 18-gauge needles were placed in the septa to vent. The round-

bottomed flask was then placed into a stainless steel Parr reaction vessel and heated to 100 ^{o}C for 10 h. The pressure typically reached approximately 100 psi. After the 10 hour heating period, the vessel was evacuated and the solvent removed *in vaccuo*. The resulting red-orange solid was adhered to silica gel and subjected to flash chromatography on silica gel (eluent 5% MeOH: CH_2Cl_2), affording compound **II-11** as a light yellow solid (2.18 g, 55% yield): mp >220 ^{o}C dec, (lit.[33]mp dec >220 ^{o}C) ^{1}H NMR ($CDCl_3$, 300 MHz) δ 1.90 (t, 2 H, *J*= 4.8 Hz), 2.70 (s, 2 H), 2.86 (t, 2 H), 4.01 (s, 4 H), 6.38 (d, 1H, *J*= 6.9 Hz), 7.12(d, 1 H, *J*= 6.9 Hz). ^{13}C NMR ($CDCl_3$, 100 MHz) δ 143.6, 141.8, 117.9, 112.0, 107.5, 64.9, 36.4, 30.2, 26.1; Mass spectrum (LRMS) ESI (M+1), m/z found 208.05 cald. for $C_{11}H_{13}NO_3$ 207.089. All values are consistent with literature. [33]

7', 8'-Dihydro-2'-methoxyspiro[1,3-dioxolane-2,6'-(5'*H*)]quinoline (II-12):[22]

Pyridone (**II-11**) (0.48 mmol, 100 mg) and Ag_2CO_3 (0.96 mmol, 264 mg) were dissolved in chloroform (80 mL). The resulting solution was sonciated for 30 min. Iodomethane (4.8 mmol, 681 mg) was slowly added to the reaction mixture. The reaction mixture was refluxed in the dark for 2 h. The mixture was filtered through celite and concentrated *in vaccuo.* The product was purified by flash chromatography on silica gel (eluent: 4:1 Hex:EtOAc) to afford **II-12** as white needle crystals (75 mg, 71% yield): mp 73-75 ^{o}C (lit.[22] mp 77.5-78.5 ^{o}C);^{1}H NMR ($CDCl_3$, 300 MHz) δ 1.97 (t, 2 H, *J*= 6.9 Hz), 2.88 (s, 2 H), δ2.97 (t, 2 H, *J*= 6.9 Hz), 3.87 (s, 3 H), 4.02 (s, 2H), 6.49 (d, 1 H, *J*= 8.1 Hz), 7.20 (d, 1 H, *J*= 8.1 Hz). ^{13}C NMR ($CDCl_3$, 100 MHz) δ 31.01, 31.70, 53.49, 64.81, 108.08, 108.27, 121.65, 140.02, 152.92,162.46. All values are consistent with literature. [22]

6-Oxo-2-methoxy-5,6,7,8-tetrahydroquinoline-5-methylcarbonyl (II-14):[22]

Compound **II-12** (73 mg, 0.33 mmol) was dissolved in a 5% HCl solution in acetone (1:1) and refluxed overnight. Acetone was removed *in vacuo*. The aqueous layer was then basified with sodium bicarbonate until no more gas evolution was noted. The resulting solution was then extracted with ethyl acetate. The combined organic layers were washed with brine, dried over $MgSO_4$ filtered and concentrated *in vacuo*. The resulting product **II-13** was used without further purification. To a solution containing

compound **II-13** (456 mg. 2.5 mmol) in dimethyl carbonate (15 mL) was added a solution sodium hydride (60% w/v in mineral oil, 240 mg, 10 mmol) in 5 mL of dimethyl carbonate. The reaction mixture was refluxed for 3 h after which the reaction was quenched with 10 mL of methanol. The solvents were removed *in vaccuo* and the neutrualized with a saturated solution of ammonium chloride. The solution was then extracted with ethyl acetate (50 mL x 3). The combined organic phases were dried over $MgSO_4$, filtered and concentrated *in vaccuo*. The product was purified by flash chromatography on silica gel (20:1 Hex:EtOAc) to afford **II-14** as an off-white solid (103 mg, 72% yield): mp 73-74 ^oC (lit.[22] mp 71-72 ^oC); ^1H NMR ($CDCl_3$, 300 MHz) δ 2.06 (t, 2H, *J*= 6. 9 Hz), 2.91 (t, 2H, *J*= 8.1 Hz), 3.90 (s, 6H), 6.55 (d, 1H, *J*= 8.7 Hz) 7.89 (d, 1H, *J*= 8.4 Hz); ^{13}C NMR ($CDCl_3$, 100 MHz) δ 29.3, 30.2, 52.0, 53.6, 98.5, 107.5, 120.0, 136.3, 151.3,161.3, 172.2, 177.0. All values are consistent with literature.[22]

2-Methylenepropane-1,3-diyl diacetate (II-7):[23]

1,3-(2-Methylene)propandiol (1.08 g, 12.27 mmol,) and 0.1 mL of pyridine were placed in a 25 mL round-bottomed flask. To this solution 8 mL of acetic anhydride was added. The mixture was then refluxed overnight. The excess acetic anhydride is removed by evaporation. After evaporation ice water was added to the resulting solution. Saturated sodium bicarbonate was then added until no more gas evolution was noted. The resulting mixture was then extracted with ethyl ether (3 x 20 mL). The combined organic phases were dried over $MgSO_4$ and concentrated to afford **II-7** as a clear colorless oil (2.16 g, 100% yield): ^1H NMR ($CDCl_3$, 300 MHz) δ 2.16 (s, 6H) 4.67 (s, 4H) 5.35 (s, 2H); ^{13}C NMR ($CDCl_3$, 100 MHz) δ 21.05, 64.72, 116.9, 138.83, 170.08. All values are consistent with literature.[23]

Dimethyl 2-methylenepropane-1,3-diyl dicarbonate (II-16):

1,3-(2-Methylene)propandiol (250 mg, 2.84 mmol) and DMAP (1.275 g, 5.68 mmol) were placed in a sealed 35 mL microwave reaction vessel and purged with nitrogen. The combined materials were dissolved in 15 mL of methylene chloride. The vessel was cooled to 0 ^oC and the methyl chloroformate (1.16 g, 8.52 mmol) was added dropwise to the stirred solution. The reaction vessel was then warmed to room temperate and placed in a microwave reactor for 90 min at 40 ^oC. The reaction was quenched with addition of

10 mL of aqueous saturated NaCl. The mixture was extracted with dichloromethane (3x 40 mL). The combined organic phases to dried over $MgSO_4$ and concentrated *in vacuo*. The resulting oil was subject flash silica gel chromatography and afforded the product **II-16** as a clear colorless oil (650 mg, 100% yield): ^{1}H NMR ($CDCl_3$, 300 MHz) δ 3.80 (s, 6H), 4.67 (s, 4H) 5.35 (s, 2H); ^{13}C NMR ($CDCl_3$, 100 MHz) δ 54.7, 67.4, 117.8, 137.6, 155.2. All data are consistent with literature values.[40]

Di-*n*-butyl 2-methylenepropane-1,3-diyl di-*n*-butyl dicarbonate (II-17):

1,3-(2-Methylene)propandiol was (250 mg, 2.84 mmol) and DMAP (1.275 g, 5.68 mmol) were placed in a sealed 35 mL microwave reaction vessel and purged with nitrogen. The combined materials were dissolved in 15 mL of dichloromethane. The vessel was cooled to 0 ^{o}C and the butyl chloroformate (1.16 g, 8.52 mmol) was added dropwise to the stirred solution. The reaction vessel was then warmed to room temperate and placed in a microwave reactor for 90 min at 40 ^{o}C. The reaction was quenched with addition of 10 mL of aqueous saturated NaCl. The mixture was extracted (3 x 40 mL) with dichloromethane. The combined organic phases were dried over $MgSO_4$ and concentrated *in vacuo*. The resulting oil was subject flash chromatography on silica gel (3:1 hexane:EtOAc) and afforded the product **II-17** was as clear colorless oil (430 mg, 53% yield): IR (NaCl plate; cm^{-1}) 2961.46,2875.34, 1747.73, 1663.07, 1582.74, 1642.81, 1396.68, 1244.15, 1156.85, 1119.03, 1156.85; ^{1}H NMR ($CDCl_3$, 300 MHz) δ 0.88(t, 6H, *J*= 7.5 Hz) 1.33 (q, 4H, *J*= 7.8 Hz), 1.59 (q, 4H, *J*= 8.1 Hz), 4.09 (t, 4H, *J*= 6.9 Hz), 4.63 (s, 4H), 5.31 (s, 2H);^{13}C NMR ($CDCl_3$, 100 MHz) δ 13.4, 18.7, 67.3, 67.9, 154.8; HRMS: pending

2-Methylenepropane-1, 3-diyl divinyl dicarbonate (II-18):

1,3-(2-Methylene)propandiol was (2.84 mmol, 250 mg) and DMAP (1.275 g, 5.68 mmol) were placed in a sealed 35 mL microwave reaction vessel and purged with nitrogen. The combined materials were dissolved in 15 mL of dichloromethane. The vessel was cooled to 0 ^{o}C and the butyl chloroformate (1.16 g, 8.52 mmol) was added dropwise to the stirred solution. The reaction vessel was then warmed to room temperate and placed in a microwave reactor for 90 min at 40 ^{o}C. The reaction was quenched with addition of 10 mL of aqueous saturated NaCl. The mixture was extracted with dichloromethane (3 x 40

mL). The combined organic phases were dried over $MgSO_4$ and concentrated *in vacuo*. The resulting oil was subject flash silica gel chromatography and afforded the product **II-18** was as clear light yellow oil (473 mg, 72% yield): IR (NaCl plate; cm^{-1}) 2928.64, 2253.95, 1761.58, 1651.24, 1460.05, 1386.28, 1300.67, 1244.02, 1156.99, 1089.33; ^1H NMR ($CDCl_3$, 300 MHz) δ 4.58 (dd, 2H, *J*=1.2 Hz, *J*= 5.4 Hz), 4.74 (s, 4H), 4.90 (dd, 2H, *J*= 0.9 Hz, *J*= 3 Hz), 5.41 (s, 2H), 7.03 (dd, 2H, *J*= 6 Hz, *J*= 21 Hz); ^{13}C NMR ($CDCl_3$, 100 MHz) δ 68.0, 98.1, 119.4, 136.7, 142.5, 152.4. HRMS: pending

2-Methylenepropane-1,3-diyl dibenzyl dicarbonate (II-19):

1,3-(2-Methylene)-propandiol was (250 mg, 2.84 mmol) and DMAP (1.275 g, 5.68 mmol) were placed in a sealed 35 mL microwave reaction vessel and purged with nitrogen. The combined materials were dissolved in 15 mL of dichloromethane. The vessel was cooled to 0 ^oC and the butyl chloroformate (1.16 g, 8.52 mmol) was added dropwise to the stirred solution. The reaction vessel was then warmed to room temperate and placed in a microwave reactor for 90 min at 40 ^oC. The reaction was quenched with addition of 10 mL of aqueous saturated NaCl. The mixture was extracted with dichloromethane (3 x 40 mL) . The combined organic phases over dried over $MgSO_4$ and concentrated *in vacuo*. The resulting oil was subject flash silica gel chromatography and afforded the product **II-19** was as clear colorless oil (430 mg, 53% yield): ^1H NMR ($CDCl_3$, 300 MHz) δ 4.76 (s, 4H)**,** 5.23 (s, 2H), 5.422(s 2H), 7.41 (m, 9H); ^{13}C NMR ($CDCl_3$, 100 MHz) δ 60.3, 67.7, 69.7, 118.2, 128.3, 128.5, 128.5, 137.4, 154.7; HRMS: pending

General Procedure for Catalytic Reactions:

A ligand (15 mol%), and a catalyst $[Pd(\eta_3\text{-}C_3H_3)Cl]2$ (2.4 mg, 2.5 mol %) and 2-methylene-1,3-propanediacetate (0.20 mmol, 34 mg) and **II-14** (100 mg, 0.13 mmol) were dissolved in 8 mL of dry solvent in a 10 mL microwave vial. The reaction mixture was then stirred at room temperature for 1 h and cooled to -45 ^oC for 30 min after which tetramethylguanidine (TMG) (37.4 mg, 0.33 mmol) was slowly added. The reaction mixture was stirred at – 45 ^oC for 12 h then warmed to room temperature and placed in a CEM Discover microwave apparatus for 90 min at 80 ^oC using the PowerMax® setting with no cooling. The mixture was transferred to a round-bottomed flask and the solvent is

removed *in vacuo*. The catalyst was removed by passing through a short silica gel plug (3:1 hexanes to ethyl acetate) and all fractions collected and concentrated. The solvent was evaporated and the resulting yellow oil was submitted to normal phase chiral HPLC with an eluent of 4% ispropanol in hexanes. The product was purified by flash chromatography on silica gel (20:1 Hexanes:EtOAc) to afford **II-8** as a light yellow oil (102 mg, 83% yield): ^{1}H NMR ($CDCl_3$, 300 MHz) δ 2.53 (2H, m), 2.75 (1H, m), 2.92 (m, 1H), 3.06 (2H, m), 3.40 (1H, dd, *J*= 18.4, *J*= 6.8), 3.78 (3H, s), 3.86 (3H, s), 4.47 (1H, s), 4.80 (1H, s), 6.54 (1H, d, *J*= 8.4 Hz), 6.94 (1H, d, *J*= 8.4 Hz); ^{13}C NMR ($CDCl_3$, 100 MHz) δ 40.4, 43.9, 45.6, 47.8, 52.6, 53.4, 62.0, 109.5, 116.3, 124.7, 137.5, 138.9, 151.3, 162.9, 171.3, 208.3. All values are consistent with literature.[24]

2.6 References

(1). (a) Söderberg, B. C. G., Transition metals in organic synthesis: highlights for the year 2002. *Coordin. Chem. Rev* **2004**, *248*, 1085-1101; (b) Tsuji, J.; Takahashi, H.; Morikawa, M., Organic synthesis bymeans of noble metal and compounds. XVII Reaction π-allylpalladium chloride with nucleophile *Tetrahedron Lett.* **1965**, *6*, 4387-4388; (c) Lu, Z.; Ma, S., Metal-catalyzed enantioselective allylation in asymmetric synthesis. *Angew. Chem. Int. Ed.* **2008**, *47*, 258-297.

(2). Evans, P. A.; Leahy, D. K., Recent developments in rhodium-catalyzed allylic substitution and carbocyclization reactions *Chemtracts* **2003**, *16*, 567.

(3). Matsushima, Y.; Onitsuka, K.; Kondo, T.; Mitsudo, T.-a.; Takahashi, S., Asymmetric catalysis of planar-chiral cyclopentadienylruthenium complexes in allylic amination and alkylation. *J. Am. Chem. Soc.* **2001**, *123*, 10405-10406.

(4). Bartels, B.; Helmchen, G., Ir-catalysed allylic substitution: mechanistic aspects and asymmetric synthesis with phosphorus amidites as ligands. *Chem. Comm.* **1999**, 741-742.

(5). Trost, B. M.; Hachiya, I., Asymmetric molybdenum-catalyzed alkylations. *J. Am. Chem. Soc.* **1998**, *120*, 1104-1105.

(6). Lloyd-Jones, G. C.; Pfaltz, A., Chiral phosphanodihydrooxazoles in asymmetric catalysis: tungsten-catalyzed allylic substitution. *Angew. Chem. Int. Ed.* **1995**, *34*, 462-464.

(7). Zijl, A. W. v.; Arnold, L. A.; Minnaard, A. J.; Feringa, B. L., Highly enantioselective copper-catalyzed allylic alkylation with phosphoramidite ligands. *Advan. Syn. Catal.* **2004**, *346*, 413-420.

(8). Trost, B. M., Asymmetric Allylic Alkylation, an enabling methodology. *J. Org. Chem.* **2004**, *69*, 5813-5837.

(9). Helmchen, G.; Kazmaier, U.; Forester, S., Enantioselective allylic substitution with carbon nucleophiles In *Catalytic Asymmetric Synthesis* Ojima, I., Ed. Wiley Hoboken 2010.

(10). Trost, B. M.; Strege, P. E., Asymmetric induction in catalytic allylic alkylation. *J. Am. Chem. Soc.* **1977**, *99*, 1649-1651.

(11). Trost, B. M.; Dietsch, T. J., New synthetic reactions. Asymmetric induction in allylic alkylations. *J. Am. Chem. Soc.* **1973**, *95*, 8200–8201.

(12). (a) Trost, B. M.; Vranken, D. L. V., Asymetric transition metal-catalyzed allylic alkylations. *Chem. Rev.* **1996**, *96*, 395-422; (b) Trost, B. M.; Verhoeven, T. R., Allylic alkylation. Palladium-catalyzed substitutions of allylic carboxylates. Stereo- and regiochemistry. *J. Am. Chem. Soc.* **1980**, *102*, 4730–4743.

(13). Trost, B. M.; Lee, C., Asymmetric allylic alkylation reactions. In *Catalytic Asymmetric Synthesis*, Ojima, I., Ed. Wiley-VCH: 2001.

(14). Trost, B. M.; Crawley, M. L., Asymmetric transition-metal-catalyzed allylic alkylations: Applications in total synthesis. *Chem. Rev.* **2003**, *103*, 2921–2944.

(15). Yoshizaki, H.; Satoh, H.; Sato, Y.; Nukui, S.; Shibasaki, M.; Mori, M., Palladium-mediated asymmetric synthesis of *cis*-3,6-disubstituted cyclohexenes. A short total synthesis of optically active (+)-γ -Lycorane. *J. Org. Chem.* **1995**, *60*, 2016-2021.

(16). Chapsal, B. D.; Ojima, I., Total synthesis of enantiopure (+)-γ-lycorane using highly efficient Pd-catalyzed asymmetric allylic alkylation. *Org. Lett.* **2005**, *8*, 1395-1398.

(17). Ernst, M.; Helmchen, G., A novel route to iridoids: enantioselective syntheses of isoiridomyrmecin and α-skytanthine *Synthesis* **2002**, *14*, 1953-1955.

(18). (a) Trost, B. M.; Schroeder, G. M., Palladium-catalyzed asymmetric allylic alkylation of barbituric acid derivatives: Enantioselective syntheses of cyclopentobarbital and pentobarbital. *J. Org. Chem.* **2000**, *65*, 1569-1573; (b) Trost, B. M.; Radinov, R.; Grenzer, E. M., Asymmetric alkylation of β-ketoesters. *J. Am. Chem. Soc.* **1997**, *119*, 7879–7880.

(19). Trost, B. M.; Chisholm, J. D.; Wrobleski, S. T.; Jung, M., Ruthenium-catalyzed alkene-alkyne coupling: Synthesis of the proposed structure of amphidinolide A. *J. Am. Chem. Soc.* **2002**, *124*, 12420–12421.

(20). Trost, B. M.; Tang, W., An efficient enantioselective synthesis of (-)-galanthamine *Angew. Chem. Int. Ed.* **2002**, *41*, 2795-2797.

(21). Rajendran, V.; Rong, S.-B.; Saxena, A.; Doctor, B. P.; Kozikowski, A. P., Synthesis of a hybrid analog of the acetylcholinesterase inhibitors huperzine-A and huperzine-B *Tetrahedron Lett.* **2001**, *42*, 5359-5361.

(22). Kozikowski, A. P.; Xia, Y., A practical synthesis of the Chinese "nootropic" agent Huperzine A: A possible lead in the treatment of Alzheimer's disease. *J. Am. Chem. Soc.* **1989**, *111*, 4116-4117.

(23). Campiani, G.; Sun, L.-Q.; Kozikowski, A. P.; Aagaard, P. a.; McKinney, M., A palladium-catalyzed route to huperzine A and Its analogues and their anticholinesterase activity. *J. Org. Chem.* **1993**, *58*, 7660-7669.

(24). Kaneko, S.; Yoshino, T.; Katoh, T.; Terashima, S., A novel enantioselective synthesis of the key intermediate of (-)-huperzine A employing asymmetric palladium-catalyzed bicycloannulation *Tetrahedron: Asymmetry* **1997**, *8*, 829-832.

(25). He, X.-C.; Wang, B.; Yu, G.; Bai, D., Studies on the asymmetric synthesis of huperzine A. Part 2: Highly enantioselective palladium-catalyzed bicycloannulation of the β-keto-ester using new chiral ferrocenylphosphine ligands. *Tetrahedron: Asymmetry* **2001**, *12*, 3213-3216.

(26). Chassaing, C.; Haudrechy, A.; Langlois, Y., Asymmetric palladium annulation: formal synthesis of (+)-huperzine-A *Tetrahedron Lett.* **1999**, *40*, 8805-8809.

(27). Ma, X.; Gang, D. R., The lycopodium alkaloids. *Nat. Prod. Rep.* **2004**, *21*, 752 - 772.

(28). Bai, D., Development of huperzine A and B for the treatment of Alzheimer's disease *Pure Appl. Chem.* **2007**, *79*, 469-479.

(29). Kozikowski, A. P.; Tuckmantel, W., Chemistry, pharmacology, and clinical efficacy of the Chinese nootropic agent uperzine A. *Acc. Chem Res.* **1999**, *32*, 641-650.

(30). (a) Xiao, X. Q.; Yang, J. W.; Tang, X. C., Huperzine A protects rat pheochromocytoma cells against hydrogen peroxide-induced injury. *Neurosci. Lett.* **1999**, *275*, 73-76; (b) Xiao, X. Q.; Zhang, H. Y.; Tang, X. C., Huperzine A attenuates amyloid -peptide fragment 25-35-induced apoptosis in rat cortical neurons via inhibiting reactive oxygen species formation and caspase-3 activation. *J. Neurosci. Res.* **2001**, *67*, 30-36.

(31). Aisen, P. S. http://clinicaltrials.gov/ct2/show/NCT00083590. (accessed June 3).

(32). Brookmeyera, R.; Johnsona, E.; Ziegler-Grahamb, K.; Arrighic, H. M., Forecasting the global burden of Alzheimer's disease. *Alzheimer's & Dementia* **2007**, *3*, 186-191.

(33). Kozikowski, A. P.; Reddy, E. R.; Miller, C. P., A simplified route to a key intermediate in the synthesis of the Chinese nootropic agent Huperizine-A. *J. Chem. Soc. Perkin Trans* **1990**, 195-197.

(34). Campiani, G.; Sun, L. Q.; Kozikowski, A. P.; Patricia Aagaard; McKinney, M., A palladium-catalyzed route to huperzine A and its analogs and their anticholinesterase activity. *J. Org. Chem.* **1993**, *58*, 7660-7669.

(35). Choi, H., Quaterly Report. 2003.

(36). Shi, C.; Ojima, I., Asymmetric synthesis of 1-vinyltetrahydroisoquinoline through Pd-catalyzed intramolecular allylic amination. *Tetrahedron* **2007**, *63*, 8563-8570.

(37). Kappe, C. O., Controlled microwave heating in modern organic synthesis. *Angew. Chem. Int. Ed.* **2004**, *43*, 6250-6284.

(38). Gabriel, C.; Gabriel, S.; Grant, E. H.; Halstead, B. S. J.; Mingos, D. M. P., Dielectric parameters relevant to microwave dielectric heating. *Chem. Soc. Rev.* **1998**, *27* 213-223

(39). Gottlieb, H. E.; Kotlyar, V.; Nudelman, A., NMR chemical shifts of common laboratory solvents as trace impurities. *J. Org. Chem.* **1997**, *62*, 7512-7515.

(40). Salamone, S. G.; Dudley, G. B., A Ring-Expansion Approach to Roseophilin. *Org, Lett.* **2005**, *7*, 4443-4445.

Chapter 3

Introduction to Cyclohydrocarbonylation

3.0 Introduction

The development of highly efficient chemical processes for the synthesis of natural and unnatural nitrogen-based heterocycles of biological interest has been a focus within modern organic chemistry. One of the most widely studied methods for the synthesis of these compounds utilizes transition metal-catalyzed cyclizations.[1] Such transformations allow simple acyclic systems to be converted into complex mono-, bi- and tricyclic compounds in an atom economical fashion. The catalytic construction of heterocyclic molecules has been classified into two distinctive processes: (1) carbon-carbon bond formation (2) carbon-heteroatom bond formation from the corresponding acyclic systems as shown in **Figure III-1**.[1]

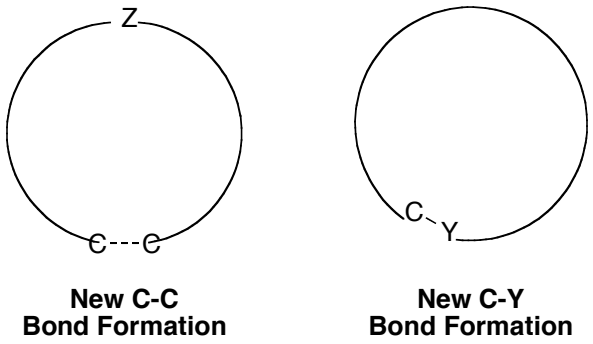

Figure III-1: Classification of heterocyclic formations

Among these cyclization processes, cyclohydrocarbonylation has emerged as a powerful reaction in the synthesis of various nitrogen-based and other heteroatom based cyclization reactions.[2] Cyclohydrocarbonylation is an intramolecular cascade process that commences with hydroformylation of a functionalized olefin to form an aldehyde intermediate, followed by concomitant intramolecular nucleophilic addition to the newly formed aldehyde resulting in a cyclization. Furthermore, the intermediate acyl-metal species formed during the formylation process may also undergo nucleophilic addition affording cyclic carbonyl adducts (**Scheme III-1**).

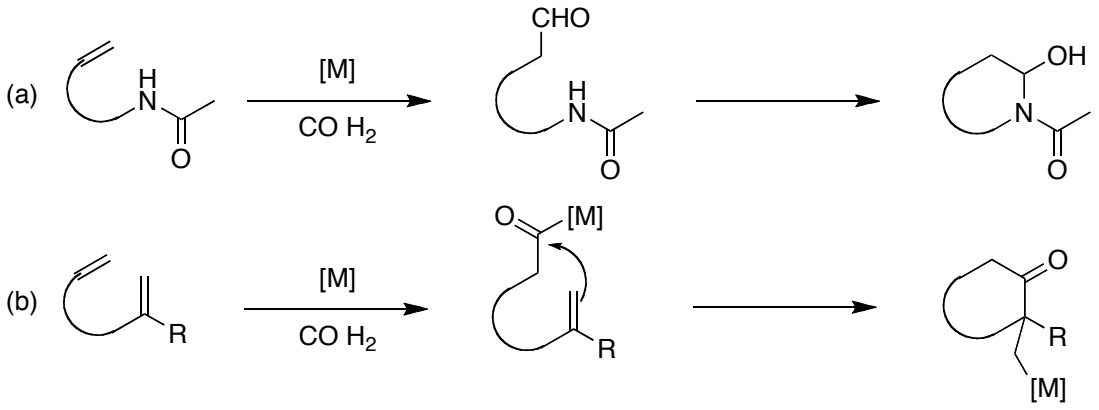

Scheme III-1: Cyclohydrocarbonylation reaction (a) nucleophilic attack to the aldehyde (b) nucleophilic attack of the acyl-metal species

In order to gain further insight into this powerful reaction, we need to deconstruct the cascade process into the following individual processes: hydroformylation, *N*-acyliminum formation and the subsequent nucleophilic addition. We will first examine the hydroformylation process.

3.1 Hydroformylation

In the presence of a metal catalyst and carbon monoxide, hydroformylation converts alkenes into the corresponding linear or branched aldehyde (**Scheme III-2**).[3]

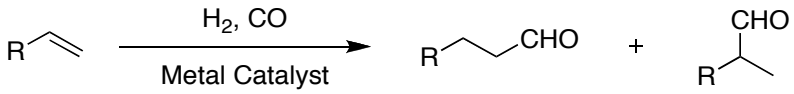

Scheme III-2: Hydroformylation reaction

The hydroformylation process was first discovered in 1938 by Otto Roelen using $HCo(CO)_4$ generated *in situ* from $Co_2(CO)_8$ under high temperatures and high pressures of carbon monoxide and hydrogen.[4]The power of this reaction was quickly understood, and the reaction was employed on an industrial scale in 1947 by Ruhrchemie for the synthesis of *n*-butanal although a substantial amount of the branched aldehyde was also produced.[5]

Over the years, several other metal species, including, platinum and ruthenium, were investigated for this reaction in efforts to improve the linear to branch selectivity. Cobalt, however, remained more advantageous, as it was more efficient than either platinum or ruthenium.[3] A dramatic change in metal preference came in the late 1960s Wilkinson and co-workers published the first paper formally detailing the use of a rhodium-phosphine-based catalyst for the hydroformylation of various alkenes. They employed $RhH(CO)(PPh_3)_2$ as a catalyst which afforded nearly 95% of the straight chain aldehyde at ambient temperature and pressure.[6] As time progressed, rhodium became the metal of choice mainly because it has a higher turnover value and requires lower temperatures and pressures in comparison to cobalt. Although rhodium is far more expensive, (trading at $79/g) than cobalt ($0.04/g) it is still the preferred metal for industrial reactions as it can be recovered and recycled more easily than cobalt. In fact, Rhone-Poulenc has a commercialized process for the production of butanal using a water-soluble rhodium catalyst.[7]

The mechanism of cobalt-catalyzed hydroformylation has been extensively studied and was detailed by Breslow and Heck in 1961.[8] The mechanism of the rhodium-catalyzed reaction is remarkably similar to the cobalt-catalyzed version with only minute variations. The generally accepted rhodium catalyzed mechanism, shown in **Scheme III-3** (only formation of the linear adduct is shown) was proposed by Wilkinson using IR and NMR methods in the same year he reported the first rhodium-catalyzed hydroformylation.[8]

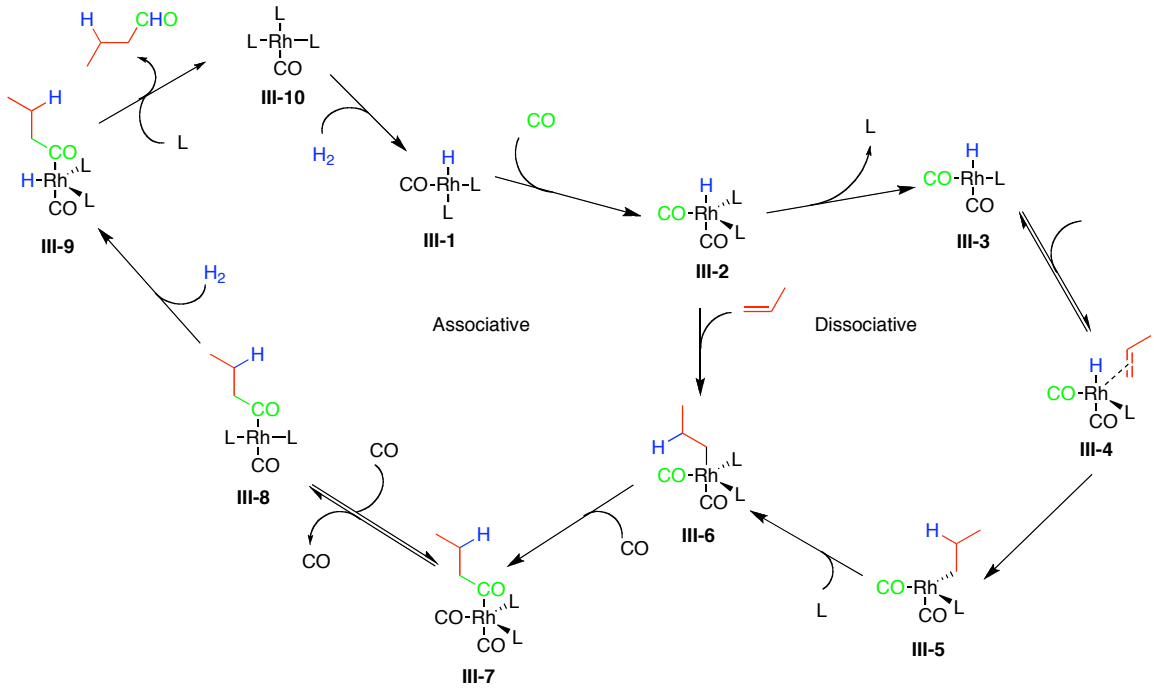

Scheme III-3: Mechanism for rhodium catalyzed hydroformylation[3]

Most mechanistic studies have suggested that the active catalyst species in the rhodium catalyzed hydroformylation reaction, species **III-2** (**Scheme III-3**). This active 18-electron species is typically generated *in situ* by the acquisition of one CO molecule and the loss of a ligand, typically a phosphine. Following the generation of hydrido-metal species **III-2**, two varying mechanistic pathways emerge. The associative pathway dominates at catalyst concentrations >6 mM, while the dissociative pathway involves a second more active catalyst species **III-3**. Under traditional industrial methods, the associative pathway dominates, as those reactions typically use a large excess of triphenylphosphine. Both pathways converge to form the alkyl metal species **III-6** formed by migratory insertion of hydrogen, which is followed by a second migratory insertion of CO to form the acyl-rhodium species **III-7**. Following formation of the acyl-rhodium species, association of CO and hydrogen gives intermediate species **III-9**. Reductive elimination then affords the desired oxo-product and regenerate the catalyst **III-10**.

In the originally proposed associative mechanism, it was suggested that coordination of the olefin (shown in red, **Scheme III-3**) with **III-2** afforded a hexacoordinate 20-electron Rh-olefin species. However, the formation of a 20-electron

species was later found to violate the generally accepted 18-electron rule for transition metals.[9] Thus, an alternative mechanism to accommodate the 18-electron rule was proposed and is shown below in **Scheme III-4**.

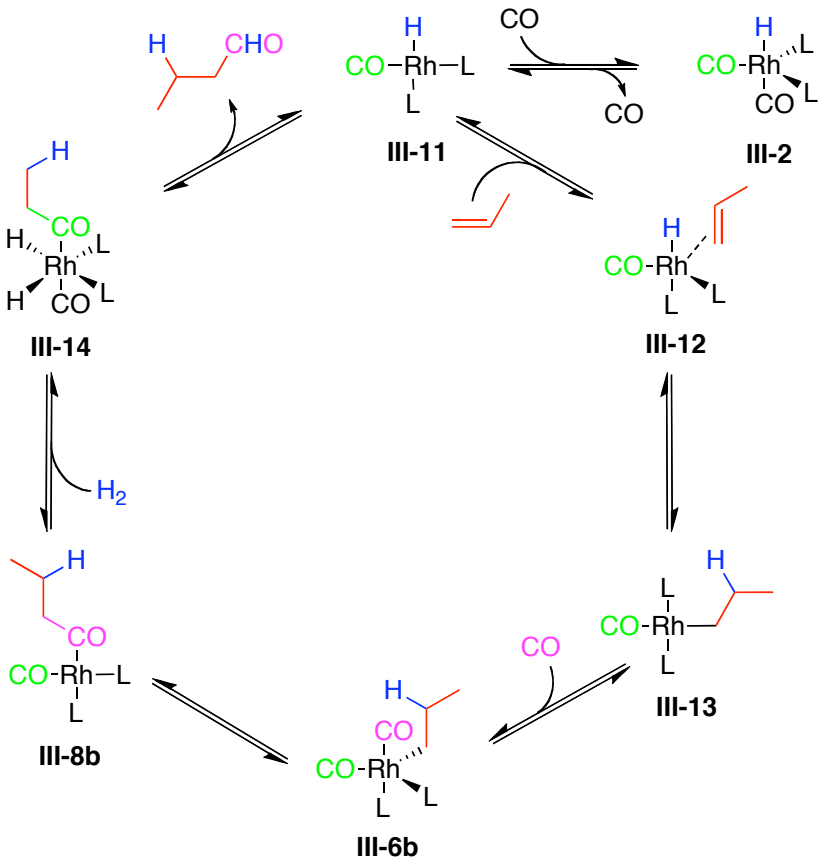

Scheme III-4: Alternative mechanism for rhodium catalyzed hydroformylation[3]

In the modified mechanism, there is an equilibrium between **III-2** and **III-11** with net loss of the CO ligand in the catalytic process, making **III-11** the active catalyst. This equilibrium avoids the 20-electron hexa-coordinate rhodium species seen in the first mechanism. Following the formation of **III-11**, association of the olefin affords complex **III-12** that is quickly converted to the species **III-13** with a 1,2-migratory insertion of hydrogen. This process is followed by CO coordination to give **III-6b** that undergoes a 1,1-migratory insertion of CO giving the acyl-Rh species **III-8b**. Finally, oxidative addition of hydrogen generates species **III-14** (an 18-electron system) that undergoes reductive elimination to afford the oxo-product, which may be the linear or the branched

adduct depending on the reaction conditions. Although only a single adduct is shown in **Scheme III-4**, the so-called branch adduct is also a product of this reaction.

Industrial applications of hydroformylation are focused on the production of linear aldehydes. Thus, the regioselective control of hydroformylation has been well studied.[3-4;10] As with most transition metal-catalyzed reactions, stereoelectronic control as dictated by ligands has been vital in affecting the stereo- and regiochemistry of hydroformylation. Considerable efforts have been put forth in examining the stereoelectronic role of various ligand types. High regioselectivities have been reported for both diphosphine and diphosphite-modified catalysts.[11] The mechanism indicates that selectivity is determined in the step that converts the penta-coordinate Rh-alkene (**III-12**) species into either the branched or linear Rh-alkyl species shown in **Scheme III-5**.[12]

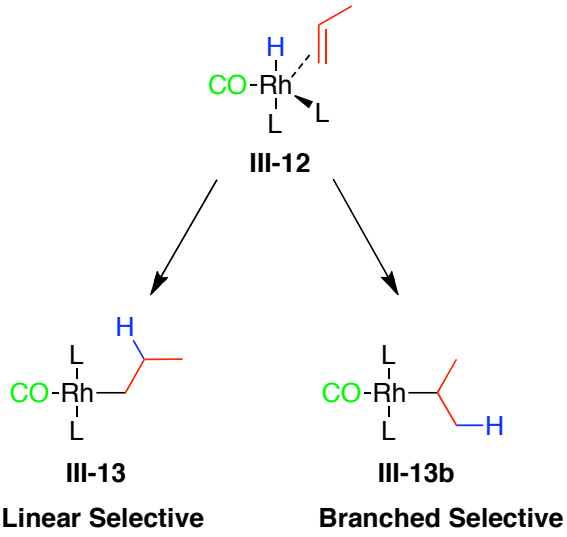

Scheme III-5: Linear and branched adducts

In turn, complex **III-12** is judged to play a critical role in controlling the regioselectivity. Resulting from their extensive use in catalysis, the influence of phosphine ligands has been studied in great detail.[13] As a result, several ligands effective for linear selective hydroformylation have been developed (**Figure III-2**).

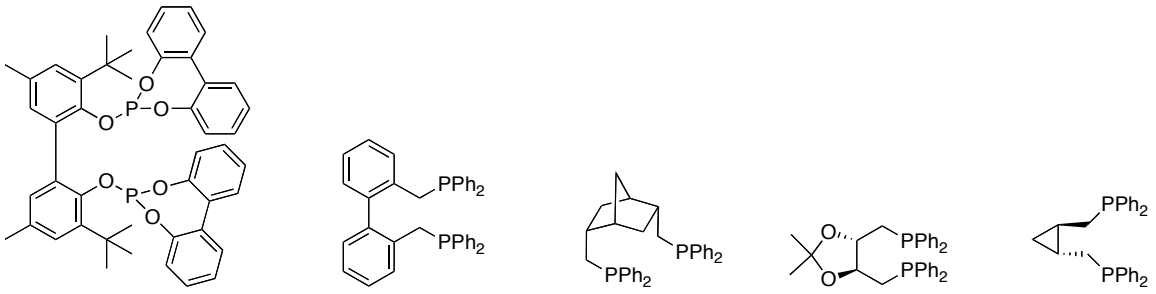

Figure III-2: Phosphine ligands for linear selective hydroformylation

It has long been suggested that ligand bite angles play a significant role in affecting the stereo- and regio-selectivity of various transition metal-catalyzed reactions. A summary of the selectivity distribution in the hydroformylation reaction as a function of bite-angle (phosphorus-metal-phosphorus) measurements are summarized in **Table III-1**.

Table III-1: Summary of ligand selectivity and bite angles[4]

Entry	Ligand	Bite Angle	*n/i (normal:iso)*
1	**III-15**	119.5	53
2	**III-16**	113/120	25
3	**III-17**	126	2.6-4.3
4	**III-18**	102	40.-8.5
5	**III-19**	107	4.4-12
6	**PPh_3**	-	2.4

As shown in **Table III-1** ligands with a bite angle near 120^o give higher linear to branch selectivity. Diphosphine ligands are known to be in equilibrium between the diequatorial (ee) and equatorial-apical (ea) configuration as shown for triphenylphosphine in **Scheme III-6**.

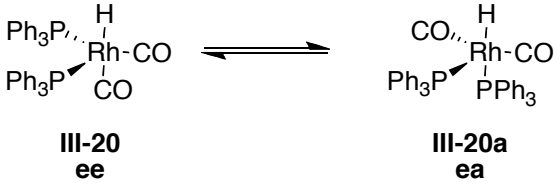

Scheme III-6: Ligand equilibrium

Casey attributed the observed correlation between bite-angle and selectivity to the diequatorial coordination mode of the bisphosphine ligands.[11b] He suggested that ligands with bite angles close to 120^{o} afford linear selectivity as a result of the ee-ea equilibrium, primarily resulting from steric hindrance. However, van Leeuwen and co-workers found no correlation between natural bite angles and the ligand backbones. They found no increase in ee chelation preference in ligands with naturally wider bite angles. They further noted that, bite angle does not have a clear effect on hydroformylation selectivity. They did, however, note that chelation control is determined by bite angles in ligands with naturally large and narrow bite angles.[12] It still remains unclear how bite angles influence hydroformylation selectivity. However, it is clear that bulkier ligands tend to afford the linear adduct. In an effort to classify the stereoelectronic effects of the various ligands, Tolman introduced the cone angle concept θ as a measure of steric bulk and ν parameter as a measure of electronic properties.[14] These two conditions may be stronger predictors of normal to isomeric selectivity.

Hydroformylation, in addition to affording two major isomeric products, is also a highly regioselective process. In general, simple-vinyl, and unfunctionalized olefins are quite reactive towards hydroformylation requiring only ambient temperature and pressure for the reactions.[3;6] More substituted olefins, such as geminal and vicinal disubstituted olefins, tend to be several orders of magnitude less reactive than the vinyl olefins, requiring temperature much above 80 ^{o}C and pressures upwards of 10 atmospheres. Trisubstituted olefins are much less reactive towards hydroformylation requiring pressures upwards of 100 atm. A summary of the reactivity trends is shown in Figure **III-3**.

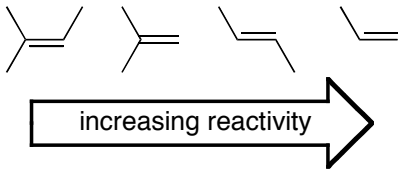

Figure III-3: Olefin reactivity

These distinct conditions required for the various substituted olefins can be exploited as hydroformylation is applied in the synthetic pathway. Accordingly, a molecule containing more than one type of olefin can be hydroformylated with excellent selectivity for a targeted olefin. Domino reactions that involve hydroformylation can take particular advantage of this regioselective feature, making hydroformylation a more synthetically versatile process. With in depth understanding of hydroformylation, we can now explore the cyclohydrocarbonylation process.

3.2 Cyclohydrocarbonylation

Cyclohydrocarbonylation (CHC) was first developed by Izawa in 1971[15] in the cobalt-catalyzed carbonylation for the synthesis of *trans*-6-methypipecolic acid owing origination to Wakamatsu's aminocarbonylation process.[16] The overall cyclohydrocarbonylative process was further developed with rhodium and applied in a variety of syntheses by Ojima and co-workers.[17] The complete application of this process to organic synthesis was primarily due to the development of various linear selective phosphorus ligands for hydroformylation. The CHC reaction has been classified into four basic reactions: (1) amidocarbonylation (2) aminocarbonylation (3) cyclohydrocarbonylation with carbon-nucleophiles (4) and other types of cyclohydrocarbonylation reactions as shown in Scheme **III-7**.

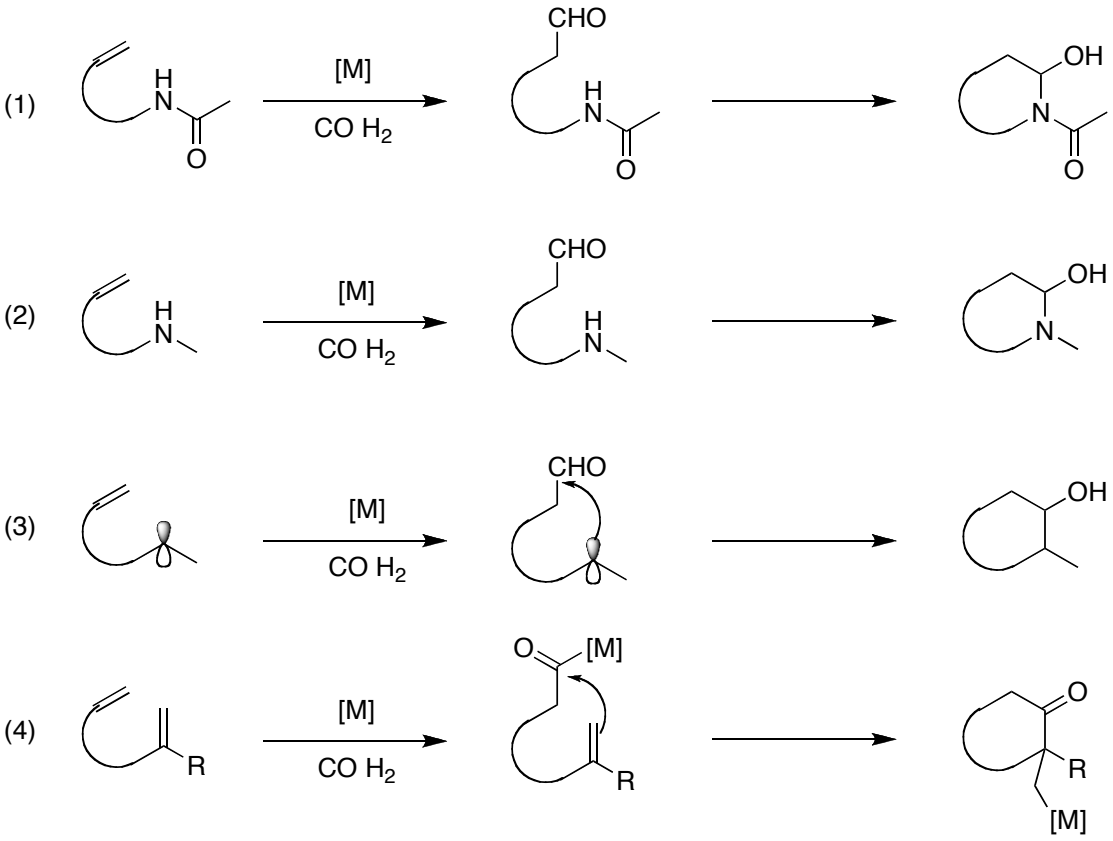

Scheme III-7: (1) Amidocarbonylation (2) Aminocarbonylation (3) CHC with carbon nucleophiles (4) Acyl-metal trapping [18]

Intramolecular amidocarbonylation is defined as hydroformylation of an olefin followed by concomitant cyclization *via* nucleophilic addition of either an amide or carbamate functional groups. Furthermore, the hemiamidal intermediate can be further dehydrated to afford either the enamide or the *N*-acyliminium ion, both of which can be further trapped by a secondary nucleophile species in both an inter and intramolecular fashion as seen in **Scheme III-8**.[19] This secondary cyclization for both types of reactions has been long used in synthesis, but only a few synthetic routes have utilized this strategy as a one-pot two-step process.

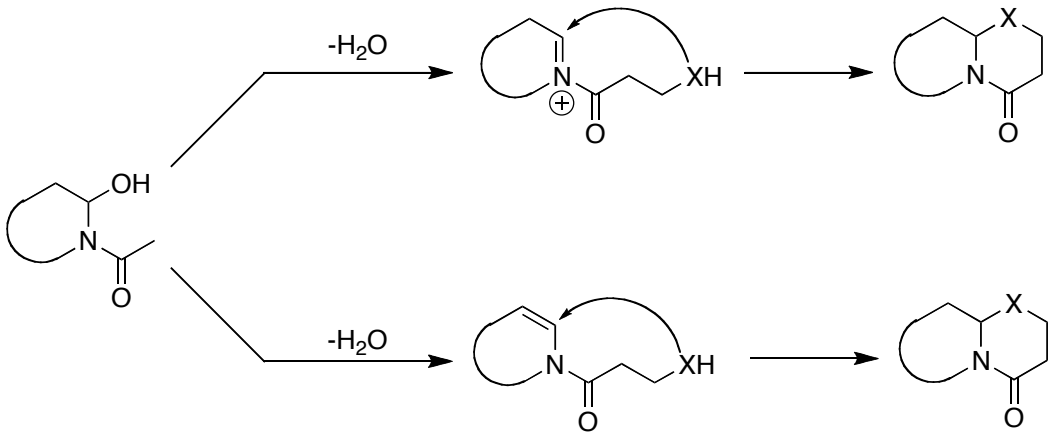

Scheme III-8: Secondary cyclization of N-acyliminium and enamide species

Ojima and co-workers employed this method in their synthesis of pyrollizidine alkaloids (+/-)-isoretronecanol (**III-24**) and (+/-)-trachlanthamidine (**III-25**) as shown below in **Scheme III-9**. [20]

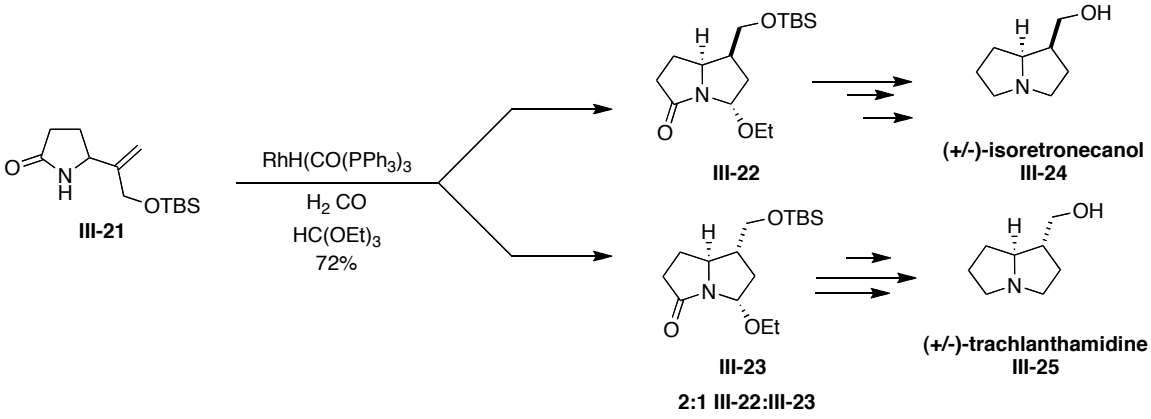

Scheme III-9: Cyclohydrocarbonylation reaction toward pyrollizidine alkaloids

It is noteworthy to mention here that the aminocarbonylation reaction is identical to amidocarbonylation, but the underlying difference is the intermediate species that is formed. In aminocarbonylation, a less reactive iminium ion is formed. This decrease in activity is easily observed when comparing electron density diagrams obtained from PC Spartan (version 8.0, PM3 semi-empirical method) calculation shown in **Figure III-3** below. The *N*-acyliminium species shows lower electron density (deeper blue color) around the electrophilic carbon, whereas in the case of the iminium the same is not observed.

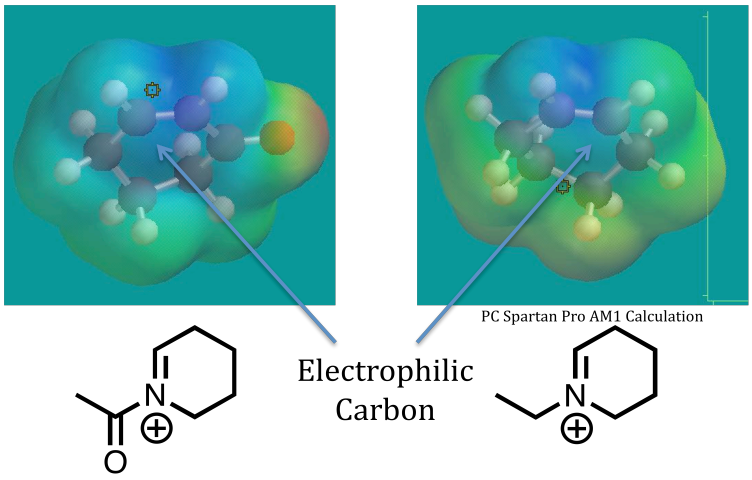

Figure III-4: Electron density of intermediate species

Thus, one can easily envision why *N*-acyliminium cyclizations are more facile. In spite of this notion, iminium-cyclizations are still employed. In 1995, Campi *et al*. reported rhodium-catalyzed aminocarbonylation as a rapid means for the synthesis of the quinazoline skeleton from 2(*N*-allylaminomethyl)aniline (**III-26**) shown below in **Scheme III-10**.[21]

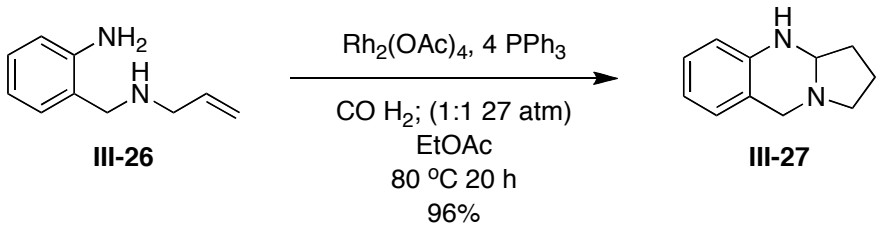

Scheme III-10: CHC access to quinazoline skeleton

Following the application of the linear selective ligand BIPHEPHOS by UnionCarbide and then Buchwald,[22] Ojima and co-workers reported an efficient CHC-mediated route toward pipecolic acid derivatives starting with vinylglycine derivates as shown in **Scheme III-11**. The protected-pipecolate adduct (**III-29**) was obtained in quantitative yield following the CHC reaction and were modified to afford compound **III-30**.

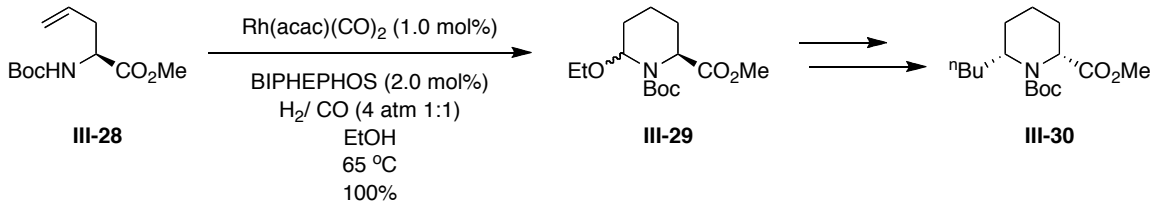

Scheme III-11: CHC application to pipecolic acid [23]

They further applied this process to a short total synthesis of Prosopinine employing a Rh-BIPHEPHOS-catalyzed aminocarbonylation as the key-step (**Scheme III-12**).[17f]

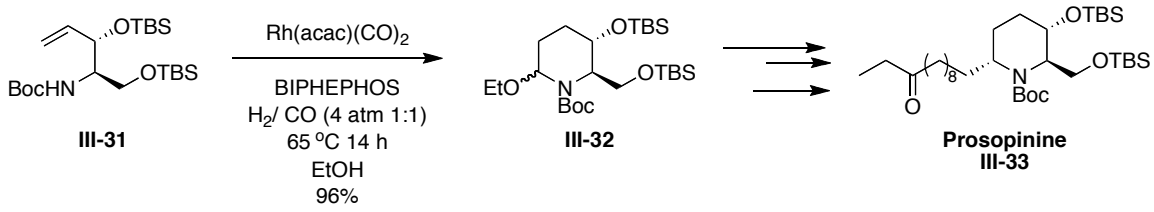

Scheme III-12: Synthesis of prosopinine

More recently, Ojima and co-workers successfully applied the CHC process in the synthesis of enantiopure derivatives of kainic acid or homokainoids, which are conformationally rigidified (*S*)-glutamic acids as shown in **Scheme III-13**. [17b;24] The CHC process afforded key intermediate **III-35** in near quantitative yields which was then transformed to the desired homokainic acid **III-36**.

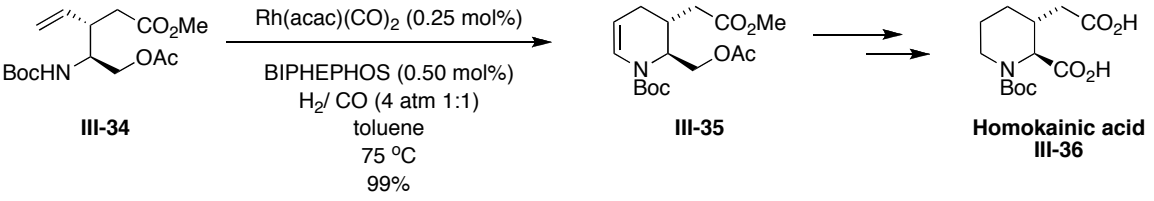

Scheme III-13: CHC-application to Kainic acid derivatives[17b;24]

Moreover, Chiou employed the CHC-process in the synthesis of enantiopure 3-hydroxypiperidine (**III-38**) derivatives which were afforded in 91% isolated yield; following a direct reductive-cleavage of the α-methoxy enamide adduct using a boron trifluoride etherate complex and a hydrosilane following the CHC reaction (**Scheme III-14**).[23]

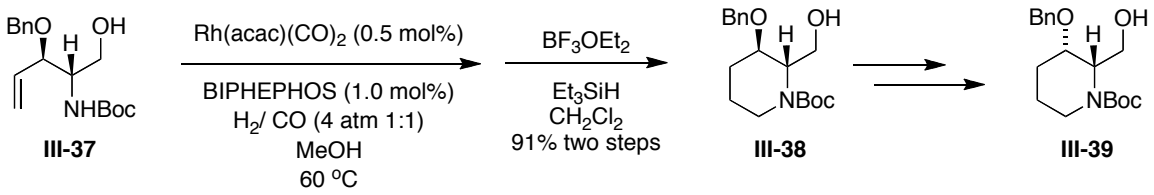

Scheme III-14: CHC application to 3-hydroxypiperidine [23]

The reports shown above demonstrate the versatility of the CHC reaction in its application toward the synthesis of the various alkaloid types. Applications of the CHC-reaction are limited only to how creatively it can be applied to synthesis. The overall reaction has been shown to be versatile and tolerant of various functional groups including –Boc, -*O*-benzyl, silyl-ethers, and esters. Thus, continued development of this process is invaluable to the development of alkaloid analogues, particularly ones with promising pharmacological efficacy.

3.3 References

(1). Nakamura, I.; Yamamoto, Y., Transition-Metal-Catalyzed Reactions in Heterocyclic Synthesis. *Chem. Rev.* **2004**, *104*, 2127–2198.

(2). (a) Chiou, W.-H.; Lee, S.-Y.; Ojima, I., Recent advances in cyclohydrocarbonylation reactions *Can. J. Chem.* **2005**, *83*, 681-692; (b) Ojima, I., New cyclization reaction in organic syntheses. *Pure Appl. Chem* **2002**, *74*, 159-166; (c) Varchi, G.; Ojima, I., Synthesis of heterocycles through hydrosilylation, silylformylation, silylcarbocyclization and cyclohydrocarbonylation reactions. *Current Org. Chem.* **2006**, *10*, 1341-1362.

(3). Ojima, I.; Tsai, C. Y.; Tzarmarioudaki, M.; Bonafoux, D., The hydroformylation reaction. In *Organic Reactions* J. Wiley & Son: 2000; pp 1-354.

(4). Yamashita, M.; Nozaki, K., Hydroformylation other hydrocarbonylations and oxidative alkoxycarbonylation. In *Comprehensive Organometallic Chemistry III*, Mingos, D. M. P.; Carbtree, R. H., Eds. Elsevier 2007.

(5). Cornils, B.; Herrmann, W. A.; Rasch, M., Otto Roelen, pioneer in industrial homogeneous catalysis. *Angew. Chem. Int. Ed.* **1994**, *33*, 2144-2163.

(6). Evans, D.; Osborn, J. A.; Wilkinson, G., Hydroformylation of alkenes by use of rhodium complex catalysts. *J. Chem. Soc.* **1968**, 3133-3142.

(7). Cornils, B.; Kuntz, E. G., Introducing TPPTS and related ligands for industrial biphasic processes. *J. Organomet.. Chem.* **1995**, *502*, 177-186.

(8). Heck, R. F.; Breslow, D. S., The reaction of cobalt hydrotetracarbonyl with olefins. *J. Am. Chem. Soc.* **1961**, *83*, 4023-4027.

(9). Carbtree, R. H., *The organomettalic chemistry of the transitions metals* 4th ed.; John Wiley and Sons Hoboken, New Jersey **2005**.

(10). (a) Agbossou, F.; Carpentier, J.-F.; Mortreux, A., Asymmetric hydroformylation. *Chem. Rev.* **1995**, *95*, 2485–2506; (b) van Leeuwen, P. W. N. M.; Claver, C., *Rhodium catalyzed hydroformylation* Kluwer Dordrecht, **2000**.

(11). (a) Buisman, G. J. H.; Veen, L. A. v. d.; Klootwijk, A.; Lange, W. G. J. d.; Kamer, P. C. J.; Leeuwen, P. W. N. M. v.; Vogt, D., Chiral cooperativity in diastereomeric diphosphite ligands: effects on the rhodium-catalyzed

enantioselective hydroformylation of styrene. *Organmetallics* **1997**, *15*, 2929-2939; (b) Casey, C. P.; Whiteker, G. T.; Melville, M. G.; Petrovich, L. M.; Jr., J. A. G.; Powell, D. R., Diphosphines with natural bite angles near 120" increase selectivity for n-aldehyde formation in rhodium-catalyzed hydroformylation. *J. Am. Chem. Soc.* **1992**, *114*, 5535-5545; (c) Kranenburg, M.; Burgt, Y. E. M. v. d.; Kamer, P. C. J.; Leeuwen, P. W. N. M. v.; Goubitz, K.; Fraanje, J., New diphosphine ligands based on heterocyclic aromatics inducing very high regioselectivity in rhodium-catalyzed hydroformylation: effect of the bite angle. *Organometallics* **1995**, *14*, 3081–3089.

(12). Veen, L. A. v. d.; Keeven, P. H.; Schoemaker, G. C.; Reek, J. N. H.; Kamer, P. C. J.; Leeuwen, P. W. N. M. v.; Lutz, M.; Spek, A. L., Origin of the bite angle effect on rhodium diphosphine catalyzed hydroformylation *Organmetallics* **2000**, *19*, 872-883.

(13). Beller, M.; Cornils, B.; Frohning, C. D.; Kohlpaintner, C. W., Progress in hydroformylation and carbonylation. *J. Mol. Catal. A* **1995**, *104*, 17-85.

(14). Tolman, C. A., Steric effects of phosphorus ligands in organometallic chemistry and homogeneous catalysis. *Chem. Rev.* **1977**, *77*, 313–348.

(15). Izawa, K.; Nishi, S.; Asada, S., Synthesis of N-acyl-α-amino esters via cobalt-catalyzed carbonylation of N-acyl-α-alkoxyamines. *J. Mol. Catal.* **1987**, *41*, 135-146.

(16). Wakamatsu, H.; Uda, J.; Yamaka, N., Synthesis of *N*- acyl amino-acids by a carbonylation reaction *J. Chem. Soc. D.* **1971**, 1540.

(17). (a) Chiou, W.-H.; Mizutani, N.; Ojima, I., Highly efficient synthesis of azabicyclo[x.y.0]alkane amino acids and congeners by means of Rh-catalyzed cyclohydrocarbonylation. *J. Org. Chem.* **2007**, *72*, 1871; (b) Chiou, W.-H.; Shoenfelder, M.; Sun, L.; Mann, A.; Ojima, I., Rhodium-Catalyzed Cyclohydrocarbonylation Approach to the Syntheses of Enantiopure Homokainoids. *J. Org. Chem.* **2007**, *72*, 9418; (c) Ojima, I.; Iula, D. M.; Tzamarioudaki, M., Efficient synthesis of functionalized piperidines through extremely regioselective Rh-catalyzed cyclohydrocarbonylation of Amido-ω−diene. *Tetrahedron Lett.* **1998**, *39*, 4599-4602; (d) Ojima, I.; Korda, A., New routes to nitrogen heterocycles through intramolecular amidocarbonylation of alkenamides catalyzed by rhodium complexes. *Tetrahedron Lett.* **1989**, *30*, 6283-6286; (e) Ojima, I.; Tzamarioudaki, M.; Eguchi, M., New and efficient route to pipecolic acid derivative by means of Rh-catalyzed intramolecular

cyclohydrocarbonylation *J. Org. Chem.* **1995**, *60*, 7078-7079; (f) Ojima, I.; Vidal, E. S., Rhodium-catalyzed cyclohydrocarbonylation: Application to the synthesis of (+)-prosopinine and (-)-deoxyprosphylline *J. Org. Chem.* **1998**, *63*, 7999-8003.

(18). Chiou, W.-H.; Lee, S.-Y.; Ojima, I., Recent Advances in cyclohydrocarbonylation reactions *Can. J. Org. Chem* **2005**, *83*, 681-692.

(19). Maryanoff, B. E.; Zhang, H.-C.; Cohen, J. H.; Ignatius J. Turchi; Maryanoff, C. A., Cyclizations of N-Acyliminium Ions. *Chem. Rev.* **2004**, *104*, 1431–1628.

(20). Eguchi, M.; Zeng, Q.; Korda, A.; Ojima, I., Synthesis of pyrrolizidine alkaloids via rhodium-catalyzed silylformylation and amidocarbonylation. *Tetrahedron Lett.* **1993**, *34*, 915-918.

(21). Campi, E.; Habsuda, J.; Jackson, W.; Jonasson, C.; Mccubbin, Q., The stereochemistry of organometallic compounds. XLII. The preparation of [2,1-b] quinazolines involving rhodium-catalysed hydroformylation of 2-amino-*N*-alkenylbenzylamines *Aust. J. Chem.* **1995**, *48*, 2023-2033.

(22). Cuny, G. D.; Buchwald, S. L., Practical, high-yield, regioselective rhodium-catalyzed hydroformylation of functionalize a-olefins. *J. Am. Chem. Soc.* **1993**, *115*, 2066-2068.

(23). Chiou, W.-H.; Lin, G.-H.; Liang, C.-W., Facile syntheses of enantiopure 3-hydroxypiperidine derivatives and 3-hydroxypipecolic acids *J. Org. Chem.* **2010**, *75*, 1748-1751.

(24). Chiou, W.-H.; Schoenfelder, A.; Mann, A.; Ojima, I., Application of rhodium-catalyzed cyclohydrocarbonylation to the syntheses of enantiopure homokainoids. *Pure Appl.Chem.* **2008**, *80*, 1019-1024.

Chapter 4

Application of Cyclohydrocarbonylation to the Synthesis of Izidine Alkaloids

4.0 Introduction

Alkaloids are defined as natural products containing a basic nitrogen atom.[1] They also account for compounds with neutral or even moderately acidic properties. In addition to containing the standard elements carbon, hydrogen and nitrogen some alkaloids also contain phosphorus, sulfur and more rarely bromine and chlorine.[1] Alkaloids are typically produced by a variety of biological systems including plants, animals and microorganisms. Organic chemists have been interested in alkaloids for a number of years, primarily due to the varying pharmacological properties held by this class of compounds.

Alkaloids can be classified into several structure-based specific categories. Among these categories, izidine alkaloids account for more than 800 compounds.[1] The izidine alkaloids can be further classified into three major divisions; the pyrollizidine, indolizidine, and quinolizidine alkaloids each based on the core structures, shown below in **Figure IV-1**.

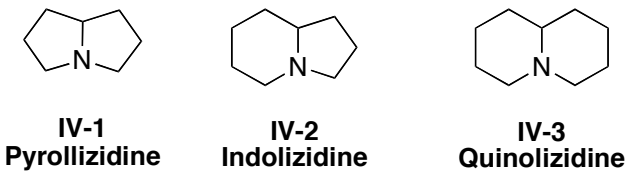

Figure IV-1: Classes of izidine alkaloids

The pyrollizidine class of izidine alkaloids has been targeted for its pharmacological and insecticidal properties as well as its unique five-five fused bicyclic ring structure.[2] The indolizidine alkaloids are synthetic targets mainly due to their antifungal and antibacterial properties.[3] The quinolizidines are pursued primarily for their antipyretic, hallucinogenic, and oxytocic properties.[3] Several examples of the various alkaloids in the different classes can be seen in **Table IV-1.**

Table IV- 1: Izidine alkaloid examples

Pyrollizidine	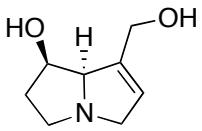 **Retronecine IV-4**	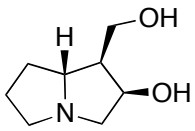 **Macronecine IV-5**	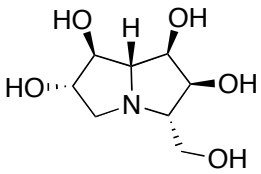 **Casuarine IV-6**
Indolizidine	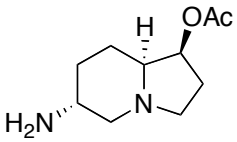 **Slaframine IV-7**	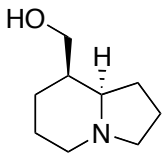 **Tashiromine IV-8**	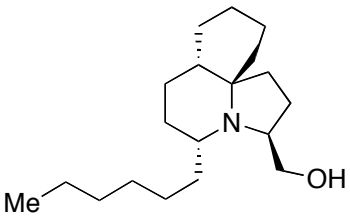 **Lepadiformine IV-9**
Quinolizidine	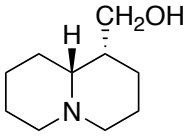 **Lupinine IV-10**	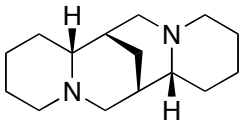 **α–Isosparteine IV-11**	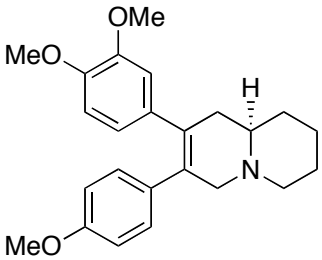 **Juladine IV- 12**

Many of the current synthetic routes to the izidine alkaloids and other similar alkaloids have employed an *N*-acyliminium cyclization involving an intramolecular nucleophilic addition as the key-step process to form the bicyclic core structure.[4] In most cases that employ the *N*-acyliminium cyclization, a two step process is required: (1) formation of the aminol species by intramolecular nucleophilic attack of the aldehyde by an amide species followed by (2) Brönsted or Lewis acid driven dehydration of the aminol affording an *N*-acyliminium which is subsequently trapped by a second nucleophile. These cyclizations have employed both heteroatomic and carbon nucleophile species, the latter being more widely applied. One of the more well-known and useful reactions is the trapping of an *N*-acyliminium species with electron-rich aromatics (Pictet-Spengler reaction). In 2006, Kuntiyong and co-workers proposed a

short synthetic route (**Scheme IV-1**) to the tricylic core of Schulzeines alkaloid (**IV-C**), which are promising natural products with excellent biological efficacy. They employed a facile and stereoselective *N*-acyliminium cyclization with an electron rich aromatic species to afford the tricyclic core **IV-B** in excellent yield (**Scheme IV-1**).[5]

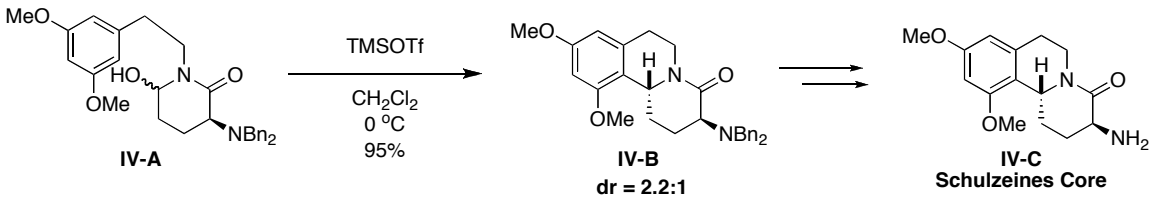

Scheme IV-1: Short synthesis to Schulzeines core[5]

Another type of nucleophile species that has also been employed are the allylsilane species. Hiemstra and co-workers employed a step-wise allylsilane directed cyclization in the synthesis of epilupinin (**IV-F**) (**Scheme IV-2**) affording a modest 74% yield.[6]

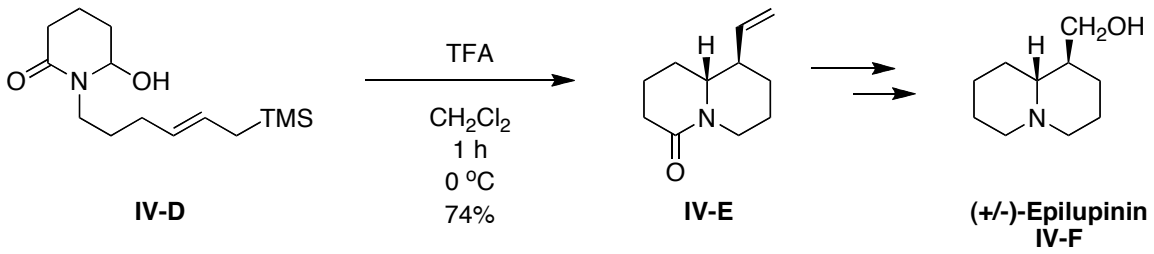

Scheme IV-2: Synthesis of Epilupinin[6]

In both of the noted cases, the formation of the desired product is complete in two independent, although closely related synthetic steps. One can envision that the formation of *N*-acyliminium ion can be accomplished in a single-step, rather than a stepwise process where the aminol is isolated. The domino process will be more atom-economical as well as a greener and more environmentally friendly method.

The desire to develop domino reaction processes requires the generation of reactive intermediates that can be quickly and efficiently transformed to other more stable adducts in a single pot. The increased use of hydroformylation in synthesis has also increased the use of domino hydroformylation-based reactions, such a

cyclohydrocarbonylation, hydroformylation-Wittig reaction, hydroformylation-Michael additions, and hydroformylation-aldol condensations.[7] The application of hydroformylation in synthesis is owed in part to development of the linear selective phosphine-based ligands such as BIPHEPHOS, BISBI, and XANTPHOS (**Figure IV-2**) and several others noted in chapter 3.[8]

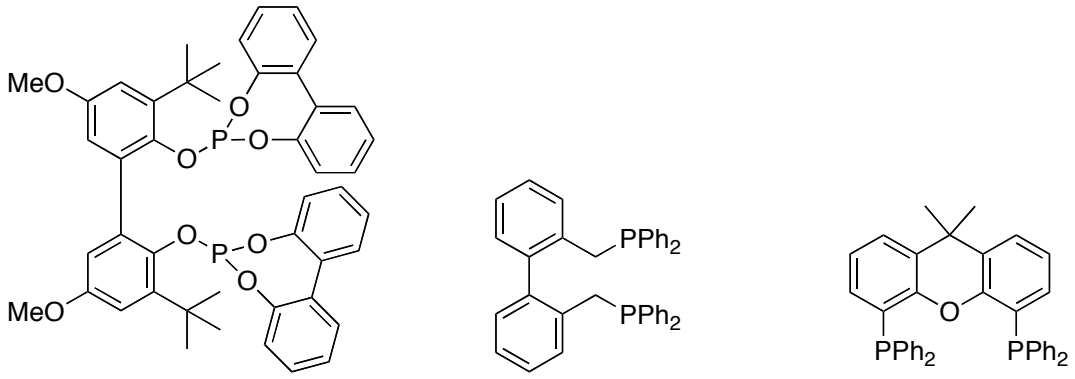

III-15
BIPHEPHOS

III-16
BISBI

IV-13
XANTPHOS

Figure IV-2: Linear selective bisphosphine ligands for hydroformylation

Cyclohydrocarbonylation has found particular utility with the synthesis of these alkaloids because it is a one-pot reaction requiring generally environmentally benign solvents. Recently, our laboratory demonstrated that heteroatom nucleophiles can serve as excellent diastereoselective trapping agents in the cyclohydrocarbonylative process depicted in **Scheme IV-3** for the synthesis of azabicyclo[2.2.0]alkane amino acids. [9]

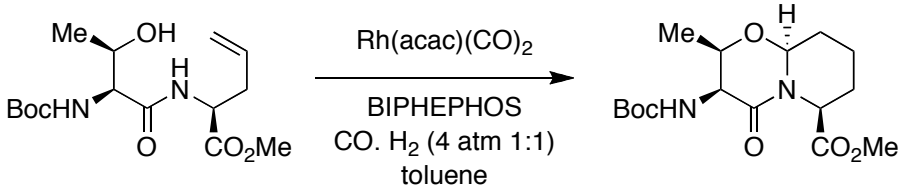

IV-14

IV-15

Scheme IV-3:Application of CHC using heteroatomic nucleophiles

A logical expansion of this process would include the use of carbon-based nucleophile systems where such an application would allow access to the izidine type alkaloids. The

process of trapping *N*-acyliminium ions with carbon-rich nucleophiles has been applied widely in synthesis as noted earlier, however to our knowledge no concomitant process has been used for electron rich carbon atoms.[4c] Herein, we report on the application of the cyclohydrocarbonylative trapping of *N*-acyliminium ions with carbon-based nucleophiles as applied toward the synthesis of the izidine alkaloids.

4.1 Synthetic Application of the CHC-reaction

4.1.1 Synthetic Strategy

Carbon nucleophiles comprise a wide range of electron-rich carbon atoms. In the consideration of carbon nucleophiles we must distinguish between charged and neutral nucleophilic carbon atoms. There are charged carbon nucleophiles, which require the addition of a strongly basic species to be generated. There are neutral nucleophilic carbons, which are simply carbon nucleophiles that do not require the addition of a strongly basic species. There are at least four types of neutral electron-rich carbon atoms. The first, and likely most utilized neutral carbon nucleophile species is the electron rich aromatic system.[4c] This system typically consists of a substituted benzene ring containing one or more electron donating species establishing a high region of electron density at the *para* and *ortho* positions indicated by the red and blue dots, respectively in **Figure IV-3**. The second widely used species are the allylsilanes.[10] The nucleophilic nature of allylsilanes can be best described by the resonance shown in **Figure IV-3** where a clear depolarization is shown generating a carbon anion species.

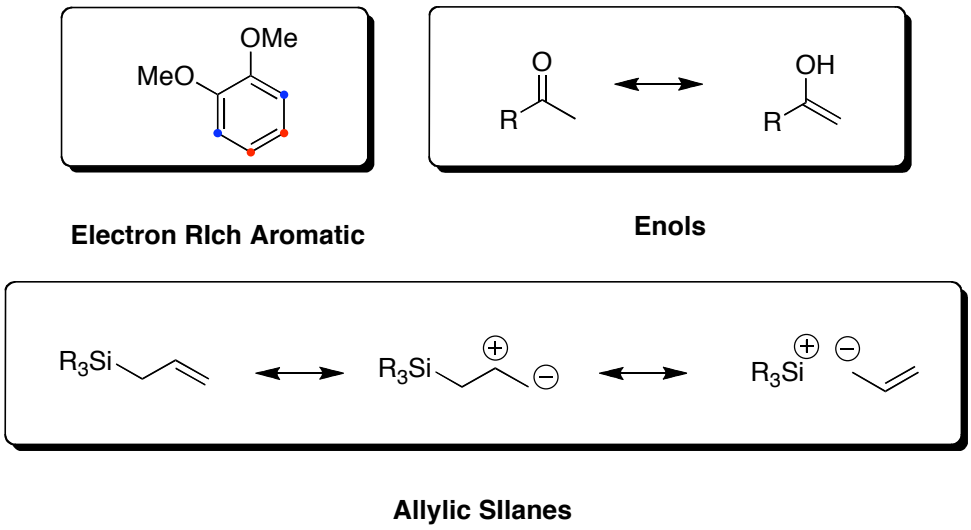

Figure IV-3: Neutral electron rich carbon species

This polarization is a direct effect of silicon's ability to stabilize β-cations.[11]Finally the most well know nucleophile species, the enol species which has been applied in synthesis for sometime.[4c] There are several well known reactions that involve enol nucleophiles including, aldol, Claisen-Schmidt, and Mannich reactions.

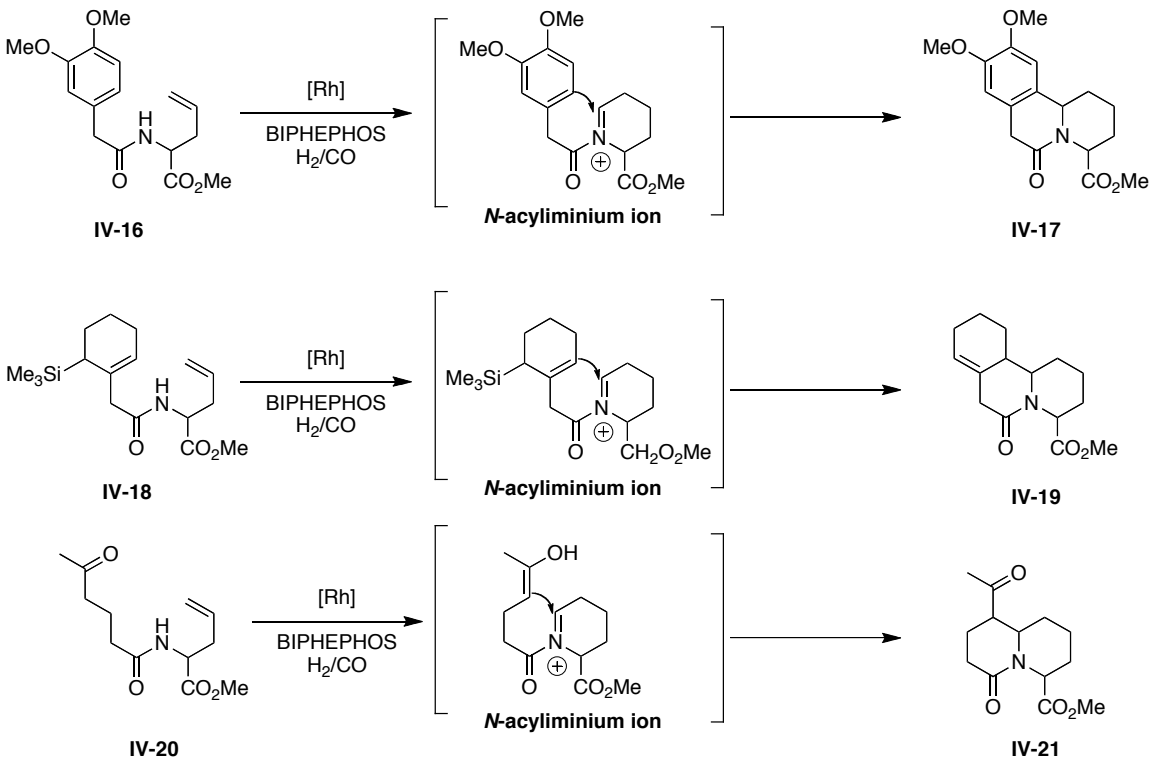

Scheme IV-4: Cyclohydrocarbonylative route to izidine alkaloid cores (adapted from Ojima NSF Prosposal)

These various neutral carbon nucleophiles can be used to access the izidine alkaloids bicyclic core as shown in **Scheme IV-4** where a cyclohydrocarbonylation reaction generates an *N*-acyliminium species which is subsequently trapped by one of the carbon nucleophile systems described. The following section will contain an in-depth discussion of the synthesis and application of these various carbon nucleophile species in the CHC reactions.

4.1.2 Application of CHC trapping using electron rich aromatics

The study of electron rich aromatics began with synthesis of the linear selective hydroformylation ligand BIPHEPHOS (*vide supra*). The di-*t*-butyl-dimethoxy-biphenol backbone of BIPHEPHOS was constructed by homo-oxidative coupling with potassium iron ferricyanide from commercially available *t*-butyl-(hydroxy)anisole (**IV-22**). The bis-biphenol moieties were prepared by formation of the phosphorochloridite **IV-25** from

commercially available 2,2'-biphenol (**IV-24).** Following high vacuum distillation and purity check by ^{31}P NMR, compound **IV-25** was then reacted with biphenol **IV-23** to afford **BIPHEPHOS** in 17% isolated yield as shown in **Scheme IV-5**.

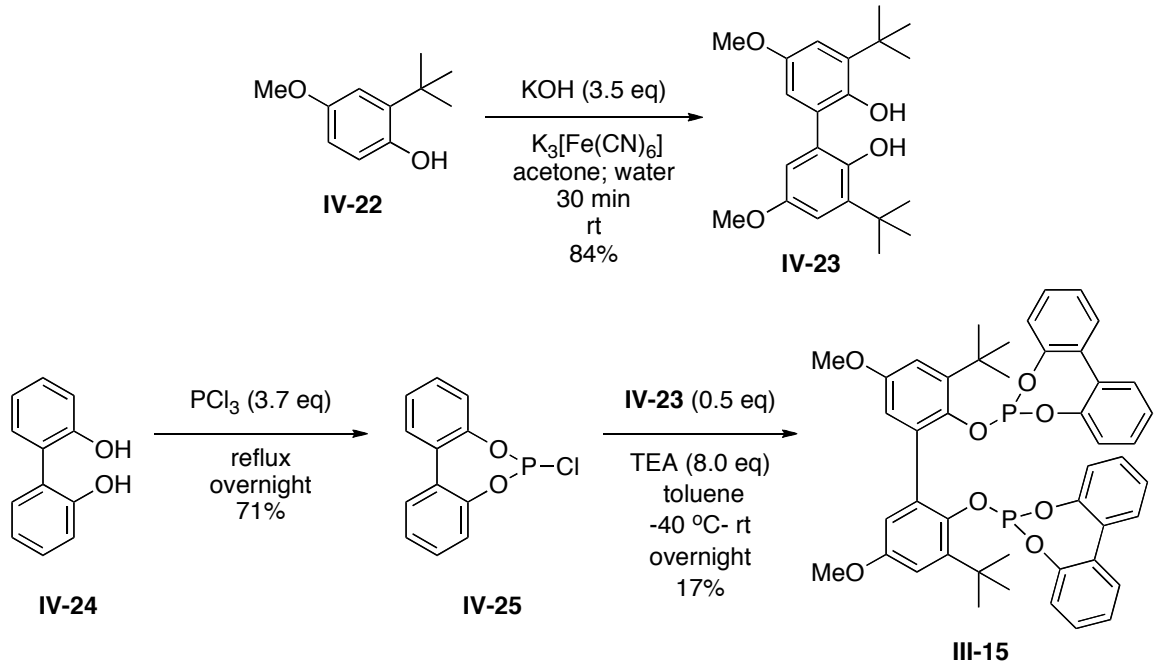

Scheme IV-5: Synthesis of BIPHEHOS

The application of the CHC-reaction commenced with the synthesis of the designed aromatic substrate as shown in **Scheme IV-4**. This substrate was chosen because it was readily accessible from commercially available materials, allylglycine and (4,5-dimethoxy)-phenylacetic acid. Furthermore, the predicted product is the 6-6-6-fused tricyclic ring system (*vide supra*) that should be thermodynamically favorable. The synthesis began with esterification of commercially available racemic allylglycine in the presence of thionyl chloride in methanol to afford the desired allylglycine methyl ester (**IV-27**) in quantitative yield after an overnight reaction (**Scheme IV-6**).

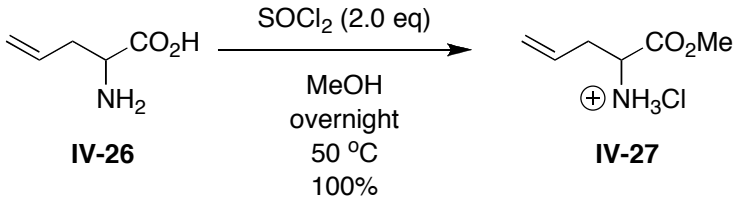

Scheme IV-6: Esterification of vinyl glycine

Having obtained compound **IV-27** in excellent yield, its was then coupled to phenylacetic acid **IV-28** in the presence of EDC to afford amide **IV-29** is 58% isolated yield as shown in **Scheme IV-7**.

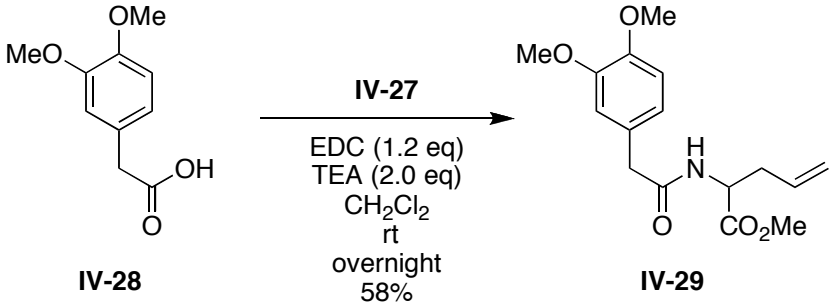

Scheme IV-7: Amide coupling

The precursor for a 6-7-6-fused (**Figure IV-4**) ring system was also synthesized for preliminary screening.

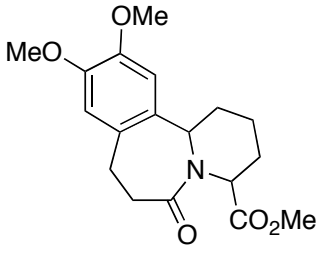

Figure IV-4: Proposed 6-7-6 fused-ring proposed product

The synthesis of this substrates began with commercially available 3,4-dimethoxyphenyl-propanoic acid (**IV-30**) under EDC coupling conditions with racemic allylglycine methyl ester **IV-27** to afford amide **IV-31** in 68% isolated yield as shown in **Scheme IV-8**.

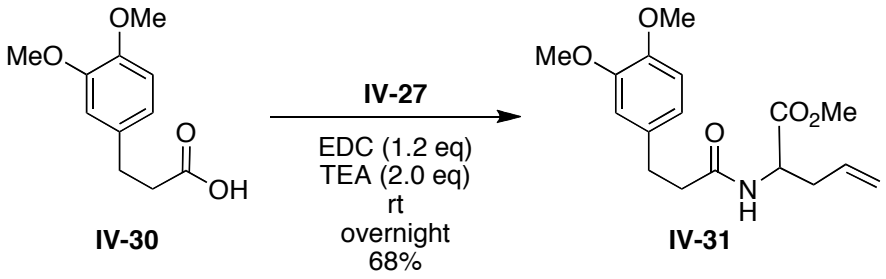

Scheme IV-8: Synthesis of 6-7-6-precursor

Having obtained two substrates in hand, the search for the best conditions for the CHC reaction began. The previously successful conditions for the heteroatomic nucleophiles, using $Rh(acac)(CO)_2$ with BIPHEPHOS and catalytic amount of *p*-TSA were chosen as the starting point for condition screening.[9] In addition, sodium sulfate was added as a dehydrating agent to facilitate the formation of the *N*-acyliminium ion. When compound **IV-31** was subjected to CHC conditions given in **Scheme IV-9** a mixture of the expected product and the enamide **IV-32-B** was observed by NMR and mass spectrometry analysis. Based on relative integration values, compound **IV-32-B** was dominant.

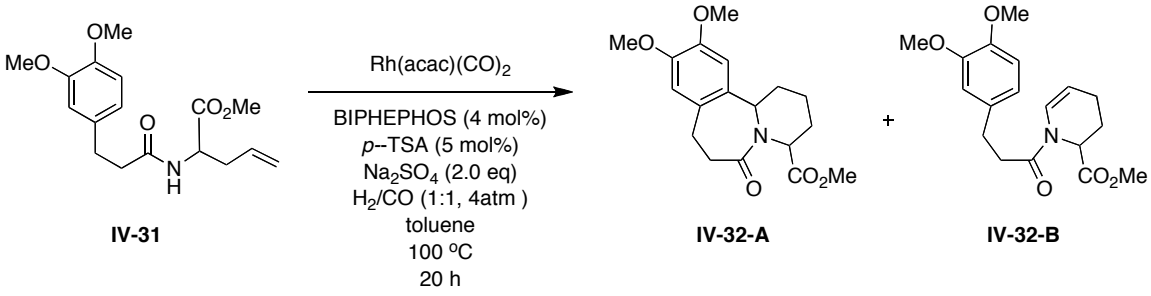

Scheme IV-9: CHC reaction form 6-7-6 izidine alkaloid ring system

However, these two compounds were not separable by TLC and thus could not be isolated by column chromatography. The enamide product in this case is not unexpected, as the alpha-proton of the newly formed *N*-acyliminium is quite acidic, thus deprotonation by either water or the conjugate base of *p*-TSA would facilitate the formation of enamide **IV-32-B** (**Scheme IV-10**).

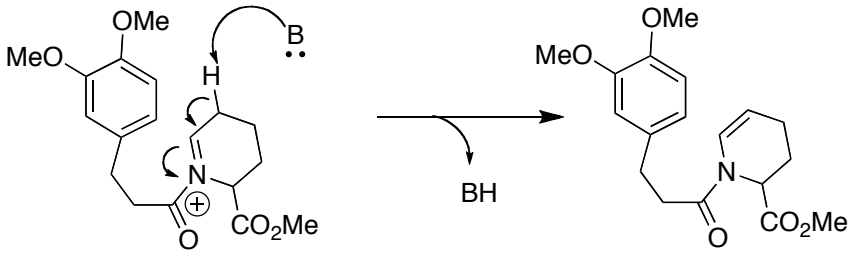

IV-32-I **IV-32-B**

Scheme IV-10: Mechanism of the enamide formation

This initial screening result supported our hypothesis that CHC-formed *N*-acyliminium could be trapped by carbon nucleophile species. Furthermore, it was thought the 7-endo-*trig* cyclization might be less facile than the 6-endo *trig* cyclization. Thus, we continued screening reaction conditions for the formation of 6-6-6 fused-ring system. The same conditions noted in **Scheme IV-9** were applied to six-membered ring substrate, which afforded the enamide product and the hydrogenated starting material (**IV-33-H**) both of which were confirmed by NMR and mass spectrometry fragmentation analysis. The products were not isolated (**Scheme IV-11**).

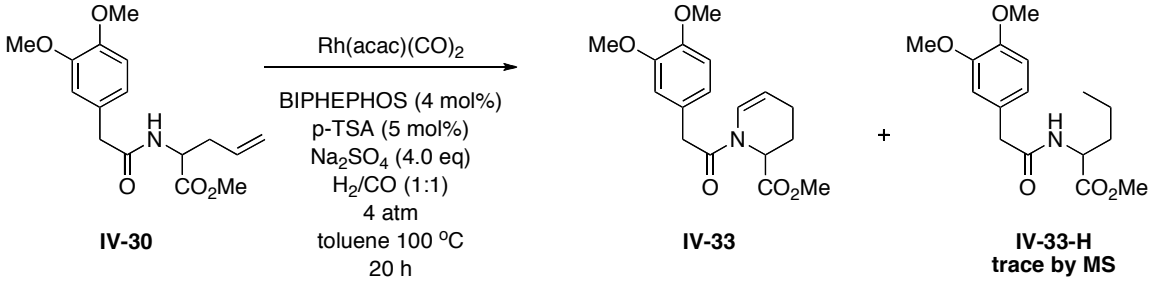

IV-30 **IV-33** **IV-33-H trace by MS**

Scheme IV-11: Preliminary screening conditions for the 6-6-6-ring system

After having obtained no fully cyclized product in the case of the six-member ring system, the substrate was modified slightly to include more electron donating species as shown in **Scheme IV-12**. The 3,4,5-trimethoxyphenyl acetic acid was coupled to allylglycine methyl ester under EDC conditions to afford the 3,4,5-trimethoxy amide **IV-35** (**Scheme IV-12**) in a modest 63% isolated yield.

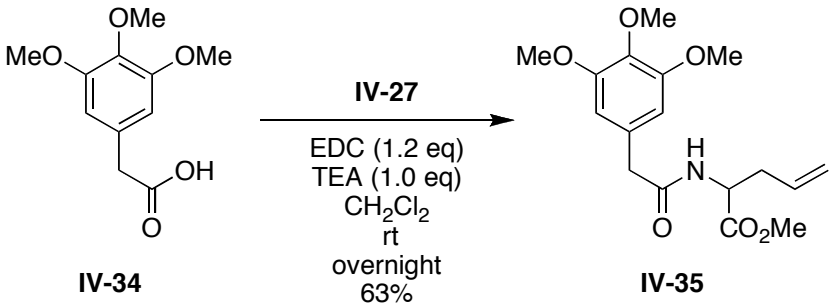

Scheme IV-12: Synthesis of the trimethoxy-substrate

In an exhaustive review, Maryanoff and co-workers noted that the addition of strong acid species such as trifluoroacetic (TFA) or formic acid affords higher yields in the step-wise application of the nucleophilic addition to *N*-acyliminium species.[4c] Thus, we employed TFA as a reaction additive. However the product afforded was a complex mixture that could not be determined nor purified as shown in **Scheme IV-13**.

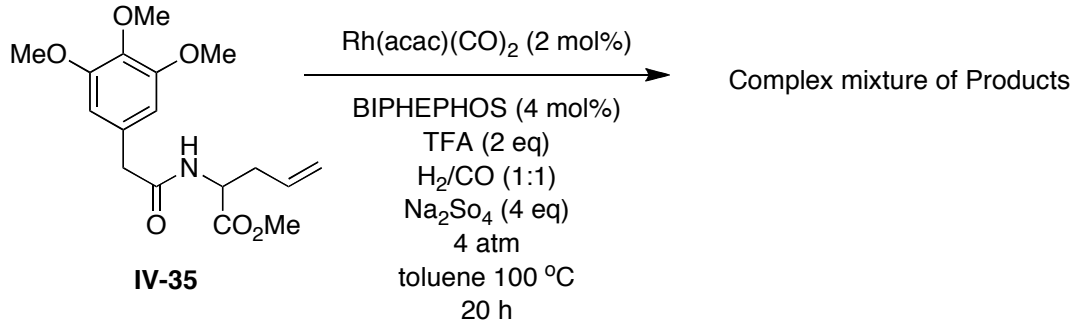

Scheme IV-13: Result with TFA additive

In the case of the trimethoxy substrate **IV-35** the addition of TFA appears to be detrimental to the reaction, it is likely to either cause degradation to the product or the starting material. Thus, the dimethoxy substrate was subjected to similar conditions as shown in **Scheme IV-14**.

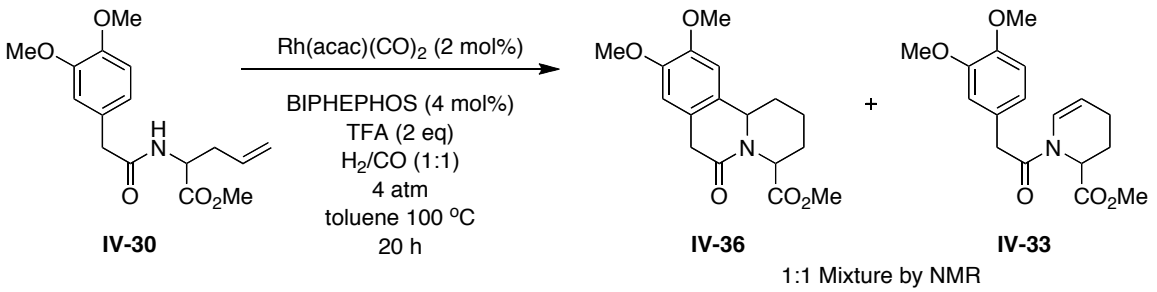

IV-30 **IV-36** **IV-33**

1:1 Mixture by NMR

Scheme IV-14: Result with TFA additive for Dimethoxy-substrate

The use of TFA additive in the case of the dimethoxy substrate afforded a 1:1 mixture of the desired product (**IV-36**) and side-product enamide (**IV-33**) as determined by ^{1}H NMR. The integration values of the three distinct chemical shifts were compared. The α-amino proton of **IV-33** (d 4.30 ppm) was compared to same of **IV-36** (d 4.36 ppm) and found to have similar integration values. Furthermore, the ^{13}C NMR shows carbonyl carbons and α-amino carbons consistent with a mixture of the compound **IV-36** and **IV-33** (See Appendix A). Thus the presence of a Brönsted acid promoted the nucleophilic trapping of the intermediate acyliminium ion. With early-optimized conditions in hand the substrate was modified slightly to incorporate an allylamine moiety instead of allyglycine moiety resulting primarily from the high cost of allylglycine. The synthesis of this new substrate was complete under similar EDC conditions as previous affording the desired product **IV-37** in 83% yield (**Scheme IV-15**).

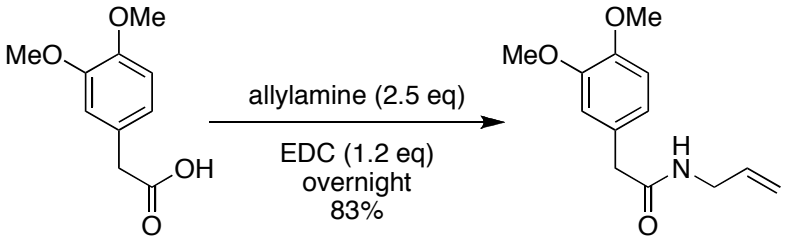

IV-30 **IV-37**

Scheme IV-15: Synthesis of allylamine base substrate

Following the previous success of a Brönsted acid as additive to the reaction, a variety of Lewis and Brönsted acids additives were screened and the results shown below in **Table IV-2.**

Table IV-2: Results of Lewis and Brönsted acids in CHC reaction

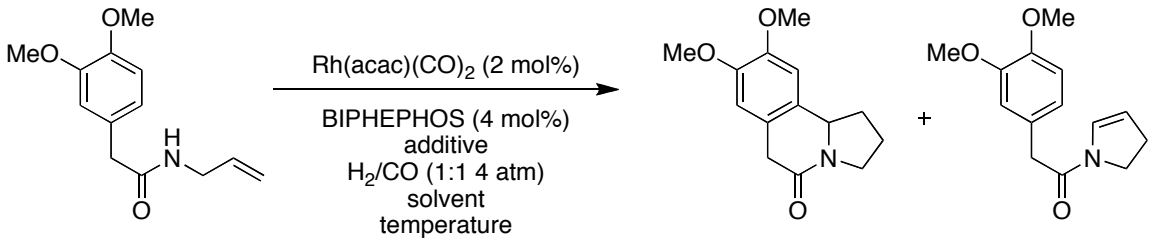

IV-37 **IV-38** **IV-39**

Entry	Solvent	Additive [a]	Temperature (°C)	Major Product	Isolated Yield(%)
1	toluene	$AlCl_3$	60	-	-
2	toluene	$ZnCl_2$	60	-	-
3	AcOH	-	60	**IV-38**	87
4	toluene	AcOH	100	**IV-38**	-
5	toluene	H_2SO_4 [b]	90	-	-
6	toluene	AcOH [c]	60	**IV-39**	78
7	toluene	TFA	60	**IV-39**	-
8	toluene	KOAc	60	**IV-38**	-

[a] Additive we used in 1 molar equivalent to the starting material.
[b] 18 M mole/vol added [c] Used a 1:1 mixture with toluene

The addition of a Lewis acid afforded no reaction in all cases (entries 1 and 2). It is likely that the Lewis acid may have deactivated the rhodium catalyst altogether. The effectiveness of the Brönsted acid additive is dependent on both concentration and acid strength, higher concentrations appear to drive the final cyclization, while lower concentration appear to have no real effect (entries 3 and 4). Furthermore, stronger acids appear to be detrimental to the reaction (entry 5), which may be a result of ligand or catalyst degradation. The high concentrations of the weak acid afforded the best results.

Following the successful trapping of the CHC-generated *N*-acyliminium ion, efforts to reproduce the reaction and yield shown in **Table IV-2** were made. However only modest isolated yields 46 and 52% could be obtained from these conditions (**Scheme IV-16**).

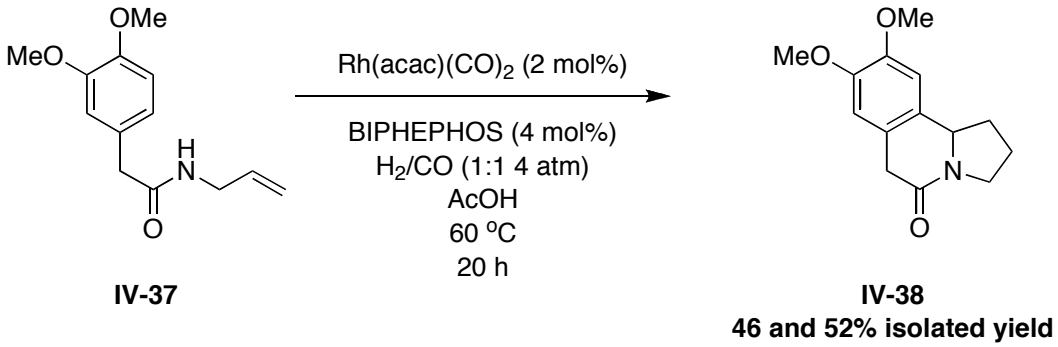

IV-37 **IV-38**
46 and 52% isolated yield

Scheme IV-16: Resynthesis of IV-38

Furthermore, no secondary product was observed on analysis by LC-MS of the crude reaction mixture. As such, it is necessary to continue screening conditions to afford the desired product in good to excellent yield.

It is noteworthy to mention that only the *para*-position adduct was obtained; no *ortho*-position adduct was observed in any of the reactions. A simple sterics explanation is not sufficient to explain the observed results as some product distribution is to be expected in the case of a methyl ether moiety. Although we traditionally do not consider cations in the Wheland intermediate as discrete species, crude analysis using PC Sparatan (AM1 semiempirical methods) of the isolated discrete cations show an approximately 12 kcal/mol difference between the *ortho*- and *para*-positions (**Figure IV-5**).

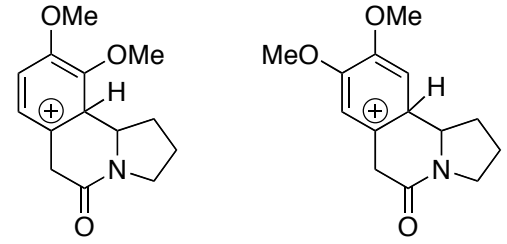

102.64 kcal/mol **90.18 kcal/mol**

Figure IV-5: Intermediate cation stability

Additionally, analysis of the HOMO-LUMO of the starting materials shows the presence of a node at the *ortho*-position, thus one should expect only to observe the *para*-postion adduct (**Figure IV-6**). Although only preliminary, these two ideas offer some insight into the selectivity bias that is observed.

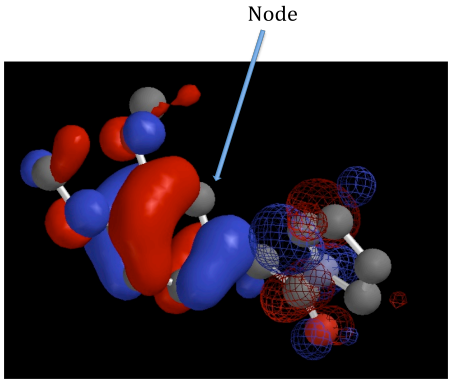

Figure IV-6: HOMO-LUMO analysis

During the screening process a private communication was received from Dr. Chiou, an Ojima laboratory alumus and co-workers detailing optimized conditions for the same process. Subsequently, a collaborative effort was put forth and published.[12] The most effective conditions are shown below in **Scheme IV-17**.

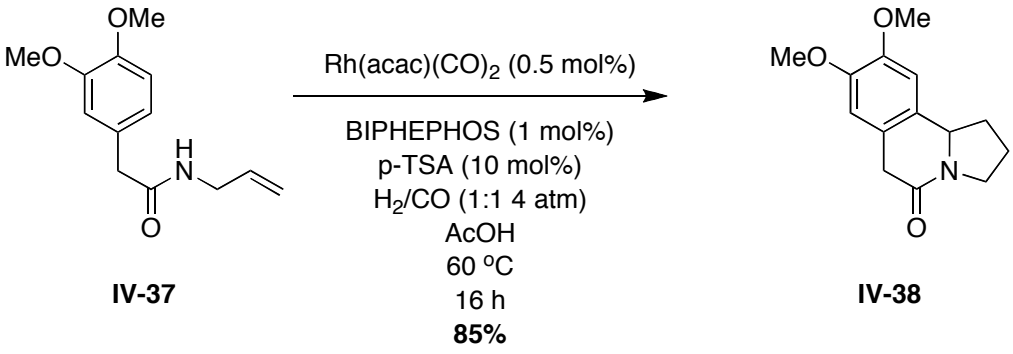

Scheme IV-17: Optimized condition from Choiu *et al.*[12]

Thus, no further efforts were put forth on the electron rich aromatic species. Although, we continue to explore applications of this reaction.

Recently, Romo and co-workers published the total synthesis Schulzeines B and C, alkaloids isolated from the marine sponge *Penares schulzei* by Fusetani.[13]

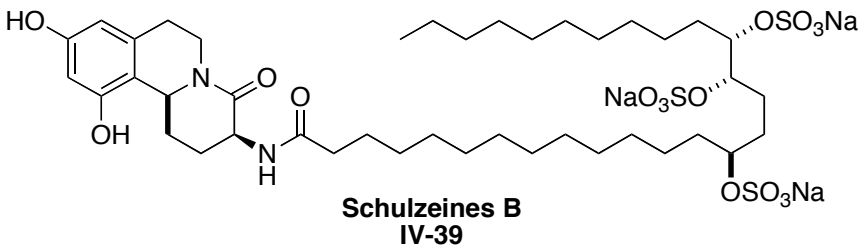

Figure IV-7: Structure of Schulzeines B

These alkaloids has drawn particular attention as they have been found be to potent viral neuraminidase inhibitor and α-glycosidase inhibitor.[13b] The synthesis of the core tricyclic moiety required more than 11 steps to arrive at the coupling ready primary amine (**B, Figure IV-8**). The application of our CHC-carbon nucleophile process would considerably shorten access to compound **B**, as shown in **Figure IV-8**. Compound **D** can be subject to CHC-reaction conditions affording compound **B** in a one-pot process. Following the proposed route we can access the tricyclic core in a total of three steps from compound **E**. This would represent a considerable improvement in the total synthesis of these molecules. Furthermore, it improves upon methods published by Kuntiyong by creating a one pot process for the formation of the tricyclic core (*vide supra,* **Scheme IV -1**).[5]

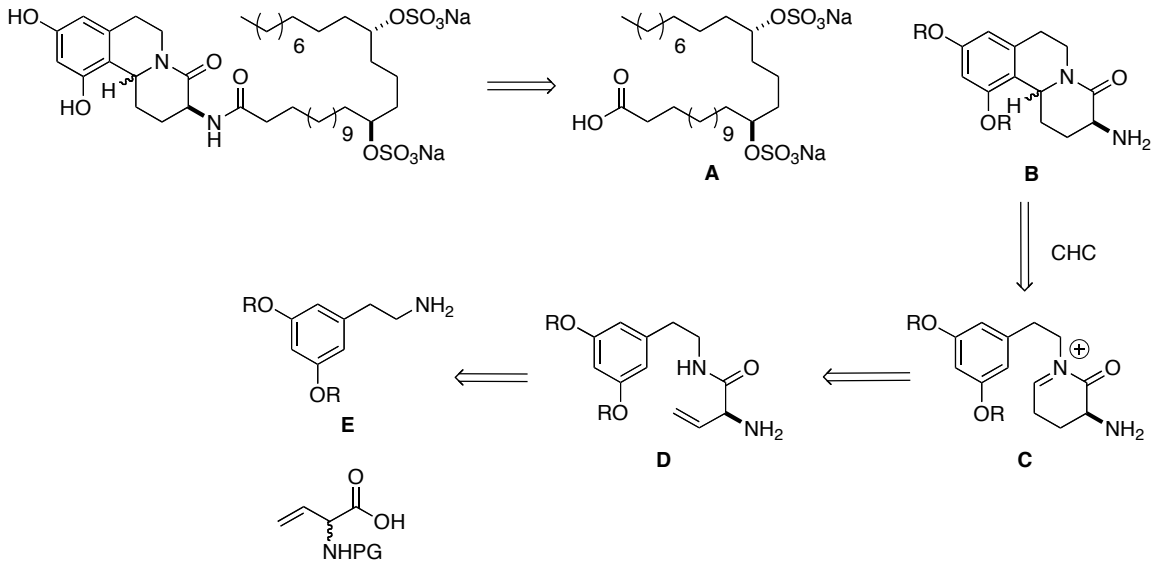

Figure IV-8: Retrosynthesis of Schulzeines

Thus, we began with a known method to access compound **E**.[14] The synthesis began with the reduction of commercially available **IV-40** by lithium aluminum hydride to give alcohol **IV-41** in 98% isolated yield, which was subsequently oxidized in the presence of a chromate regent to afford aldehyde **IV-42** (**Scheme IV-18**). A two-step process is preferred here as the yield is more consistent and higher.

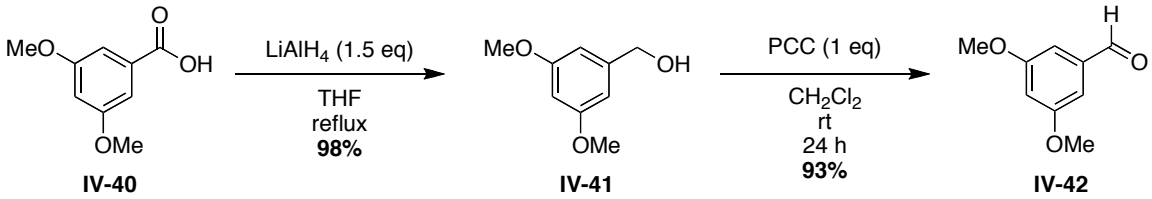

IV-40 **IV-41** **IV-42**

Scheme IV-18: Synthesis of aldehyde IV-42

Compound **IV-42** was subsequently transformed to nitroalkene **IV-43** *via* a Henry reaction using nitromethane (**Scheme IV-19**) giving the desired product in 42% isolated yield following two crystallizations from ethanol.

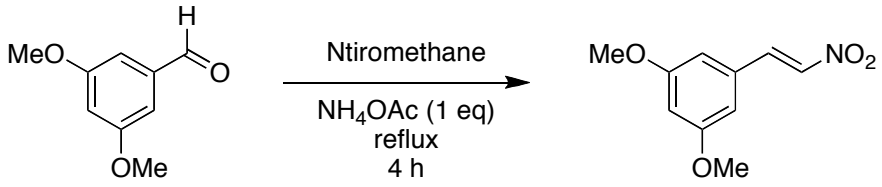

IV-42 **IV-43**

Scheme IV-19: Henry reaction to give IV-43

The reduction of nitroalkene **IV-43** to amine **IV-44** was completed on an as needed basis and used without purification in the subsequent coupling reaction (**Scheme IV-19**). The coupling reaction of **IV-44** with vinylglycine **IV-45** in the presence of HOBot (hydroxybenzyltriazole) and EDC failed to afford the desired product **IV-46** but instead afforded the isomerized product **IV-46A** (**Scheme IV-20**). The isomerization of vinylglycines is well established under basic conditions however it is also known to isomerize under neutral and strongly acidic conditions as well.

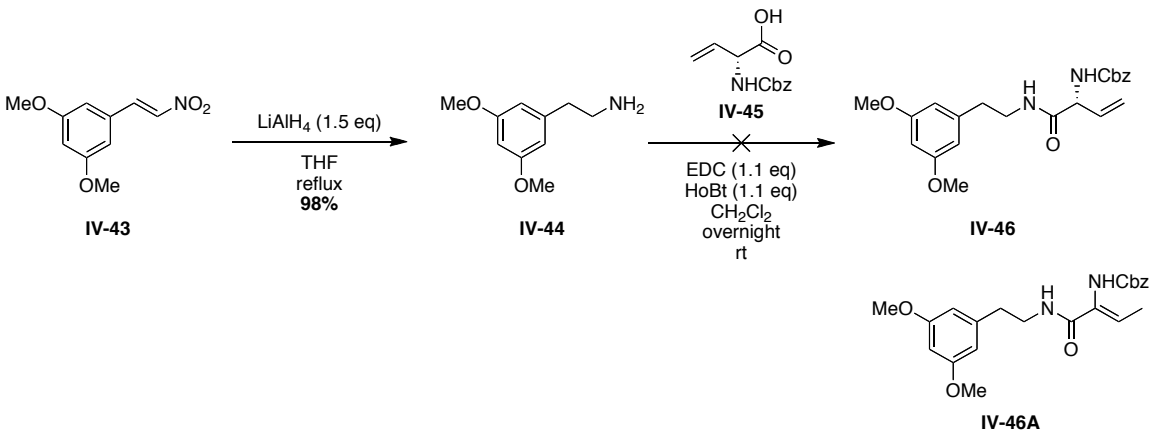

Scheme IV-20: Coupling of vinylglycine

Efforts to obtain the desired compound **IV-46** are still underway.

4.1.3 Application of CHC trapping using allylsilanes

The initially proposed allylsilane system (**Scheme IV-21**) allows for facile access to 6-6-6 alkyl quinolizidine alkaloids. However the synthesis of the precursor **IV-18** is in and of itself a synthetic challenge and does not provide the ideal scenario for reaction condition screening.

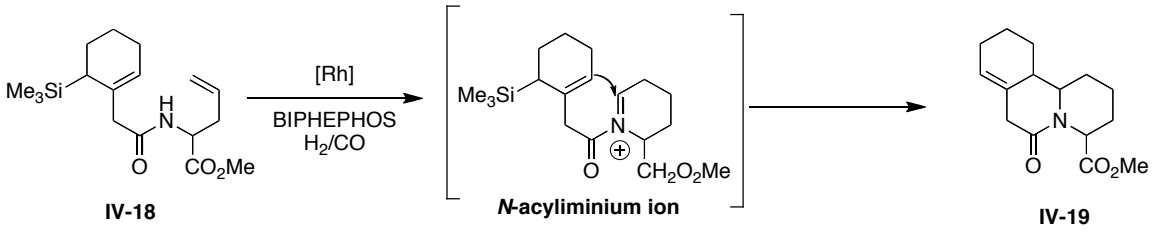

Scheme IV-21: Allyl silane trapping using CHC

Thus a similar more easily synthesized substrate (**IV-47)** was designed (**Scheme IV-22**) to accomplish the initial studies into this new system.

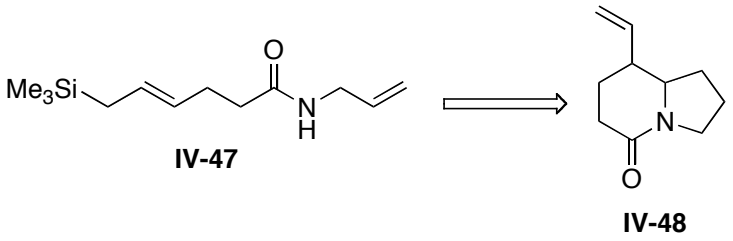

Scheme IV-22: Substrate modification

The double bond in the desired product is anticipated to either be hydroformylated or reduced. This distribution can be controlled by extending the reaction time to allow for the hydroformylation of the resultant olefin. A very simple retrosynthesis can be envisioned for compound **IV-47**, with the first cut forming the silyl-hexeneoic acid (**IV-49**) and commercially available allyl amine. The resultant compound **IV-49** can be accessed by the olefin metathesis of commercially available materials allyl silane and penteneoic acid (**Scheme IV-23**).

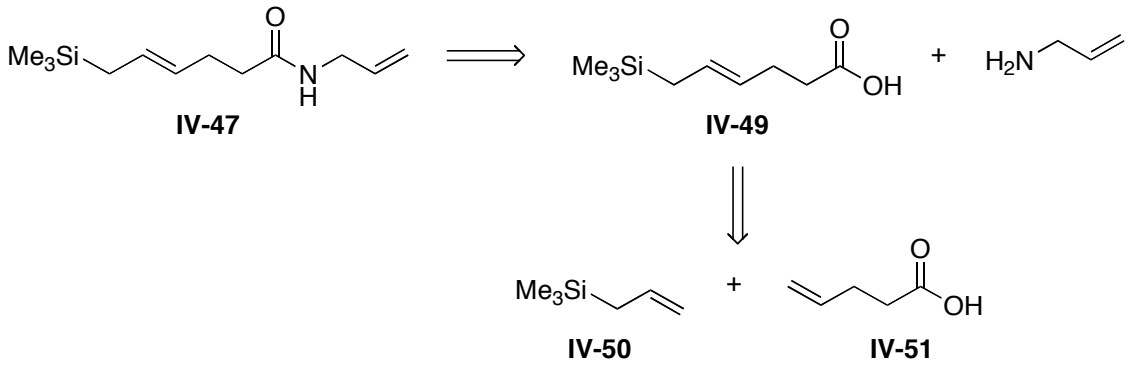

Scheme IV-23: Retrosynthesis of compound IV-47

Thus, the targeted synthesis of compound **IV-47** began with the cross metathesis of commercially available allylsilane (**IV-50**) and 4-pentenoic acid (**IV-51**) catalyzed by the Grubbs-Hoveyda catalyst, giving the desired compound **IV-49** in 58% isolated yield with a 3:1 *E*:*Z* diastereoselectivity ratio. The resultant product was then coupled to allylamine using EDC, affording the desired amide (**IV-47**) in 71% isolated yield (**Scheme IV-24**).

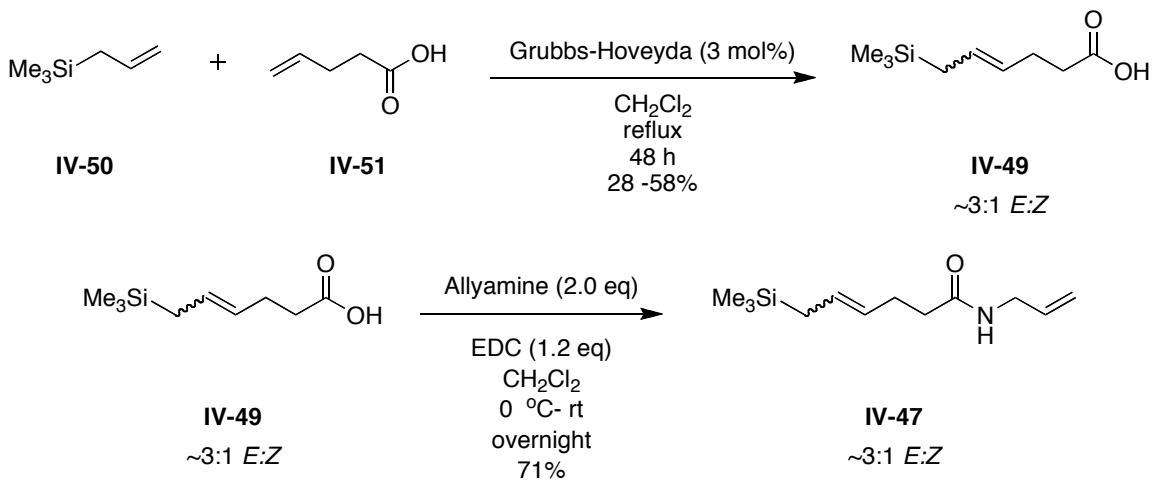

Scheme IV-24: Synthesis of the allylsilane amide

Compound **IV-47** was subjected to CHC preliminary screening (*vide supra*) conditions using *p*-TSA as the additive (**Scheme IV-25**). The reaction afforded two major adducts, the predicted cyclized hydrogenated product (**IV-47a**) in 10.8 mg and uncyclized enamide product (**IV-47b**) not quantified but observed by NMR and mass spectrometry analyses of crude reaction mixture.

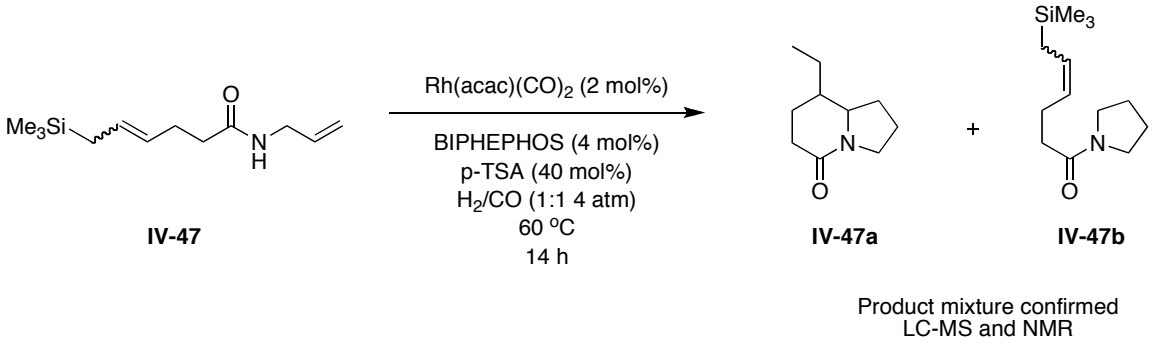

Scheme IV-25: CHC-application with allylsilane

An accurate ratio of the products was not determined because the enamide product was not isolated. The mixture of the two products may be due to several factors, one principle factor is that cyclization of the ring may be dependent on the olefin type, that is *E*-isomer may cyclize faster than *Z*-isomer or vice versa. In order to rule out this kinetic resolution effect, preparation of a single olefin is highly desired.

The difficult portion of the synthesis of compound **IV-47** is the installation of the C-Si bond. In 1980, Corrui[15] reported using hexamethyldisilane (**IV-52**), an alkali-metal hydride and an allylic halide for the synthesis of the allylsilane (**IV-53**) as seen in **Scheme IV-26.**

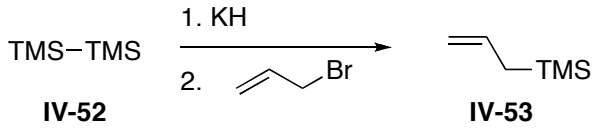

Scheme IV-26: Silicon metallating reaction[15]

Thus one conceives of using this reaction concept in the synthesis of the compound **IV-47,** where 3-hexenonic acid (**IV-54**) is converted into an allylsilane (**IV-55**) *via* an S_N2 type reaction. It is important to note that compound **IV-54** may also undergo an $S_N2`$ reaction affording an undesired terminal olefin. No literature precedent was found for a silicon metallation of an internal olefin.

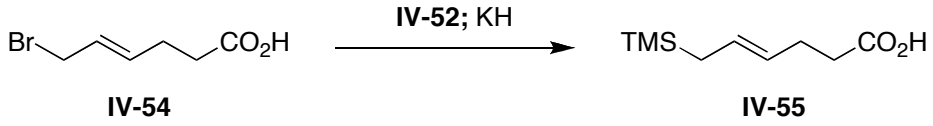

Scheme IV-27: Application silicon metallation to compound IV-47

In order to test the feasibility of the reaction shown in **Scheme IV-27**, the synthesis of the compound **IV-54** began with monomalonation of *trans*-1,4-dibromo-2-butene (**IV-56**) toward the monomalonate ester (**IV-57**) in 90% isolated yield and expected dimalonate byproduct (**IV-58**) in 8% yield as shown in **Scheme IV-28**. The desired monomalonate was then decarboxylated under basic conditions in a microwave reactor to afford alcohol (**IV-59**). The alcohol product **IV-59** was subjected directly to coupling conditions with EDC and the Boc-protected allylamine (**Scheme IV-28**). The presence of the alcohol group in compound **IV-60** was confirmed by infrared spectroscopy.

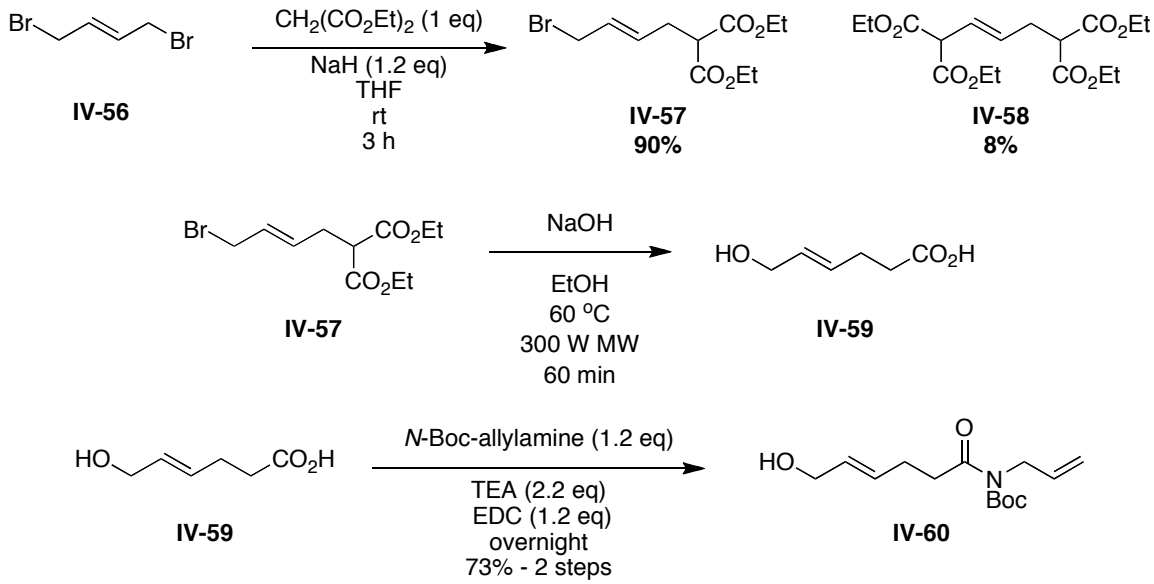

Scheme IV-28: Synthesis of the Single allylsilane isomer

The alcohol functionality on compound **IV-60** was then converted into the –OTs moiety to afford a more facile leaving group giving compound **IV-61** in 86% isolated yield (**Scheme IV-29**). The installation of the silyl moiety began with formation of metallosilyl species (**IV-62**) from hexamethyldisilane (**IV-52**) and potassium hydride which was added to **IV-61** and furnished a completely unexpected Boc-deprotection (**IV-64)** instead of the expected S_N2 or $S_N2`$ substitution at the allyl moiety. It appears that the carbonyl of the Boc- moiety was more electron deficient than either of the allylic positions. The deprotection may also have been driven by the oxophilic nature of the silicon anion.

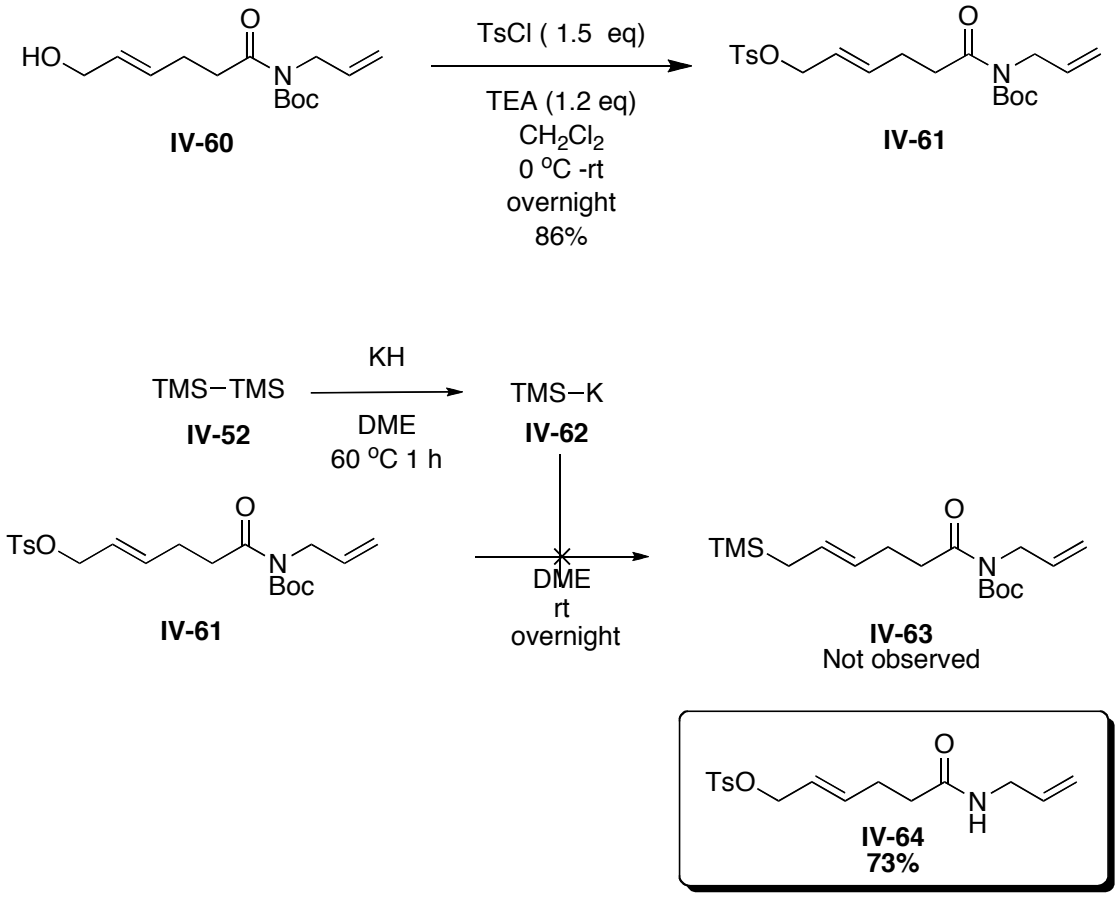

Scheme IV-29: Addition of the metallosilane species

Efforts to continue the development of this reaction were stopped following the discovery of a publication by Taddei and Mann detailing the optimized conditions for the allylsilane trapping of the CHC-generated *N*-acyliminium ion as shown in **Scheme IV-30**.[16]

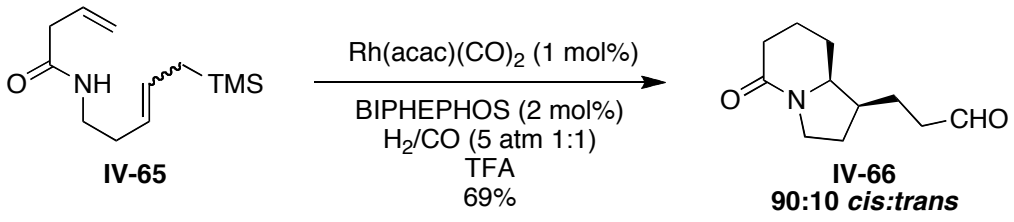

Scheme IV-30: Results from Taddei and Mann[16]

4.1.4 Application of CHC trapping using enols

The use of enols are nucleophilic trapping agents of *N*-acyliminium ions is well established process.[4c] Thus, it seems obvious to attempt to use these nucleophiles as trapping agents in the CHC- reaction as shown below in **Scheme IV-31**.

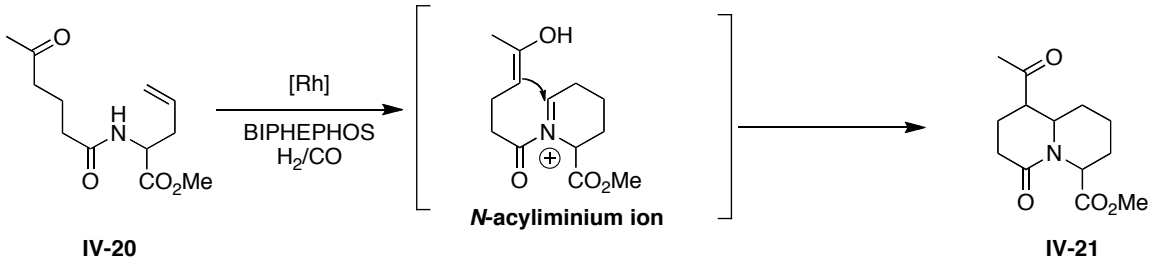

IV-20 **IV-21**

Scheme IV-31: Strategy for trapping of CHC-adduct using enols

The synthesis of compound **IV-20** is very straightforward as the free acid of the desired amide is commercially available. The free acid was first transformed into lactone **IV-68** in the presence of acetic anhydride and catalytic amounts of *p*-TSA. Lactone **IV-68** was immediately opened under mild conditions with allyl amine to afford amide **IV-69** in 96% isolated yield over two steps (**Scheme IV-32**).

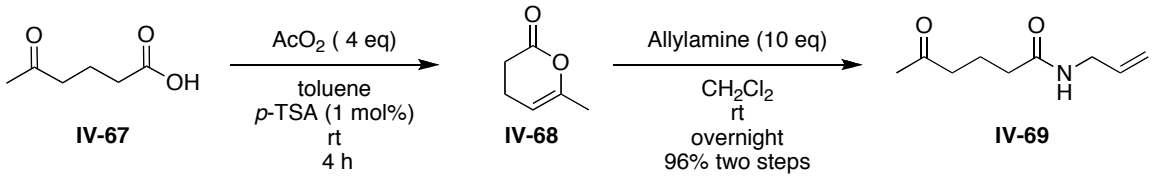

IV-67 **IV-68** **IV-69**

Scheme IV-32: Synthesis of the enol substrate

Amide **IV-69** was subjected directly to CHC-reaction screening conditions. Several CHC-reactions under various conditions were attempted with substrate **IV-72**, FIA mass analysis showed conversion of the starting material. However, no product was obtained. The lack of product in this is likely due to the inability to observe the product on TLC

because it lacks a chromophore and fails to stain with standard laboratory staining agents; although, compound **IV-69** can be observed on TLC by staining with sulfuric acid ethanol mixture. Thus, the substrate was modified at the ketone terminus to incorporate a phenyl, which can be obtained from commercially available **IV-70**. The new substrate bearing the phenyl moiety at the keto-terminus was transformed to the desire amide under similar conditions as compound **IV-69** to give amide **IV-72** in 90% isolated yield (**Scheme IV-33**).

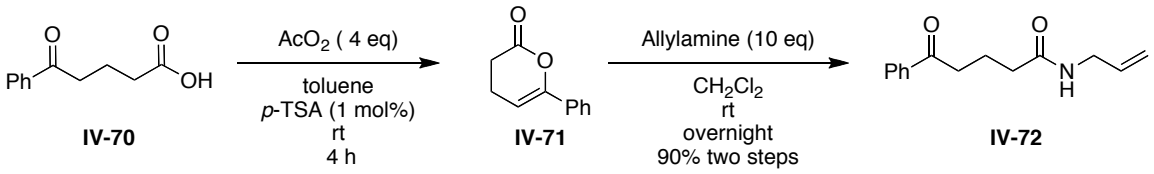

Scheme IV-33:Synthesis of modified phenyl substrate

Amide **IV-72** was subjected directly to CHC-reaction screening conditions. The exploratory conditions chosen were based on previous conditions employing strongly acidic media, where *N*-acyliminum ion were trapped in a step-wise manner with enols.[4c] Thus, acetic acid was chosen as the solvent and acid source based on the previous positive results obtained with acetic acid as solvent. The results shown in Scheme **IV-34** are based on preliminary HPLC and FIA results. Mass analysis showed a molecular weight corresponding to the hydrogenated enamide and a mass corresponding to the desired product, which also has the same molecular weight as the enamide byproduct. Analysis by HPLC confirmed three peaks in approximately 1:1:1, which indirectly confirmed the results observed by mass (**Scheme IV-34**).

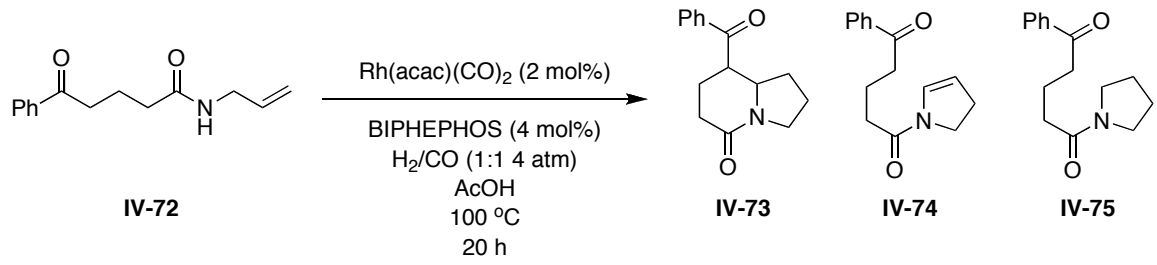

Scheme IV-34: CHC conditions for enol nucleophiles

Continued LC-MS analysis is necessary in order to obtain definitive results. Furthermore, continued screening of optimized conditions is ongoing.

4.2. Experimental Methods

General Information:

All chemicals were obtained from Sigma-Aldrich, TCI-America or Acros Organic and used as is unless otherwise noted. All reactions were performed under Schlenk conditions with oven-dried glassware unless otherwise noted. Anhydrous methylene chloride, toluene, tetrahydrofuran, and ethyl ether were kept under nitrogen and were dried using the PURESOLV system (Innovative Technologies, Newport, MA). Anhydrous dimethoxyethane (DME) was obtained from Acros Organics and used without further purification. Anhydrous methanol was obtained by distillation over calcium hydride. ^{1}H, ^{13}C and ^{31}P NMR data were obtained using either 300 MHz Varian Gemni 2300 (75 MHz ^{13}C, 121 MHz ^{31}P) spectrometer or the 400 MHz Varian INOVA 400 (100 MHz ^{13}C, 162 MHz ^{31}P) spectrometer in $CDCl_3$ as a solvent unless other wise noted. Chemical shifts (δ) are reported in ppm and standardized with solvent as internal standard based on literature reported values. Melting points were measured on Thomas Hoover Capillary melting point apparatus and are uncorrected. GC/MS was performed on Agilent 6890 GC/ 5973 Mass selective detector with electron ionization. LC/MS was performed using FIA (flow-injection analysis) using Agilent 1100 LS-MSD electrospray ionization (ESI) single quadrupole mass spectrometer. Purification using chromatography was performed either manually using standard flash chromatography on silica gel or automatically using Yamazen W-Prep 2XY A type automated chromatography system and prefabricated silica gel columns.

3,3'-Di-*tert*-butyl-5,5'-dimethoxybiphenyl-2,2'-diol (IV-23):[17]

Potassium hydroxide (13.06 g, 232.75 mmol), and potassium ferricyanide (21.92 g, 66.5 mmol) were dissolved in 100mL of water. The 4-methoxy-6-*t*-butylphenol (12.00 g, 66.5 mmol) dissolved in 100 mL of acetone was added drop-wise with stirring. The reaction mixture was stirred for 5 min. The mixture was extracted with three 150 mL portions of ethyl acetate. The resulting organic phase was dried over $MgSO_4$. The crude mixture was concentrated to afford a brown solid that was recrystallized from hexanes, to afford a fine white powder (10.0 g, 84% yield): ^{1}H NMR (300 MHz, $CDC1_3$) δ 1.47 (s, 18H),

3.78 (s, 6 H), 5.05 (d, 2 H, *J*= 3 Hz), 6.64 (d, 2H, *J*= 3 Hz) 6.68 (d, 2H, *J*= 3 Hz). All values are in agreement with literature reported.[18]

BIPHEPHOS, (6,6'-[(3,3'-di-*t*-butyl-5,5'-dimethoxy-1,1'-biphenyl-2,2'-diyl)bis(oxy)]bis(dibenzo[d,f][1,3,2]dioxaphosphepin) (III-15):[19]

Phosphorous trichloride (8 ml, 82.58 mmol) was added neat to 2,2'-biphenol (4.00 g, 21.5 mmol). The mixture was refluxed for 2 h. The product was immediately distilled by Kugelhor (200 ^{o}C, 0.5 mmHg), affording the desired phosphochloridite (**IV-25**) as clear viscous oil (3.75 g, 70% yield) ^{31}P NMR (125 MHz, $CDCl_3$) d 180.56. The resulting phosphorchloridite was dissolved in 12 mL of toluene and added drop-wise to a stirred solution of 48 mL of toluene, TEA (9.03 g, 89.3 mmol) at -40 ^{o}C. The resulting mixture was warmed to room temperature and stirred overnight. Water was added until a precipitate formed. The resulting mixture was filtered. The solid was then recrystallized from acetonitrile to afford compound **III-15** was white powder solid (2.23 g, 17% yield): mp 166-167 ^{o}C (lit mp[19] 147-150 ^{o}C); ^{1}H (300 MHz, $CDCl_3$) δ 1.46 (s, 18H), 3.39 (s, 6H), 6.90-7.32 (m, 20H); ^{31}P NMR (125 MHz, $CDCl_3$) δ 146.96. All values are in agreement with literature reported.[19]

Allylglycine methyl ester (IV-27):[9]

Allylglycine hydrochloride (1.00 g, 8.69 mmol) in 100 mL round-bottomed flask charged with nitrogen was dissolved in MeOH (30 mL). This solution was then cooled to 0 ^{o}C and thionyl chloride (2.07 g, 17.4 mmol) was added drop-wise. The reaction mixture was slowly warmed to room temperature and was then heated to 50 ^{o}C overnight. After the heating the solvent was evaporated to afford **IV-27** as a light yellow oil. The product was used as is for the subsequent reactions: ^{1}H NMR (300 MHz, $CDCl_3$) δ 2.84 (s, 2 H), 3.80 (s, 3 H), 4.26 (s, 1 H), 5.23 (m, 2 H), 5.84 (m, 1 H), 8.21 (bs, 2 H). All values are consistent with literature.[9]

Methyl 2-[2-(3,4-dimethoxyphenyl)acetamido]pent-4-enoate (IV-29):[9]

(3,4-Dimethoxyphenyl)acetic acid (1.18 g, 6.04 mmol) and EDC HCl (1.273 g, 6.64 mmol) was placed in a 25 mL round-bottomed flask and dissolved in 6 mL of

dichloromethane. After a short stirring period allylglycine (1.00 g, 6.04 mmol) in 6 mL of dichloromethane was added drop-wise to the stirred solutions. The reaction mixture was stirred overnight followed by the addition 4 mL of saturated sodium hydrogen carbonate to the reaction mixture. The mixture was extracted three times with 20 mL portions of ethyl acetate. The combined organic layers were washed twice with 20 mL saturated aqueous ammonium chloride. The organic layer was dried over $MgSO_4$ and the solvent removed. The crude material was subjected to flash column chromatography silica gel with hexanes:EtOAc (3:1) to afford compound **IV-29** as an off white solid (1.07 g, 58% yield): mp 45-47 ^oC; ^1H NMR (300 MHz, $CDCl_3$) δ 2.42 (m, 2H), 3.54 (s, 2 H), 3.71(s, 3H), 3.88 (s, 6H), 4.64 (td, 1H, *J*= 5.4, *J*= 1.8 Hz), 4.94(m, 1H), 4.94 (m, 2H), 5.51 (m, 1H), 6.78 (m, 3H); ^{13}C NMR (100 MHz, $CDCl_3$) δ 36.2, 43.6, 51.9, 56.1, 56.5, 111.6, 112.9, 116.4 122.9, 131.5, 132.7, 148.7, 150.3, 171.5, 171.6.; FIA ESI found m/z 307 [M+] calcd. for $C_{16}H_{21}NO_5$ 307.14 .

Methyl 2-[3-(3,4-dimethoxyphenyl)propanamido]pent-4-enoate (IV-31): [9]

(3,4-Dimethoxyphenyl)propanoic acid (1.18 g, 6.04 mmol) and EDC HCl (1.273 g, 6.64 mmol) was placed in a 25 mL round-bottomed flask and dissolved in 6 mL of dichloromethane. After a short stirring period allyl glycine (1.00 g, 6.04 mmol) in 6 mL of dichloromethane was added drop-wise to the stirred solution. The reaction mixture was stirred overnight followed by addition 4 mL of saturated sodium hydrogen carbonate reaction mixture. The mixture was extracted three times with 20 mL portions of ethyl acetate. The combined organic layers were washed twice with 20 mL saturated aqueous ammonium chloride. The organic layer was dried over $MgSO_4$ and the solvent removed. The crude material was then subjected to flash column chromatography on silica gel chromatography hexanes:EtOAc (3:1) to afford compound **IV-31** a yellow solid (1.07 g, 58% yield): mp 69-71 ^oC; ^1H NMR (300 MHz, $CDCl_3$) δ 2.45 (m, 2H), 2.90 (t, 1H, *J*= 4.6 Hz), 3.75 (s, 3H), 3.85 (s, 6H), 4.65 (m, 2H), 5.05 (m, 2H) 5.45(m, 1H), 6.70 (d, 2H) 6.73 (s, 1H); ^{13}C NMR (100 MHz, $CDCl_3$) δ 31.9, 36.1, 36.7, 52.3, 56.5, 56.7, 56.8, 113.1, 114.0, 116.7, 122.5, 132.7, 133.2, 147.0, 149.7, 171.5, 173.3; FIA ESI found m/z 322 [M+H] calc. for $C_{17}H_{23}NO_5$ 321.16

Methyl 2-[2-(3,4,5-trimethoxyphenyl)acetamido]pent-4-enoate (IV-35):[9]

(3,4,5-Trimethoxyphenyl)acetic acid (157 mg, 0.60 mmol,) and EDC HCl (126 mg, 0.66 mmol,) was placed in a 25 mL round-bottomed flask and dissolved in 2 mL of dichloromethane. After a short stirring period allylglycine (115 mg, 0.69 mmol) and TEA (60.6 mg, 0.60) in 3 mL of dichloromethane were added drop-wise to the stirred solutions. The reaction mixture was stirred overnight followed by addition of 4 mL of saturated sodium bicarbonate to the reaction mixture. The reaction mixture was extracted with ethyl acetate (3 x 20 mL). The combined organic layers were washed twice with 20 mL saturated aqueous ammonium chloride. The organic phase was dried over $MgSO_4$ and the solvent removed. The crude material was subject to flash column chromatography on silica gel with hexanes:EtOAc (2:1) as eluent to afford compound **IV-35** as clear light yellow oil (146 mg, 63% yield): ^{1}H NMR (400 MHz, $CDCl_3$) δ 2.42 (m, 2H), 3.50 (s, 2H), 3.70 (s, 3H) 3.83 (s, 6H), 4.60 (dd, 1H, *J*= 6.3 Hz, *J*= 1.5 Hz), 4.93 (m, 1H), 5.51 (m, 1H), 5.96 (d, 1H, *J*= 7.6 Hz), 6.46 (s, 2H); ^{13}C NMR (100 MHz, $CDCl_3$) δ 36.7, 44.1, 51.6, 52.6, 56.4, 61.0, 106.6, 119.4, 130.2, 132.2, 153.8, 170.7, 172.2.

General Procedure for the CHC Reaction:

Substrates (100 mg, 0.425 mmol) $Rh(acac)(CO)_2$ (2.2 mg, 2 mol%), BIPHEPHOS (14 mg, 4 mol%) were placed in 30 mL vial. Solvent (6 mL) was added and the resulting solution was stirred until a light yellow color was noted. The vial was placed open into a 300 mL autoclave reactor. The reactor was sealed and purged with carbon monoxide three times, then the reactor was filled to 2 atm of carbon monoxide and the same pressure of hydrogen. The reaction vessel was placed in an oil bath and heated to the desired temperature for 18-20 hours. System was cooled and evacuated. The vial was removed and solvent evaporated *in vacuo*. The resultant crude material was subject to flash column chromatography on silica gel with hexanes:EtOAc as eluent.

***N*-Allyl-2-(3,4-dimethoxyphenyl)acetamide (IV-37):**

(3,4-Dimethoxyphenyl)acetic acid (2.00 g, 8.8 mmol) and EDC·HCl (2.53 g, 13.2 mmol) was placed in a 250 mL round-bottomed flask and dissolved in 44 mL of

dichloromethane. After a short stirring period allylamine (1.26 g, 22.1 mmol) was added drop-wise to the stirred solutions. The reaction mixture was stirred overnight and then 4 mL of saturated sodium hydrogen carbonate was added to the reaction mixture. The mixture was then extracted three times with 20 mL portions ethyl acetate. The combined organic layers were washed twice with 20 mL saturated aqueous ammonium chloride. The combined organic layers were dried over $MgSO_4$ and the solvent removed. The crude material was then subjected to flash column chromatography on silica gel (hexanes:EtOAc 4:1) to afford compound **IV-37** as white solid (1.94 g, 83% yield): mp 78-80 ^oC; ^1H NMR (300 MHz, $CDCl_3$) δ 3.54 (s, 2H), 3.82(m, 2H), 3.85 (s, 6H), 5.02 (m, 2H), 5.72 (1H, m), 6.78 (d, 1H *J*= 7.5 Hz), 6.83 (s, 1H), 6.86 (s, 1H); ^{13}C NMR (100 MHz,$CDCl_3$) δ 41.0, 43.2, 57.3, 110.2, 112.1, 116.5, 121.5, 132.1, 135.5, 149.1, 150.6 , 171.4

8,9-Dimethoxy-1,2,3,10b-tetrahydropyrrolo[2,1-*a*]isoquinolin-5(6*H*)-one (IV-38):
N-Allyl-2-(3,4-dimethoxyphenyl)acetamide (100 mg, 0.425 mmol) $Rh(acac)(CO)_2$ (2.2 mg, 2 mol%), BIPHEPHOS (14 mg, 4 mol%) were placed in 30 mL vial. Acetic acid (6 mL) was added and solution was stirred until a light yellow color was noted. The vial was placed open into a 300 mL autoclave reactor. The reactor was sealed and purged with carbon monoxide three times, then the reactor was filled with 2 atm of carbon monoxide and 2 atm of hydrogen. The reaction vessel was placed in an oil bath and heated to 60 ^oC for 18 hours. The system was cooled and purged. The vial was removed and solvent evaporated *in vacuo*. The resultant crude material was subject to column chromatography on silica gel (hexanes: EtOAc 2:1) to afford compound **IV-38** as a light yellow oil (86 mg, 42% yield): ^1H NMR (300 MHz, $CDCl_3$) δ 2.00 (t, 2H *J*= 5.7 Hz) 6.84 (s, 1H), 2.59 (t, 2H, *J*= 6 Hz), 3.79 (m, 2H), 3.83 (s, 6H), 4.20 (s, 2H), 6.82 (s, 1H); ^{13}C NMR (400 MHz, $CDCl_3$) δ 17.3, 29.9, 33.9, 42.4, 45.9, 56.1, 111.4, 113.2, 122.1, 126.79, 148.3, 149.0, 172.5, 175.5; Mass spectrum FIA LC-MS found 265.3 [M+18] calc. for $C_{14}H_{17}NO_3$: 247.29

3,5-Dimethoxyphenyl)methanol (IV-41):[14]

A flask containing lithium aluminum hydride (1.56 g, 41.7 mmol) was charged with 32 mL of dry THF. A solution containing 3,5-dimethoxybenzoic acid (5.00 g, 27.4 mmol) in THF was slowly added to lithium aluminum hydride suspension. The reaction mixture was heated to reflux for 4 h in an oil bath. After heating water was added until no further gas evolution was noted, then 50 mL of 1 M sulfuric acid was added to mixture. The resulting cloudy grey solution was extracted with dichloromethane (50 mL x 3). The combined organic layers were washed with brine (50 mL x 2). The organic layer was then dried over $MgSO_4$ and solvent removed to afford compound **IV-41** a white solid (3.65 g, 98% yield): ^{1}H NMR (400 MHz, $CDCl_3$) δ 3.80 (s, 3.80), 4.63 (s, 2H), 6.39 (s, 1H), 6.52 (s, 2H). All values are consistent with literature.[14]

3,5-Dimethoxybenzaldehyde (IV-42):[14]

Compound **IV-41** (3.65 g, 21.7 mmol) and pyridinium chlorochromate (PCC)(4.67 g, 21.7 mmol) were dissolved in 72 mL of dichloromethane and stirred under nitrogen for 24 h. After the stirring the reaction mixture was filtered through celite. The celite was washed with 1:1 mixture of hexanes ethyl acetate and filterate collected. The material was filtered through silica gel and washed with ethyl acetate. The filterate was collected and the solvent evaporated to afford a crude brown solid, which was subject to column chromatography on silica gel using Yamzen Parallel PrepXY automated chromatography system to afford the desired compound **IV-42** as a white solid (3.35 g, 93% yield): mp 38-40 ^{o}C (lit[20] mp 46-47 ^{o}C); ^{1}H NMR (300 MHz, $CDCl_3$) δ 3.84 (s, 6H), 6.85 (s, 1H), 7.02 (s, 2H), 9.91 (d, 1H, J=0.6 Hz). All values are consistent with literature.[20]

1,3-Dimethoxy-5-[(*E*)-2-nitroethenyl]benzene (IV-43):[21]

3,5-Dimethoxybenzaldehyde **(IV-42)** (3.35 g, 20.16 mmol) and ammonium acetate (1.55 g, 20.16 mmol) were dissolved in 106 mL of nitromethane. The solution was heated to reflux and the reaction carefully monitored by TLC. Upon completion the solvent was removed to afford a brown solid that was dissolved in ether and washed with water (50 mL X 3). The combined aqueous layers were extracted with ether (20 mL x 3). The combined organic layers were washed with saturated sodium bicarbonate. The organic

phase was collected and dried over $MgSO_4$ and the solvent removed to afford a brown solid. The resultant brown solid was recrystallized from ethanol twice to afford compound **IV-43** as yellow needles (42% yield, 1.77 g): mp 126-127 ^oC (lit.[22]mp 129-131 ^oC); ^1H NMR (300 MHz, $CDCl_3$) δ 3.82 (s, 6H), 6.58 (d, 1H, *J*= 2.1 Hz), 6.65 (d, 2H, *J*= 2.1 Hz), 7.25 (d, 1H, *J*= 13.5 Hz), 7.90 (d, 1H, *J*= 13.8 Hz). All values are consistent with literature. [21]

3-(*E/Z*)-*N*-(Prop-2-en-1-yl)-5-(trimethylsilyl)pent-3-enamide (IV-47):

Compound **IV-49** and EDC·HCl (102 mg, 0.547 mmol) were placed in a 10 mL round-bottomed flask and dissolved in 2 mL of dichloromethane. After a short stirring period allylamine (62 mg, 1.09 mmol) was added drop-wise to the stirred solutions. The reaction mixture was stirred overnight and 4 mL of saturated sodium hydrogen carbonate was added to the reaction mixture. The mixture was then extracted three times with 20 mL portions ethyl acetate. The combined organic layers were washed twice with 20 mL saturated aqueous ammonium chloride. The combined organic layers were dried over $MgSO_4$ and the solvent removed. The crude material was subjected to column chromatography on silica gel (hexanes:EtOAc 5:1) to afford compound **IV-47** as a light yellow oil (71% yield 87 mg): ^1H NMR (400 MHz, $CDCl_3$) δ 0.02 (s, 9H), 0.19 (m, 2H), 0.99 (m, 2H), 1.10 (m, 2H), 1.47 (m, 2H), 1.50 (m, 2H), 1.87 (d, 2H, *J*= 5.1 Hz), 4.51 (d, 1H), 5.46 (d, 1H, *J*= 18 Hz), 5.63 (m, 1H), 6.05 (m, 1H); ^{13}C NMR (100 MHz, $CDCl_3$) δ -2.0, -1.9, 16.7, 17.5, 18.1, 22.2, 30.3,126.5, 131.1*z*, 134.4, 142.9, 171.9. Mass spectrum FIA found 338 m/z [M+TFA] cald. 225.40

3-(*E*/*Z*)-5-(Trimethylsilyl)pent-3-enoic acid (IV-49)[23]:

To a solution of 3-pentenoic acid (1.0 g, 9.98 mmol) and allyltrimethylsilane (2.75 g, 24.0 mmol) in DCM (50 mL) at reflux was added the Grubbs-Hoveyda catalyst (3 mol%, 180 mg). The reaction mixture was allowed to stir at reflux for 24 h and after cooling to room temperature the solvent was removed *in vacuo*. The crude product was purified by column chromatography on silica gel (hexanes:EtOAc 6:4) to yield compound **IV-49** as yellow oil (1.04 g, 58% yield): *E/Z* 3:1: NMR data of the mixture of *E/Z* isomers: ^1H NMR (400 MHz, $CDCl_3$) δ 5.70-5.62 (m, 1H*Z*), 5.62-5.54 (m, 1H*E*), 5.46 (dt, *J*= 7.1,

10.9, Hz), 5.34 (dt, *J*= 7.1, 15.2, 1H*E*), 3.10 (d, *J*= 7.1, 2 H*Z*), 3.07 (d, *J*= 7.1, 2H*E*), 1.53-1.47 (m, 2H*E & Z*), 0.02 (s, 9H*Z*), 0.00 (s, 9H*E*); ^{13}C NMR (100 MHz, $CDCl_3$) δ -2.0, -1.9, 18.9, 22.9, 32.5, 37.9, 117.4, 118.9, 130.0*Z*, 131.8, 178.7; FIA found 204 [$M+NH_4^+$] cald. For $C_9H_{18}O_2Si$ 186.11. All values are in agreement with literature reported.[23]

***(E)*-Ethyl 2-(4-bromobut-2-enyl)malonate (IV-57):**

Sodium hydride (60% w/w in mineral oil) (2.6 g, 70.25 mmol) was suspended in dry THF (150 mL). The suspension was cooled to 0 ^{o}C with stirring. A solution of diethylmalonate (5.00 g, 31.2 mmol) in 20 mL THF was added drop-wise to the THF-suspension. A solution of *trans*-1,4-dibromo-2-butene (10.0 g, 46.83 mmol) dissolved in 20 mL of the THF was added all at once. The reaction mixture was stirred overnight. The reaction was quenched with the slow addition of the water. The resulting mixture was extracted with three 50 mL portions of the ether. The combined organic phases were washed with two 50 mL portions of brine. The organic phase was dried over $MgSO_4$ and the solvent evaporated. The resultant crude mixture was subjected to column chromatography on silica gel (hexanes:EtOAc 9:1) to afford compound **IV-57** as a clear colorless oil (8.20 g, 90% yield): ^{1}H NMR ($CDCl_3$, 300 MHz) δ 1.21 (m, 6H), 1.51 (t, 1H, *J*= 3.9 Hz), 1.63 (t, 1H, *J*= 4.8 Hz), 2.50 (q, 1H, *J*= 8.4 Hz), 3.91 (d, 1H), 4.11(m, 4H), 5.08(dd, 1H *J*= 1.8 Hz, *J*=10.2 Hz), 5.31 (m, 1H). ^{13}C NMR (100 MHz, $CDCl_3$) δ 16.1, 32.1, 34.2, 63.3, 54.2, 132.1, 138.4, 171.2.

(*E*)-*tert*-Butyl allyl(6-hydroxyhex-4-enoyl)carbamate (IV-60):

Compound **IV-58** (3.00 g, 10.7 mmmol) was dissolved in 20 mL absolute ethanol and placed in a 35 mL microwave reactor tube. 6 N potassium hydroxde (1.72 g, 30.7 mmol) was added to the solution. The mixture was heated to 80 ^{o}C in a CEM-Discover microwave reactor for 1 h. After the heating the solution was acidified to pH 2 using 12 N HCl. The resulting solution was then partitioned three times with 20 mL ethyl acetate. The resulting organic phases were combined and washed with saturated aqueous sodium bicarbonate. The organic phase was dried over $MgSO_4$ and the solvent was evaporated under reduced pressure. The resulting oil was used for the next reaction without further purification. Free acid **IV-59** (10.7 mmol) and EDC·HCl (2.34 g, 12.24 mmol) were

dissolved in 25 mL of dichloromethane. *N*-Boc-allylamine was dissolved in 5 mL of dichloromethane and added to the solution. After 5 min of stirring TEA (2.27 g, 22.4 mmol) was added drop-wise to the mixture. The reaction mixture was stirred overnight at room temperature. The reaction was quenched with water and partitioned with dichloromethane. The resulting organic phases were combined, washed with brine and dried over $MgSO_4$. The solvent was evaporated and the crude mixture was subjected to column chromatography on silica gel (hexanes:EtOAc 3:1) to afford the title compound **IV-60** as clear colorless liquid (2.00 g, 73% yield for 2 steps): IR (NaCl plate cm^{-1}) 3348, 3082, 2978, 2931, 1697, 1646, 1455, 1059; ^1H NMR ($CDCl_3$, 300 MHz) δ 1.17 (q, 2H), 1.43 (s, 9H), 3.46 (q, 2H *J*= 4 Hz), 3.73 (s, 2H), 3.95 (dd, 2H), 4.65 (bs, 1H), 5.07 (m, 2H), 5.78 (m, 2H); ^{13}C NMR ($CDCl_3$, 400 MHz) δ 15.15, 28.36, 43.08, 65.64, 70.55, 79.34, 115.64, 129.48, 134.09, 155.75;

***tert*-Butyl-*N*-[(4*E*)-6-{[(4-methylbenzene)sulfonyl]oxy}hex-4-enoyl]-*N*-(prop-2-en-1-yl)carbamate (IV-61):**

Compound **IV-60** (500 mg, 1.85 mmol) was dissolved in 10 mL of the dichloromethane and cooled to 0 ^oC. To this mixture was added a solution of *p*-toulenesulfonyl chloride (424 mg, 2.22 mmol) in 10 mL dichloromethane. The reaction mixture was stirred for several mins after which TEA (224 mg, 2.22 mmol) was added drop-wise. The reaction mixture was allowed to warm to room temperature and stirred overnight. The reaction was quenched with aqueous NH_4Cl and extracted with ether (20 mL x 3). The organic layers were combined, dried over $MgSO_4$, filtered and concentrated. The resulting crude oil was purified by flash column chromatography on silica gel (hexnanes:EtOAc 6:1) to afford the desired product **IV-61** as clear oil (673 mg, 86% yield): ^1H NMR ($CDCl_3$, 300 MHz) δ 0.87 (m, 2H), 1.23 (m, 2H), 1.28 (m, 9H), 2.44 (s, 3H), 3.74 (bs, 2H), 5.07 (m, 2H), 5.78 (m, 1H), 7.35 (d, 2H, *J*= 2.5 Hz), 7.77(d, 2H, *J*= 8.4 Hz);

References

(1). Aniszewski, T., *Alkaloids - secrets of life: alkaloid chemistry, biological significance, applications and ecological role* Elsevier Science: Amsterdam, **2007**.

(2). Liddell, J. R., Pyrrolizidine alkaloids *Nat. Prod. Rep.* **2000**, *17*, 455–462

(3). Gellert, E., The Indolizidine alkaloids. *J. Nat. Prod.* **1982**, *45*, 50–73.

(4). (a) Bardot, V.; Gardette, D.; Gelas-Mialhe, Y.; Gramain, J.-C.; Remuson, R., A synthesis of the quinolizidine alkaloids (±)-lasubine I and (±)-lasubine II. *Heterocycles* **1998**, *48*, 507-518; (b) Gardette, D.; Gelas-Mialhe, Y.; Gramain, J.-C.; Perrin, B.; Remuson, R., Enantioselective synthesis of the quinolizidine alkaloids (+)-myrtine and (-)-epimyrtine. *Tetrahedron: Asymmetry* **1998**, *9*, 1823-1828; (c) Maryanoff, B. E.; Zhang, H.-C.; Cohen, J. H.; Turchi, I. J.; Maryanoff, C. A., Cyclizations of *N*-acyliminium ions *Chem. Rev.* **2004**, *104* 1431-1628; (d) Wijdeven, M. A.; Wijtmans, R.; van den Berg, R. J. F.; Noorduin, W.; Schoemaker, H. E.; Sonke, T.; van Delft, F. L.; Blaauw, R. H.; Fitch, R. W.; Spande, T. F.; Daly, J. W.; Rutjes, F. P. J. T., *N,N*-Acetals as *N*-acyliminium ion precursors: Synthesis and absolute stereochemistry of epiquinamide. *Org, Lett.* **2008**, *10*, 4001-4003; (e) Zhang, W.; Franzen, J., Diverse asymmetric quinolizidine synthesis: A stereodivergent one-pot approach. *Advan. Syn. Catal.* **2010**, *352*, 499-518.

(5). Kuntiyong, P.; Akkarasamiyo, S.; Eksinitkun, G., Short synthetic route toward the tricyclic core of schulzeines. *Chem. Lett.* **2006**, *35*, 1008-1009.

(6). Hiemstra, H.; Sno, M. H. A. M.; Vijn, R. J.; Speckamp, W. N., Silicon directed *N*-acyliminium Ion cyclizations. highly selective syntheses of (+/-) -isoretronecanol and (+/-)-epilupinine. *J. Org. Chem.* **1985**, *50*, 4014-4020

(7). (a) Abillard, O.; Breit, B., Domino hydroformylation/enantioselective cross-aldol addition. *Adv. Synth. Catal.* **2007**, *349*, 1891-1895; (b) Airianu, T.; Spangenberg, N.; Girard, A. S.; Salvardori, J.; Taddei, M.; Mann, A., A general approach to aza-heterocycles by means of domino sequences driven by hydroformylation. *Chem. Eur. J.* **2008**, *14*, 10938-10948; (c) Farwick, A.; Helmchen, G., Stereoselective synthesis of β-proline derivatives from allylamines via domino hydroformylation/Wittig olefination and aza-Michael addition. *Adv. Synth. Catal.* **2010**, *352*, 1023-1032; (d) Marchetti, M.; Paganelli, S.; Carboni, D.; Ulgheri, F.; Del Ponte, G., Synthesis of indole derivatives by domino

hydroformylation/indolization of 2-nitrocinnamaldehydes. *J. Mol. Catal A: Chem.* **2008**, *288*, 103-108.

(8). Briet, B., Synthetic aspects of stereoselective hydroformylation *Acc. Chem Res.* **2003**, *36*, 264-275.

(9). Chiou, W.-H.; Mizutani, N.; Ojima, I., Highly efficient synthesis of azabicyclo[x.y.0]alkane amino acids and congeners by means of Rh-catalyzed cyclohydrocarbonylation. *J. Org. Chem.* **2007**, *72*, 1871.

(10). (a) Chabaud, L.; Philippe James; Landais, Y., Allylsilanes in organic synthesis − recent developments *Eur. J. Org. Chem.* **2004**, 3173-3199; (b) Sakurai, H., Reaction of allysilanes and appliction to organic synthesis *Pure Appl. Chem* **1982**, *54*, 1-22.

(11). Sugawara, M.; Yoshida, J.-i., Evaluation of β- and γ-effects of Group 14 elements using intramolecular competition. *J. Org. Chem.* **2000**, *65*, 3135–3142.

(12). Chiou, W.-H.; Lin, G.-H.; Hsu, C.-C.; Chaterpaul, S. J.; Ojima, I., Efficient syntheses of crispine-A and harmicine by Rh-catalyzed cyclohydrocarbonylation. *Org. Lett.* **2009**, *11*, 2659-2662.

(13). (a) Liu, G.; Romo, D., Enantioselective synthesis of schulzeines B and C via a β-lactone-derived surrogate for bishomoserine aldehyde. *Org. Lett.* **2009**, *11*, 1143-1146 ; (b) Takada, K.; Uehara, T.; Nakao, Y.; Matsunaga, S.; Soest, R. W. M. v.; Fusetani, N., Schulzeines A−C, new α-glucosidase inhibitors from the marine sponge *Penares schulze*. *J. Am. Chem. Soc.* **2004**, *126*, 187–193.

(14). Tahirovic, Y. A.; Geballe, M.; Gruszecka-Kowalik; Ewa; Myers, S. J.; Lyuboslavsky, P.; Le, P.; French, A.; Irier, H.; Choi, W.-b.; Easterling, K.; Yuan, H.; Wilson, L. J.; Kotloski, R.; McNamara, J. O.; Dingledine, R.; Liotta, D. C.; Traynelis, S. F.; Snyder, J. P., Enantiomeric propanolamines as selective *N*-Methyl-D-aspartate 2β receptor antagonists. *J. Med. Chem.* **2008**, *51*, 5506-5521.

(15). Corrui, R. J. P.; Guerin, C., Alkali metal hydrides : new metallating reagents at silicon *Chem. Comm.* **1980**, 168-169.

(16). Airiau, E.; Spangenberg, T.; Schoenfelder, G. A.; Salvardori, J.; Taddei, M.; Mann, A., A general approach to aza-Heterocycles by means of domino sequences driven by hydroformylation. *Chem. Eur. J.* **2008**, *14*, 10938-10948.

(17). Jana, R.; Tunge, J. A., A homogeneous, recyclable rhodium(I) catalyst for the hydroarylation of Michael acceptors. *Org, Lett.* **2009**, *11*, 971-974.

(18). Butsugan, Y.; Muto, J. M.; Kawai, M.; Araki, S.; Murase, Y.; Saitolc, K., Structures of autoxidation products of 2-*tert* -butyl-4-methoxyphenol in aqueous alkaline solution *J. Org. Chem.* **1989**, *54*, 4215-4217.

(19). Cuny, G. D.; Buchwald, S. L., Practical, high-yield, regioselective rhodium-catalyzed hydroformylation of functionalize a-olefins. *J. Am. Chem. Soc.* **1993**, *115*, 2066-2068.

(20). Bradbury, B. J.; Bartyzel, P.; Kaufman, T. S.; Nieto, M. J.; Sindelar, R. D.; Scesney, S. M.; Gaumond, B. R.; Marsh, H. C., Jr., Synthesis and complement inhibitory activity of B/C/D-ring analogues of the fungal metabolite 6,7-Diformyl-3',4',4a',5',6',7',8',8a'-octahydro-4,6',7'-trihydroxy- 2',5',5',8a'-tetramethylspiro[1'(2'H)-naphthalene-2(3H)-benzofuran]. *J. Med. Chem.* **2003**, *46*, 2697-2705.

(21). Pettit, R. K.; Pettit, G. R.; Hamel, E.; Hogan, F.; Moser, B. R.; Wolf, S.; Pon, S.; Chapuis, J.-C.; Schmidt, J. M., *E*-combretastatin and *E*-resveratrol structural modifications: Antimicrobial and cancer cell growth inhibitory β-*E*-nitrostyrenes. *Bioorg. Med. Chem.* **2009**, *17*, 6606-6612.

(22). Bridges, A. J., A synthesis of the potent A2 selective adenosine agonist N6-[2-(3,5-dimethoxyphenyl)-2-(2-methylphenyl)ethyl]adenosine, and its 5'-N-ethylribofuranuronamide derivative. *Nucleos. Nuclet.* **1989** *8*,357-366.

(23). Tredwell, M.; Luft, J. A. R.; Schuler, M.; Kenny Tenza; Kendall N. Houk; Véronique Gouverneur, D., Fluorine-Directed Diastereoselective Iodocyclization. *Angew. Chem. Int. Ed* **2007**, *47*, 357-360.

Appendix I

Spectroscopy Data

Please note most NMR data presented here were process from original FID data using MestReNova software version 6.1.1. Some NMR data, all HLPC and FIA data are scanned original spectrum

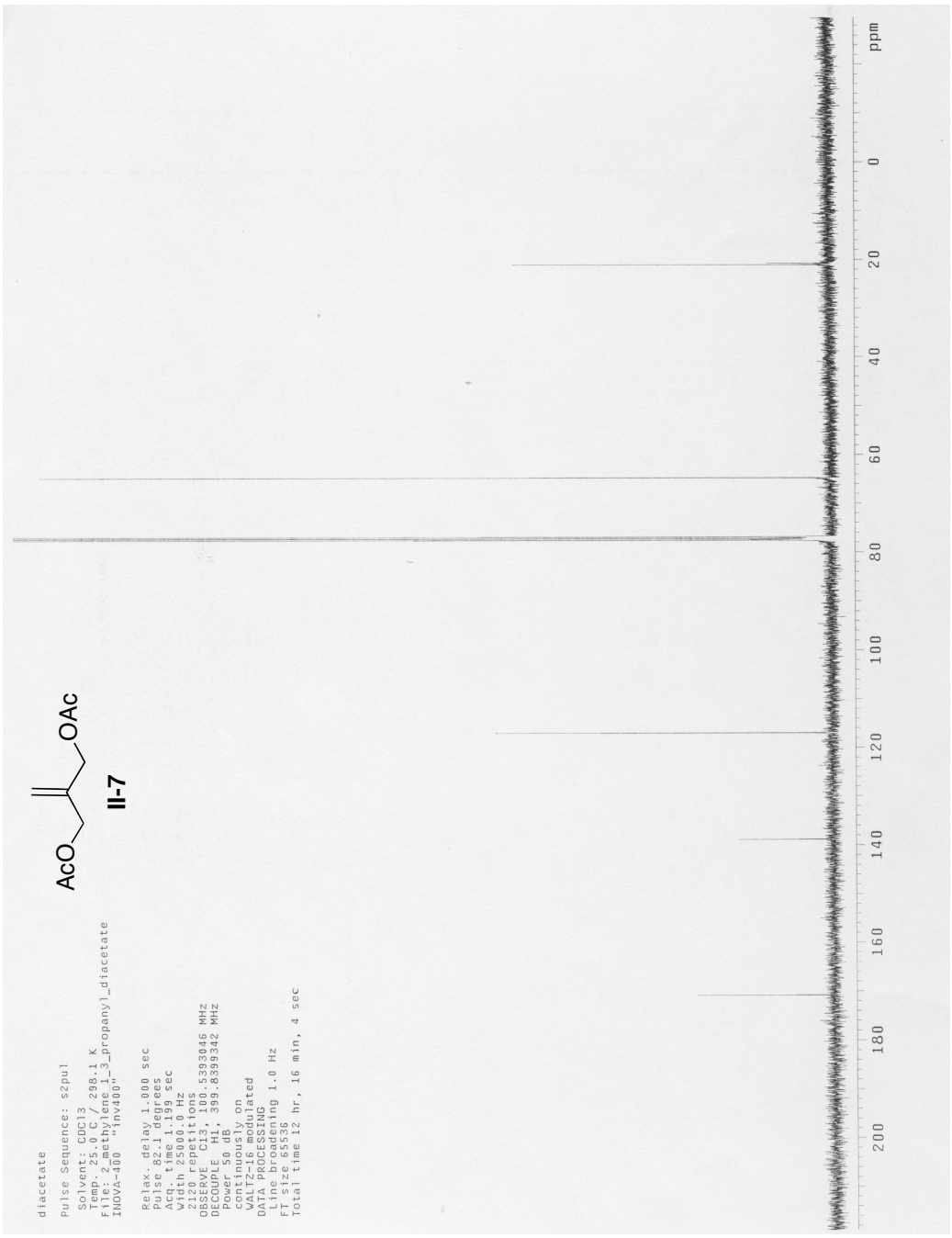
diacetate
Pulse Sequence: s2pul
Solvent: CDCl3
Temp. 25.0 C / 298.1 K
File: 2_methylene_1_3_propanyl_diacetate
INOVA-400 "inv400"
Relax. delay 1.000 sec
Pulse 82.1 degrees
Acq. time 1.199 sec
Width 25000.0 Hz
2120 repetitions
OBSERVE C13, 100.5393046 MHz
DECOUPLE H1, 399.8399342 MHz
Power 50 dB
continuously on
WALTZ-16 modulated
DATA PROCESSING
Line broadening 1.0 Hz
FT size 65536
Total time 12 hr, 16 min, 4 sec
AcO
OAc
II-7
200
180
160
140
120
100
80
60
40
20
0
ppm

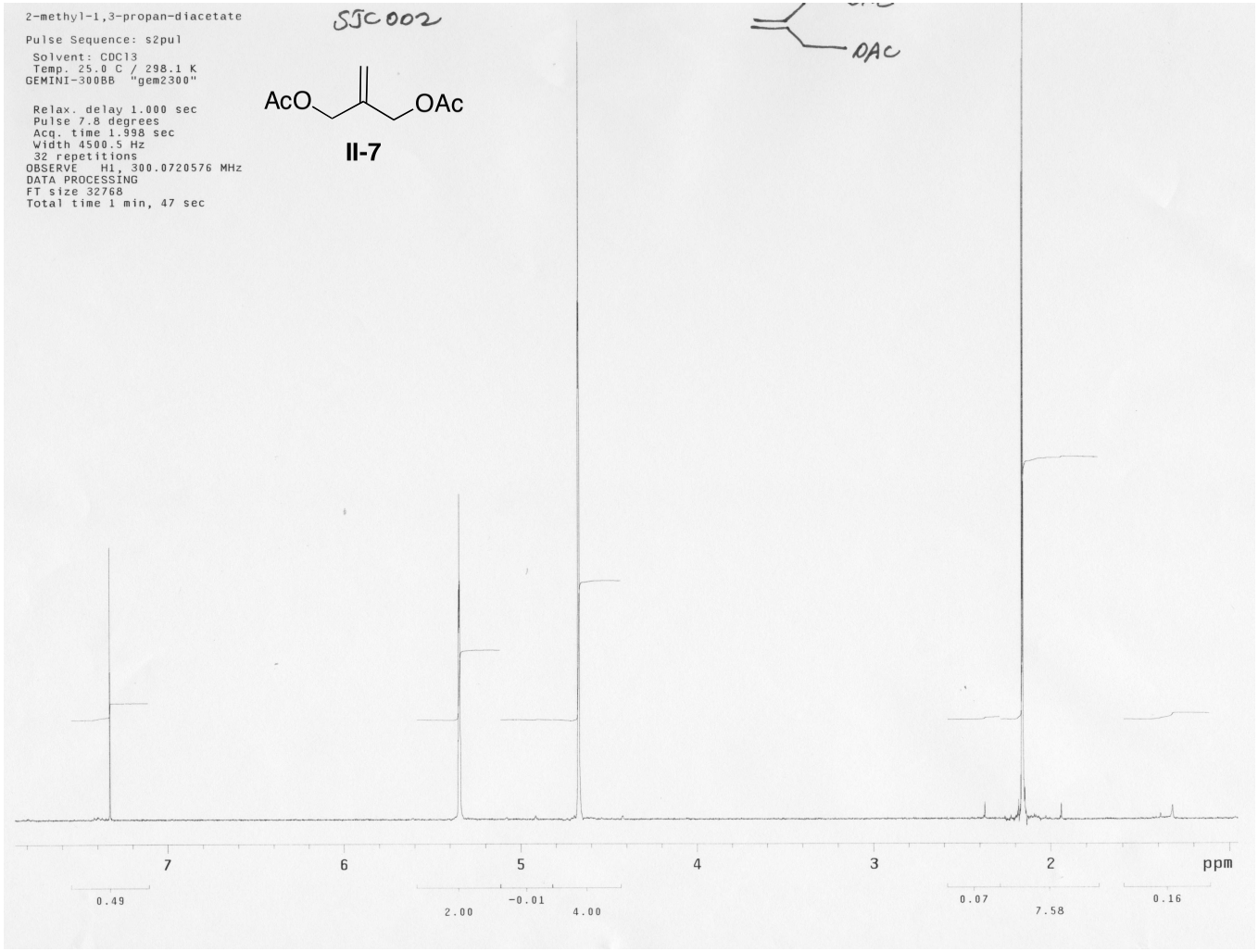
2-methyl-1,3-propan-diacetate
Pulse Sequence: s2pul
Solvent: CDCl3
Temp. 25.0 C / 298.1 K
GEMINI-300BB "gem2300"
Relax. delay 1.000 sec
Pulse 7.8 degrees
Acq. time 1.998 sec
Width 4500.5 Hz
32 repetitions
OBSERVE H1, 300.0720576 MHz
DATA PROCESSING
FT size 32768
Total time 1 min, 47 sec
SJC002
AcO
OAc
II-7
OAc
7
6
5
4
3
2
ppm
0.49
2.00
-0.01
4.00
0.07
7.58
0.16

nylethylamine biphenyl (R),(R),(R)
equence: s2pul
t: CDCl3
25.0 C / 298.1 K
300BB "gem2300"
delay 1.000 sec
50.0 degrees
ime 1.280 sec
3405.4 Hz
ei 13 cons
P31, 121.4712599 MHz
E H1, 300.0735793 MHz
34 dB
uously on
16 modulated
OCESSING
roadening 1.0 Hz
1 32772
ime 7 min, 21 sec
I-40
146.075
180
160
140
120
100
80
60
40
20
0
-20
ppm

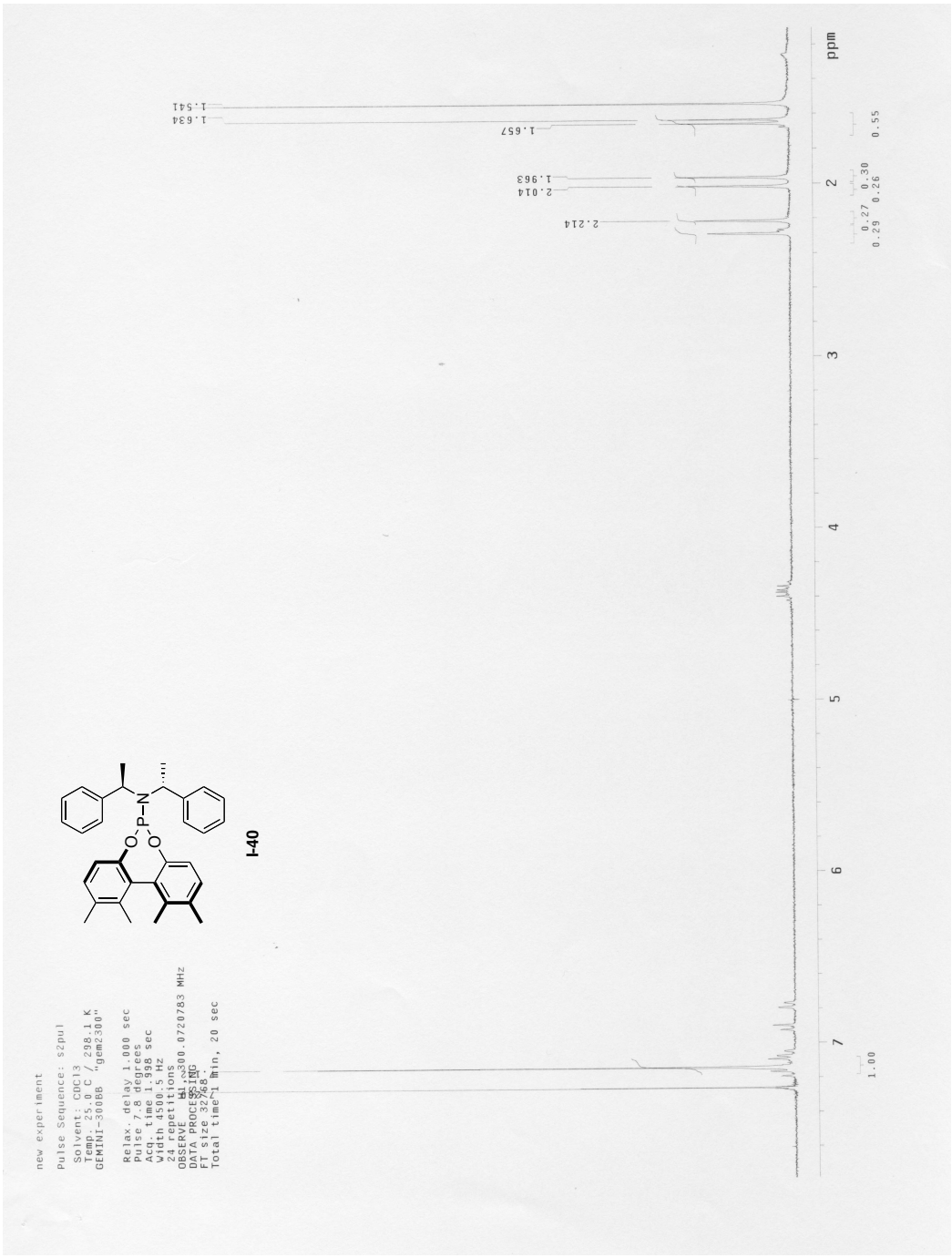
new experiment
Pulse Sequence: s2pul
Solvent: CDCl3
Temp. 25.0 C / 298.1 K
GEMINI-300BB "gem2300"
Relax. delay 1.000 sec
Pulse 7.8 degrees
Acq. time 1.996 sec
Width 4810.5 Hz
24 repetitions
OBSERVE H1, 300.0720783 MHz
DATA PROCESSING
FT size 32768
Total time 1 min, 20 sec
I-40
1.541
1.634
1.657
1.963
2.014
2.214
ppm
1.00
0.27
0.29
0.26
0.30
0.55

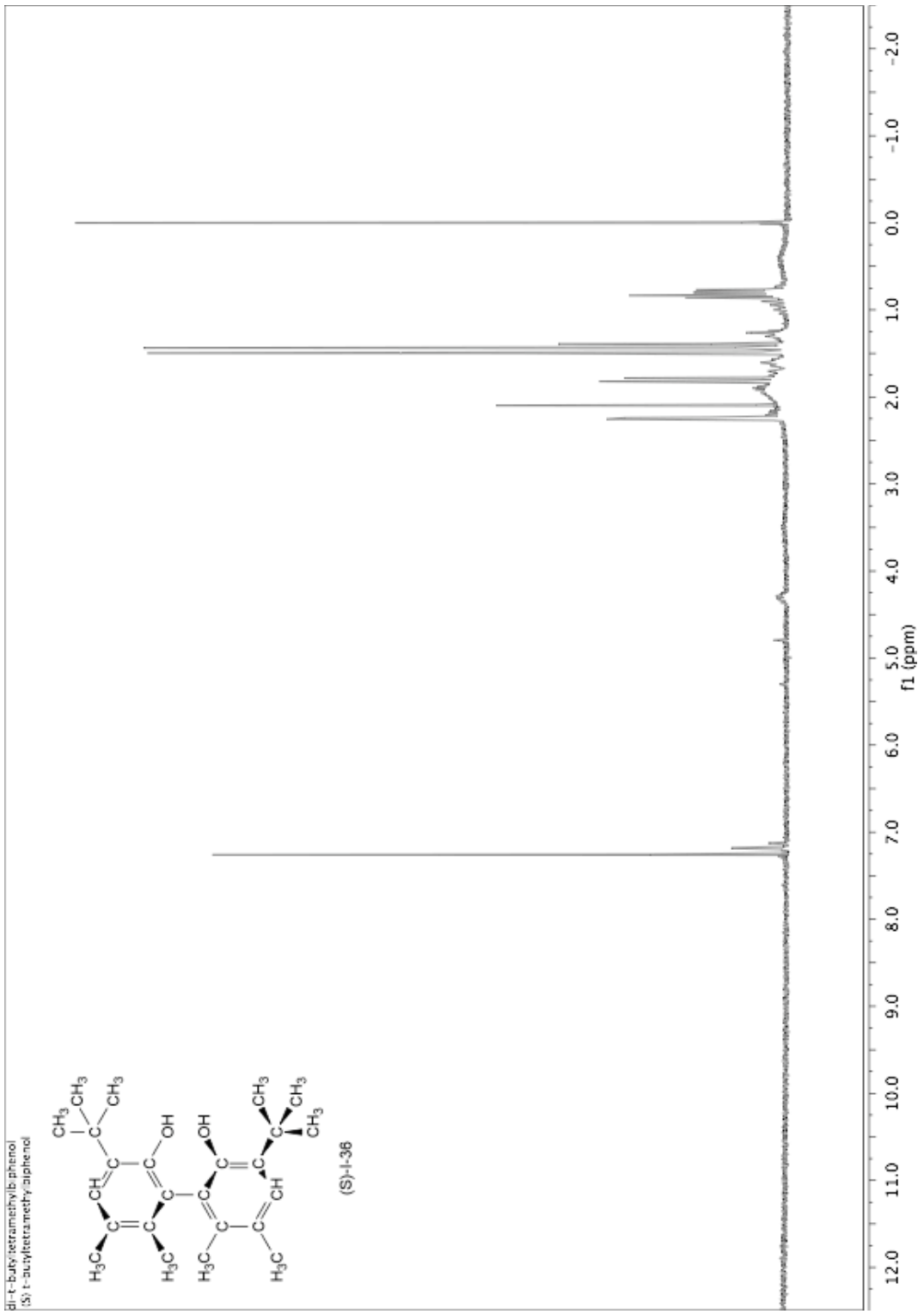
di-t-butyltetramethylbiphenol
(S)-t-butyltetramethylbiphenol
(S)-I-36
12.0
11.0
10.0
9.0
8.0
7.0
6.0
5.0
4.0
3.0
2.0
1.0
0.0
-1.0
-2.0
f1 (ppm)

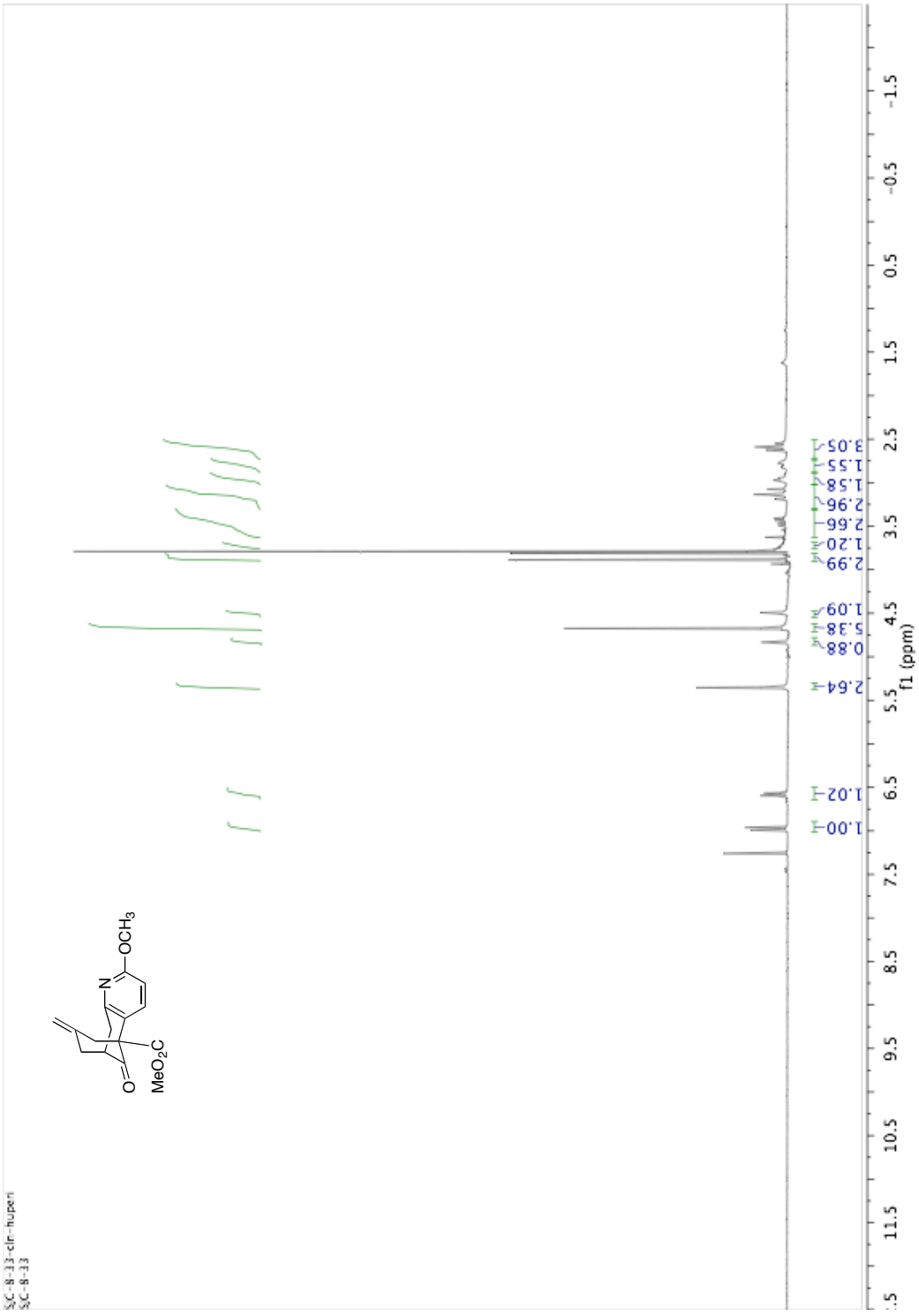
SJC-8-33-clr-huperi
SJC-8-33
OCH3
N
O
MeO2C
1.00
1.02
2.64
0.88
5.38
1.09
2.99
1.20
2.66
2.96
1.58
1.55
3.05
f1 (ppm)

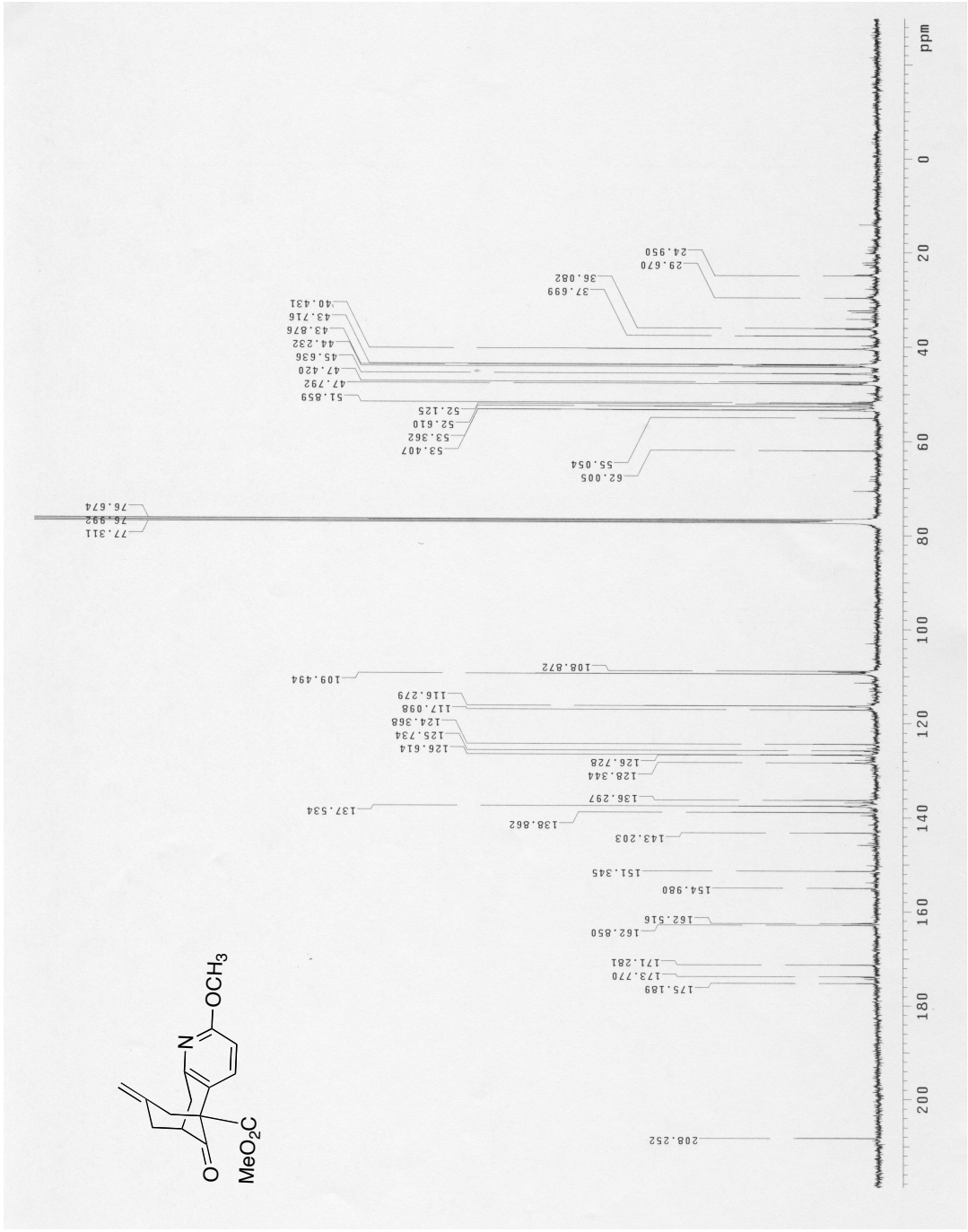
208.252
175.189
173.770
171.281
162.850
162.516
154.980
151.345
143.203
138.862
137.534
136.297
128.344
126.728
126.614
125.734
124.368
117.098
116.279
109.494
108.872
77.311
76.992
76.674
62.005
55.054
53.407
53.362
52.610
52.125
51.859
47.792
47.420
45.636
44.232
43.876
43.716
40.431
37.699
36.082
29.670
24.950
ppm
0
20
40
60
80
100
120
140
160
180
200
N
OCH3
O
MeO2C

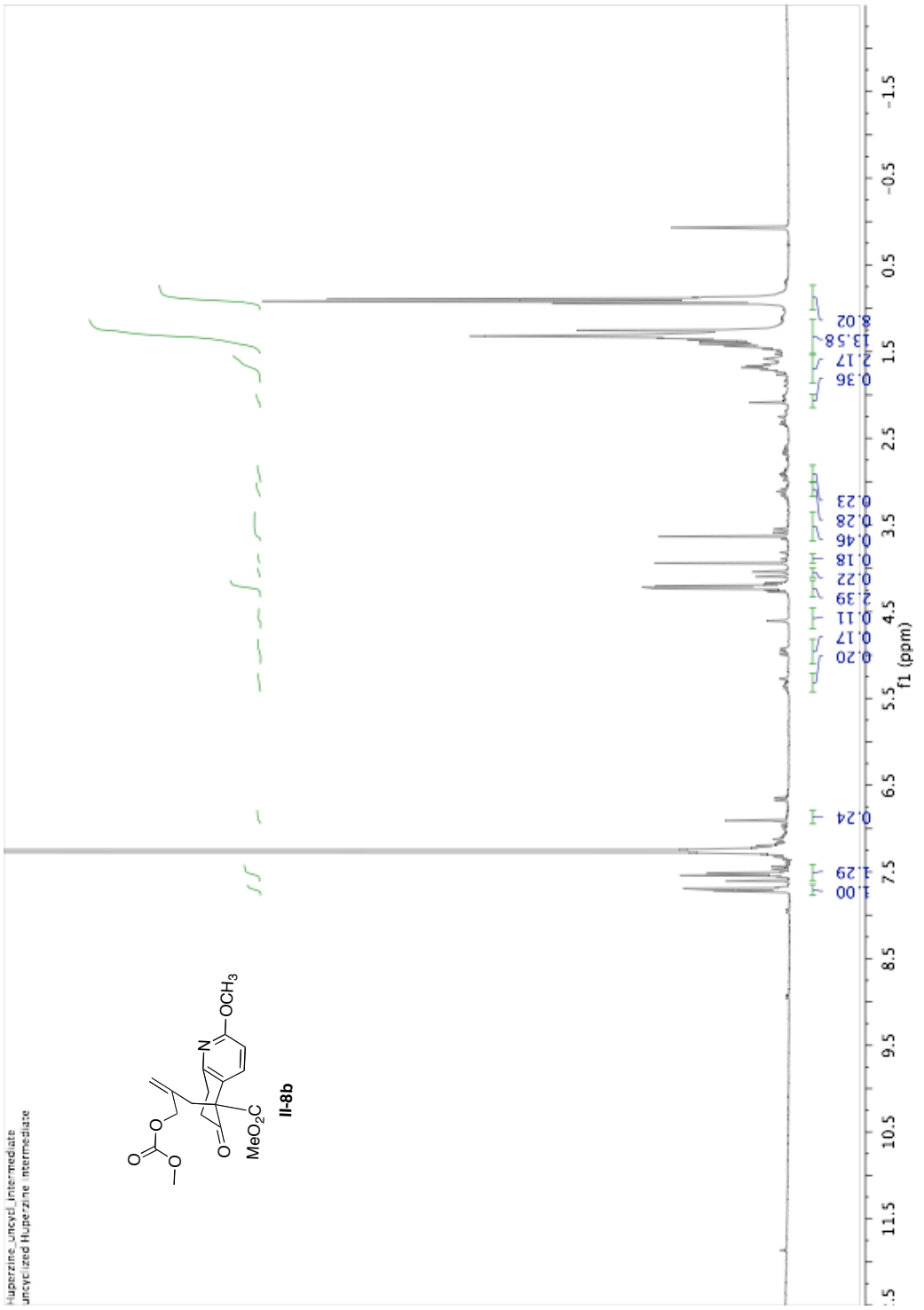
Huperzine_uncycl_intermediate
uncyclized Huperzine intermediate
II-8b
f1 (ppm)

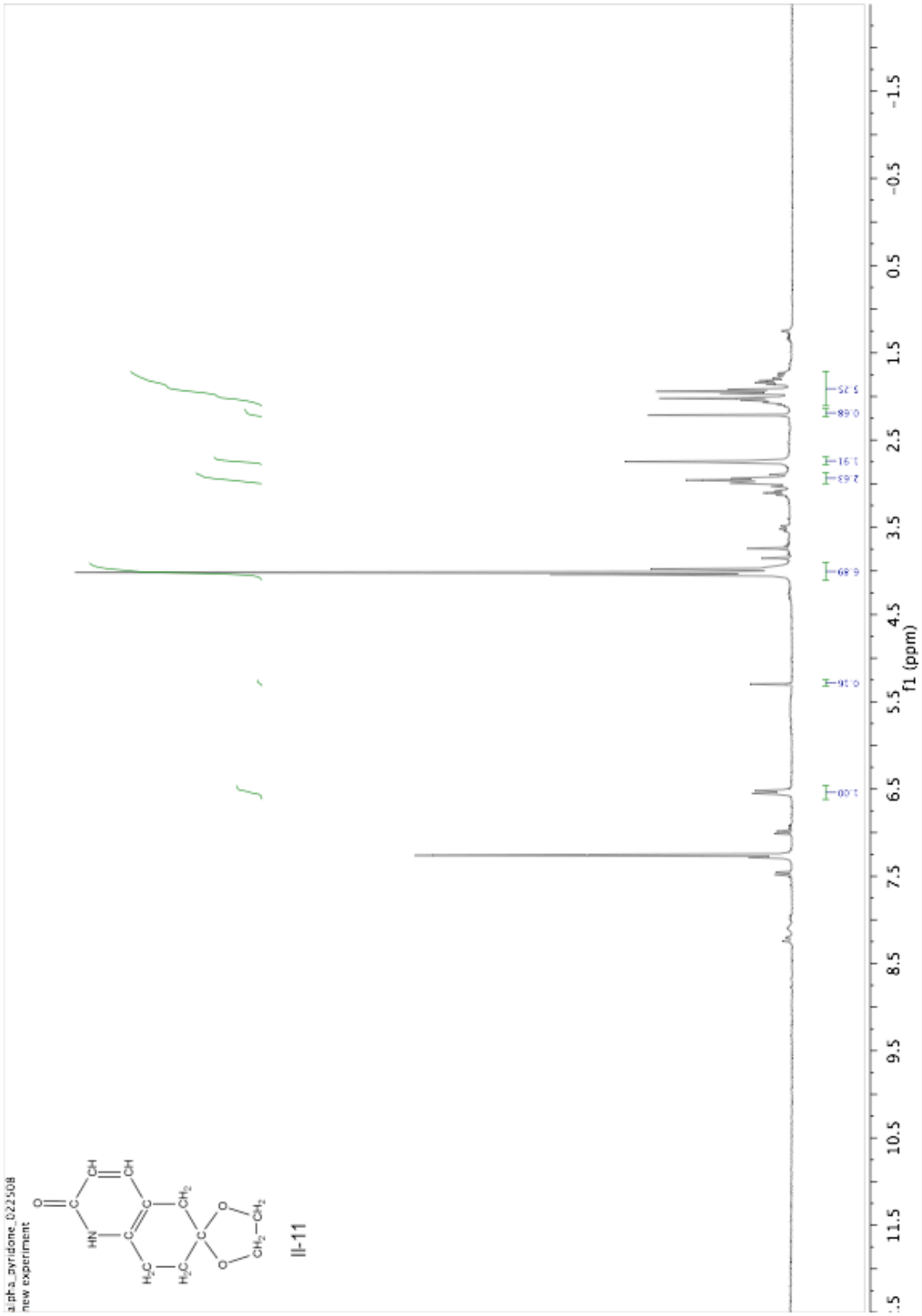
II-11
f1 (ppm)

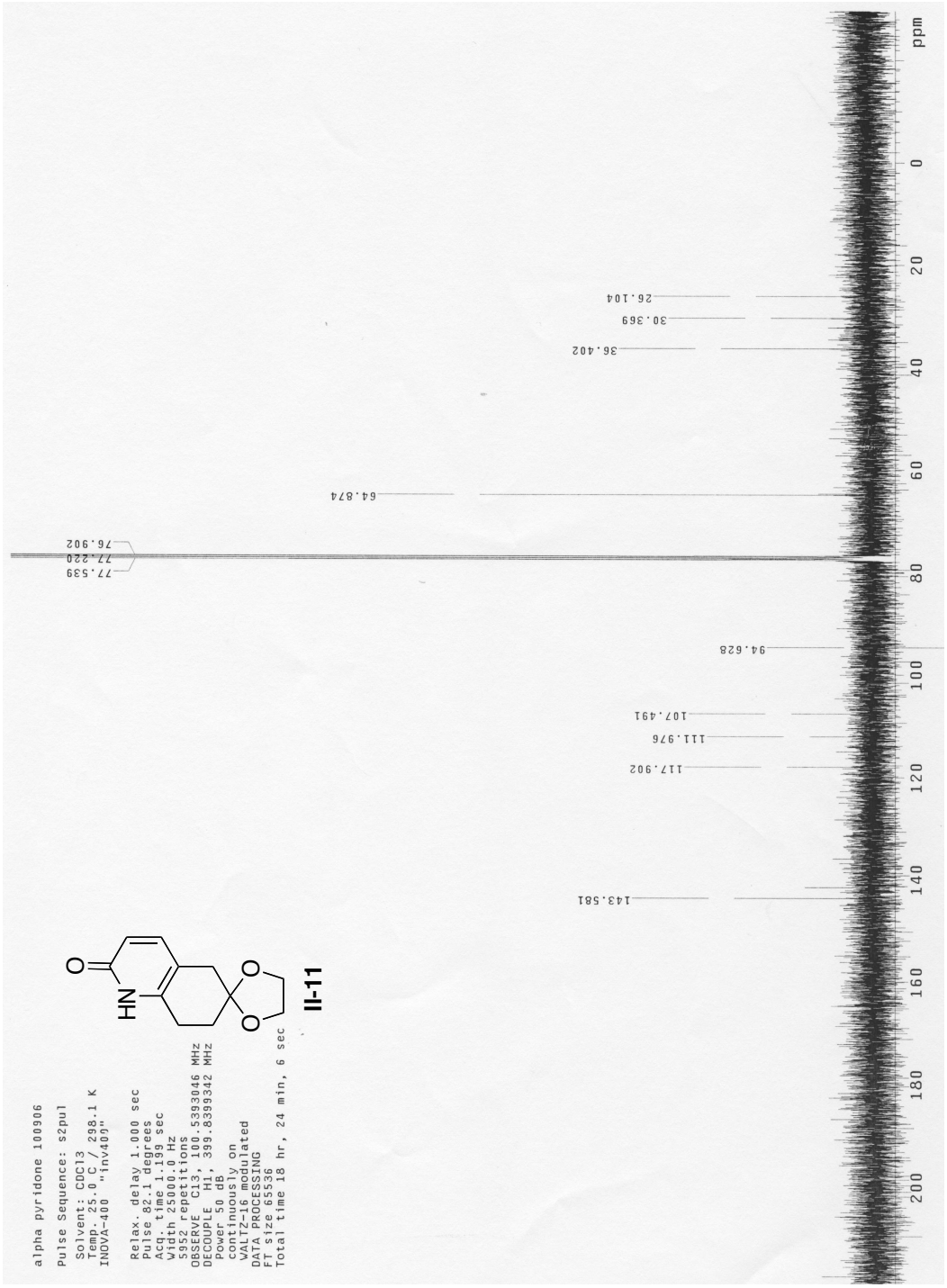
alpha pyridone 100906
Pulse Sequence: s2pul
Solvent: CDCl3
Temp. 25.0 C / 298.1 K
INOVA-400 "inv400"
Relax. delay 1.000 sec
Pulse 82.1 degrees
Acq. time 1.199 sec
Width 25000.0 Hz
5952 repetitions
OBSERVE C13, 100.5393046 MHz
DECOUPLE H1, 399.8399342 MHz
Power 50 dB
continuously on
WALTZ-16 modulated
DATA PROCESSING
FT size 65536
Total time 18 hr, 24 min, 6 sec
HN
O
O
O
II-11
143.581
117.902
111.976
107.491
94.628
77.539
77.220
76.902
64.874
36.402
30.369
26.104
ppm
0
20
40
60
80
100
120
140
160
180
200

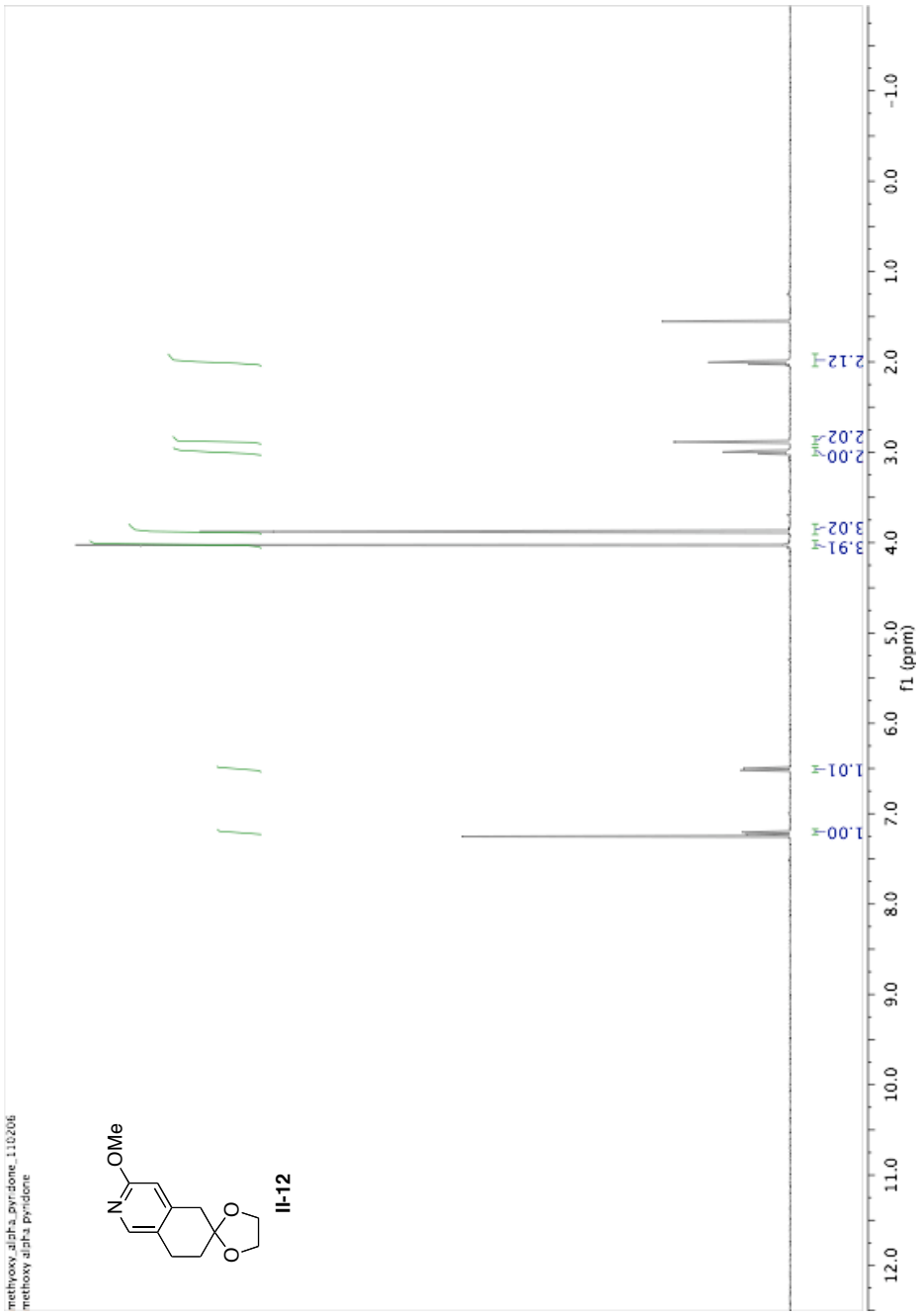
methyoxy alpha_pyridone_110206
methoxy alpha pyridone
OMe
N
O
O
II-12
2.12
2.02
2.00
3.02
3.91
1.01
1.00
f1 (ppm)

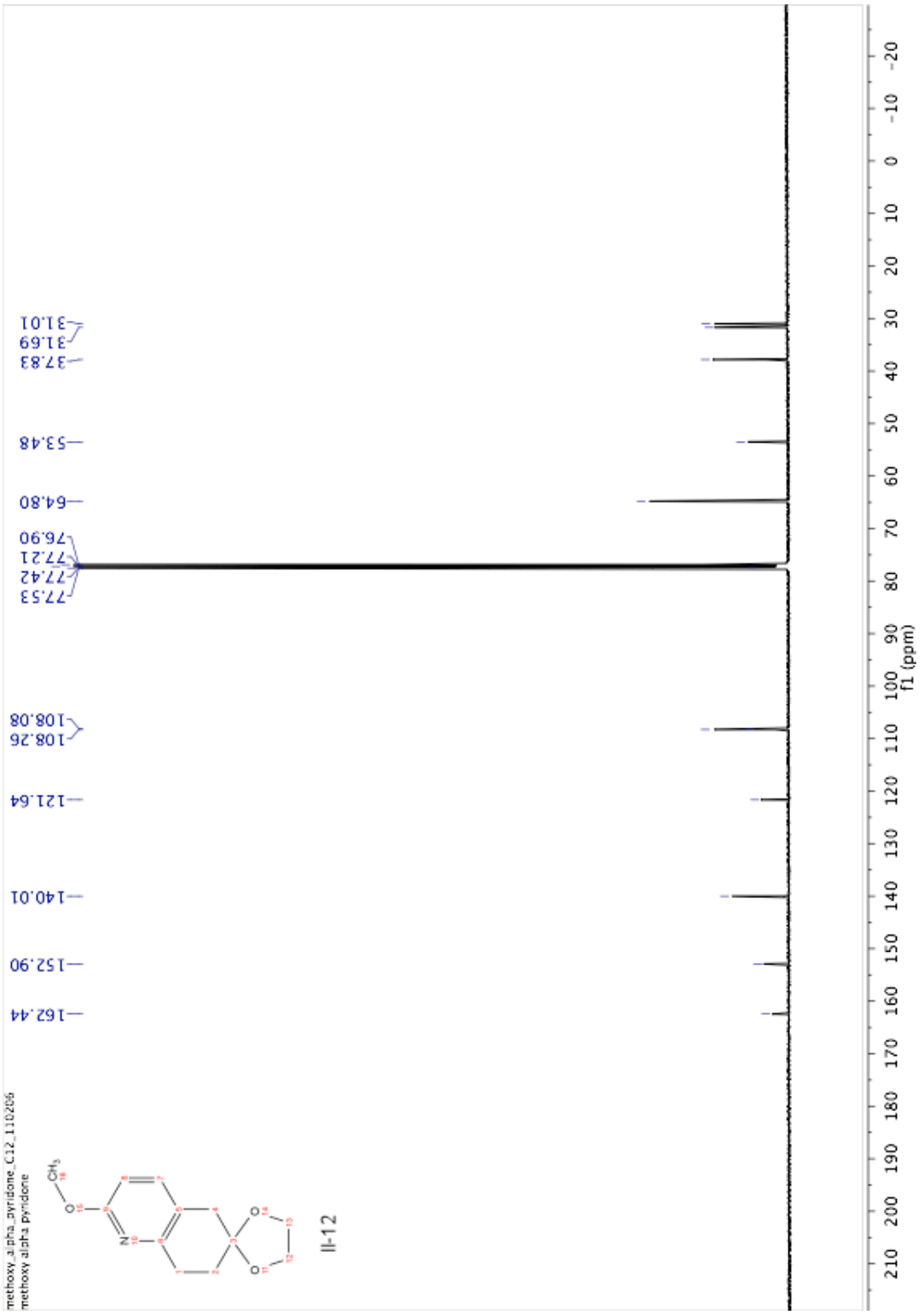
methoxy_alpha_pyridone_C12_1102D6
methoxy alpha pyridone
II-12
162.44
152.90
140.01
121.64
108.26
108.08
77.53
77.42
77.21
76.90
64.80
53.48
37.83
31.69
31.01
f1 (ppm)

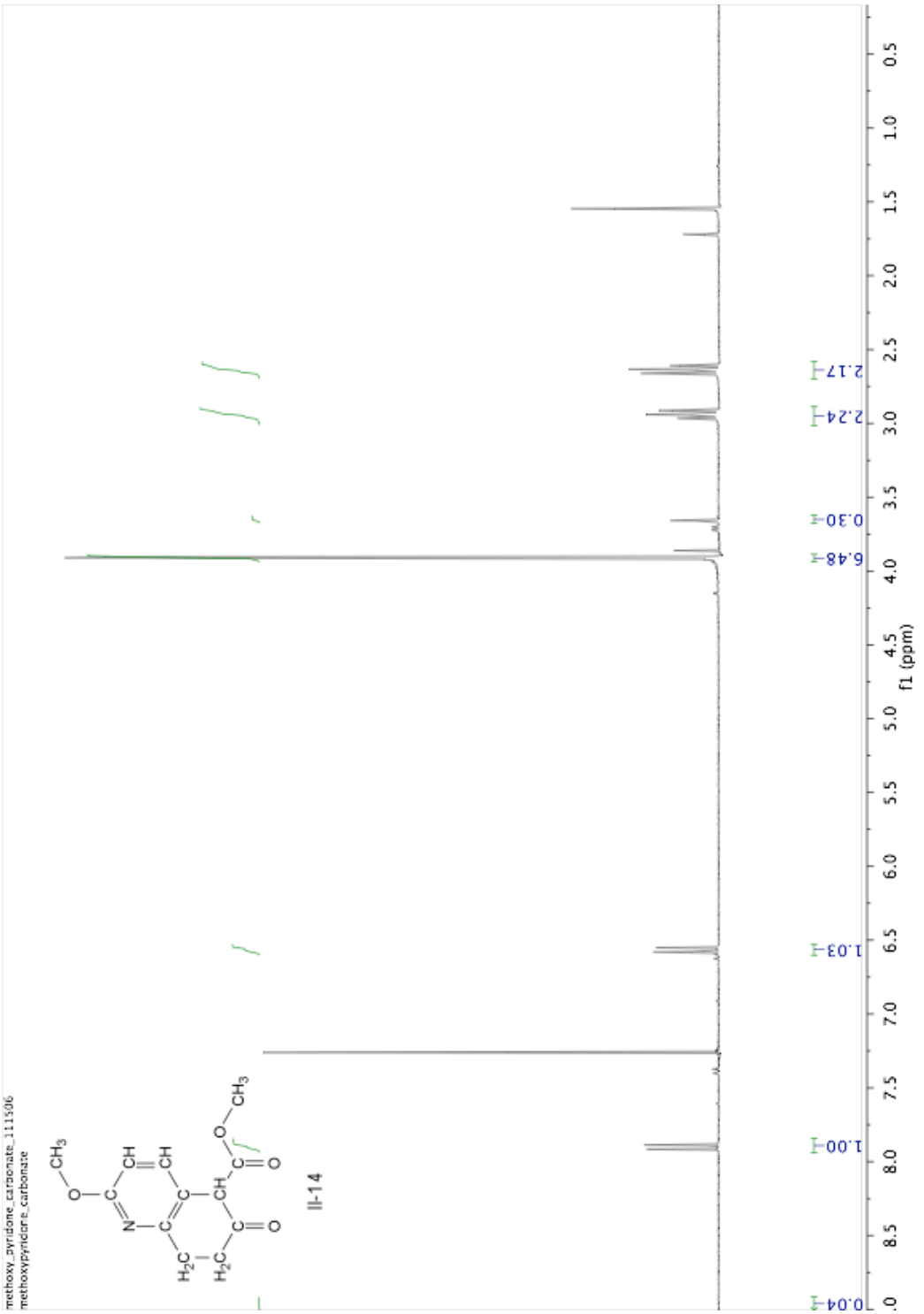
methoxy_pyridone_carbonate_111506
methoxypyridone_carbonate
II-14
2.17
2.24
0.30
6.48
1.03
1.00
0.04
f1 (ppm)

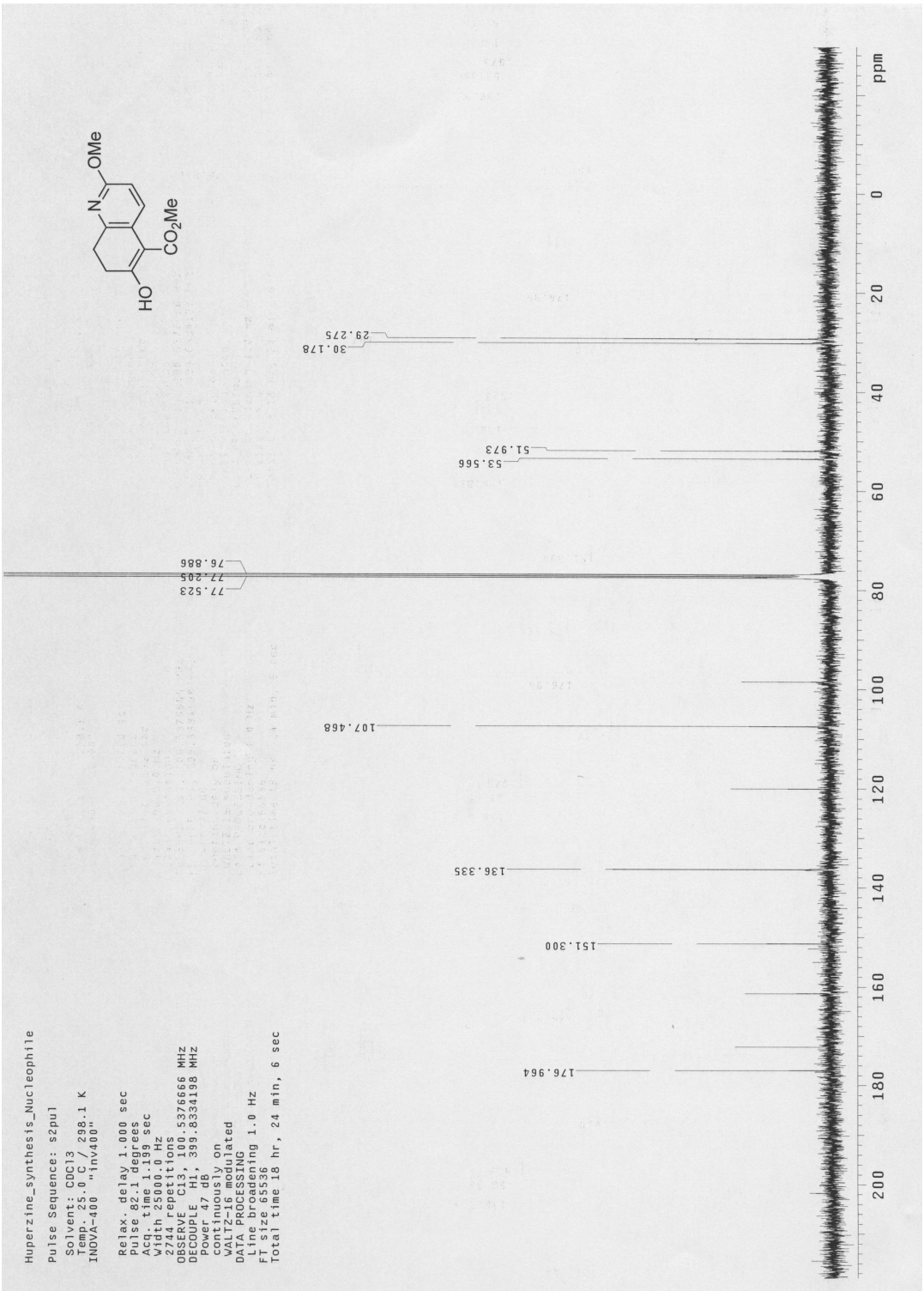
Huperzine_synthesis_Nucleophile
Pulse Sequence: s2pul
Solvent: CDCl3
Temp. 25.0 C / 298.1 K
INOVA-400 "inv400"
Relax. delay 1.000 sec
Pulse 82.1 degrees
Acq. time 1.199 sec
Width 25000.0 Hz
2744 repetitions
OBSERVE C13, 100.5376666 MHz
DECOUPLE H1, 399.8334198 MHz
Power 47 dB
continuously on
WALTZ-16 modulated
DATA PROCESSING
Line broadening 1.0 Hz
FT size 65536
Total time 18 hr, 24 min, 6 sec
OMe
N
CO2Me
HO
176.964
151.300
136.335
107.468
77.523
77.205
76.886
53.566
51.973
30.178
29.275
ppm

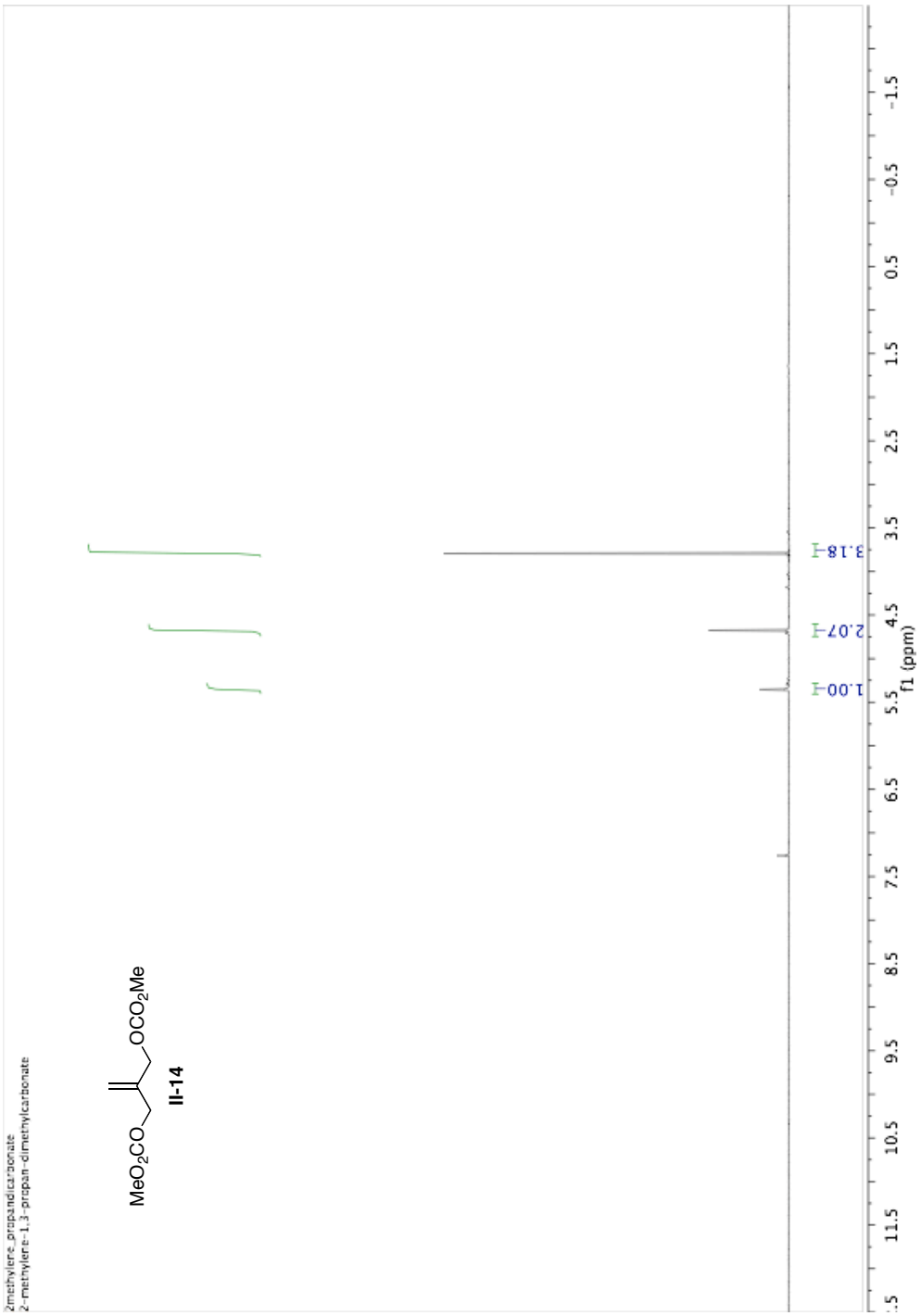
2methylene_propandicarbonate
2-methylene-1,3-propan-dimethylcarbonate
MeO2CO
OCO2Me
II-14
3.18
2.07
1.00
f1 (ppm)

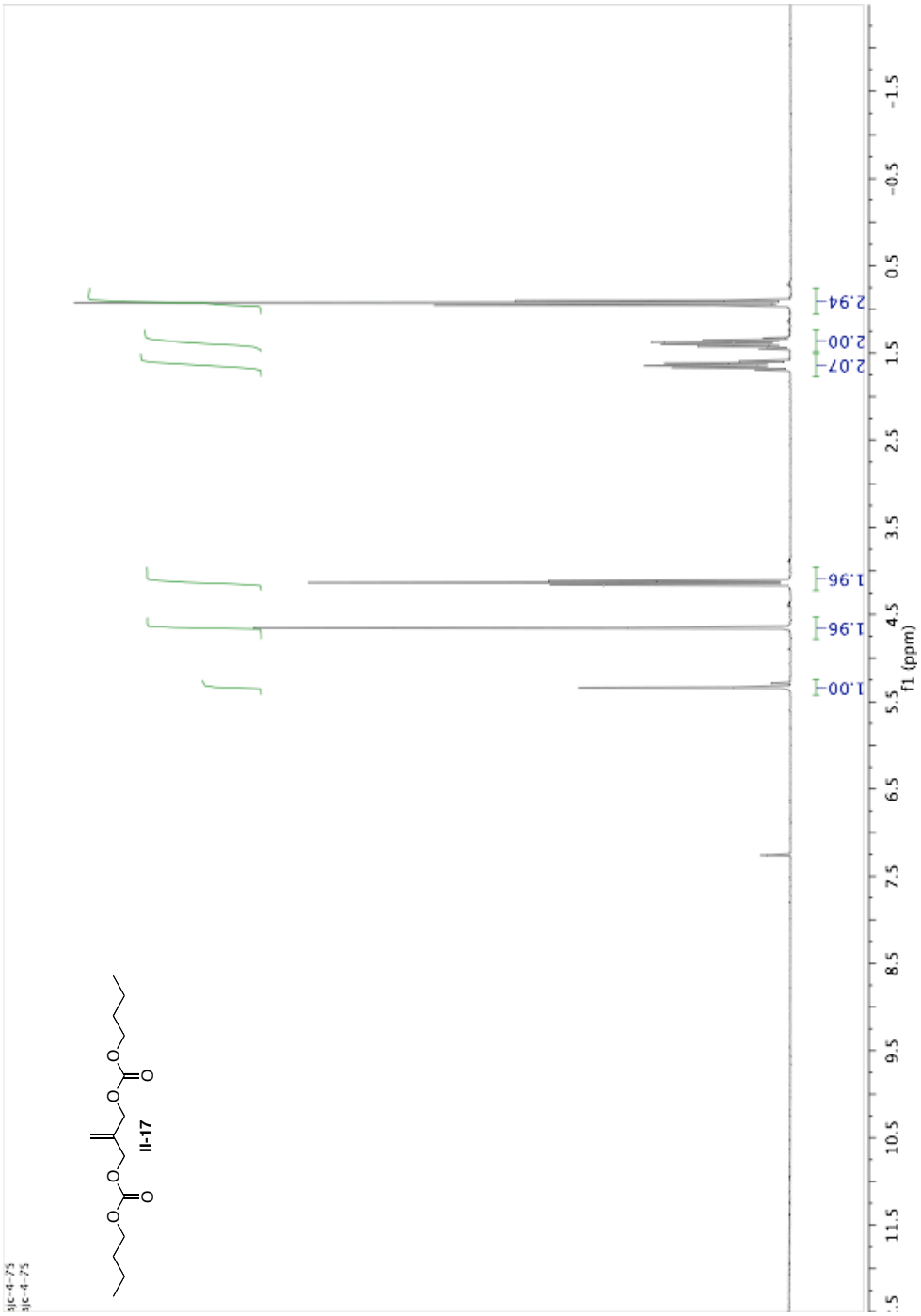
II-17
2.94
2.00
2.07
1.96
1.96
1.00
f1 (ppm)

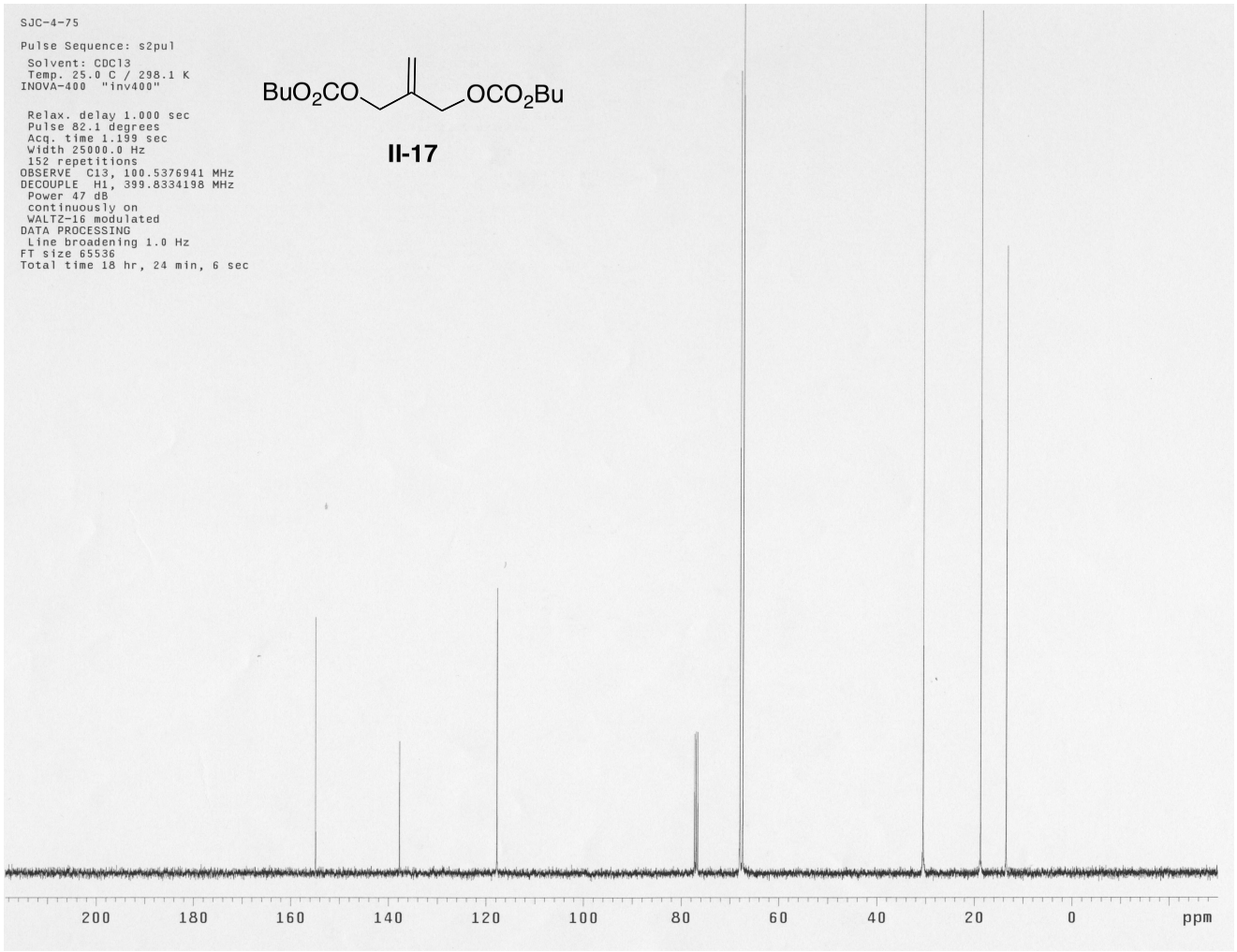
SJC-4-75
Pulse Sequence: s2pul
Solvent: CDCl3
Temp. 25.0 C / 298.1 K
INOVA-400 "inv400"
Relax. delay 1.000 sec
Pulse 82.1 degrees
Acq. time 1.199 sec
Width 25000.0 Hz
152 repetitions
OBSERVE C13, 100.5376941 MHz
DECOUPLE H1, 399.8334198 MHz
Power 47 dB
continuously on
WALTZ-16 modulated
DATA PROCESSING
Line broadening 1.0 Hz
FT size 65536
Total time 18 hr, 24 min, 6 sec
BuO2CO
OCO2Bu
II-17
200
180
160
140
120
100
80
60
40
20
0
ppm

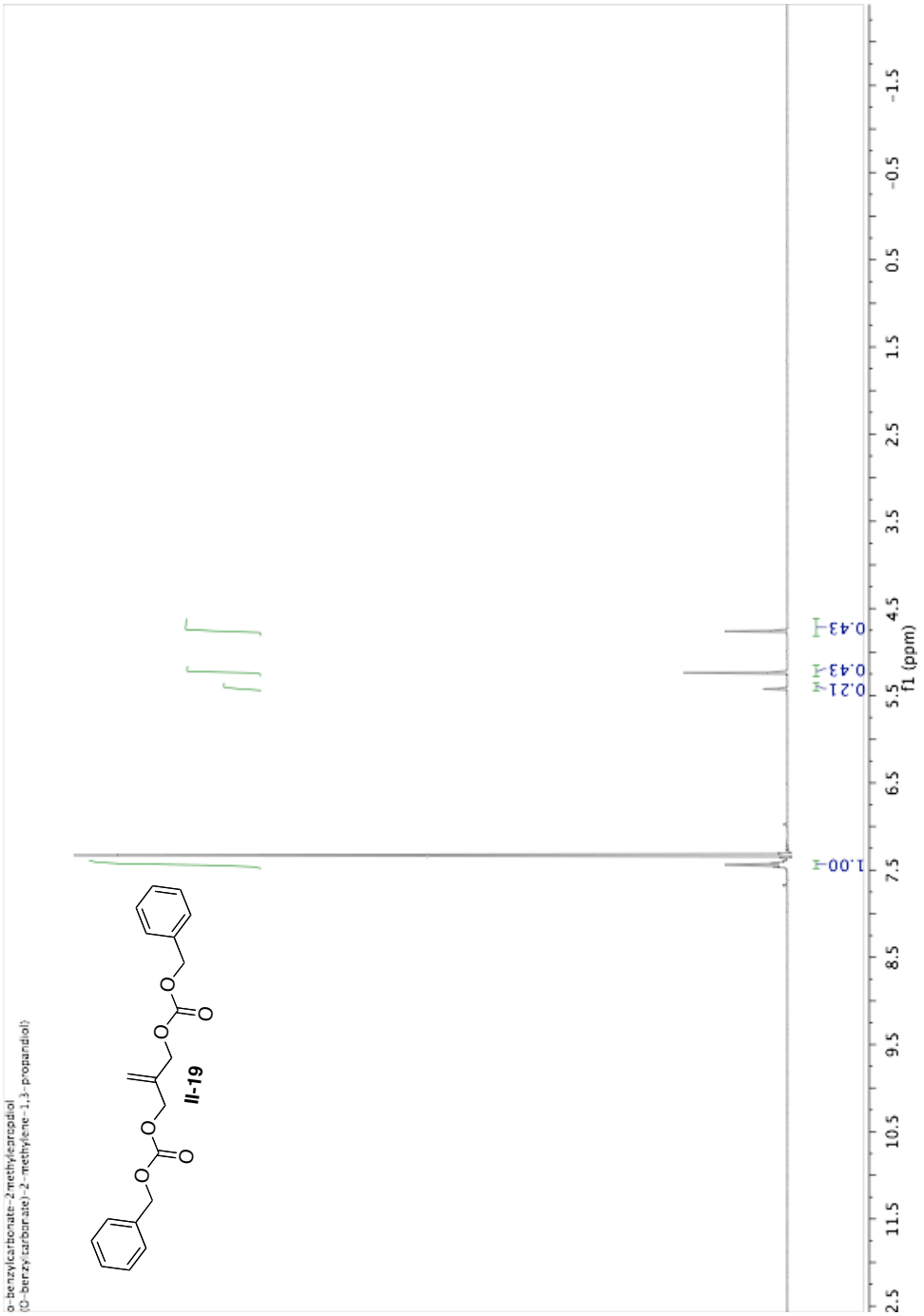
II-19
1.00
0.21
0.43
0.43
f1 (ppm)

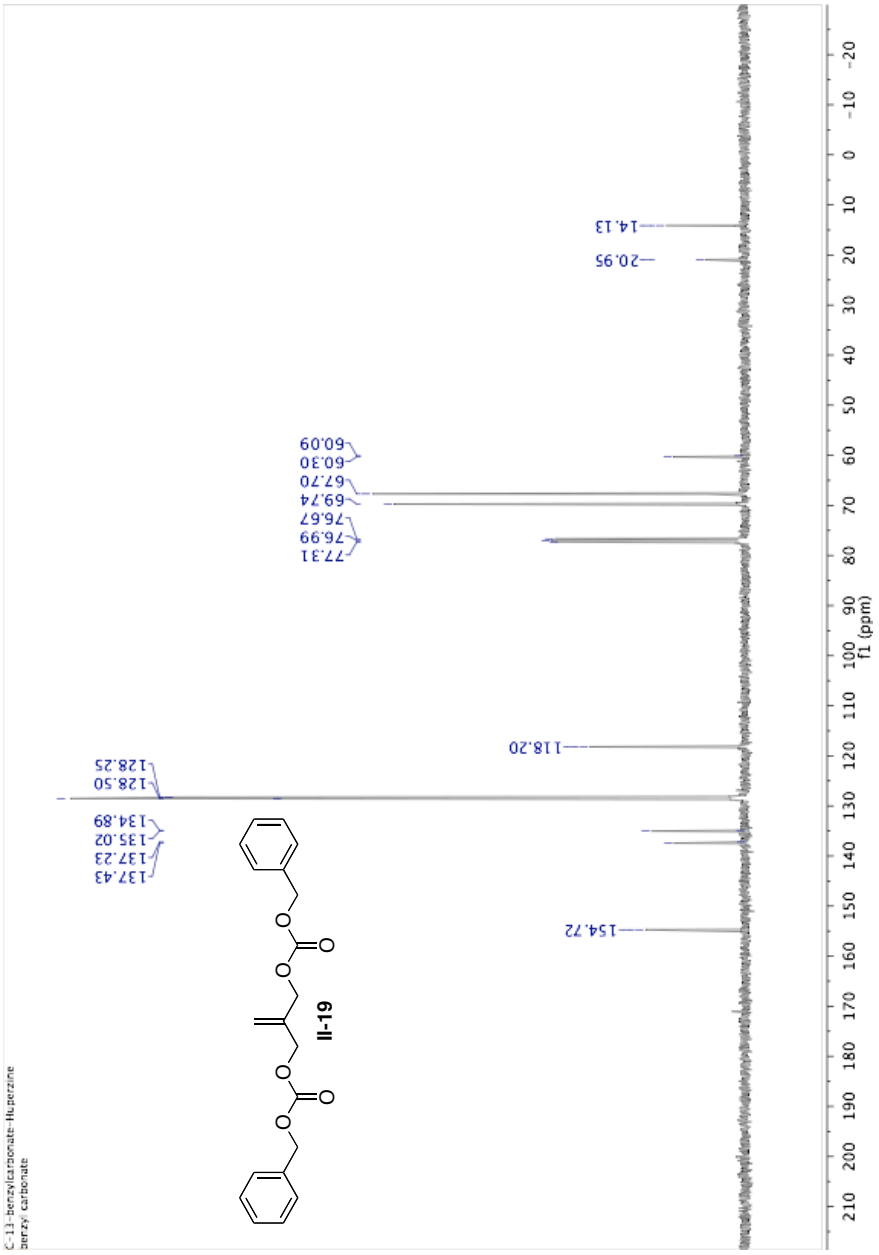
C-13-benzylcarbonate-Hyperzine
benzyl carbonate
II-19
154.72
137.43
137.23
135.02
134.89
128.50
128.25
118.20
77.31
76.99
76.67
69.74
67.70
60.30
60.09
20.95
14.13
f1 (ppm)

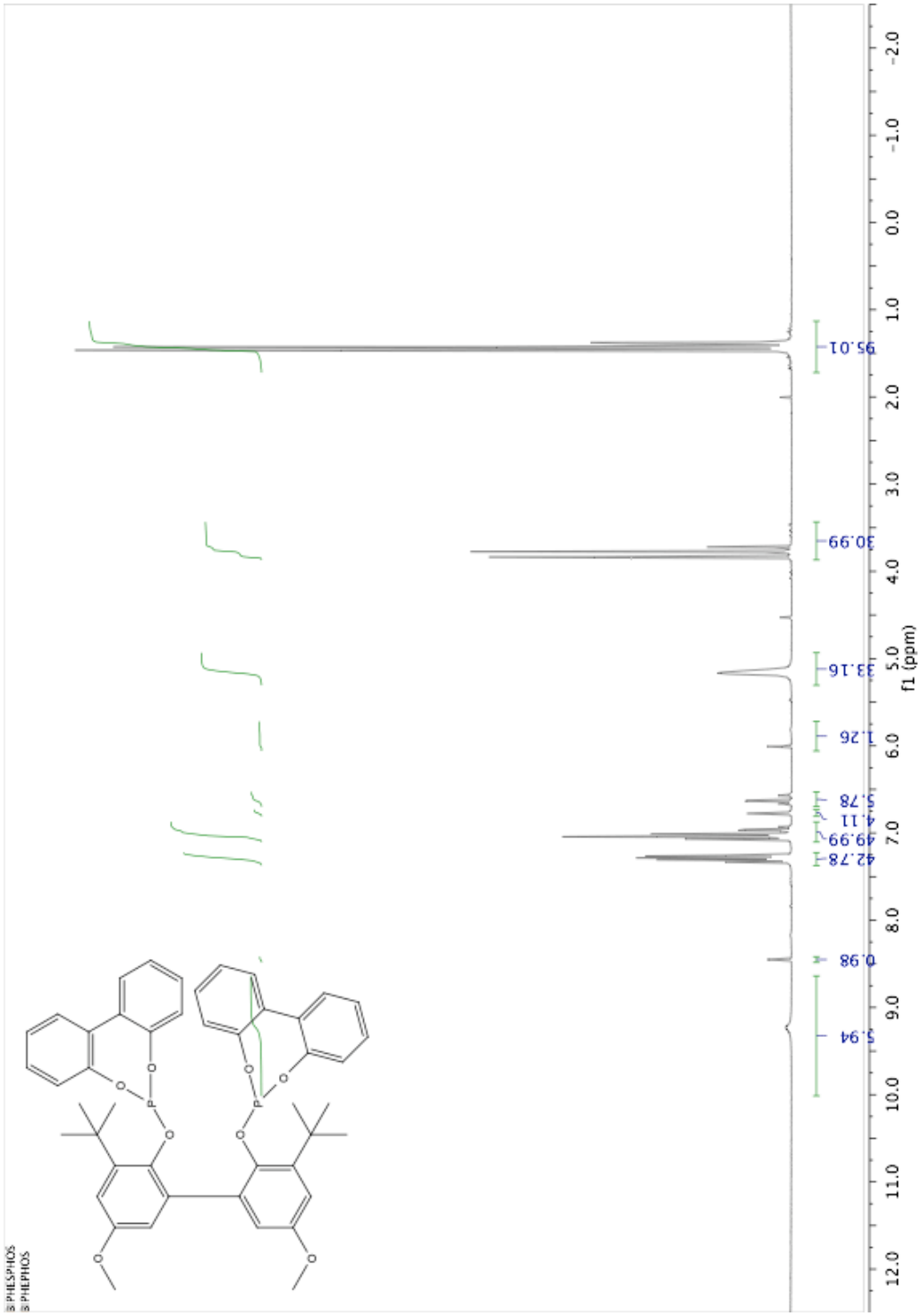
(S)-PHELSPHOS
(S)-PHELPHOS
95.01
30.99
33.16
1.26
5.78
4.11
49.99
42.78
0.98
5.94
f1 (ppm)

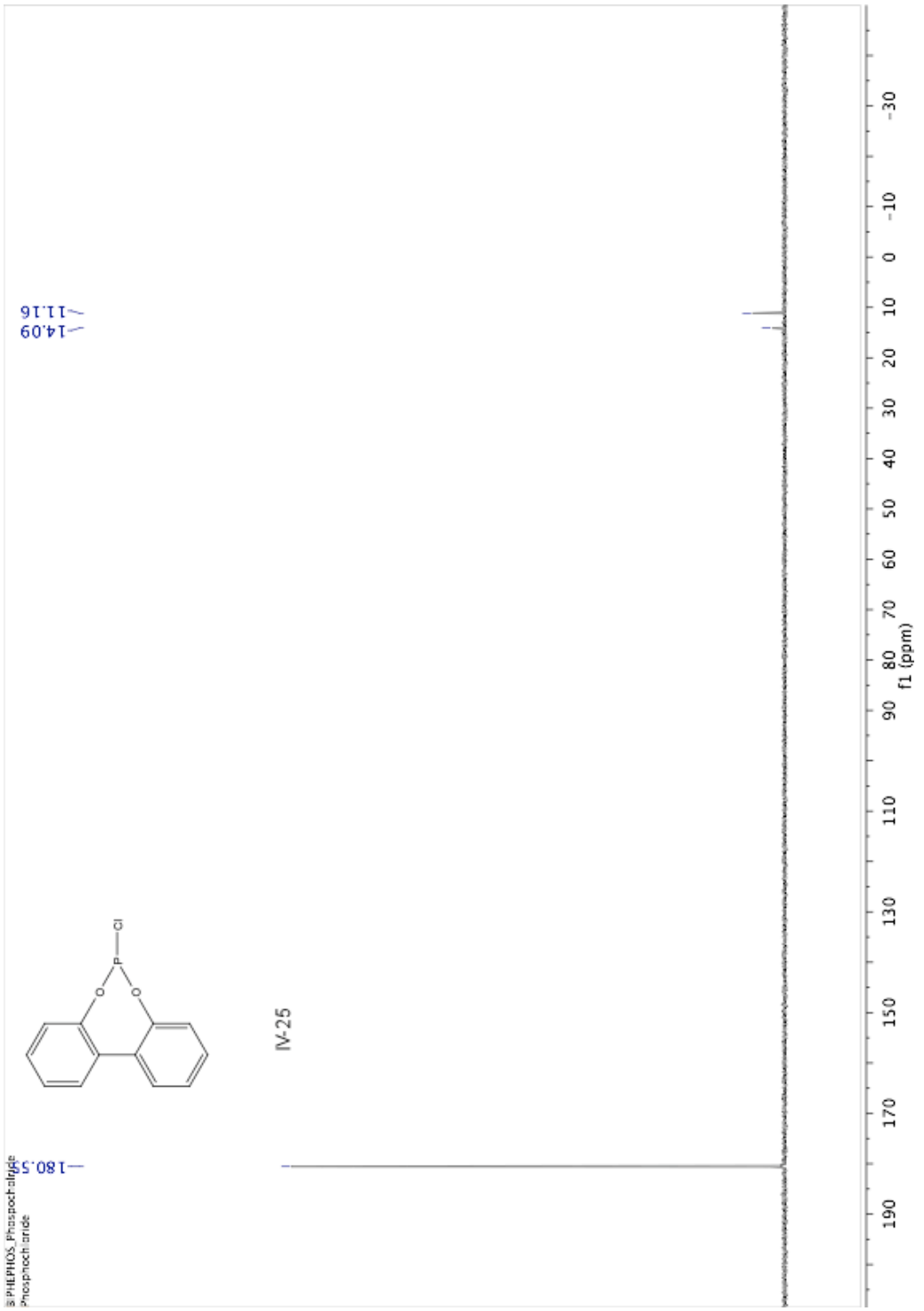
180.55
14.09
11.16
IV-25
f1 (ppm)

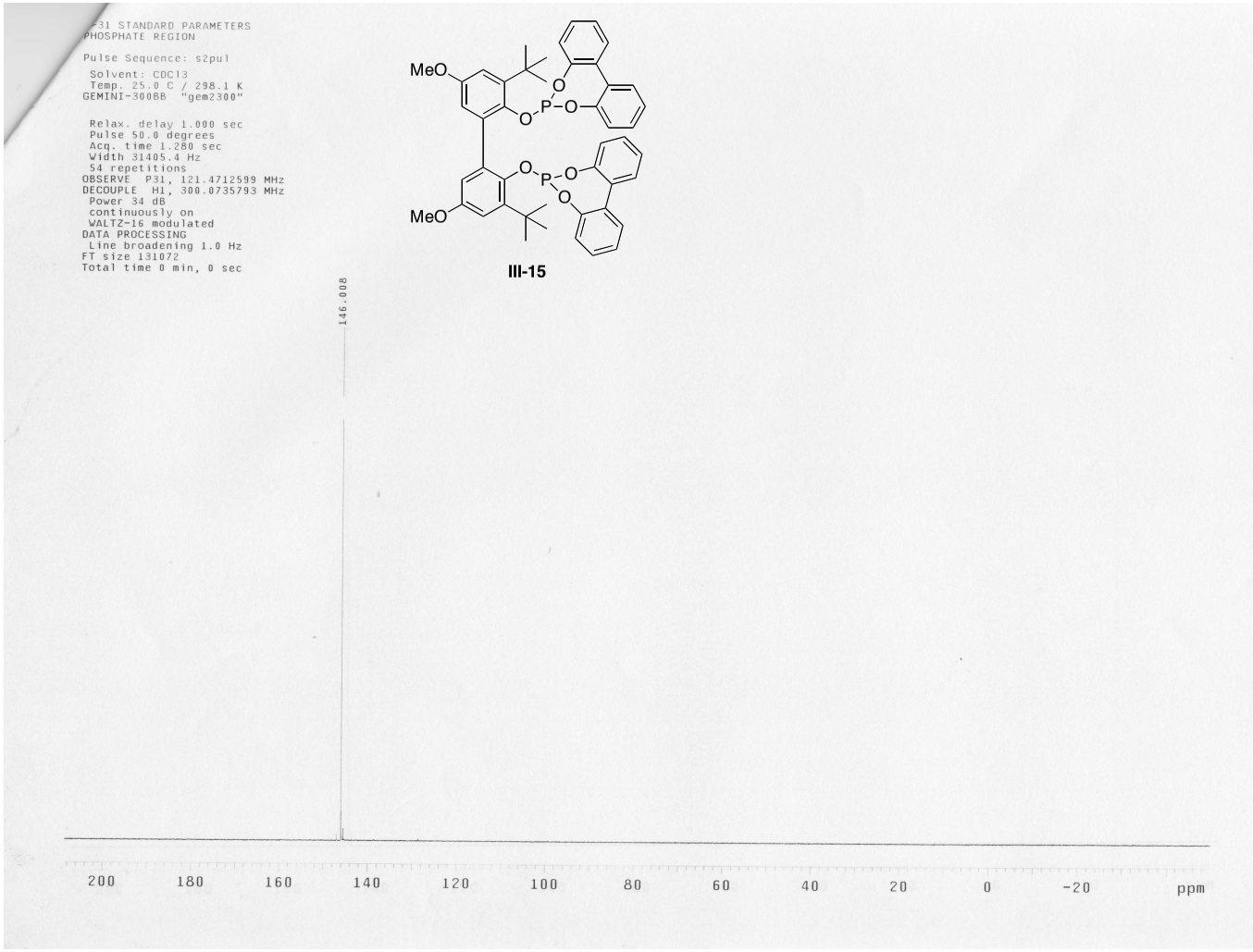
31 STANDARD PARAMETERS
PHOSPHATE REGION
Pulse Sequence: s2pul
Solvent: CDCl3
Temp. 25.0 C / 298.1 K
GEMINI-300BB "gem2300"
Relax. delay 1.000 sec
Pulse 50.0 degrees
Acq. time 1.280 sec
Width 31405.4 Hz
54 repetitions
OBSERVE P31, 121.4712599 MHz
DECOUPLE H1, 300.0735793 MHz
Power 34 dB
continuously on
WALTZ-16 modulated
DATA PROCESSING
Line broadening 1.0 Hz
FT size 131072
Total time 0 min, 0 sec
MeO
MeO
O
P
O
O
P
O
O
O
III-15
146.008
200
180
160
140
120
100
80
60
40
20
0
-20
ppm

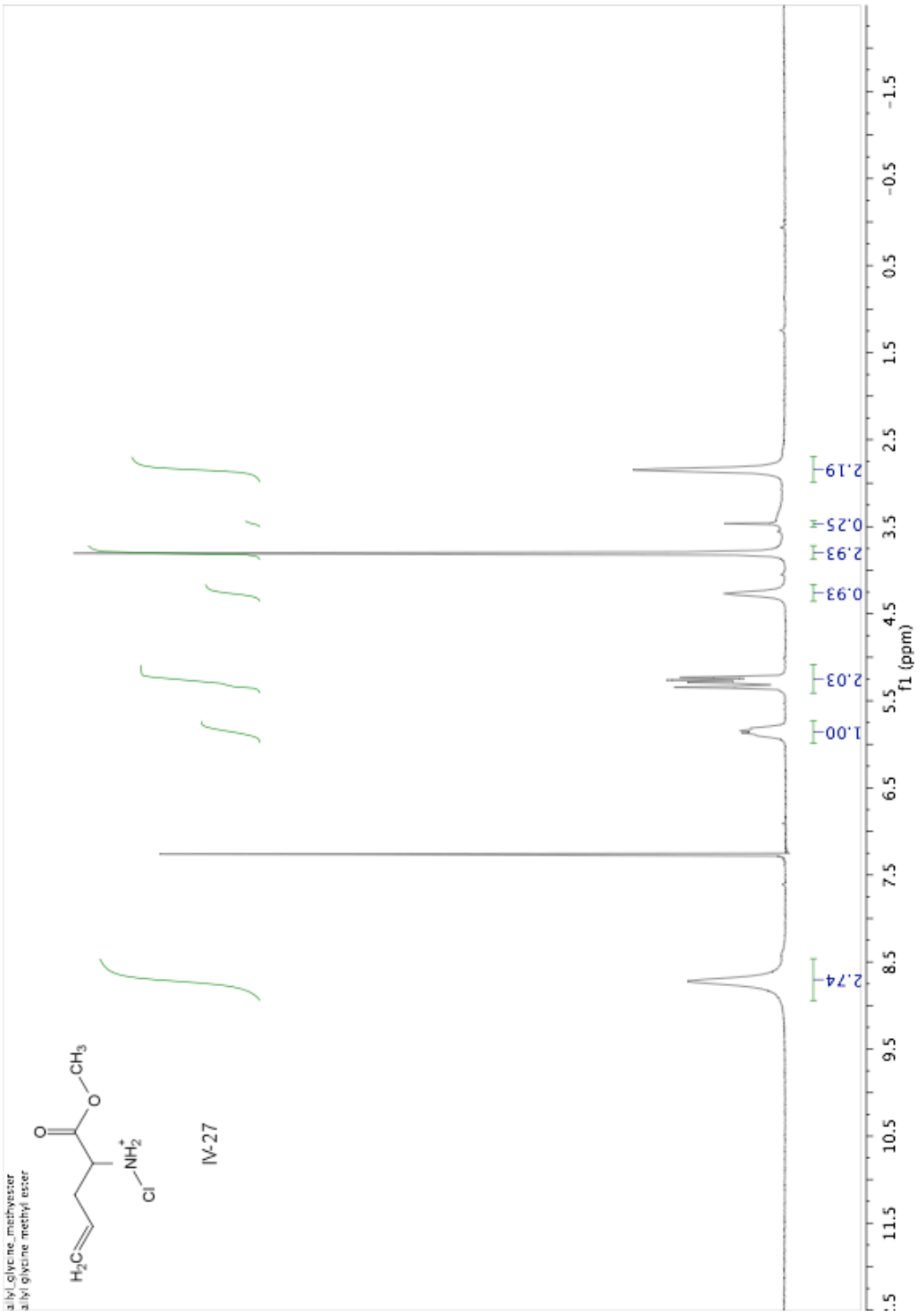
allyl_glycine_methyester
allyl glycine methyl ester
IV-27
f1 (ppm)
2.74
1.00
2.03
0.93
2.93
0.25
2.19

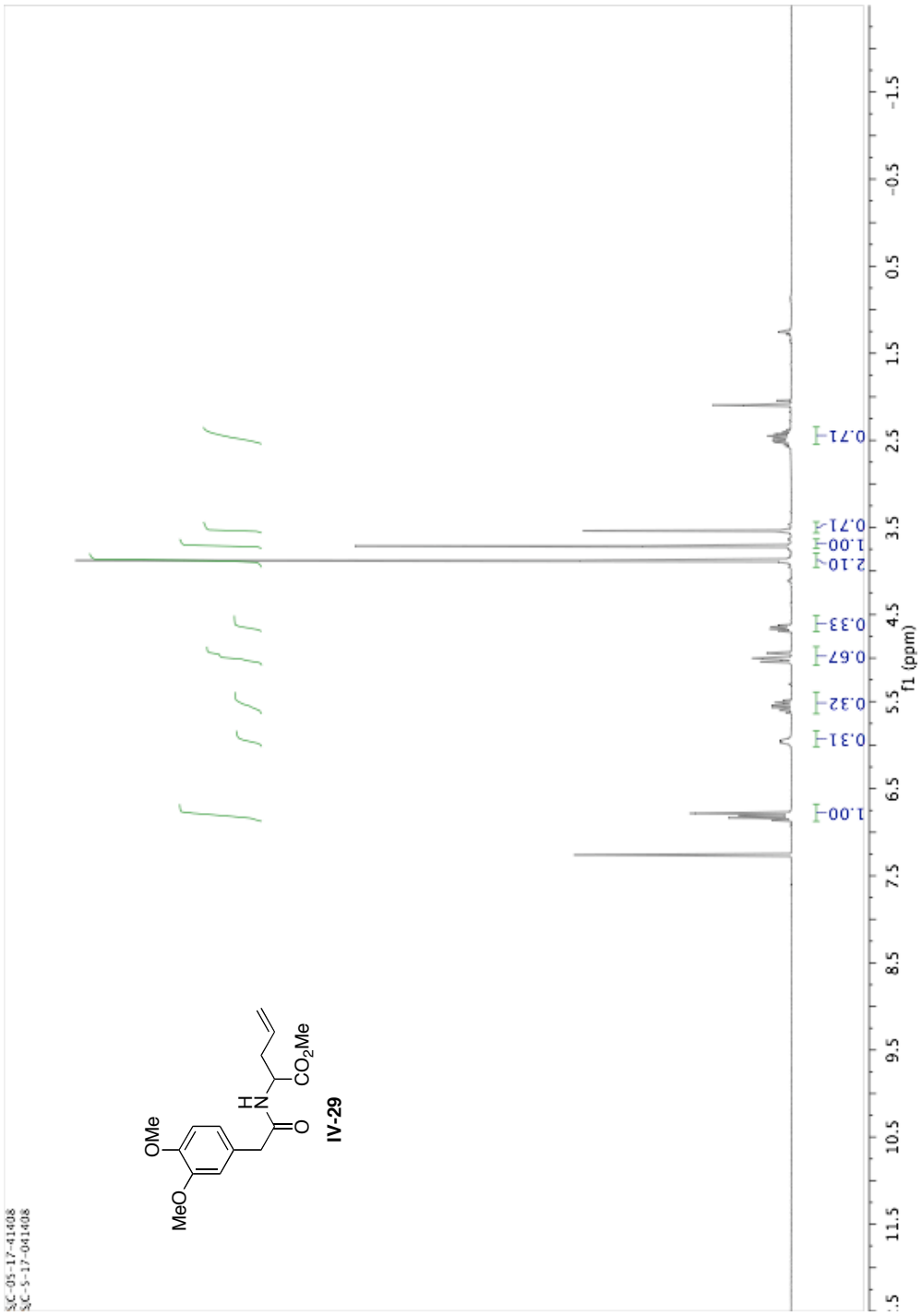
SJC-05-17-41408
SJC-5-17-041408
OMe
MeO
H
N
O
CO2Me
IV-29
0.71
1.00
2.10
0.33
0.67
0.32
0.31
1.00
f1 (ppm)

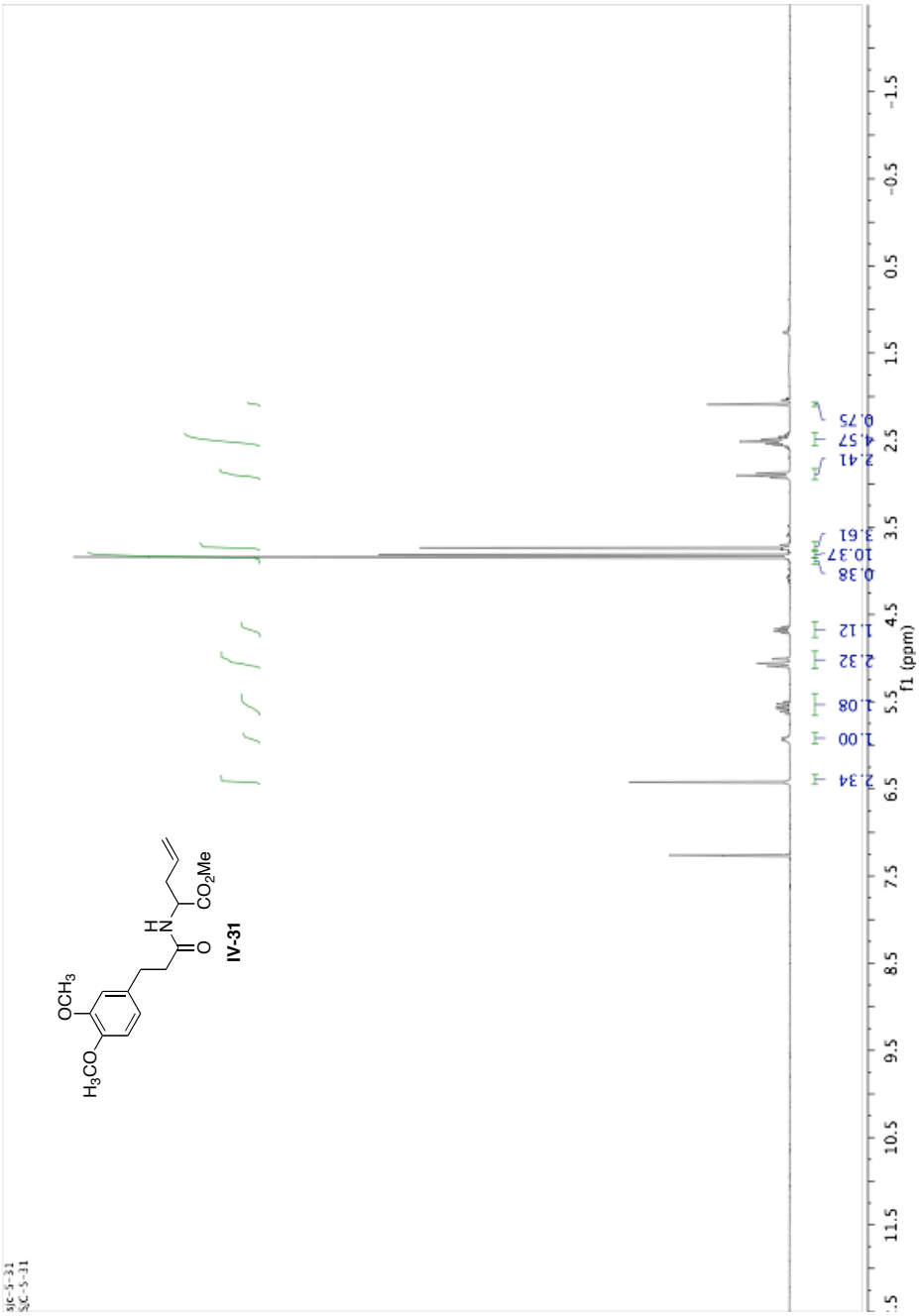
IV-31
f1 (ppm)

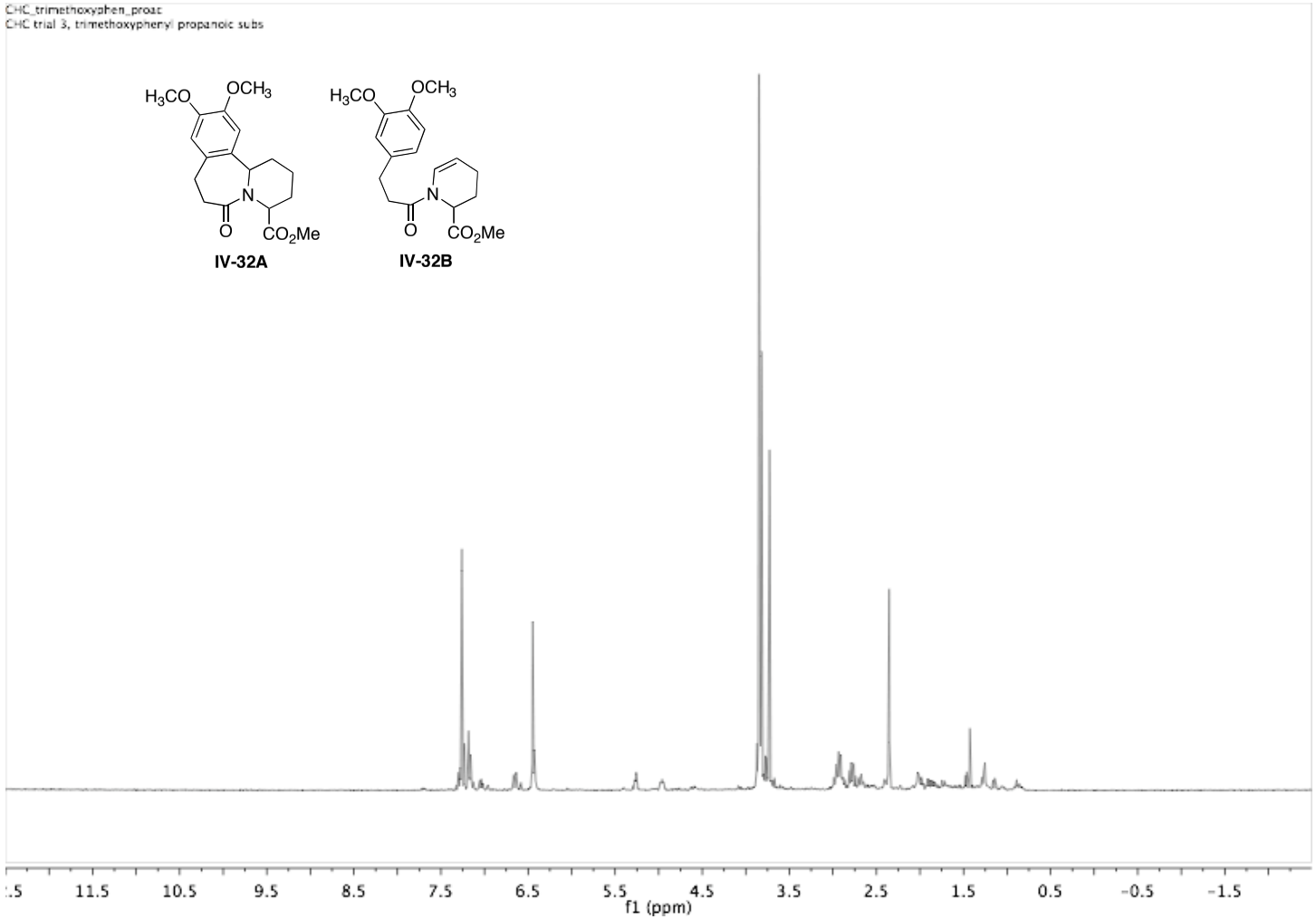
CHC_trimethoxyphen_proac
CHC trial 3, trimethoxyphenyl propanoic subs
H3CO
OCH3
N
O
CO2Me
IV-32A
IV-32B
11.5
10.5
9.5
8.5
7.5
6.5
5.5
4.5
3.5
2.5
1.5
0.5
-0.5
-1.5
f1 (ppm)

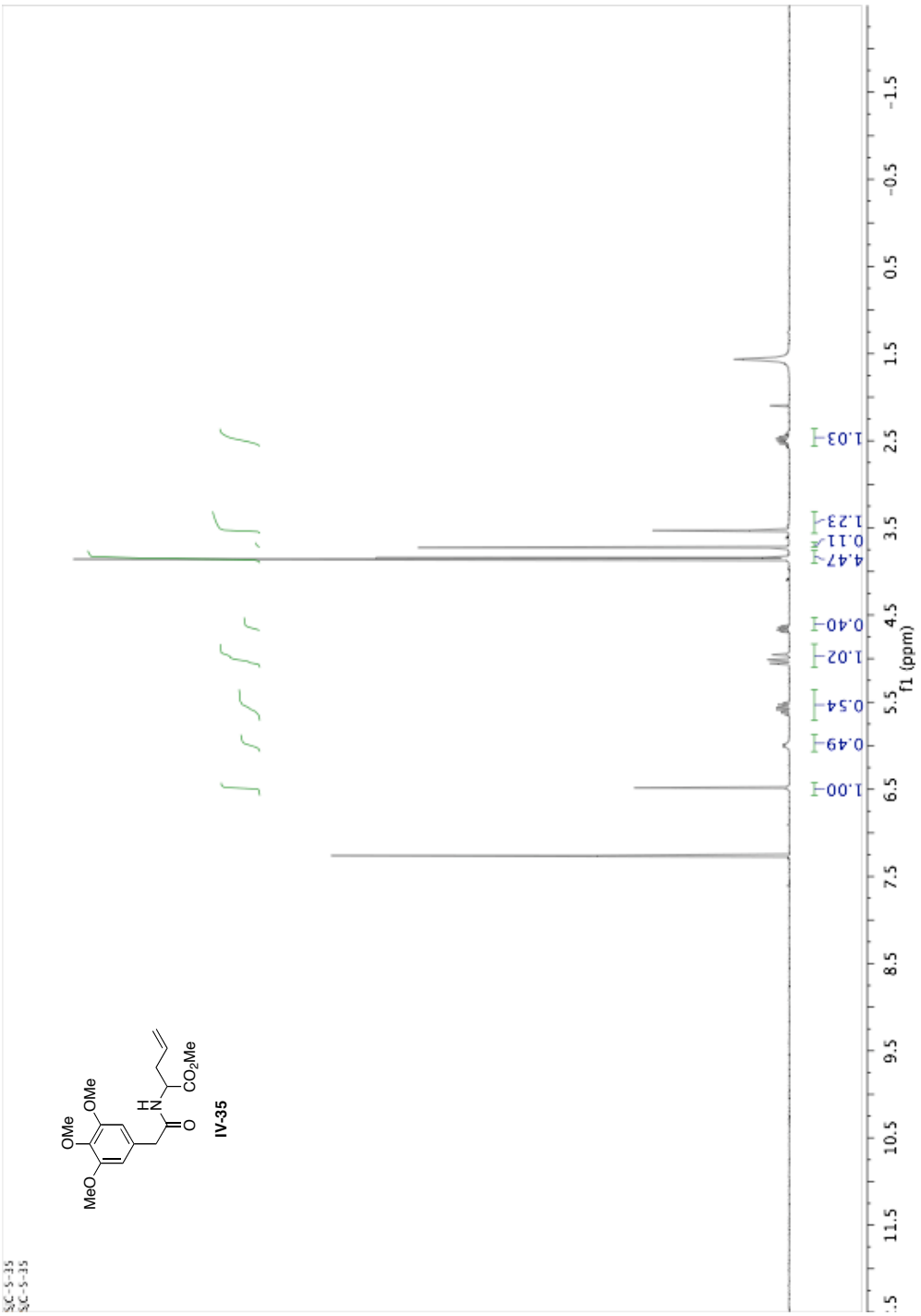
OMe
OMe
MeO
H
N
O
CO2Me
IV-35
1.00
0.49
0.54
1.02
0.40
4.47
0.11
1.23
1.03
f1 (ppm)

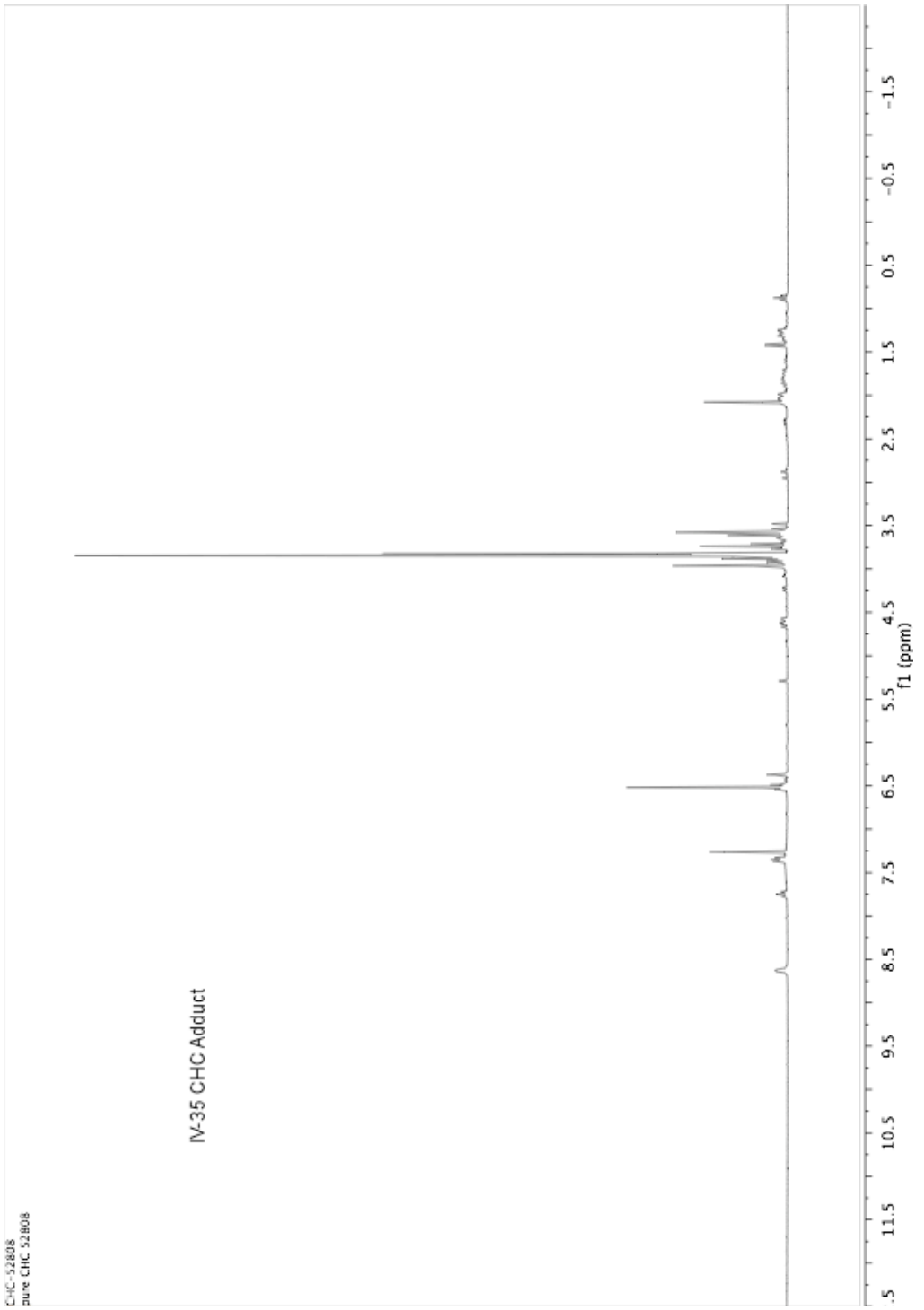
IV-35 CHC Adduct
f1 (ppm)

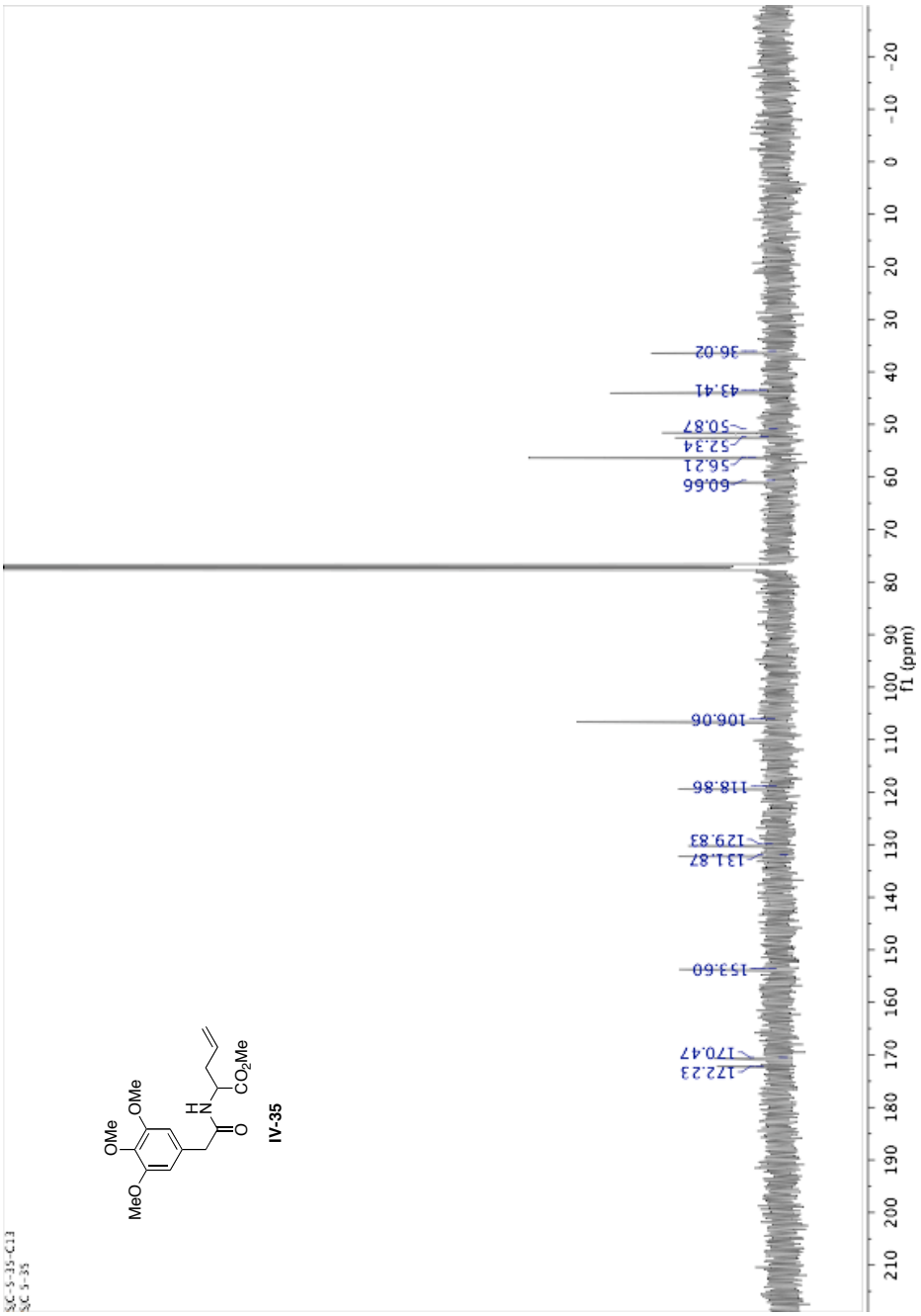
36.02
43.41
50.87
52.34
56.21
60.66
106.06
118.86
129.83
131.87
153.60
170.47
172.23
f1 (ppm)
OMe
OMe
MeO
H
N
O
CO2Me
IV-35

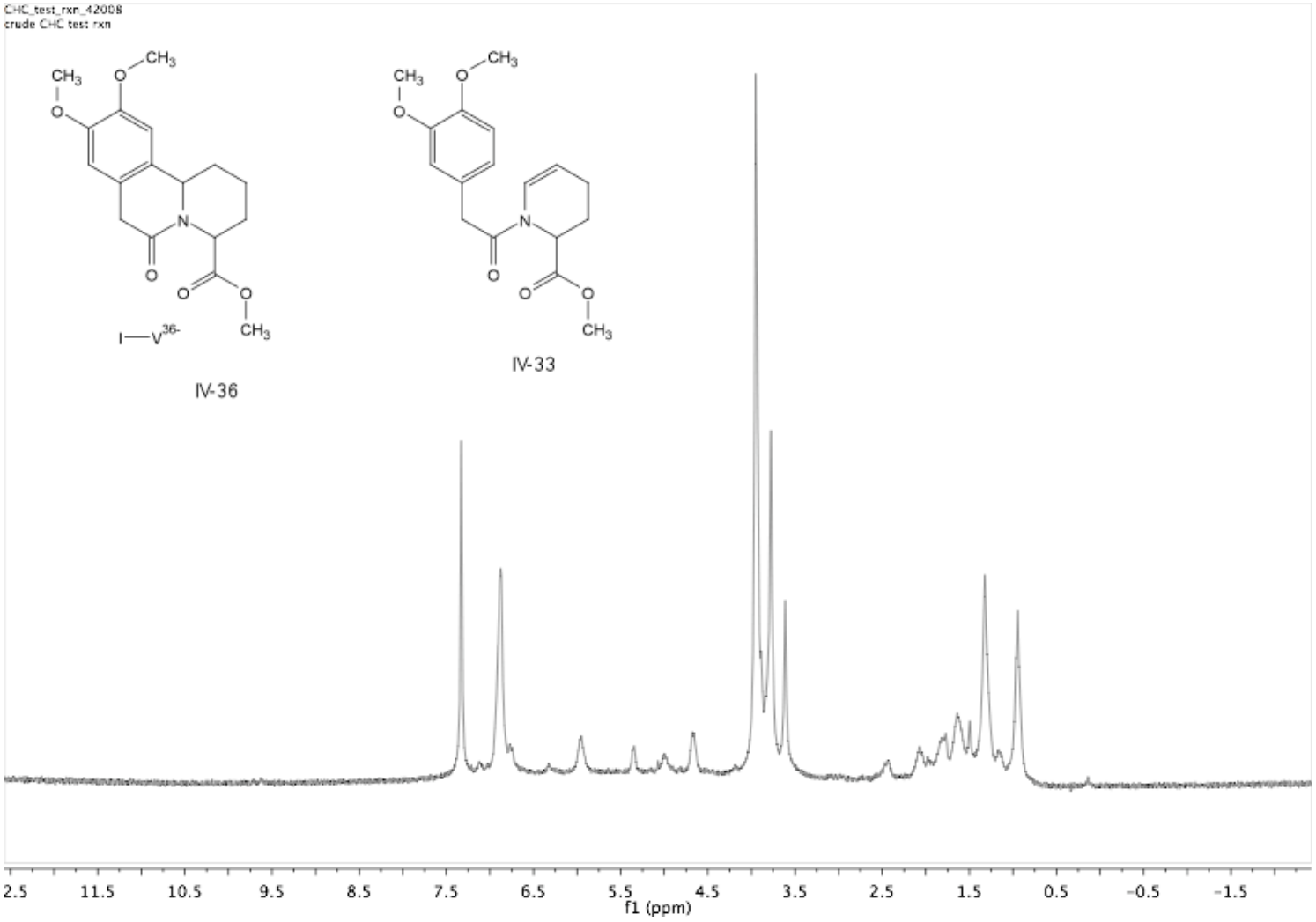
CHC_test_rxn_42008
crude CHC test rxn
IV-36
IV-33
2.5
11.5
10.5
9.5
8.5
7.5
6.5
5.5
4.5
3.5
2.5
1.5
0.5
-0.5
-1.5
f1 (ppm)

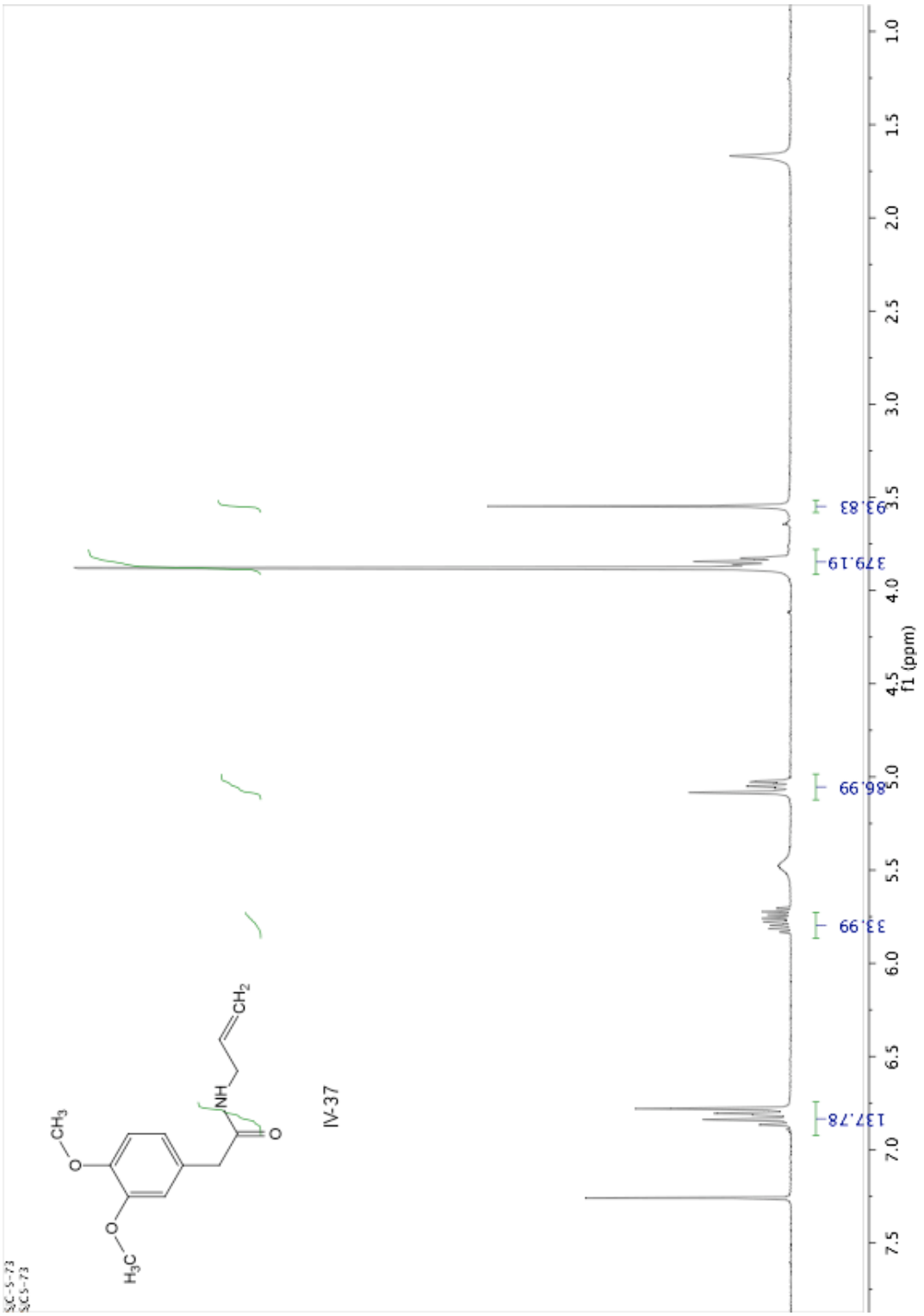
IV-37
NH
O
CH3
H3C
CH2
137.78
33.99
86.99
379.19
93.83
f1 (ppm)

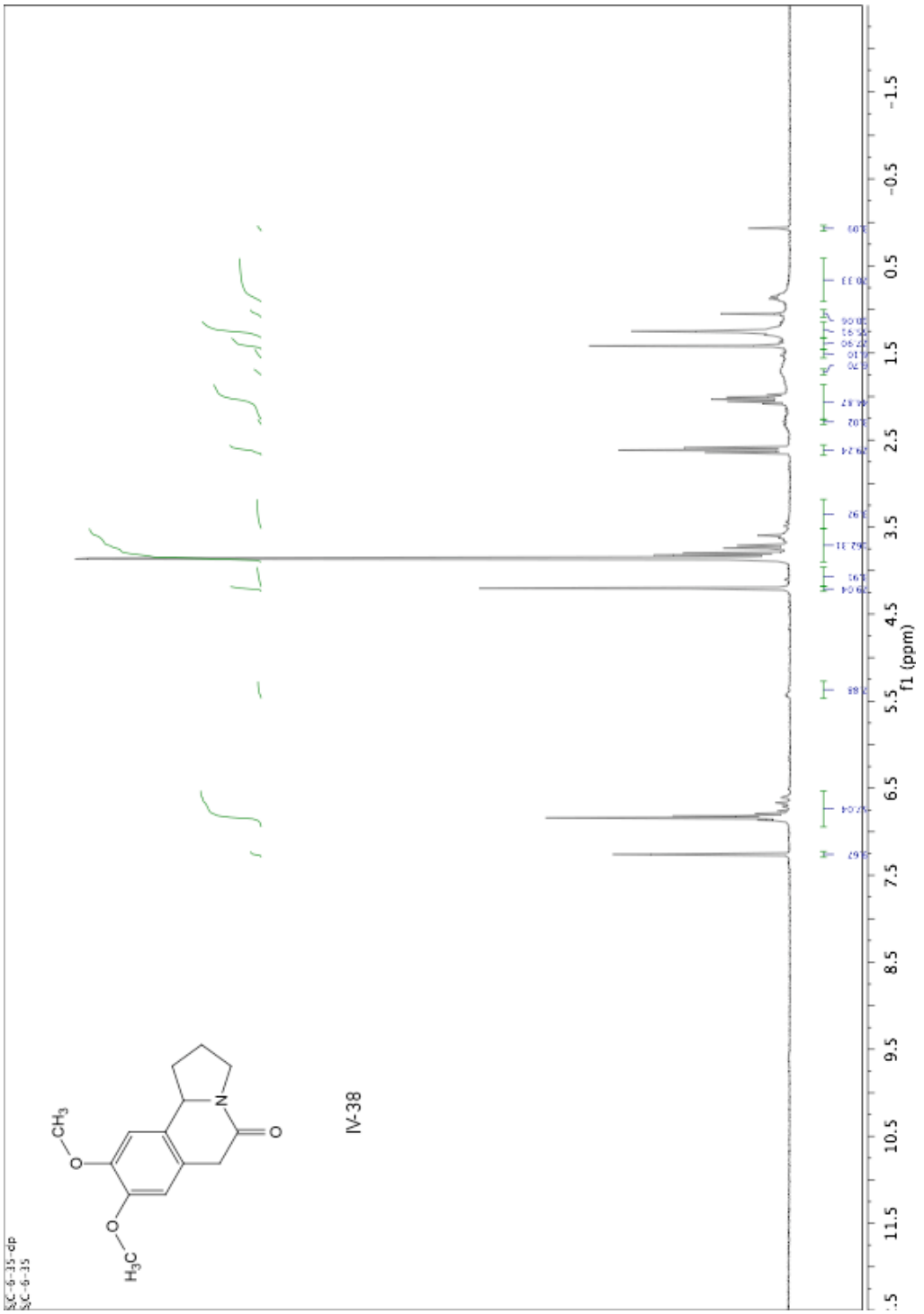
IV-38
f1 (ppm)

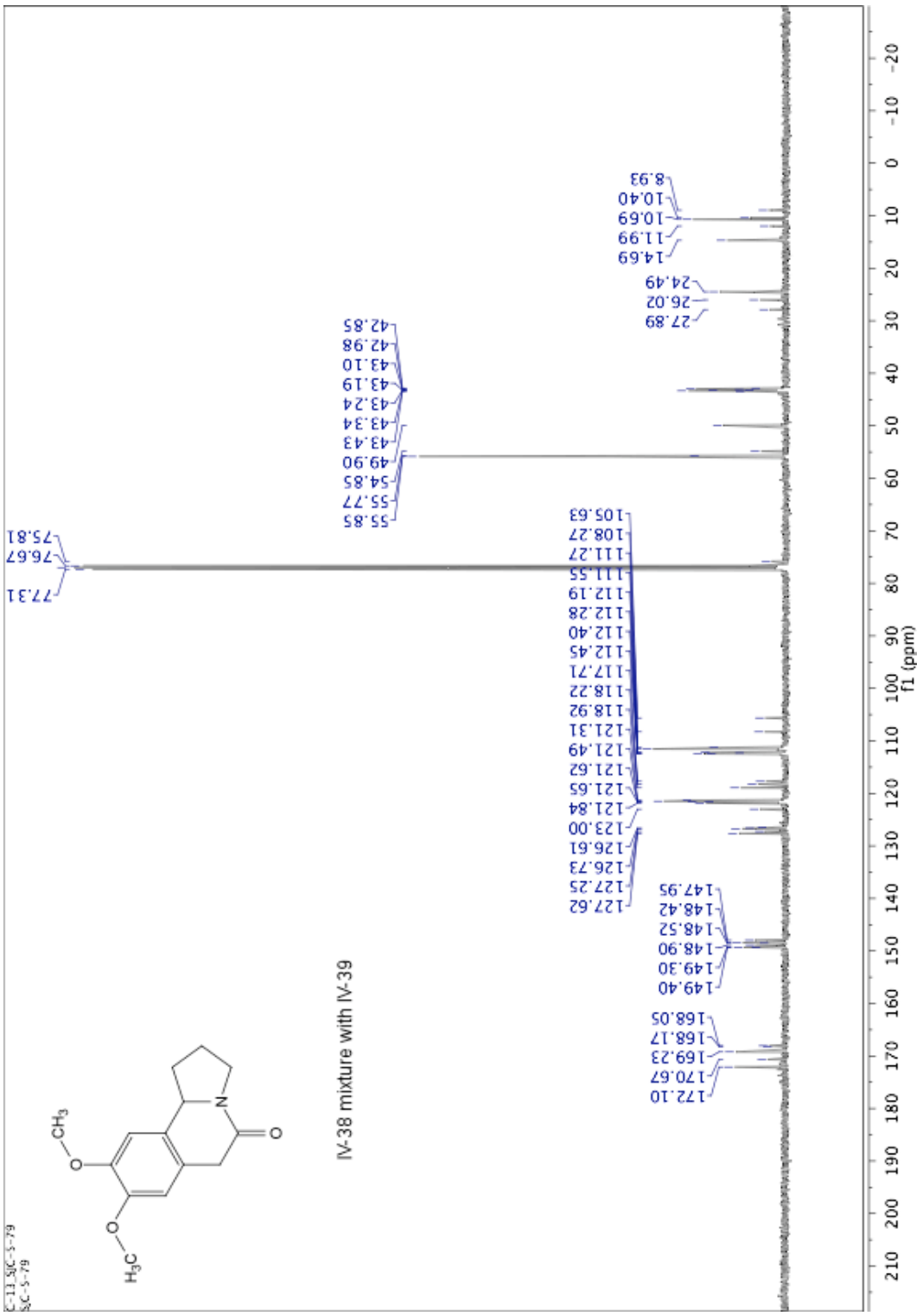
IV-38 mixture with IV-39
f1 (ppm)

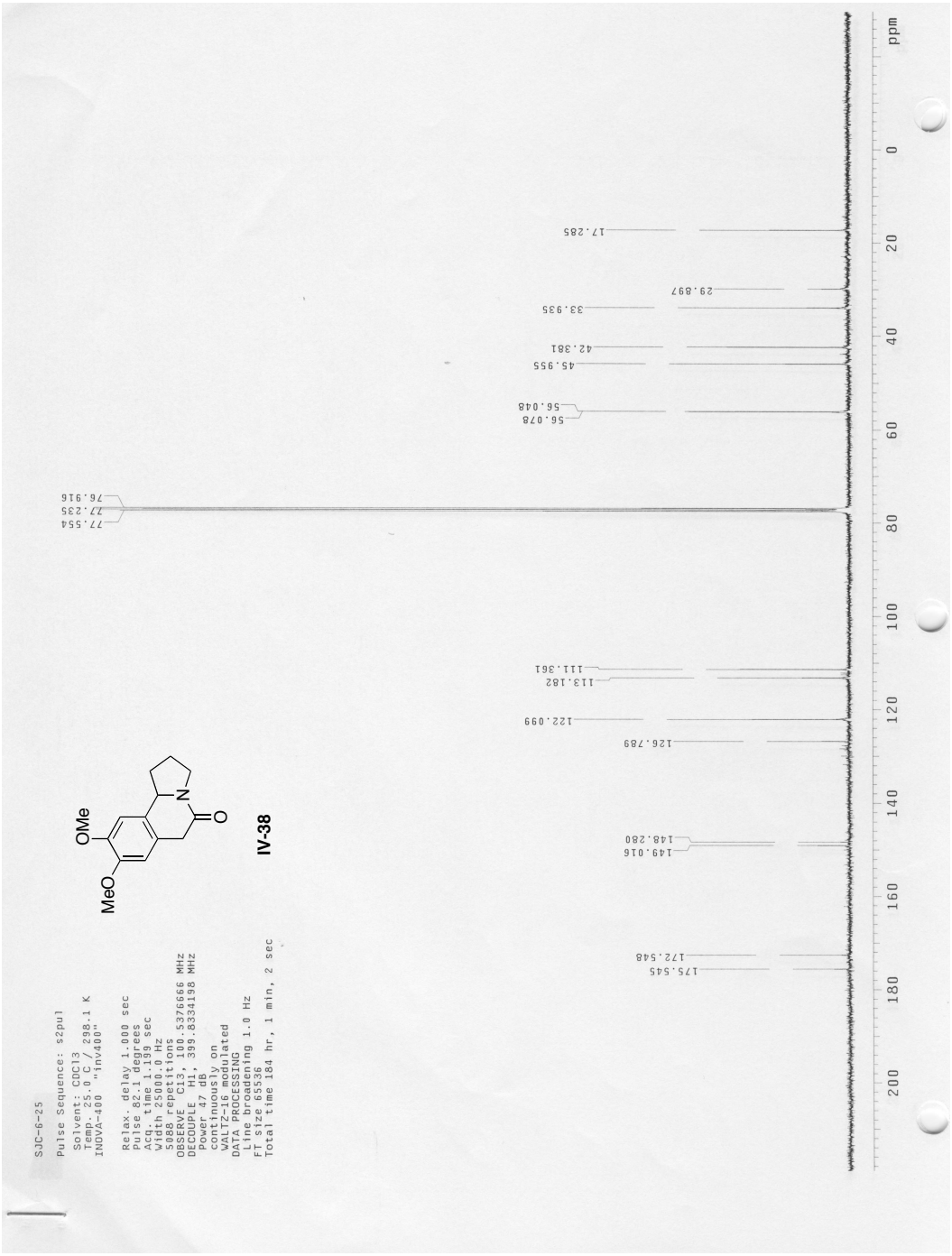
SJC-6-25
Pulse Sequence: s2pul
Solvent: CDCl3
Temp. 25.0 C / 298.1 K
INOVA-400 "inv400"
Relax. delay 1.000 sec
Pulse 82.1 degrees
Acq. time 1.199 sec
Width 25000.0 Hz
8 repetitions
OBSERVE C13, 100.5376666 MHz
DECOUPLE H1, 399.8334198 MHz
Power 47 dB
continuously on
WALTZ-16 modulated
DATA PROCESSING
Line broadening 1.0 Hz
FT size 65536
Total time 184 hr, 1 min, 2 sec
OMe
MeO
O
N
IV-38
77.554
77.235
76.916
56.078
56.048
45.955
42.361
33.935
29.897
17.285
175.545
172.548
149.016
148.280
126.789
122.099
113.182
111.361
ppm

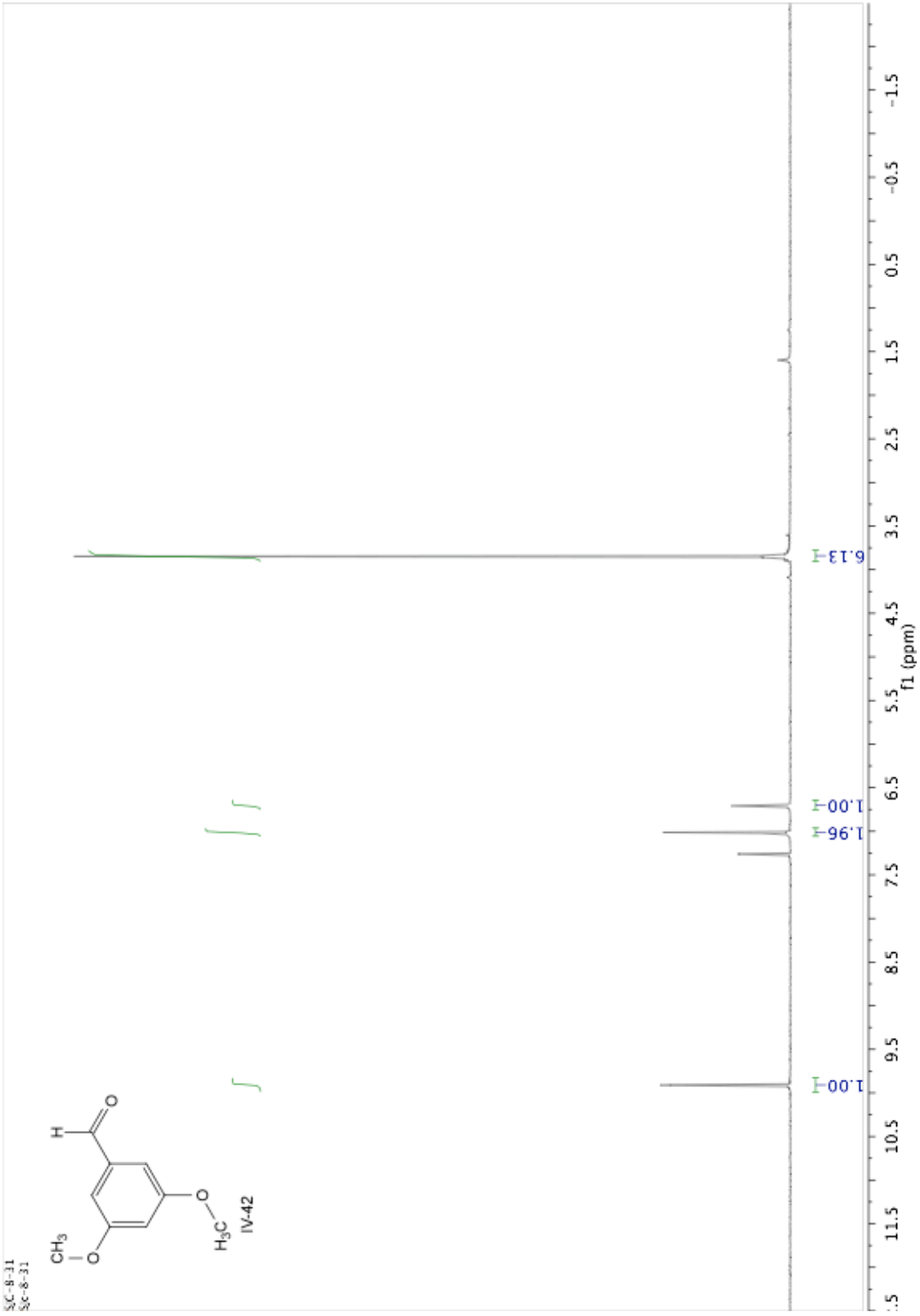
6.13
1.00
1.96
1.00
f1 (ppm)
IV-42

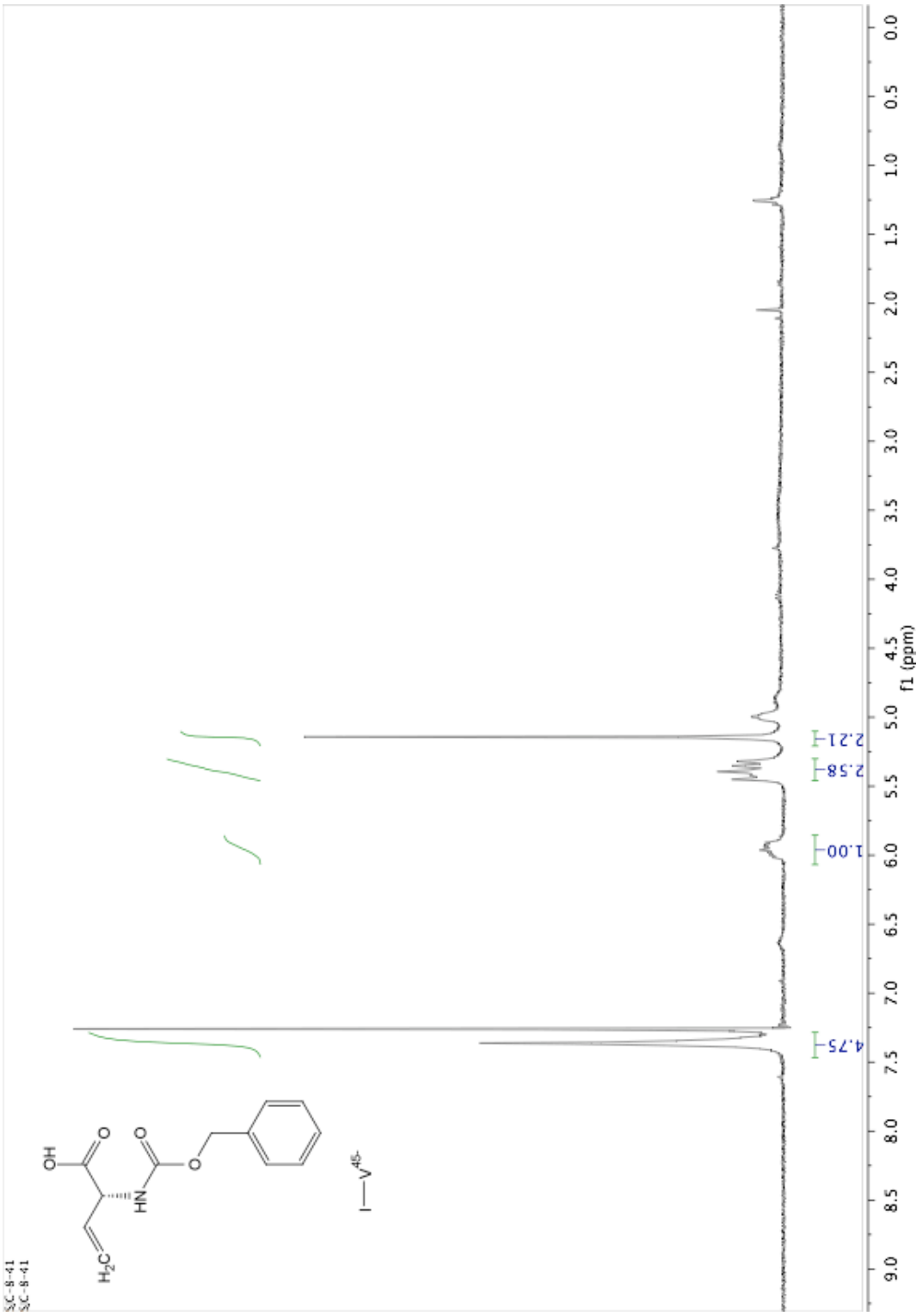
SJC-8-41
SJC-8-41
OH
O
O
HN
O
H2C
I—V45-
4.75
1.00
2.58
2.21
f1 (ppm)

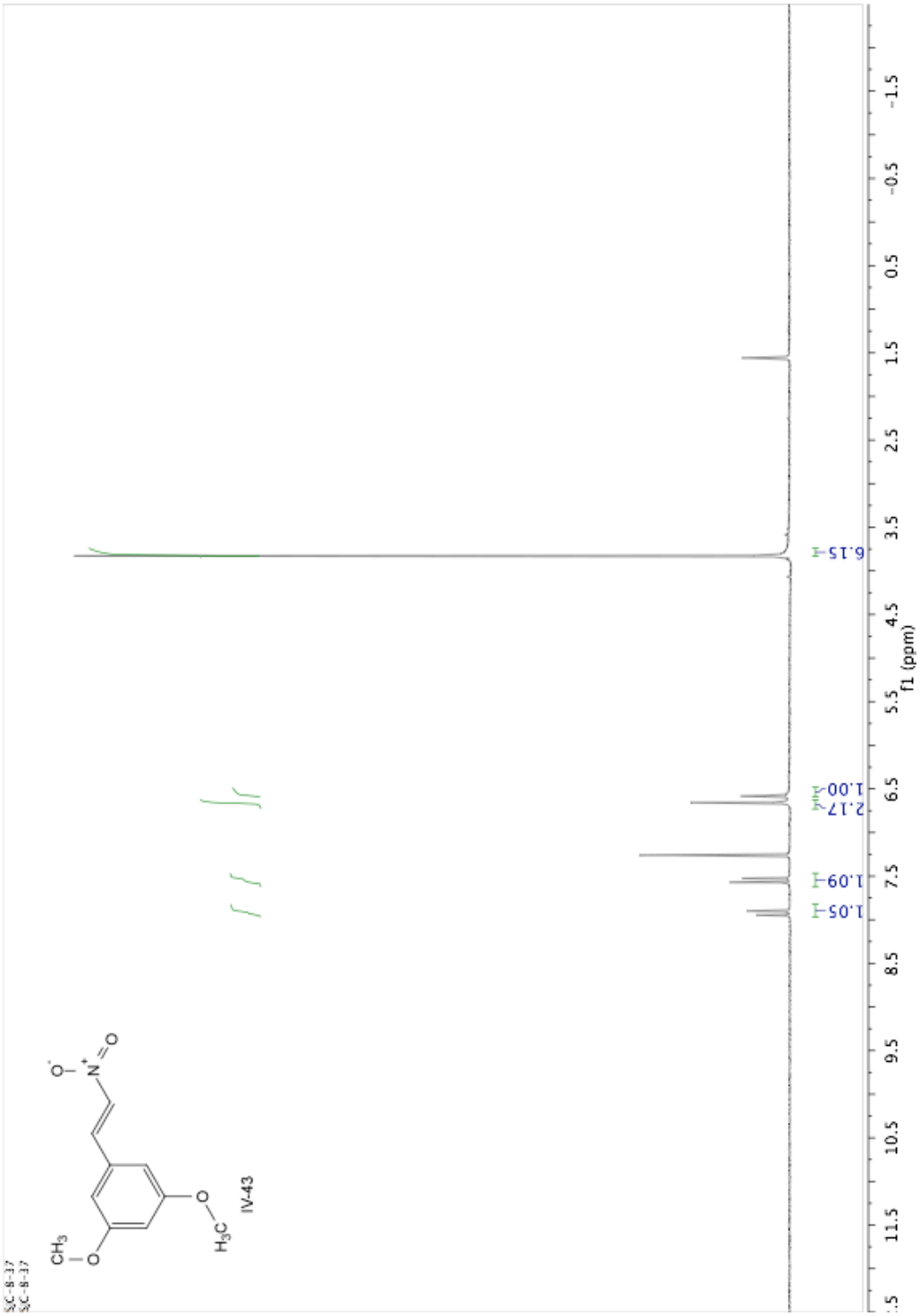
SJC-8-37
SJC-8-37
IV-43
6.15
1.00
2.17
1.09
1.05
f1 (ppm)

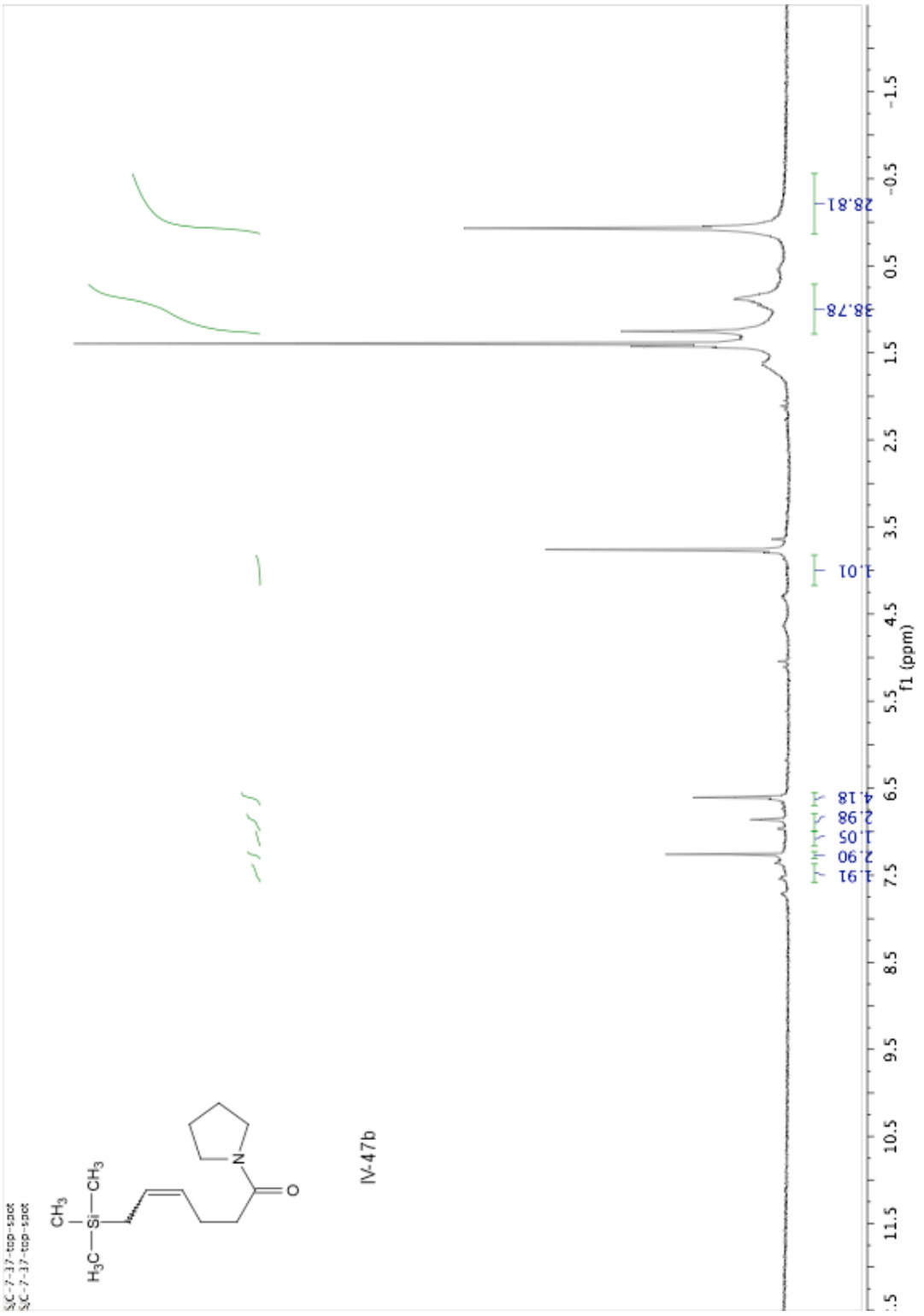
SJC-7-37-top-spot
SJC-7-37-top-spot
IV-47b
28.81
38.78
4.01
4.18
2.98
1.05
2.90
4.91
f1 (ppm)

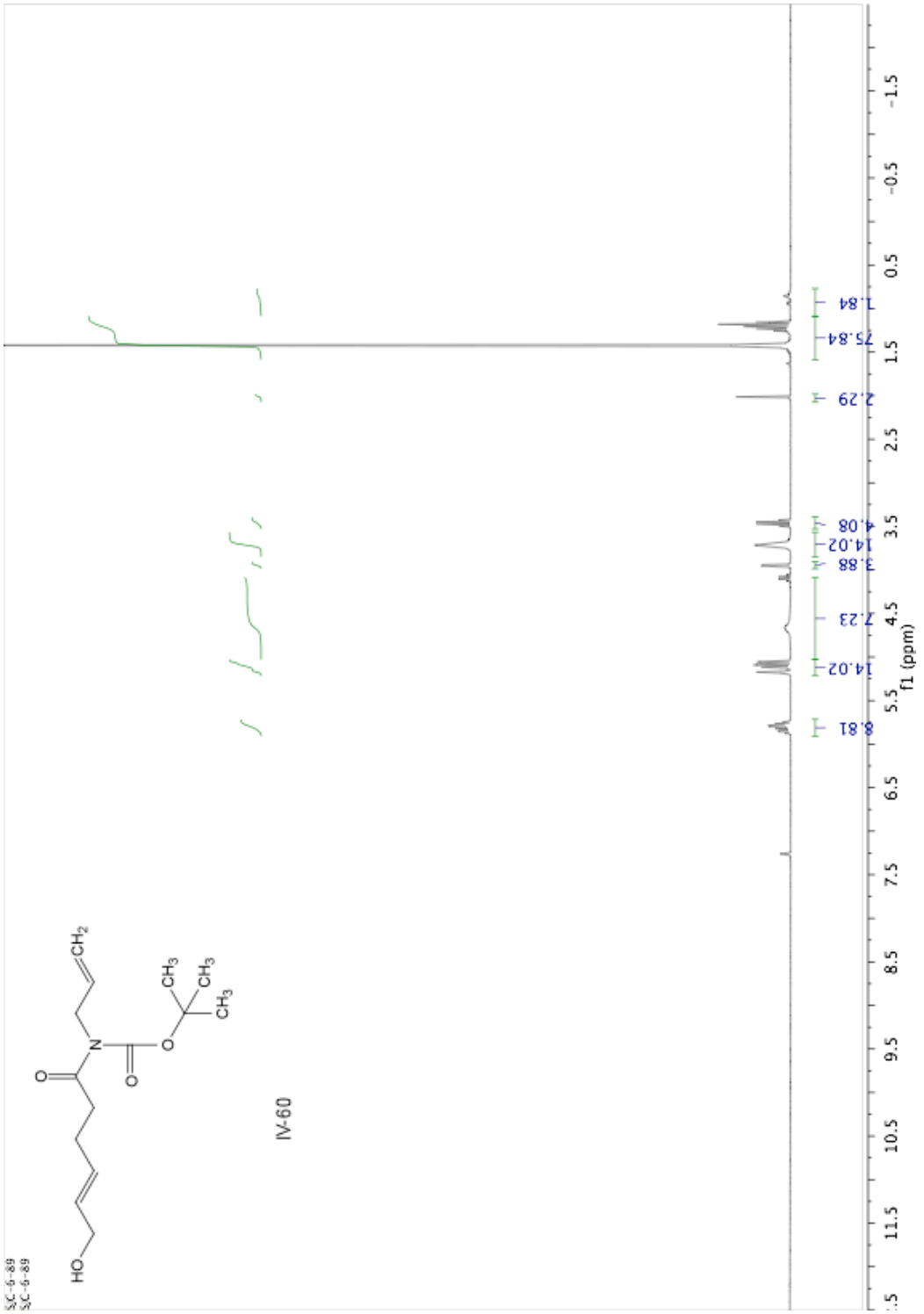
SJC-6-89
SJC-6-89
HO
O
O
N
O
O
CH3
CH3
CH3
CH2
IV-60
1.84
75.84
2.29
4.08
14.02
3.88
7.23
14.02
8.81
f1 (ppm)

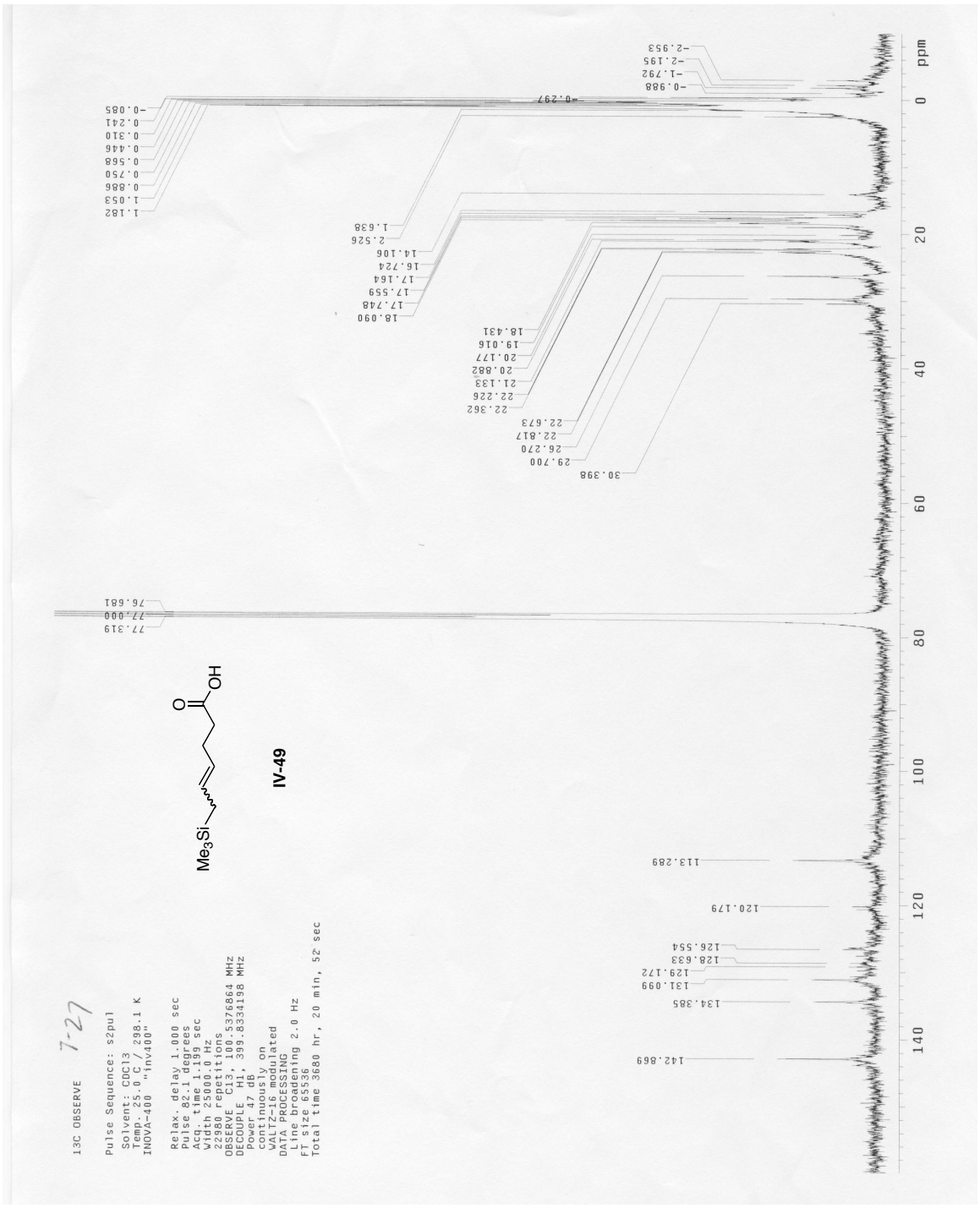
13C OBSERVE 7-27
Pulse Sequence: s2pul
Solvent: CDCl3
Temp. 25.0 C / 298.1 K
INOVA-400 "inv400"
Relax. delay 1.000 sec
Pulse 82.1 degrees
Acq. time 1.199 sec
Width 25000.0 Hz
22980 repetitions
OBSERVE C13, 100.5376864 MHz
DECOUPLE H1, 399.8334198 MHz
Power 37 dB
continuously on
WALTZ-16 modulated
DATA PROCESSING
Line broadening 2.0 Hz
FT size 65536
Total time 3680 hr, 20 min, 52 sec
Me3Si
O
OH
IV-49
77.319
77.000
76.681
142.869
134.385
131.099
129.172
128.633
126.554
120.179
113.289
30.398
29.700
26.270
22.817
22.673
22.362
22.226
21.133
20.882
20.177
19.016
18.431
18.090
17.748
17.559
17.164
16.724
14.106
2.526
1.638
1.182
1.053
0.886
0.750
0.568
0.446
0.310
0.241
0.085
-0.297
-0.988
-1.792
-2.195
-2.953
ppm
0
20
40
60
80
100
120
140

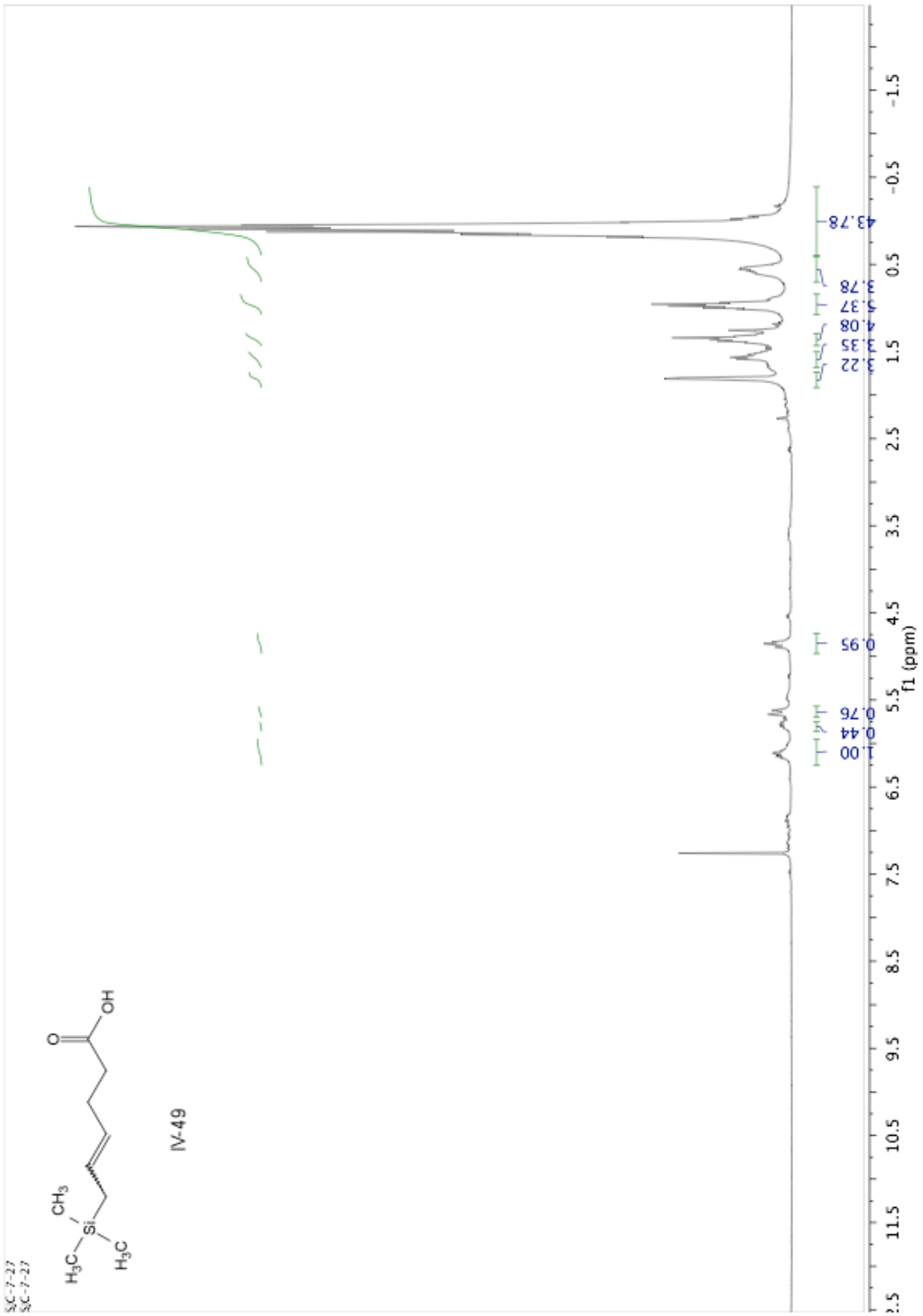
IV-49
f1 (ppm)

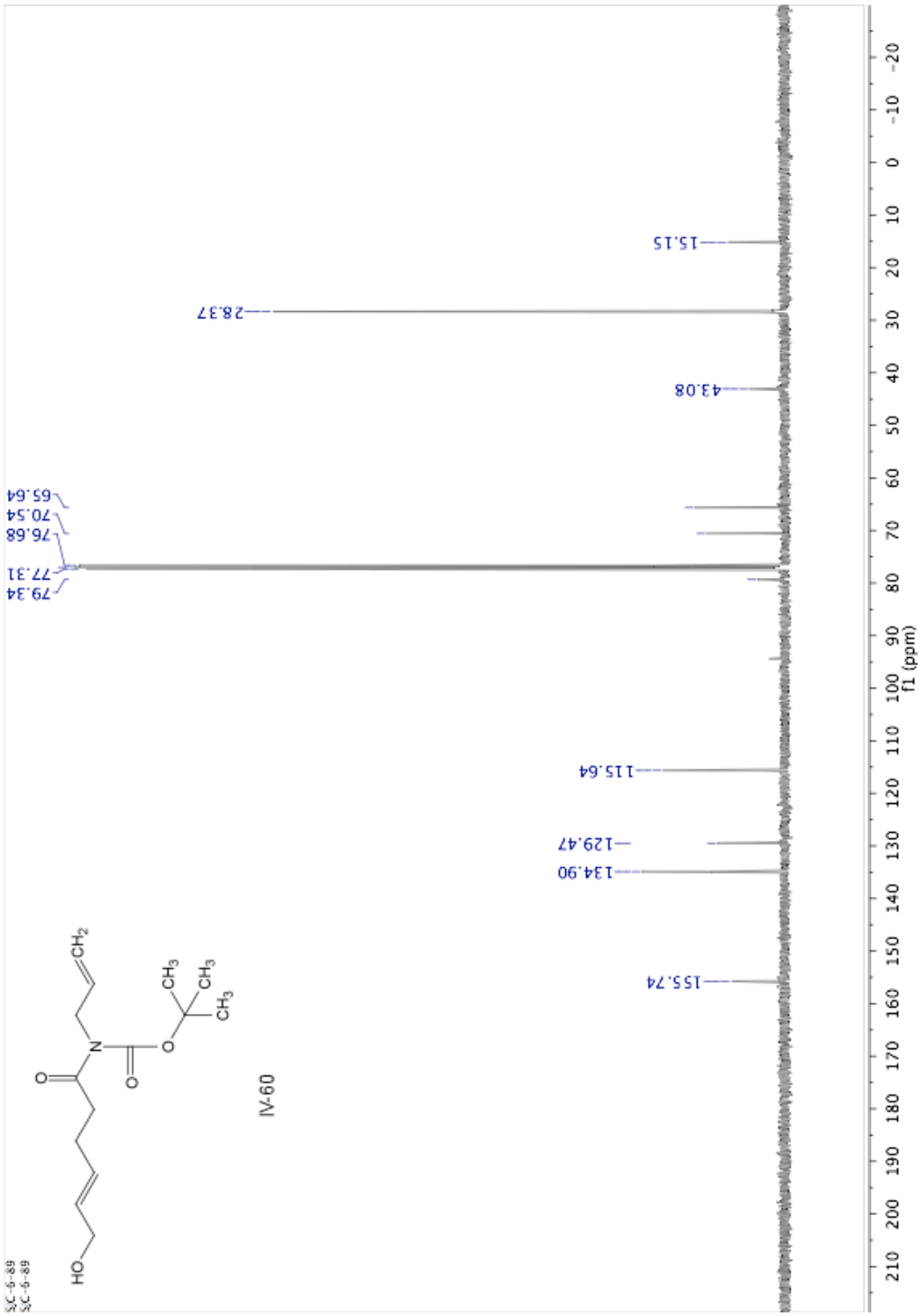
155.74
134.90
129.47
115.64
79.34
77.31
76.68
70.54
65.64
43.08
28.37
15.15
f1 (ppm)
IV-60
SC-6-89
SC-6-89

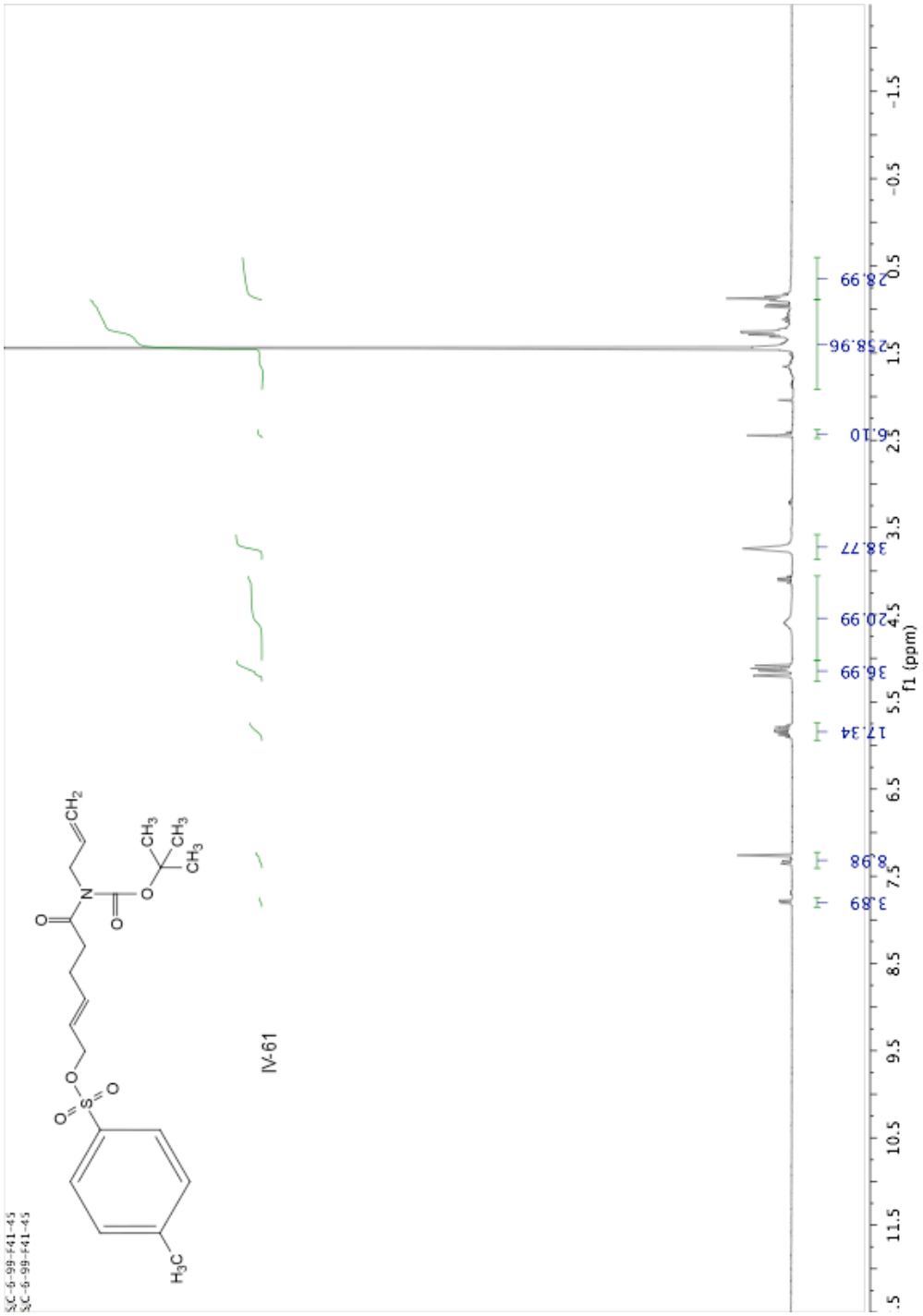
IV-61
f1 (ppm)

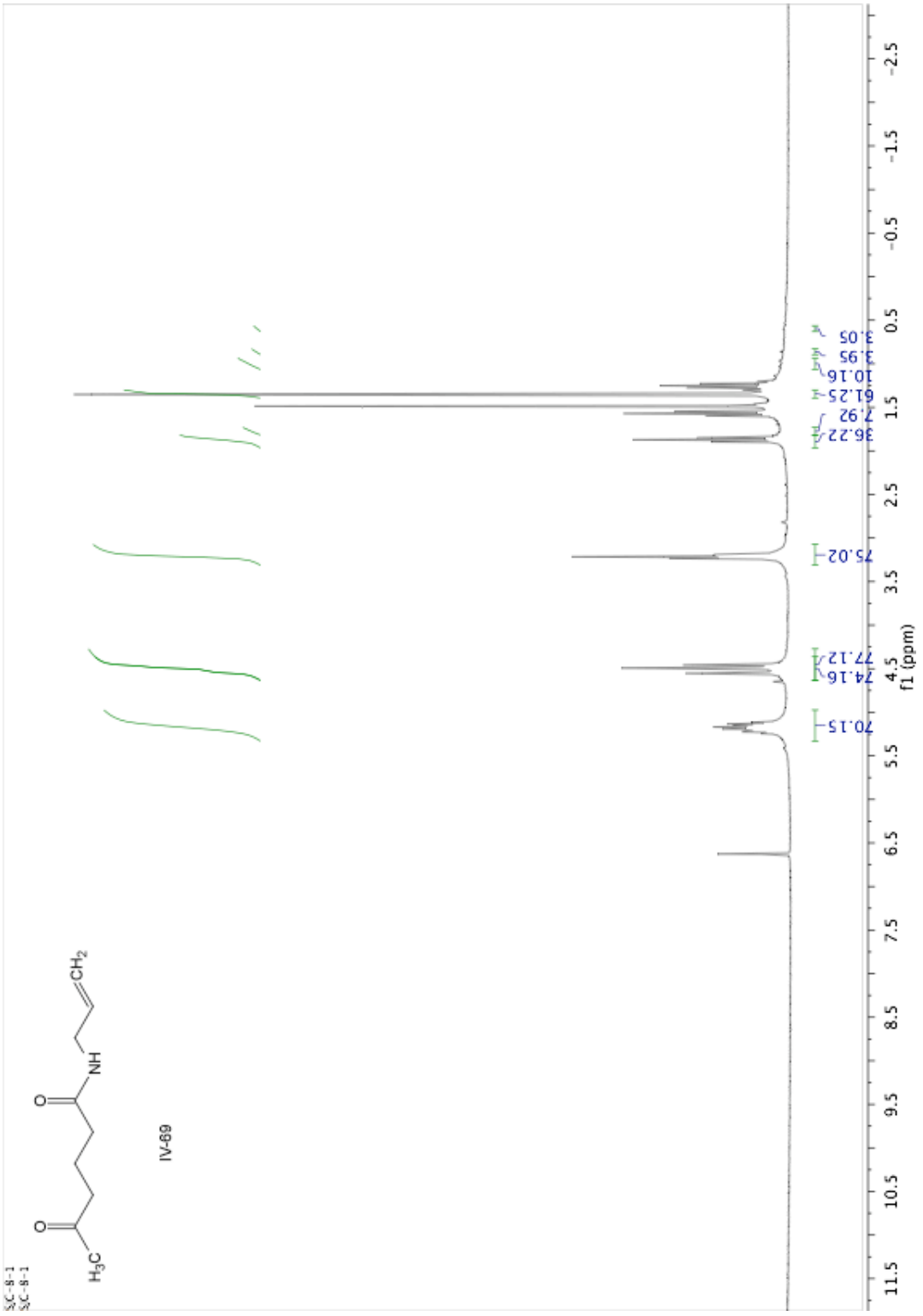
IV-69
f1 (ppm)
3.05
3.95
10.16
61.25
7.92
36.22
75.02
77.12
74.16
70.15

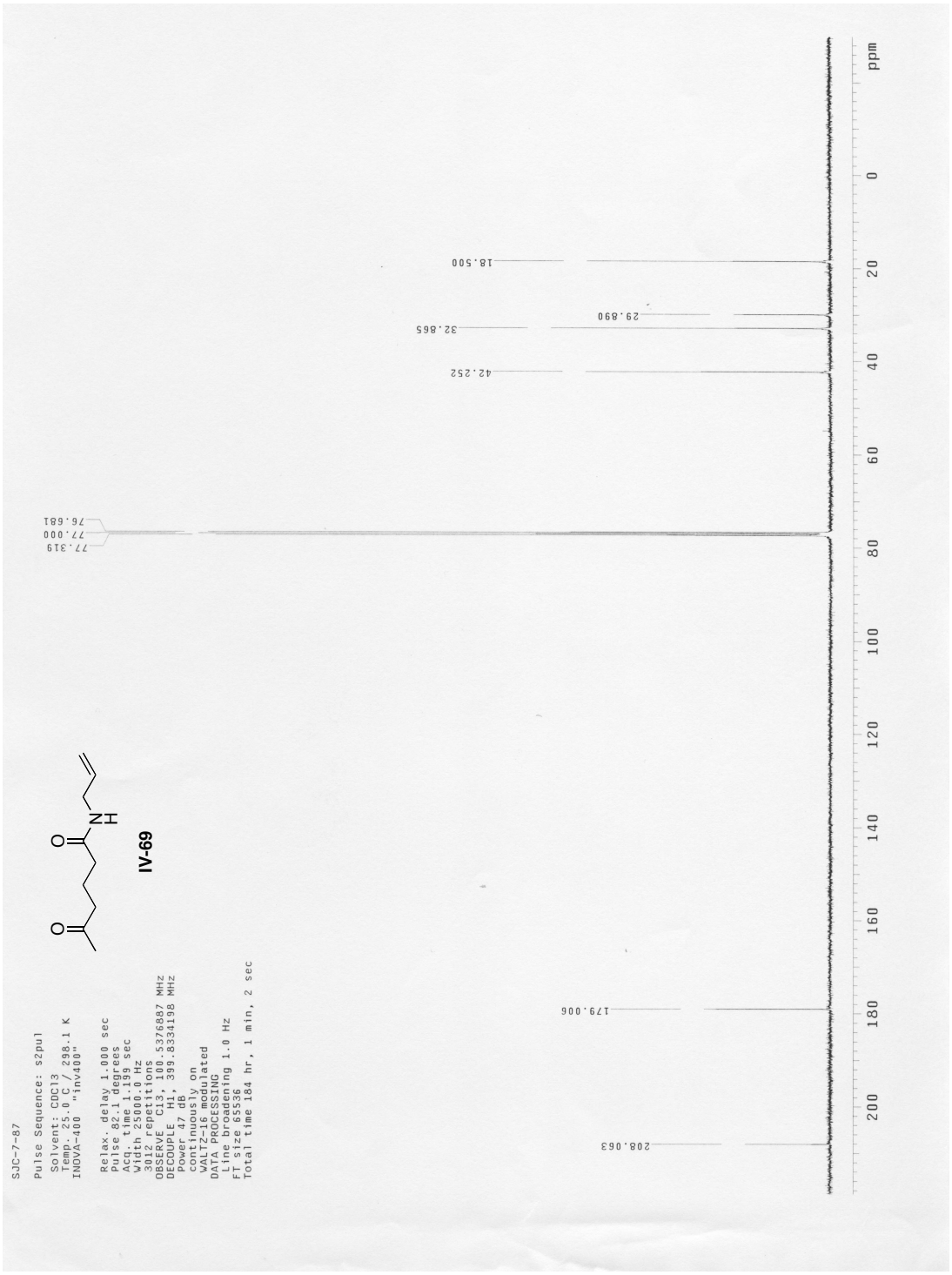
SJC-7-87
Pulse Sequence: s2pul
Solvent: CDCl3
Temp: 25.0 C / 298.1 K
INOVA-400 "inv400"
Relax. delay 1.000 sec
Pulse 92.1 degrees
Acq. time 1.199 sec
Width 25000.0 Hz
3012 repetitions
OBSERVE C13, 100.5376887 MHz
DECOUPLE H1, 399.8334198 MHz
Power 47 dB
continuously on
WALTZ-16 modulated
DATA PROCESSING
Line broadening 1.0 Hz
FT size 65536
Total time 184 hr, 1 min, 2 sec
IV-69
77.319
77.000
76.681
208.063
179.006
42.252
32.865
29.890
18.500
ppm

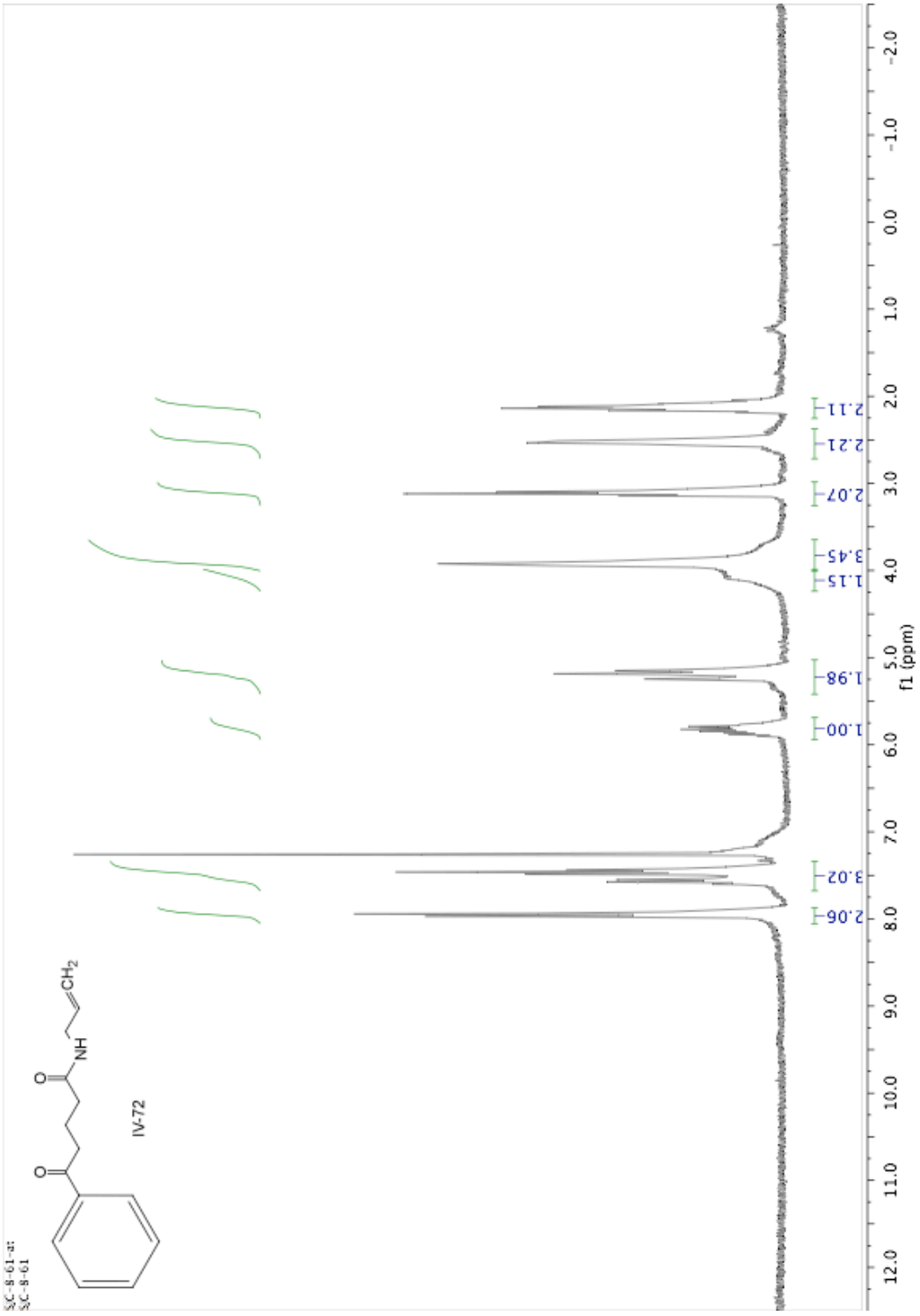
SC-8-61-a:
SC-8-61
IV-72
NH
O
O
CH2
2.06
3.02
1.00
1.98
1.15
3.45
2.07
2.21
2.11
f1 (ppm)
12.0
11.0
10.0
9.0
8.0
7.0
6.0
5.0
4.0
3.0
2.0
1.0
0.0
-1.0
-2.0

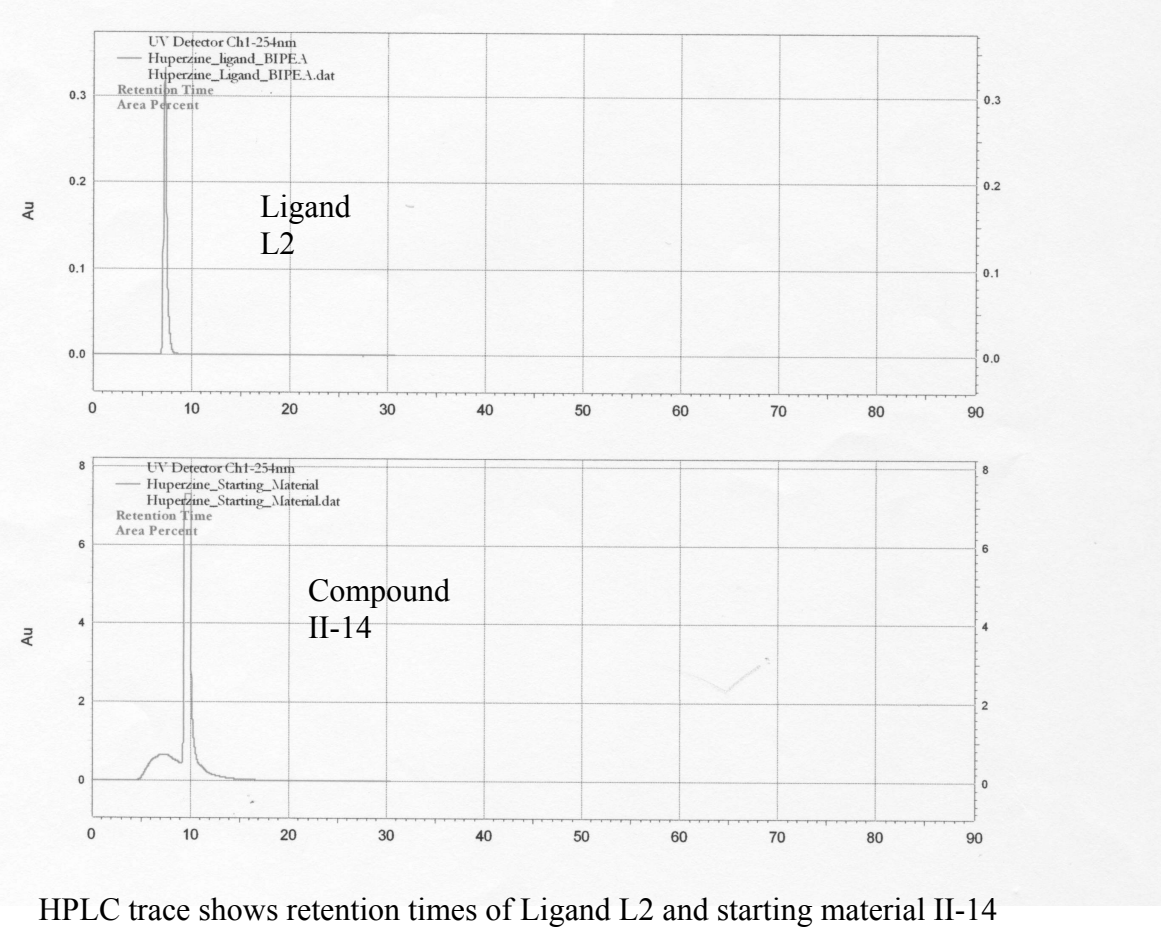

HPLC trace shows retention times of Ligand L2 and starting material II-14

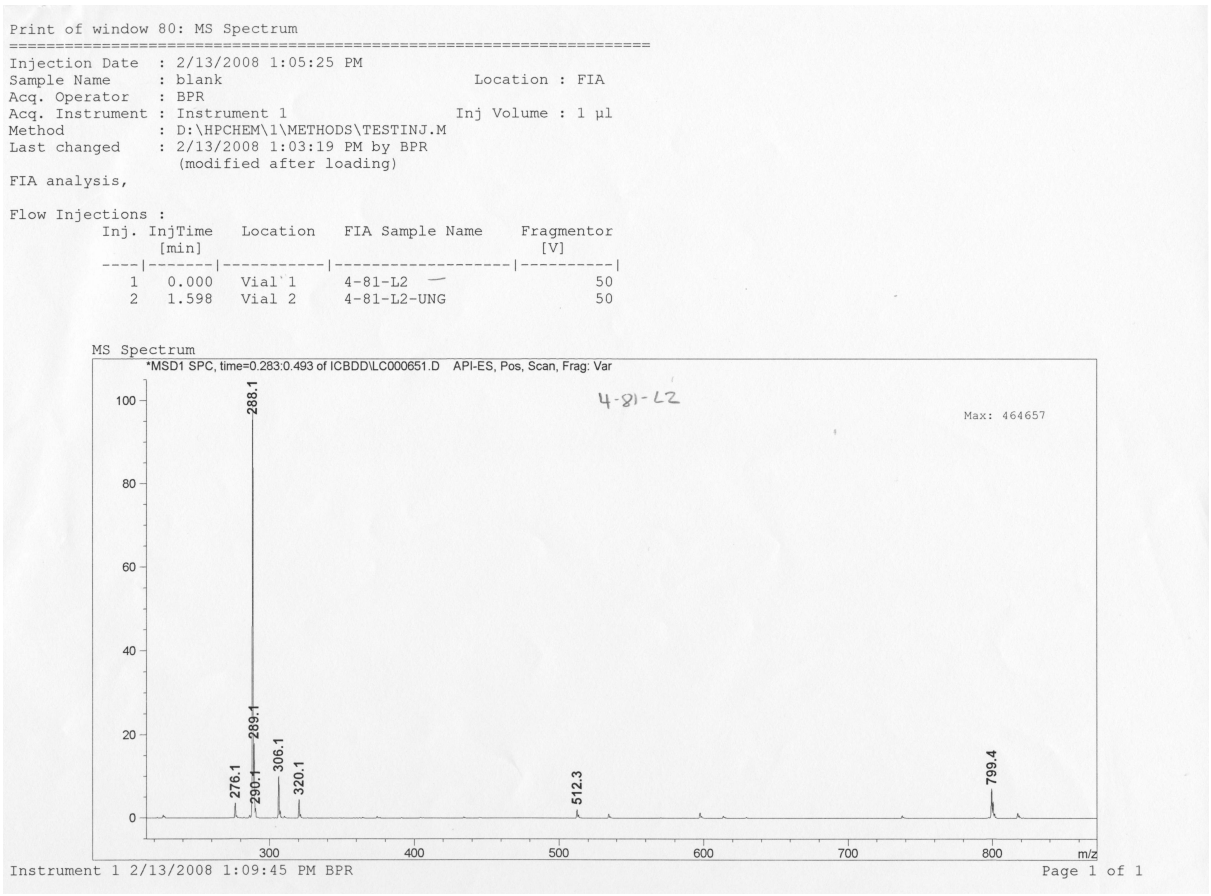

```
Print of window 80: MS Spectrum
=====================================================================
Injection Date  : 2/13/2008 1:05:25 PM
Sample Name     : blank                          Location : FIA
Acq. Operator   : BPR
Acq. Instrument : Instrument 1                Inj Volume : 1 µl
Method          : D:\HPCHEM\1\METHODS\TESTINJ.M
Last changed    : 2/13/2008 1:03:19 PM by BPR
                  (modified after loading)
FIA analysis,

Flow Injections :
          Inj. InjTime   Location   FIA Sample Name    Fragmentor
               [min]                                     [V]
          ----|-------|-----------|------------------|----------|
             1   0.000   Vial 1     4-81-L2                  50
             2   1.598   Vial 2     4-81-L2-UNG              50
```


FIA of the crude asymmetric allylic alkylation of the huperzine-A intermediate. Shows only 288 [M+H] for the completely cyclized product. No 363 or 364 (uncyclized and uncyclized+H) peak observed

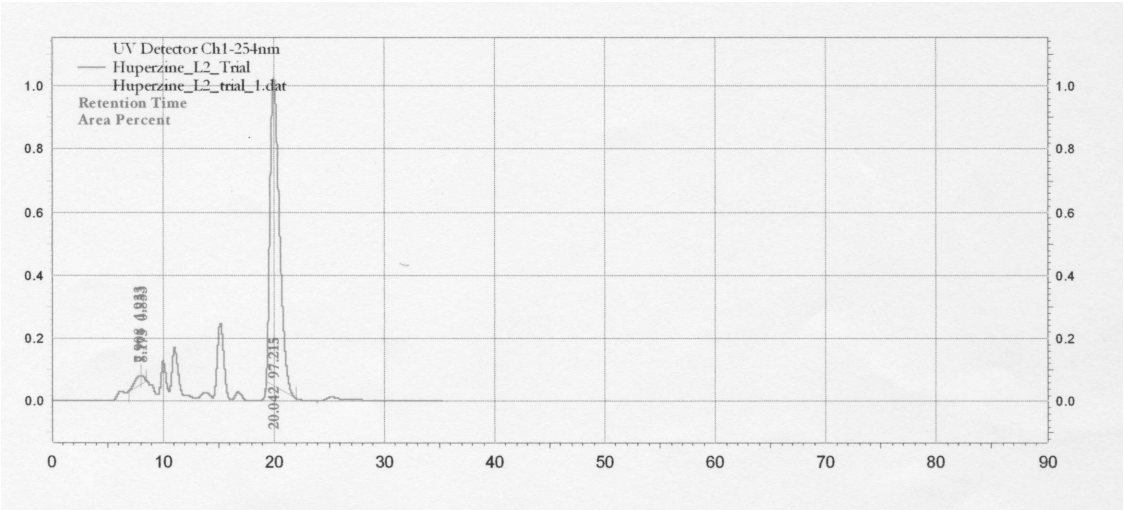

HPLC trace showing cyclized II-8 as an enantiopure compound. Peak at 15.1 min is compound II-16